

NASA Contractor Report 198529

Mechanical and Thermal Properties of Two Cu-Cr-Nb Alloys and NARloy-Z

David L. Ellis and Gary M. Michal
Case Western Reserve University
Cleveland, Ohio

October 1996

Prepared for
Lewis Research Center
Under Cooperative Agreement NCC3-94



National Aeronautics and
Space Administration

Trade names or manufacturers' names are used in this report for identification only. This usage does not constitute an official endorsement, either expressed or implied, by the National Aeronautics and Space Administration.

Table Of Contents

<i>Table Of Contents</i>	<i>i</i>
<i>Table Of Figures</i>	<i>iii</i>
<i>Table Of Tables</i>	<i>vii</i>
<i>Abstract</i>	<i>viii</i>
<i>Introduction</i>	<i>1</i>
<i>Experimental Procedure</i>	<i>2</i>
Production Of Material	<i>2</i>
Alloy Density Measurement	<i>2</i>
Identification and Analysis of Precipitates	<i>3</i>
Creep Testing	<i>3</i>
Thermal Conductivity Testing	<i>7</i>
Low Cycle Fatigue	<i>8</i>
<i>Results</i>	<i>9</i>
Alloy Chemistries	<i>9</i>
Alloy Densities	<i>11</i>
Precipitate Analysis	<i>12</i>
Creep Testing	<i>13</i>
Cu-8 Cr-4 Nb	<i>13</i>
Cu-4 Cr-2 Nb	<i>17</i>
NARloy-Z	<i>20</i>
Creep Fracture Surfaces	<i>23</i>
Modeling of Creep Properties	<i>25</i>
Thermal Conductivity Testing	<i>31</i>
Cu-8 Cr-4 Nb	<i>31</i>
Cu-4 Cr-2 Nb	<i>35</i>
Low Cycle Fatigue	<i>38</i>
<i>Discussion</i>	<i>43</i>
Creep	<i>43</i>
Low Cycle Fatigue	<i>47</i>
Thermal Conductivity	<i>47</i>
<i>Summary and Conclusions</i>	<i>50</i>
<i>Future Work</i>	<i>51</i>
<i>Acknowledgments</i>	<i>52</i>

References	53
Appendices	55
Appendix A - Creep Of Cu-8 Cr-4 Nb	56
Appendix B - Creep Of Cu-4 Cr-2 Nb	115
Appendix C - Creep Of NARloy-Z	146
Appendix D - Cu-8 Cr-4 Nb Low Cycle Fatigue Loops	185

Table Of Figures

Figure 1 - Creep Specimen Design	3
Figure 2a - Size Distribution Of Cu-4 Cr-2 Nb Powder	10
Figure 2b - Size Distribution Of Cu-8 Cr-4 Nb Powder	10
Figure 3 - Comparison Of Alloy Densities	12
Figure 4 - Typical Cu-8 Cr-4 Nb Creep Curve	14
Figure 5 - Times To 1% Creep Strain For Cu-8 Cr-4 Nb	15
Figure 6 - Steady-State Creep Rates Of Cu-8 Cr-4 Nb	15
Figure 7 - Creep Rupture Lives Of Cu-8 Cr-4 Nb	16
Figure 8 - Creep Elongations Of Cu-8 Cr-4 Nb	16
Figure 9 - Typical Cu-4 Cr-2 Nb Creep Curve	17
Figure 10 - Times To 1% Creep Strain Cu-4 Cr-2 Nb	18
Figure 11 - Steady-State Creep Rates Of Cu-4 Cr-2 Nb	18
Figure 12 - Creep Rupture Lives Of Cu-4 Cr-2 Nb	19
Figure 13 - Average Creep Elongation Of Cu-4 Cr-2 Nb	19
Figure 14 - Typical NARloy-Z Creep Curve	20
Figure 15 - Times To 1% Creep Strain For NARloy-Z	21
Figure 16 - Steady-State Creep Rates Of NARloy-Z	21
Figure 17 - Creep Rupture Lives Of NARloy-Z	22
Figure 18 - Creep Elongations Of NARloy-Z	22
Figure 19a - Typical Fracture Surface Of Cu-8 Cr-4 Nb Creep Samples (Extrusion L-3107 Tested At 500°C/84.0 MPa)	23
Figure 19b - Detail Of Cu-8 Cr-4 Nb Fracture Surface (Extrusion L-3107 Tested At 500°C/84.0 MPa)	24
Figure 19c - Typical Fracture Surface Of Cu-4 Cr-2 Nb Creep Samples (Extrusion L-3297 Tested At 650°C/37.4 MPa)	24
Figure 19d - Typical Fracture Surface Of NARloy-Z Creep Samples (Plate 3 Tested At 800°C/10.4 MPa)	25
Figure 20a - Design Space for Cu-8 Cr-4 Nb	28
Figure 20b - Design Space for Cu-4 Cr-2 Nb	28
Figure 20c - Design Space for NARloy-Z	29
Figure 21 - Average Heat Capacity Of Cu-8 Cr-4 Nb	33
Figure 22 - Average Thermal Diffusivity Of Cu-8 Cr-4 Nb	34
Figure 23 - Average Thermal Conductivity Of Cu-8 Cr-4 Nb	34
Figure 24 - Heat Capacity Of Cu-4 Cr-2 Nb	37
Figure 25 - Thermal Diffusivity Of Cu-4 Cr-2 Nb	37
Figure 26 - Thermal Conductivity Of Cu-4 Cr-2 Nb	38
Figure 27 - Typical LCF Loops For Cu-8 Cr-4 Nb (Sample 1-1 Tested At Room Temperature)	40
Figure 28a - Room Temperature Low Cycle Fatigue Lives Of Cu-8 Cr-4 Nb and NARloy-Z	41
Figure 28b - Elevated Temperature Low Cycle Fatigue Lives Of Cu-8 Cr-4 Nb and NARloy-Z	42
Figure 29 - Comparison Of Mean Times To 1% Creep	44
Figure 30 - Comparison Of Mean Creep Rates	45
Figure 31 - Comparison Of Mean Creep Lives	46
Figure 32 - Comparison Of Average Creep Elongations	46
Figure 33 - Comparison of Cu-Cr-Nb, NARloy-Z And Cu Thermal Conductivities	48
Figure A - 1 - Extrusion L-3097 Tested At 500°C/72.9 MPa	61
Figure A - 2 - Extrusion L-3104 Tested At 500°C/72.9 MPa	62
Figure A - 4 - Extrusion L-3106 Tested At 500°C/72.9 MPa	64
Figure A - 5 - Extrusion L-3107 Tested At 500°C/72.9 MPa	65
Figure A - 6 - Extrusion L-3108 Tested At 500°C/72.9 MPa	66
Figure A - 7 - Extrusion L-3097 Tested At 500°C/84.0 MPa	67
Figure A - 8 - Extrusion L-3104 Tested At 500°C/84.0 MPa	68
Figure A - 9 - Extrusion L-3105 Tested At 500°C/84.0 MPa	69

<i>Figure A - 10 - Extrusion L-3106 Tested At 500°C/84.0 MPa</i>	70
<i>Figure A - 11 - Extrusion L-3107 Tested At 500°C/84.0 MPa</i>	71
<i>Figure A - 12 - Extrusion L-3108 Tested At 500°C/84.0 MPa</i>	72
<i>Figure A - 13 - Extrusion L-3097 Tested At 500°C/92.8 MPa</i>	73
<i>Figure A - 14 - Extrusion L-3104 Tested At 500°C/92.8 MPa</i>	74
<i>Figure A - 15 - Extrusion L-3105 Tested At 500°C/92.8 MPa</i>	75
<i>Figure A - 16 - Extrusion L-3106 Tested At 500°C/92.8 MPa</i>	76
<i>Figure A - 17 - Extrusion L-3107 Tested At 500°C/92.8 MPa</i>	77
<i>Figure A - 18 - Extrusion L-3108 Tested At 500°C/92.8 MPa</i>	78
<i>Figure A - 19 - Extrusion L-3097 Tested At 650°C/37.4 MPa</i>	79
<i>Figure A - 20 - Extrusion L-3104 Tested At 650°C/37.4 MPa</i>	80
<i>Figure A - 21 - Extrusion L-3105 Tested At 650°C/37.4 MPa</i>	81
<i>Figure A - 22 - Extrusion L-3106 Tested At 650°C/37.4 MPa</i>	82
<i>Figure A - 23 - Extrusion L-3107 Tested At 650°C/37.4 MPa</i>	83
<i>Figure A - 24 - Extrusion L-3108 Tested At 650°C/37.4 MPa</i>	84
<i>Figure A - 25 - Extrusion L-3097 Tested At 650°C/44.3 MPa</i>	85
<i>Figure A - 26 - Extrusion L-3104 Tested At 650°C/44.3 MPa</i>	86
<i>Figure A - 27 - Extrusion L-3105 Tested At 650°C/44.3 MPa</i>	87
<i>Figure A - 28 - Extrusion L-3106 Tested At 650°C/44.3 MPa</i>	88
<i>Figure A - 29 - Extrusion L-3107 Tested At 650°C/44.3 MPa</i>	89
<i>Figure A - 30 - Extrusion L-3108 Tested At 650°C/44.3 MPa</i>	90
<i>Figure A - 31 - Extrusion L-3097 Tested At 650°C/49.8 MPa</i>	91
<i>Figure A - 32 - Extrusion L-3104 Tested At 650°C/49.8 MPa</i>	92
<i>Figure A - 33 - Extrusion L-3105 Tested At 650°C/49.8 MPa</i>	93
<i>Figure A - 34 - Extrusion L-3106 Tested At 650°C/49.8 MPa</i>	94
<i>Figure A - 35 - Extrusion L-3107 Tested At 650°C/49.8 MPa</i>	95
<i>Figure A - 36 - Extrusion L-3108 Tested At 650°C/49.8 MPa</i>	96
<i>Figure A - 37 - Extrusion L-3097 Tested At 800°C/19.2 MPa</i>	97
<i>Figure A - 38 - Extrusion L-3104 Tested At 800°C/19.2 MPa</i>	98
<i>Figure A - 39 - Extrusion L-3105 Tested At 800°C/19.2 MPa</i>	99
<i>Figure A - 40 - Extrusion L-3106 Tested At 800°C/19.2 MPa</i>	100
<i>Figure A - 41 - Extrusion L-3107 Tested At 800°C/19.2 MPa</i>	101
<i>Figure A - 42 - Extrusion L-3108 Tested At 800°C/19.2 MPa</i>	102
<i>Figure A - 43 - Extrusion L-3097 Tested At 800°C/23.3 MPa</i>	103
<i>Figure A - 44 - Extrusion L-3104 Tested At 800°C/23.3 MPa</i>	104
<i>Figure A - 45 - Extrusion L-3105 Tested At 800°C/23.3 MPa</i>	105
<i>Figure A - 46 - Extrusion L-3106 Tested At 800°C/23.3 MPa</i>	106
<i>Figure A - 47 - Extrusion L-3107 Tested At 800°C/23.3 MPa</i>	107
<i>Figure A - 48 - Extrusion L-3108 Tested At 800°C/23.3 MPa</i>	108
<i>Figure A - 49 - Extrusion L-3097 Tested At 800°C/26.8 MPa</i>	109
<i>Figure A - 50 - Extrusion L-3104 Tested At 800°C/26.8 MPa</i>	110
<i>Figure A - 51 - Extrusion L-3105 Tested At 800°C/26.8 MPa</i>	111
<i>Figure A - 52 - Extrusion L-3106 Tested At 800°C/26.8 MPa</i>	112
<i>Figure A - 53 - Extrusion L-3107 Tested At 800°C/26.8 MPa</i>	113
<i>Figure A - 54 - Extrusion L-3108 Tested At 800°C/26.8 MPa</i>	114
<i>Figure B - 1 - Extrusion L-3284 Tested At 500°C/72.9 MPa</i>	118
<i>Figure B - 2 - Extrusion L-3296 Tested At 500°C/72.9 MPa</i>	119
<i>Figure B - 3 - Extrusion L-3297 Tested At 500°C/72.9 MPa</i>	120
<i>Figure B - 4 - Extrusion L-3298 Tested At 500°C/72.9 MPa</i>	121
<i>Figure B - 5 - Extrusion L-3296 Tested At 500°C/84.0 MPa</i>	122
<i>Figure B - 6 - Extrusion L-3298 Tested At 500°C/84.0 MPa</i>	123
<i>Figure B - 7 - Extrusion L-3284 Tested At 500°C/92.8 MPa</i>	124

<i>Figure B - 8 - Extrusion L-3296 Tested At 500°C/92.8 MPa</i>	125
<i>Figure B - 9 - Extrusion L-3297 Tested At 500°C/92.8 MPa</i>	126
<i>Figure B - 10 - Extrusion L-3298 Tested At 500°C/92.8 MPa</i>	127
<i>Figure B - 11 - Extrusion L-3284 Tested At 650°C/37.4 MPa</i>	128
<i>Figure B - 12 - Extrusion L-3296 Tested At 650°C/37.4 MPa</i>	129
<i>Figure B - 13 - Extrusion L-3297 Tested At 650°C/37.4 MPa</i>	130
<i>Figure B - 14 - Extrusion L-3298 Tested At 650°C/37.4 MPa</i>	131
<i>Figure B - 16 - Extrusion L-3284 Tested At 650°C/49.8 MPa</i>	133
<i>Figure B - 17 - Extrusion L-3296 Tested At 650°C/49.8 MPa</i>	134
<i>Figure B - 18 - Extrusion L-3297 Tested At 650°C/49.8 MPa</i>	135
<i>Figure B - 19 - Extrusion L-3298 Tested At 650°C/49.8 MPa</i>	136
<i>Figure B - 20 - Extrusion L-3296 Tested At 800°C/19.2 MPa</i>	137
<i>Figure B - 21 - Extrusion L-3298 Tested At 800°C/19.2 MPa</i>	138
<i>Figure B - 22 - Extrusion L-3296 Tested At 800°C/23.3 MPa</i>	139
<i>Figure B - 23 - Extrusion L-3298 Tested At 800°C/23.3 MPa</i>	140
<i>Figure B - 24 - Extrusion L-3284 Tested At 800°C/26.8 MPa</i>	141
<i>Figure B - 25 - Extrusion L-3296 Tested At 800°C/26.8 MPa</i>	142
<i>Figure B - 26 - Extrusion L-3298 Tested At 800°C/26.8 MPa</i>	143
<i>Figure B - 27 - Extrusion L-3284 Tested At 800°C/44.3 MPa</i>	144
<i>Figure B - 28 - Extrusion L-3297 Tested At 800°C/44.3 MPa</i>	145
<i>Figure C - 2 - Plate 5 Tested At 500°C/62.1 MPa</i>	150
<i>Figure C - 3 - Plate 6 Tested At 500°C/62.1 MPa</i>	151
<i>Figure C - 4 - Plate 8 Tested At 500°C/62.1 MPa</i>	152
<i>Figure C - 6 - Plate 5 Tested At 500°C/72.9 MPa</i>	154
<i>Figure C - 7 - Plate 6 Tested At 500°C/72.9 MPa</i>	155
<i>Figure C - 8 - Plate 8 Tested At 500°C/72.9 MPa</i>	156
<i>Figure C - 9 - Plate 3 Tested At 500°C/84.0 MPa</i>	157
<i>Figure C - 10 - Plate 5 Tested At 500°C/84.0 MPa</i>	158
<i>Figure C - 11 - Plate 6 Tested At 500°C/84.0 MPa</i>	159
<i>Figure C - 12 - Plate 8 Tested At 500°C/84.0 MPa</i>	160
<i>Figure C - 13 - Plate 3 Tested At 650°C/17.9 MPa</i>	161
<i>Figure C - 15 - Plate 6 Tested At 650°C/17.8 MPa</i>	163
<i>Figure C - 16 - Plate 8 Tested At 650°C/17.8 MPa</i>	164
<i>Figure C - 17 - Plate 3 Tested At 650°C/27.6 MPa</i>	165
<i>Figure C - 18 - Plate 5 Tested At 650°C/27.6 MPa</i>	166
<i>Figure C - 19 - Plate 6 Tested At 650°C/27.6 MPa</i>	167
<i>Figure C - 20 - Plate 8 Tested At 650°C/27.6 MPa</i>	168
<i>Figure C - 21 - Plate 3 Tested At 650°C/37.4 MPa</i>	169
<i>Figure C - 22 - Plate 5 Tested At 650°C/37.4 MPa</i>	170
<i>Figure C - 23 - Plate 6 Tested At 650°C/37.4 MPa</i>	171
<i>Figure C - 24 - Plate 8 Tested At 650°C/37.4 MPa</i>	172
<i>Figure C - 25 - Plate 3 Tested At 800°C/6.2 MPa</i>	173
<i>Figure C - 26 - Plate 5 Tested At 800°C/6.2 MPa</i>	174
<i>Figure C - 27 - Plate 6 Tested At 800°C/6.2 MPa</i>	175
<i>Figure C - 28 - Plate 8 Tested At 800°C/6.2 MPa</i>	176
<i>Figure C - 29 - Plate 3 Tested At 800°C/10.4 MPa</i>	177
<i>Figure C - 30 - Plate 5 Tested At 800°C/10.4 MPa</i>	178
<i>Figure C - 31 - Plate 6 Tested At 800°C/10.4 MPa</i>	179
<i>Figure C - 32 - Plate 8 Tested At 800°C/10.4 MPa</i>	180
<i>Figure C - 33 - Plate 3 Tested At 800°C/14.6 MPa</i>	181
<i>Figure C - 34 - Plate 5 Tested At 800°C/14.6 MPa</i>	182
<i>Figure C - 35 - Plate 6 Tested At 800°C/14.6 MPa</i>	183

<i>Figure C - 36 - Plate 8 Tested At 800°C/14.6 MPa</i>	<u>184</u>
<i>Figure D - 1 - Cu-8 Cr-4 Nb Sample 1-1 LCF Tested At Room Temperature / 2.0% Total Strain</i>	<u>186</u>
<i>Figure D - 2 - Cu-8 Cr-4 Nb Sample 6-2 LCF Tested At Room Temperature / 2.0% Total Strain</i>	<u>187</u>
<i>Figure D - 3 - Cu-8 Cr-4 Nb Sample 1-5 LCF Tested At 538°C (1000°F) / 0.7% Total Strain</i>	<u>188</u>
<i>Figure D - 4 - Cu-8 Cr-4 Nb Sample 7-4 LCF Tested At 538°C (1000°F) / 0.7% Total Strain</i>	<u>189</u>
<i>Figure D - 5 - Cu-8 Cr-4 Nb Sample 6-4 LCF Tested At 538°C (1000°F) / 1.2% Total Strain</i>	<u>190</u>
<i>Figure D - 6 - Cu-8 Cr-4 Nb Sample 7-1 LCF Tested At 538°C (1000°F) / 1.2% Total Strain</i>	<u>191</u>
<i>Figure D - 7 - Cu-8 Cr-4 Nb Sample 1-2 LCF Tested At 650°C (1200°F) / 0.7% Total Strain</i>	<u>192</u>
<i>Figure D - 8 - Cu-8 Cr-4 Nb Sample 7-3 LCF Tested At 650°C (1200°F) / 0.7% Total Strain</i>	<u>193</u>
<i>Figure D - 9 - Cu-8 Cr-4 Nb Sample 1-4 LCF Tested At 650°C (1200°F) / 1.2% Total Strain</i>	<u>194</u>
<i>Figure D - 10 - Cu-8 Cr-4 Nb Sample 6-1 LCF Tested At 650°C (1200°F) / 1.2% Total Strain</i>	<u>195</u>

Table Of Tables

<i>Table 1a - Cu-8 Cr-4 Nb Creep Test Matrix</i>	5
<i>Table 1b - Cu-4 Cr-2 Nb Creep Test Matrix</i>	6
<i>Table 1c - NARloy-Z Creep Test Matrix</i>	7
<i>Table 2 - Chemistries Of Cu-4 Cr-2 Nb, Cu-8 Cr-4 Nb and NARloy-Z Samples</i>	9
<i>Table 3 - Densities Of Cu, Cu-Cr-Nb Alloys and NARloy-Z</i>	11
<i>Table 4 - Lattice Parameters Of Extracted Precipitates</i>	12
<i>Table 5 - Chemical Analysis Of Precipitates and Matrix</i>	13
<i>Table 6 - Creep Model Coefficients</i>	27
<i>Table -7 - 95% Confidence Minimum Predicted Stresses For 1, 10 and 100 Hour Creep Lives</i>	31
<i>Table 8 - Average Thermal Properties Of Cu-8 Cr-4 Nb</i>	33
<i>Table 9 - Thermal Properties Of Cu-4 Cr-2 Nb</i>	36
<i>Table 10 - Low Cycle Fatigue Results</i>	39
<i>Table A - 1 Results of Cu-8 Cr-4 Nb Creep Testing</i>	56
<i>Table B - 1 Results of Cu-4 Cr-2 Nb Creep Testing</i>	115
<i>Table C - 1 Results of NARloy-Z Creep Testing</i>	146

Abstract

A series of creep tests were conducted on Cu-8 Cr-4 Nb (Cu-8 at.% Cr-4 at.% Nb), Cu-4 Cr-2 Nb (Cu-4 at.% Cr-2 at.% Nb), and NARloy-Z (Cu-3 wt.% Ag-0.5 wt.% Zr) samples to determine their creep properties. In addition, a limited number of low cycle fatigue and thermal conductivity tests were conducted.

The Cu-Cr-Nb alloys showed a clear advantage in creep life and sustainable load over the currently used NARloy-Z. Increases in life at a given stress were between 100% and 250% greater for the Cu-Cr-Nb alloys depending on the stress and temperature. For a given life, the Cu-Cr-Nb alloys could support a stress between 60% and 160% greater than NARloy-Z.

Low cycle fatigue lives of the Cu-8 Cr-4 Nb alloy were equivalent to NARloy-Z at room temperature. At elevated temperatures (538°C and 650°C), the fatigue lives were 50% to 200% longer than NARloy-Z samples tested at 538°C.

The thermal conductivities of the Cu-Cr-Nb alloys remained high, but were lower than NARloy-Z and pure Cu. The Cu-Cr-Nb thermal conductivities were between 72% and 96% that of pure Cu with the Cu-4 Cr-2 Nb alloy having a significant advantage in thermal conductivity over Cu-8 Cr-4 Nb. In comparison, stainless steels with equivalent strengths would have thermal conductivities less than 25% the thermal conductivity of pure Cu.

The combined results indicate that the Cu-Cr-Nb alloys offer an attractive alternative to current high temperature Cu-based alloys such as NARloy-Z.

Introduction

A series of Cu-Cr-Nb alloys produced by Chill Block Melt Spinning (CBMS) was examined previously (1). The results strongly indicated that the alloys possessed exceptional high temperature strength and creep resistance while maintaining good electrical and thermal conductivities. Based on the creep properties and electrical conductivities, the decision was made to scale-up the Cu - 8 at. % Cr - 4 at. % Nb (Cu- 8 Cr-4 Nb) alloy for extensive mechanical testing. In addition, the thermal conductivity of the alloy would be directly tested. For making the alloy in large quantities, CBMS was replaced with conventional argon gas atomization to produce powder. Based on work by Anderson et al. (2, 3), it was felt that there was a chance to increase the thermal conductivity significantly with a minimal reduction in strength. Therefore, as a higher thermal conductivity option, a Cu - 4 at. % Cr - 2 at.% Nb (Cu-4 Cr-2 Nb) was also examined.

The Cu-Cr-Nb alloys derive their strength from the very stable intermetallic phase Cr_2Nb . This phase is stable in solid and liquid Cu to temperatures above 1600°C . The constituents, Cr and Nb, have minimal solubilities in solid Cu, limiting the decrease in conductivity. The high stability of the Cr_2Nb also contributes to the microstructural stability of the alloy during subsequent elevated temperature exposures.

NARloy-Z (Cu - 3 wt.% Ag - 0.5 wt.% Zr) derives its strengthening from a combination of solid solution and precipitation strengthening by Ag and precipitation strengthening by the Cu_xZr ($x=4$ or 5) phase. The Cu_xZr phase is also important in raising the temperature at which the alloy loses the benefits of work hardening.

Experimental Procedure

The testing focused primarily on creep resistance. In addition, the thermal conductivity and low cycle fatigue behavior of the Cu-Cr-Nb alloys were examined less extensively.

Production Of Material

The Cu-Cr-Nb alloys were purchased from Special Metals Corporation as metal powder. The powder was sieved to -150 mesh (less than 106 μm), but the average powder particle size was approximately 45 μm . The powder was canned in 51.4 mm (2 inch) diameter 1020 carbon steel cans. The cans were evacuated and sealed. The canned powder was extruded at 857°C (1575°F) using a round die which produced a 16:1 reduction in area. The result was a round bar nominally 1 meter (39 inches) long with a diameter of 12.7 mm (0.5 inches). The usable Cu-Cr-Nb alloy core was typically 9.53 mm (0.375 inches) in diameter.

NARloy-Z was supplied to NASA LeRC by Don Ulmer of Rocketdyne in the form of a 191 mm x 305 mm x 37 mm (7" x 12" x 1.5") plate in the as-hot rolled condition. The plate was cut into several smaller pieces for ease of handling. The smaller pieces were solution heat treated at 900°C (1650°F) for 1 hour and water quenched. The samples were aged at 482°C (900°F) for 3 hours and air cooled. All samples were placed in Sen/Pak¹ heat treat envelopes that were filled with Ar to prevent oxidation of the surfaces during the heat treatment steps.

Alloy Density Measurement

Samples of the alloys and pure copper were weighed using a Ainsworth AA-160 balance. To determine the volume and density of the samples, the volume of the samples was determined using a Micromeritics Accupyc 1330 gas pycnometer. High purity helium gas was used as the working gas. The unit determined the volume of the samples and, from the provided weight, the volume. The unit was purged 20 times prior to taking data. Fifty repetitions of measuring the volume of the samples were taken automatically by the pycnometer. Following the runs, the unit averaged the fifty density measurements to calculate the density of the samples.

¹ Sen/Pak is the registered trademark of the Sentry Company, Foxboro, MA

Identification and Analysis of Precipitates

Previous work by Kuo (4) indicated that up to a quarter of the Cr atoms in the very similar Cr_2Ta phase could be substituted for by Cu. The stability of the hexagonal phase of Cr_2Nb in melt spun ribbons (1, 5) indicated the possibility that the same was occurring in Cr_2Nb .

To determine if Cu was substituting for Cr in material produced from atomized powder, precipitates were extracted from the Cu matrix. A 1 g ammonium sulfate-1 g citric acid-100 ml H_2O electrolyte solution was used to electrolytically dissolve away the Cu matrix. The precipitates were collected from the solution using a 0.1 μm filter paper.

The collected precipitates were analyzed using X-ray diffraction to determine the phases present and the lattice parameters. Following X-ray diffraction analysis, the precipitates and dissolved Cu matrix were chemically analyzed.

Creep Testing

The results of preliminary creep testing conducted at NASA LeRC have been reported elsewhere (6, 7). Only data on as-extruded material tested in a design level test matrix allowing for determination of confidence limits on the various tensile results will be presented in this final report.

The sample geometry used for creep testing appears in Figure 1. The subsize samples conform to ASTM standard E 8 (8). The sample used threaded ends to accommodate existing fixturing. The sample had a nominal 16.26 mm (0.640 inch) gauge length.

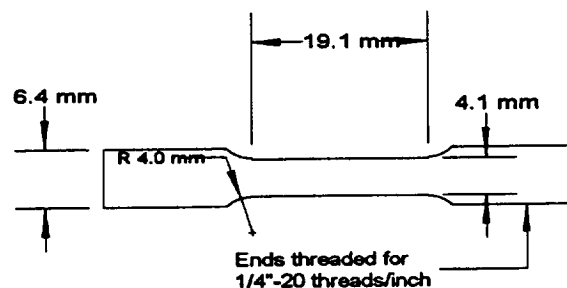


Figure 1 -
Creep Specimen Design

Creep testing was conducted in vacuum at temperatures between 500°C and 800°C. Based on previous work, a test matrix was designed to allow for accurate prediction of the creep life and creep rate of the alloys. Three stresses

were selected at each temperature to give nominal 30, 100 and 300 hour lives. The test matrices are given in Table 1. The column headings indicate the extrusion run or plate piece for each sample. Samples from the same column come from the same starting stock. Within the table the numbers represent the testing order of the samples. For the Cu-4 Cr-2 Nb extrusions, sufficient samples were not available from some bars to allow for testing the complete test matrix. In that case, the intermediate stress tests were not performed.

During the allocation of Cu-4 Cr-2 Nb samples, several samples were moved from lower temperatures to higher temperatures to accommodate the lower number of available samples. This allowed for a low-high stress / low-medium-high temperature with some medium stress data points. Unfortunately in the case of Cu-4 Cr-2 Nb, the spreadsheet did not recalculate the stresses correctly due to an error in the spreadsheet formula. As a result, some high temperature samples had a higher stress than intended. These differences are reflected in Table 1 and later in the design space. As will be discussed later, the higher stresses still produced valid results.

Select samples were examined using scanning electron microscopy (SEM). The general features of the surface were investigated, and precipitates and other features on the surface were examined to determine if there was any correlation between the precipitates and failure sites.

Table 1a -
Cu-8 Cr-4 Nb Creep Test Matrix

		Extrusion					
Temperature (°C)	Stress (MPa)	L-3097	L-3104	L-3105	L-3106	L-3107	L-3108
500	92.8	19	20	18	41	3	50
	84.0	5	43	25	45	49	6
	72.9	10	47	39	36	29	28
650	49.8	27	17	4	37	23	2
	44.3	38	26	12	7	1	13
	37.4	46	24	40	48	35	11
800	26.8	34	44	33	21	53	22
	23.3	32	14	30	52	8	42
	19.2	54	9	31	51	15	16

Table 1b -
Cu-4 Cr-2 Nb Creep Test Matrix

Temperature (°C)	Stress (MPa)	Extrusion			
		L-3284	L-3296	L-3297	L-3298
500	92.8	29	7	6	9
	84.0		17	15	4
	72.9	8	30	23	1
650	49.8	27	19	20	5
	44.3		11		3
	37.4	29	25	13	16
800	44.3	10		12	
	26.8	14	22		28
	23.3		21		18
	19.2		2		26

Table 1c -
NARloy-Z Creep Test Matrix

Temperature (°C)	Stress (MPa)	Plate			
		3	5	6	8
500	84.0	16	18	7	30
	72.9	15	21	26	13
	62.1	24	9	29	2
650	37.4	33	8	10	32
	27.6	12	19	5	25
	17.8	35	34	3	6
800	14.6	1	27	23	11
	10.4	28	22	20	17
	6.2	36	14	31	4

Thermal Conductivity Testing

A limited number of thermal conductivity tests were conducted on the Cu-8 Cr-4 Nb and Cu-4 Cr-2 Nb alloys. For NARloy-Z, design level data were already available (9). For the Cu-8 Cr-4 Nb alloy, one sample from each of the six extrusions were sent to the Thermophysical Properties Research Laboratory (TPRL) at Purdue University. Only one Cu-4 Cr-2 Nb sample was tested at TPRL.

Thermal conductivity testing was conducted by the laser flash method. The method calculates the thermal conductivity of the material using the formula

$$\lambda_{(T)} = \rho_{RT} \alpha_{(T)} C_{P(T)} \quad [1]$$

where $\lambda_{(T)}$ is the thermal conductivity at temperature T (W/mK), ρ_{RT} is the room temperature bulk density (g/cm³), $\alpha_{(T)}$ is the thermal diffusivity at temperature T (cm²/s) and $c_{p(T)}$ is the heat capacity at temperature T (J/gK).

The heat capacity was measured using a Perkins-Elmer DSC-2 Differential Scanning Calorimeter. Sapphire was used as the standard. The thermal diffusivity was measured using an apparatus consisting of a Korad 2 laser to irradiate the sample and an infrared detector to record the temperature rise on the opposite face. The diffusivity was calculated from the time it took the sample to reach half its maximum temperature rise ($t_{1/2}$) using the formula

$$\alpha_{(T)} = \frac{WL^2}{t_{1/2}} \quad [2]$$

Here L is the thickness of the sample, and W is a dimensionless parameter specific to the individual machine and specimen relating to the heat loss from the specimen. In the ideal case of no heat loss, the value of W is 0.139. The maximum temperature rise was typically less than 1°C. For elevated temperature diffusivities, the sample was placed in an evacuated bell jar and heated using a Ta heater to the desired temperature prior to testing.

Low Cycle Fatigue

Low cycle fatigue (LCF) testing of the Cu-8 Cr-4 Nb alloy was conducted on an older batch of material processed using the same conditions as the material produced for the creep tests. Based on a comparison of the creep properties of the prior and current materials, there were no discernible differences between the two batches of materials.

LCF testing was performed at room temperature, 538°C and 650°C (1000°F and 1200°F). Fully-reversed, strain-controlled fatigue tests were performed using a triangular waveform at a constant strain rate of 0.12/min (0.002/s). An 89 kN (20,000 lbf) MTS hydraulic test machine fitted with an environmental chamber was used. A 1.27 cm (0.5 inch) gauge length extensometer was attached to the specimen for strain measurement and control. For the elevated temperature tests, the specimens were heated using an inductively heated SiC susceptor. A thermocouple inserted from the bottom between the susceptor and the specimen was used to monitor and control the temperature. Oxygen gettered Ar gas was flowed over the sample at a rate of 4 l/min (0.14 SCFM) to prevent oxidation of the sample during testing.

Results

Alloy Chemistries

The actual chemistries of the Cu-4 Cr-2 Nb, Cu-8 Cr-4 Nb and NARloy-Z alloys used in the testing are presented in Table 2. In addition to the composition of the consolidated material, the chemistries supplied by Special Metals for the powders is also presented.

The critical need for the Cu-Cr-Nb alloys is to maintain an atomic Cr to Nb ratio of 2 or slightly greater. By maintaining a Cr-rich Cr_2Nb precipitate hydrogen embrittlement can be controlled or eliminated (10). Table 2 also lists the atomic Cr to Nb ratio.

Table 2 -
Chemistries Of Cu-4 Cr-2 Nb, Cu-8 Cr-4 Nb and NARloy-Z Samples

Alloy	Ag	Cr	Cu	Nb	O*	Zr	Cr:Nb
Cu-4 Cr-2 Nb — Powder [†]		3.27	Bal.	2.92	251		2.00
Cu-4 Cr-2 Nb		3.8	Bal.	3.6	N.A.		1.89
Cu-8 Cr-4 Nb — Powder [†]		6.45	Bal.	5.49	455		2.10
Cu-8 Cr-4 Nb		6.5	Bal.	5.5	640		2.11
NARloy-Z	3.0		Bal.		N.A.	0.5	

All chemistries in weight percent

*O is in ppm by weight

[†]Chemistry supplied by Special Metals

Special Metals Corporation also supplied an analysis of the powder sizes for the Cu-4 Cr-2 Nb and Cu-8 Cr-4 Nb powders. The powder size distributions are supplied in Figure 2. Over 25% of both powders were -500 mesh and 75% of both powders were -200 mesh.

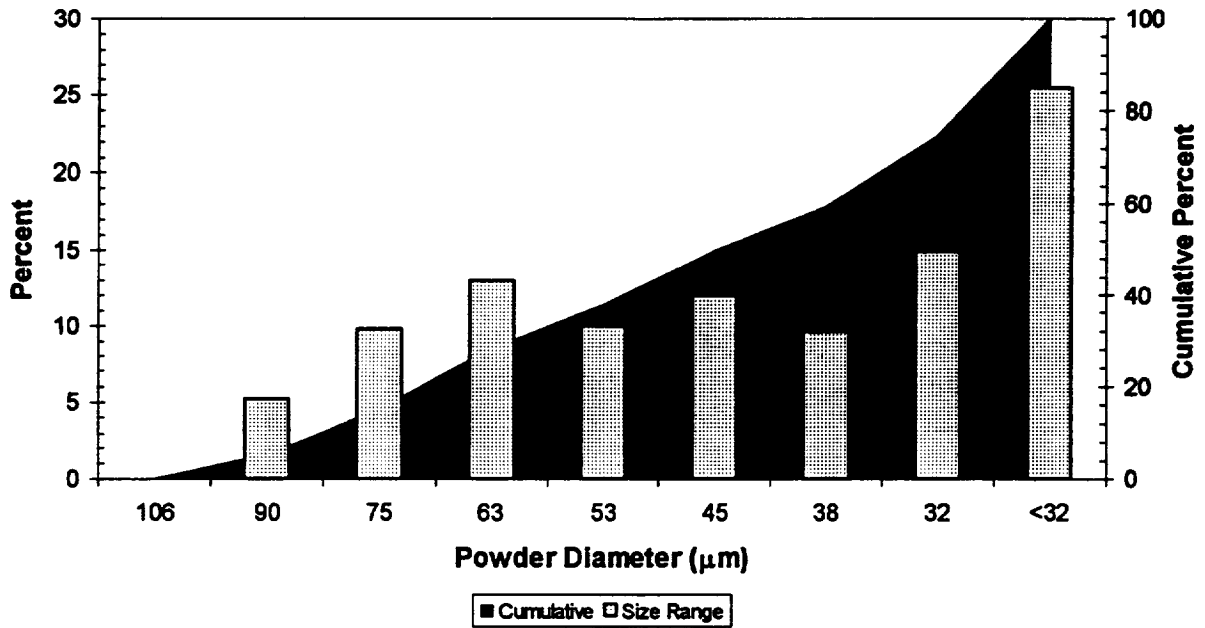


Figure 2a -
Size Distribution Of Cu-4 Cr-2 Nb Powder

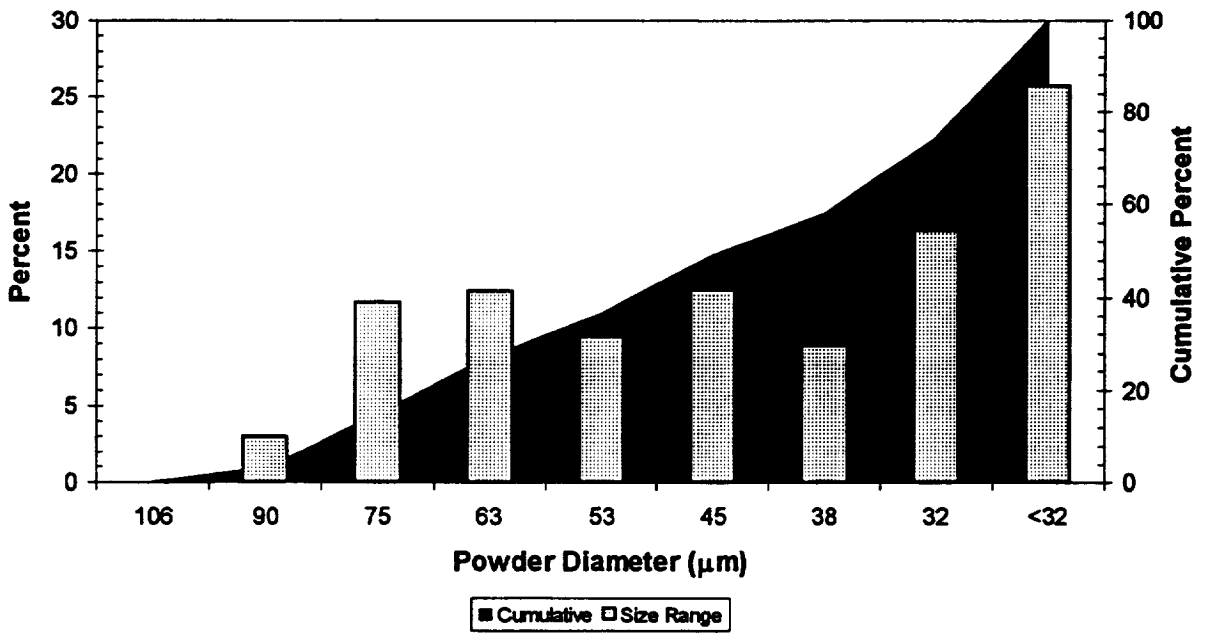


Figure 2b -
Size Distribution Of Cu-8 Cr-4 Nb Powder

Alloy Densities

The densities of the alloys are dependent on the actual chemistries of the alloys. The calculated density of Cr₂Nb is 7.657 compared to 8.94 g/cm³ for pure Cu (11). Therefore the density of the Cu-Cr-Nb alloys decreases as the amount of Cr and Nb and hence the volume fraction of Cr₂Nb increases. For the studied compositions, the densities are listed in Table 3 and graphically compared in Figure 3. Table 3 also includes the accepted values for Cu and NARloy-Z.

Table 3 -
Densities Of Cu, Cu-Cr-Nb Alloys and NARloy-Z

Sample	Experimental Density (g/cm ³)	Accepted Density (g/cm ³)
Cu	8.920	8.94 (Ref. 11)
Cu-4 Cr-2 Nb	8.850	
Cu-8 Cr-4 Nb	8.756	
NARloy-Z	9.130	9.131 (Ref. 9)

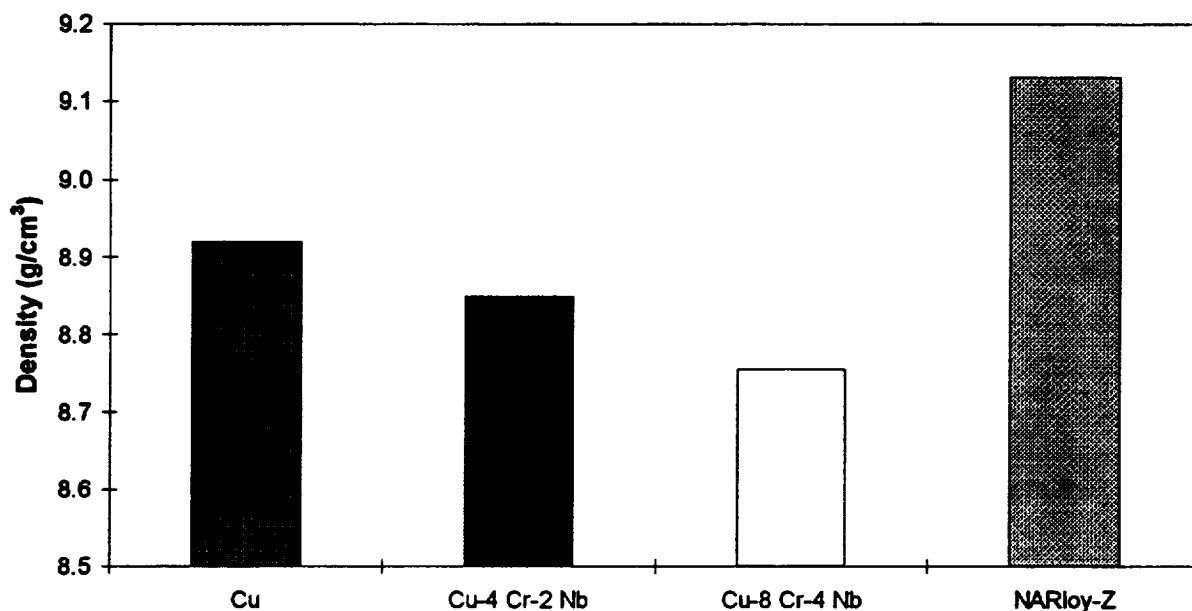


Figure 3 -
Comparison Of Alloy Densities

Precipitate Analysis

The material extracted from the Cu-8 Cr-4 Nb alloy was identified by X-ray diffraction as consisting of a Cu solid solution, FCC Cr₂Nb, and a Cr solid solution. The Cu came from undissolved matrix incorporated into the sample. The lattice parameters of the phases are presented in Table 4. Because only one small peak was observed for the Cr, no lattice parameter is given. The results showed no change in the lattice parameters from the values for the pure materials.

Table 4 -
Lattice Parameters Of Extracted Precipitates

Precipitate	Lattice Parameter (nm)
Cr ₂ Nb	0.6993 ± 0.0001
Cu (ss)	0.3617 ± 0.0001
Cr (ss)	Present (1 peak)

The results of the chemical analysis of the precipitates are presented in Table 5. The matrix showed nothing but pure Cu. This supports the design work on the alloy and previous contentions that the matrix should be nearly pure Cu. The chemical analysis of the precipitates is complicated by the presence of unknown amounts of Cu and Cr precipitates. However, one can assume that the amount of elemental Cr is small (<5%). The theoretical values for $Cr_{1.5}Cu_{0.5}Nb$ are given in Table 5. Assuming that Cu substitutes for Cr as shown by Kuo (4) for Cr_2Ta , the atomic ratio of Cr to Nb should shift to lower values. Looking at the measured Cr to Nb ratio on an atomic basis, the results fall within the stoichiometric limits for Cr_2Nb . This indicates that there was no significant substitution of Cu for Cr in the Cr_2Nb .

Table 5 -
Chemical Analysis Of Precipitates and Matrix

Element	Matrix (wt.% / at.%)	Precipitates (wt.% / at.%)	Theoretical $Cr_{1.5}Cu_{0.5}Nb$ (wt.% / at.%)
Cr	0 / 0	27.2 / 33.9	38.5 / 50.0
Cu	100 / 100	47.7 / 48.7	15.7 / 16.7
Nb	0 / 0	25.0 / 17.4	45.8 / 33.3
Cr : Nb	N/A	1.09 / 1.94	0.84 / 1.5

Creep Testing

The results for the creep tests were examined to determine four main parameters; time to 1% creep strain, rupture life, steady-state creep rate and elongation at failure. In addition, the times spent in first, second and third stage creep were determined. The 1% creep strain was chosen as a way to compare the Cu-Cr-Nb alloys to the NARloy-Z samples which had considerably different creep behavior under the testing conditions. The value of 1% was arbitrarily chosen as an amount greater than the first stage creep strain for most of the tests.

Cu-8 Cr-4 Nb

A typical creep curve for Cu-8 Cr-4 Nb is presented in Figure 4. The alloy typically has a very short third stage creep regime. The total creep elongation

of the sample is also fairly low. All the creep data and curves for the Cu-8 Cr-4 Nb alloy are presented in Appendix A.

A summary of the time to 1% creep strain is presented in Figure 5. Figure 6 shows the steady-state creep rates for Cu-8 Cr-4 Nb while Figure 7 presents the creep rupture lives. The creep elongation of Cu-8 Cr-4 Nb is displayed in Figure 8.

The time to 1% creep, steady-state creep rate and creep life follow a logarithmic dependency. Because of this, the geometric mean was used instead of the average. The geometric mean was calculated from the formula

$$\text{Geometric Mean} = 10^{\frac{\sum_{i=1}^n \log x}{n}} \quad [3]$$

where x is either the time or rate. For the elongation, the simple average was used. The mean is presented in each figure for easy comparison. The detailed analysis of the creep behavior used all data points.

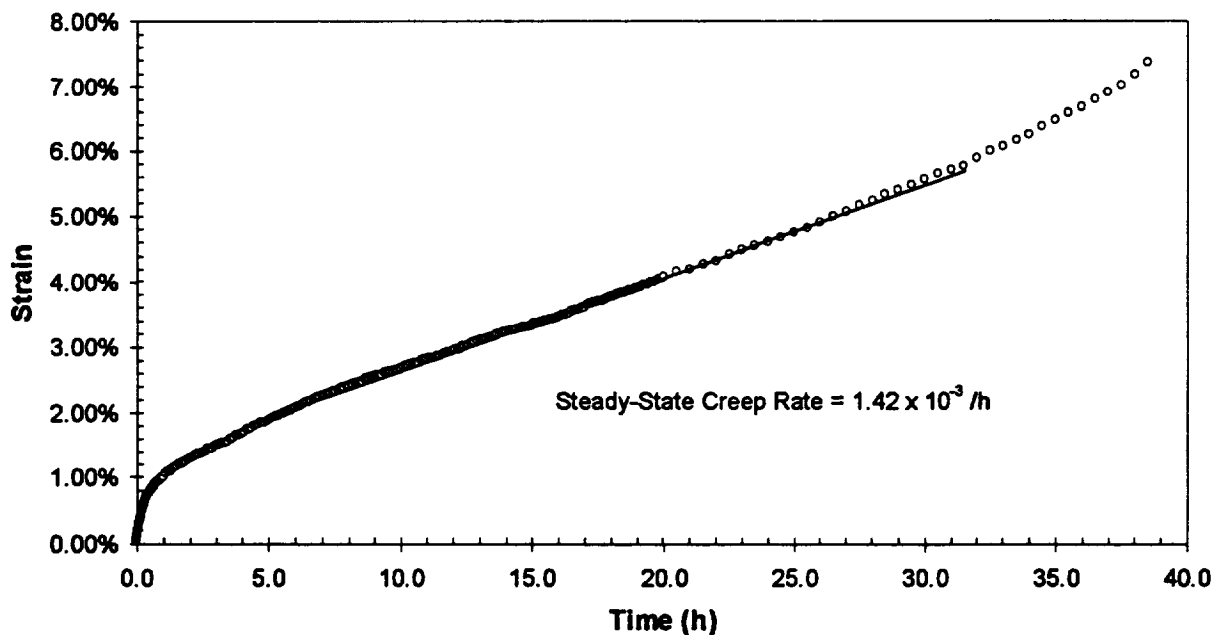


Figure 4 -
Typical Cu-8 Cr-4 Nb Creep Curve
(Extrusion L-3107 Tested At 800°C/19.2 MPa)

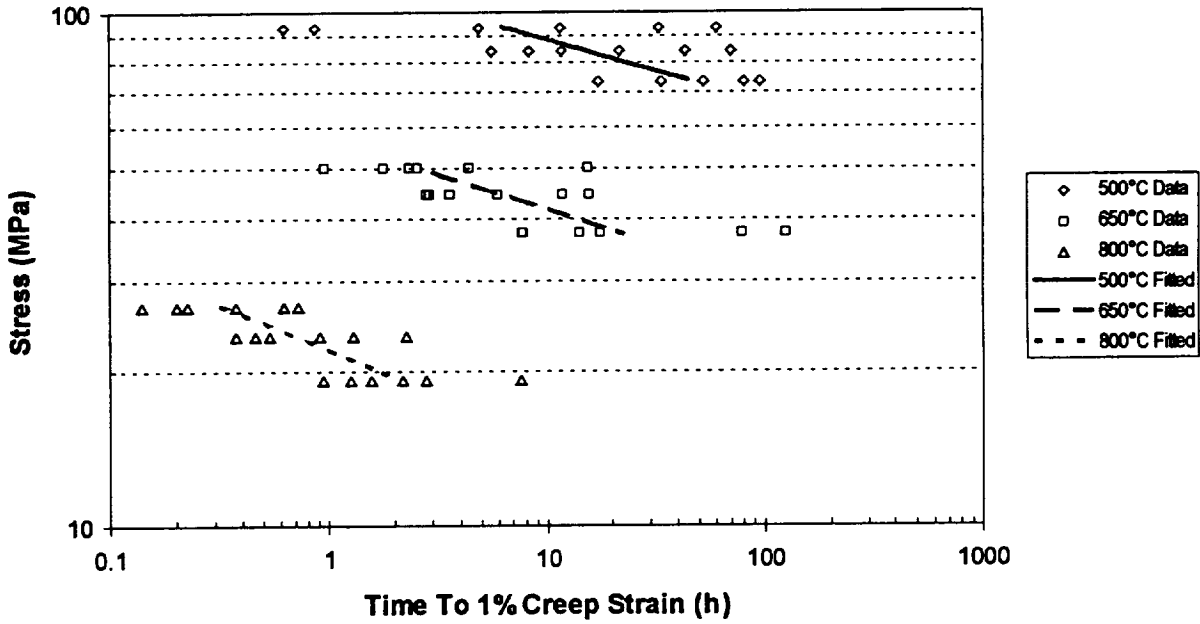


Figure 5 -
Times To 1% Creep Strain For Cu-8 Cr-4 Nb

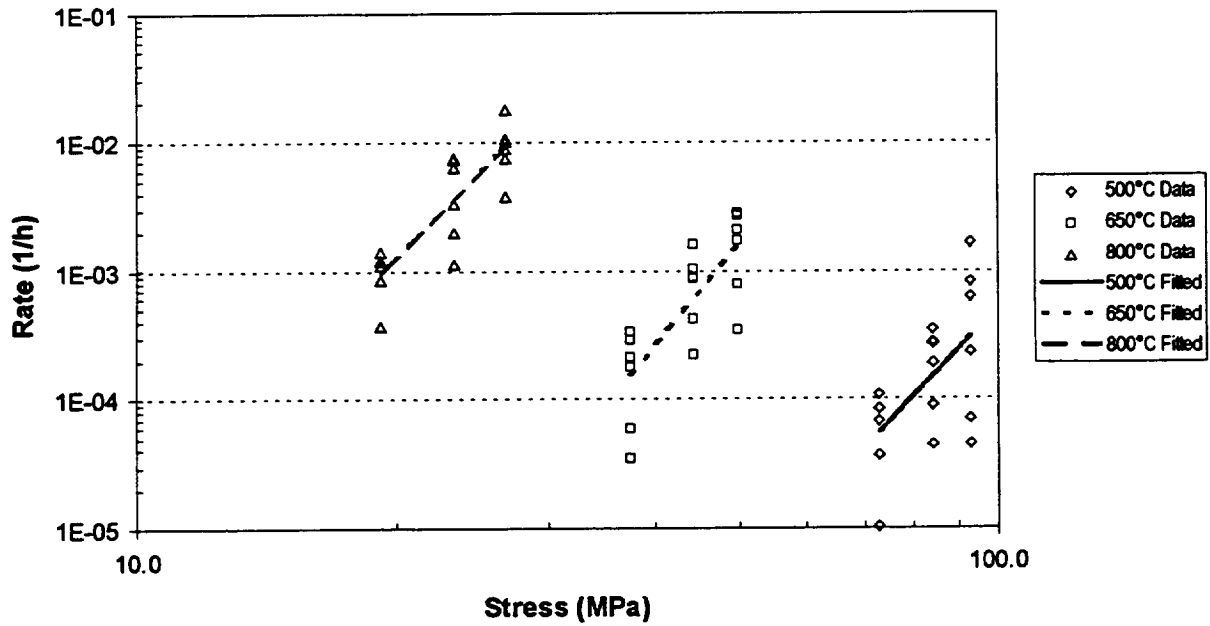


Figure 6 -
Steady-State Creep Rates Of Cu-8 Cr-4 Nb

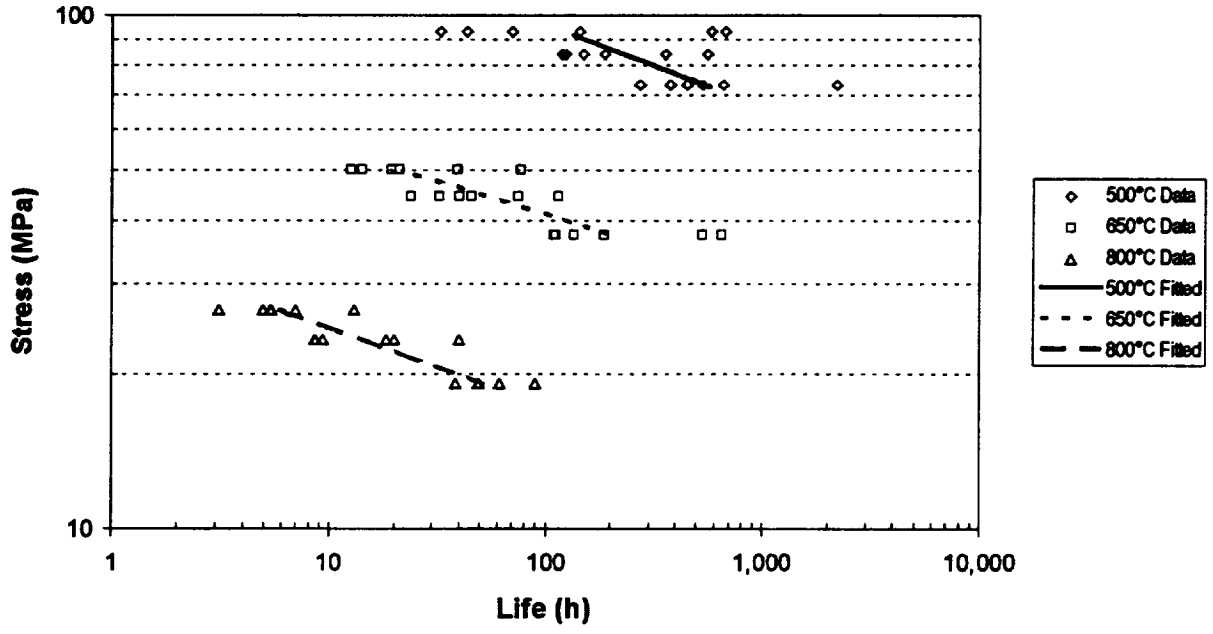


Figure 7 -
Creep Rupture Lives Of Cu-8 Cr-4 Nb

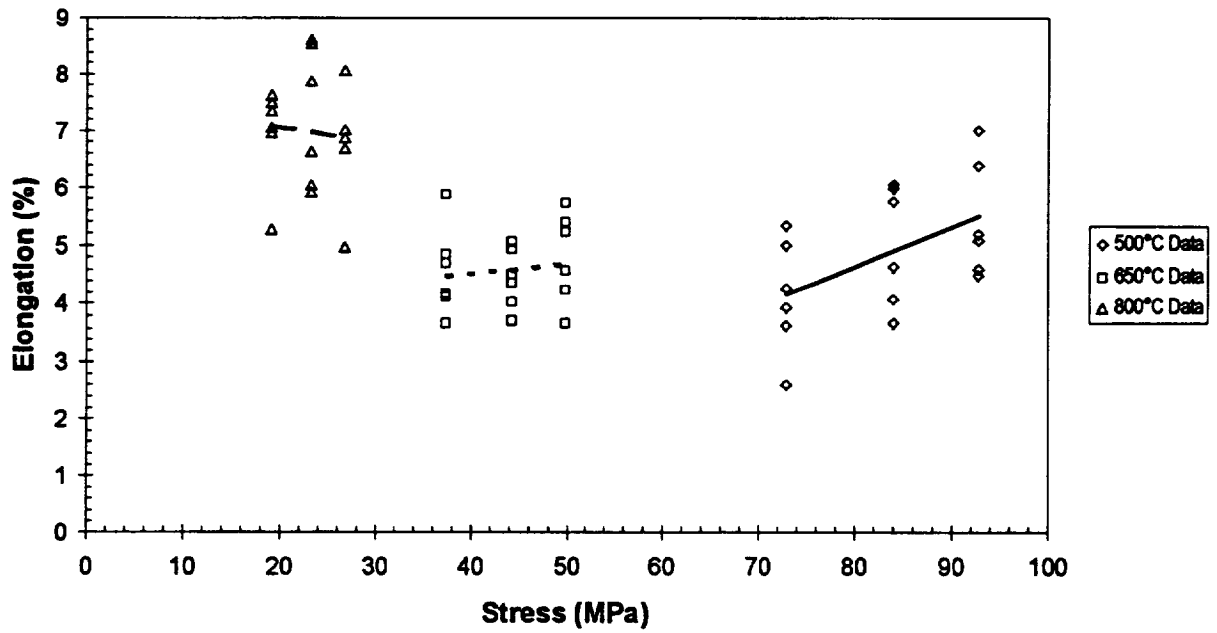


Figure 8 -
Creep Elongations Of Cu-8 Cr-4 Nb

Cu-4 Cr-2 Nb

A typical creep curve for Cu-4 Cr-2 Nb is presented in Figure 9. The alloy typically has a third stage creep regime in contrast to the Cu-8 Cr-4 Nb alloy. The creep elongations of the samples are higher than Cu-8 Cr-4 Nb. All the creep curves for the Cu-4 Cr-2 Nb alloy are presented in Appendix B.

A summary of the time to 1% creep strain is presented in Figure 10. As with the Cu-8 Cr-4 Nb results, the geometric mean of the data is plotted in Figure 10. Figure 11 shows the steady-state creep rates for Cu-4 Cr-2 Nb while Figure 12 presents the creep rupture life of Cu-4 Cr-2 Nb. The creep elongations for Cu-4 Cr-2 Nb are given in Figure 13.

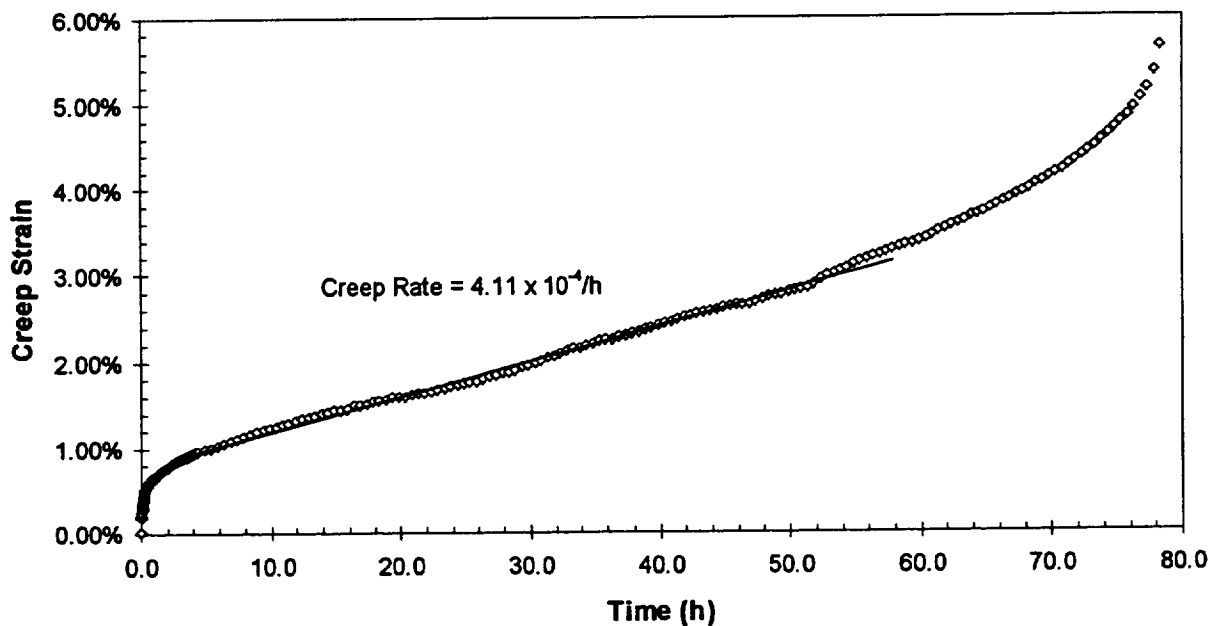


Figure 9 -
Typical Cu-4 Cr-2 Nb Creep Curve
(Extrusion L-3298 Tested At 650°C/44.3 MPa)

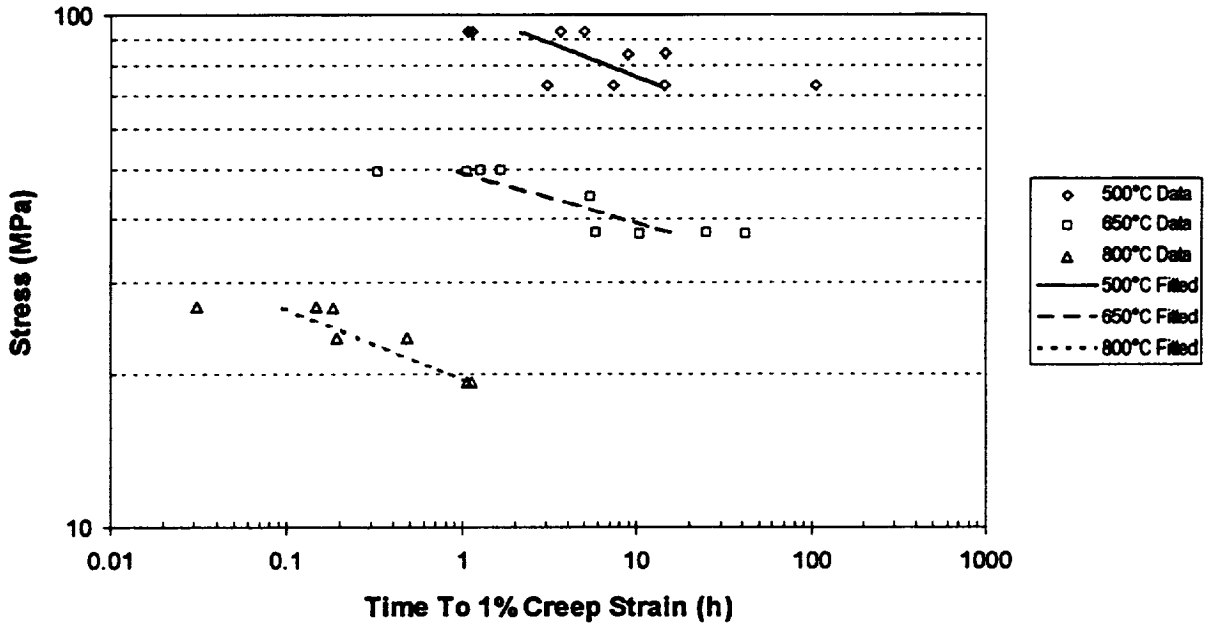


Figure 10 -
Times To 1% Creep Strain Cu-4 Cr-2 Nb

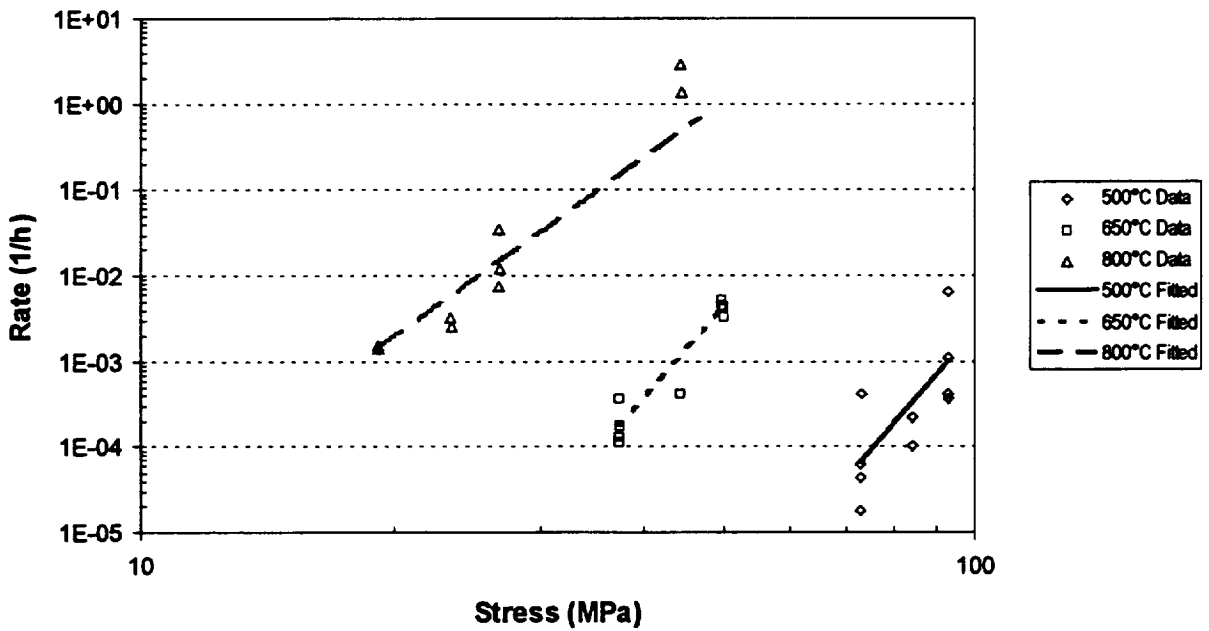


Figure 11 -
Steady-State Creep Rates Of Cu-4 Cr-2 Nb

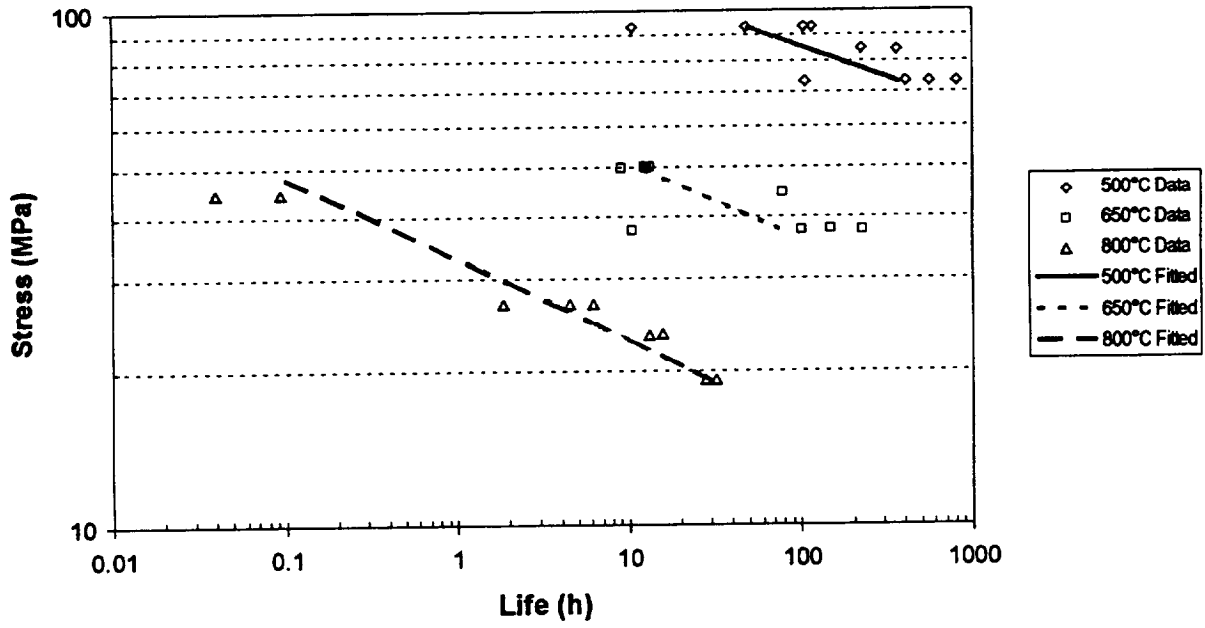


Figure 12 -
Creep Rupture Lives Of Cu-4 Cr-2 Nb

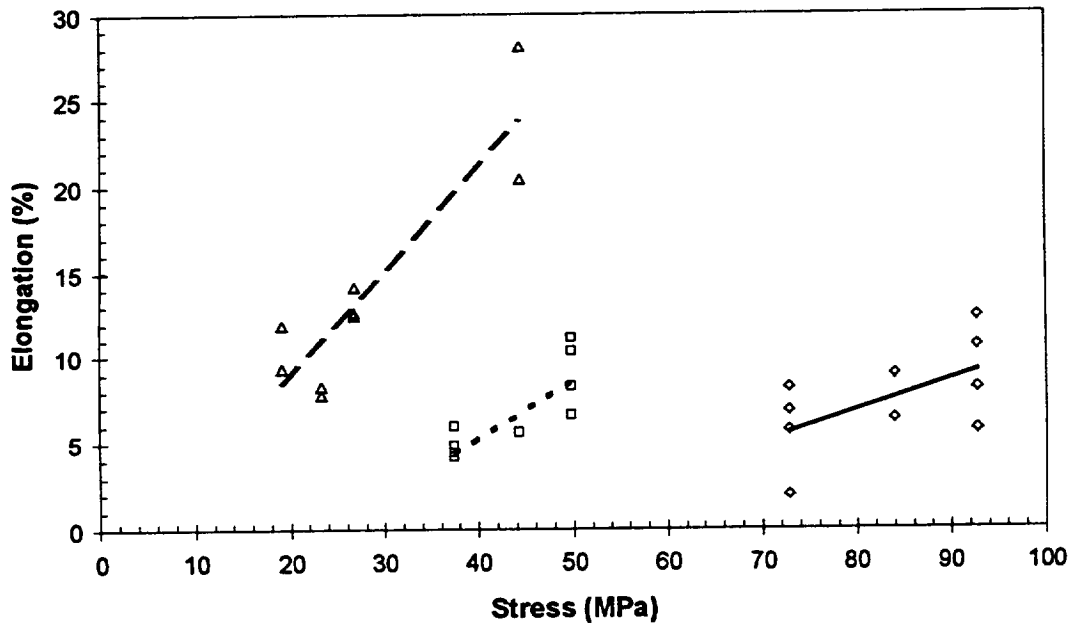


Figure 13 -
Average Creep Elongation Of Cu-4 Cr-2 Nb

NARloy-Z

NARloy-Z exhibited a very different behavior from the Cu-Cr-Nb alloys. From the previously available data (9), it was known that the alloy needed lower stresses over the temperature range used in the testing to achieve similar lives. The test matrix was modified to reflect this. What was not expected was the sometimes very high total creep elongations and extended third stage creep observed. Figure 14 shows a typical creep curve. In addition to much greater creep elongations, the alloy tends to exhibit a relatively short second stage creep. Appendix C contains all of the creep curves.

A summary of the time to 1% creep strain is presented in Figure 15. Figure 16 shows the steady-state creep rates for NARloy-Z. The creep rupture lives of NARloy-Z is presented in Figure 17. Figure 18 gives the creep elongation.

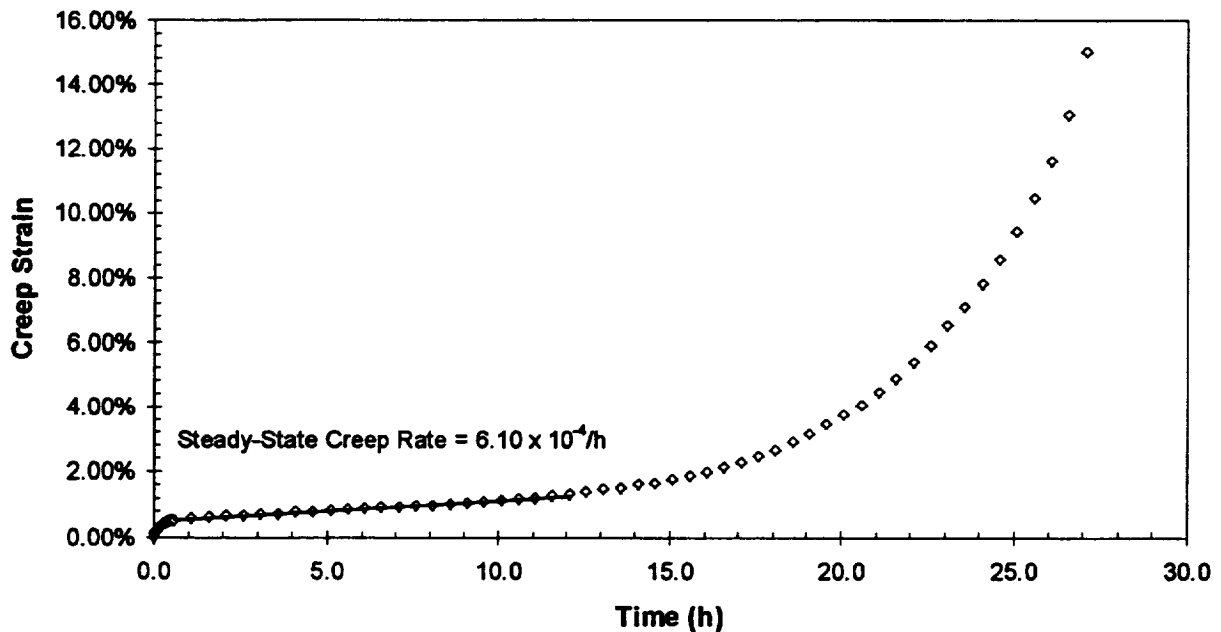


Figure 14 -
Typical NARloy-Z Creep Curve
(Plate 3 Tested At 650°C/27.6 MPa)

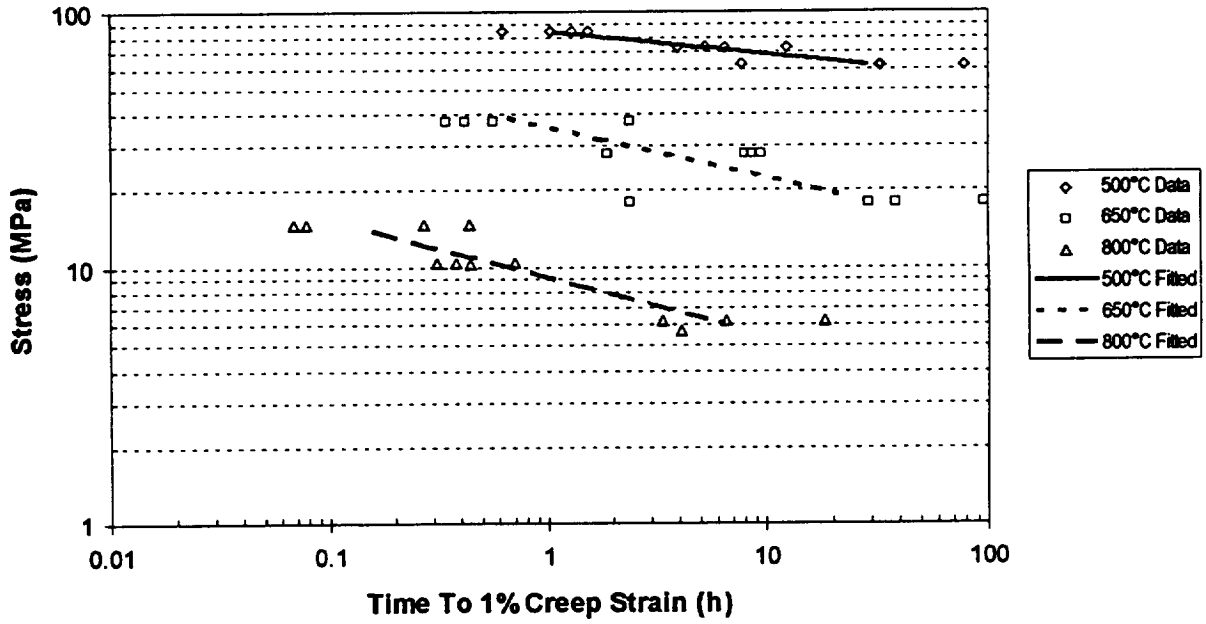


Figure 15 -
Times To 1% Creep Strain For NARloy-Z

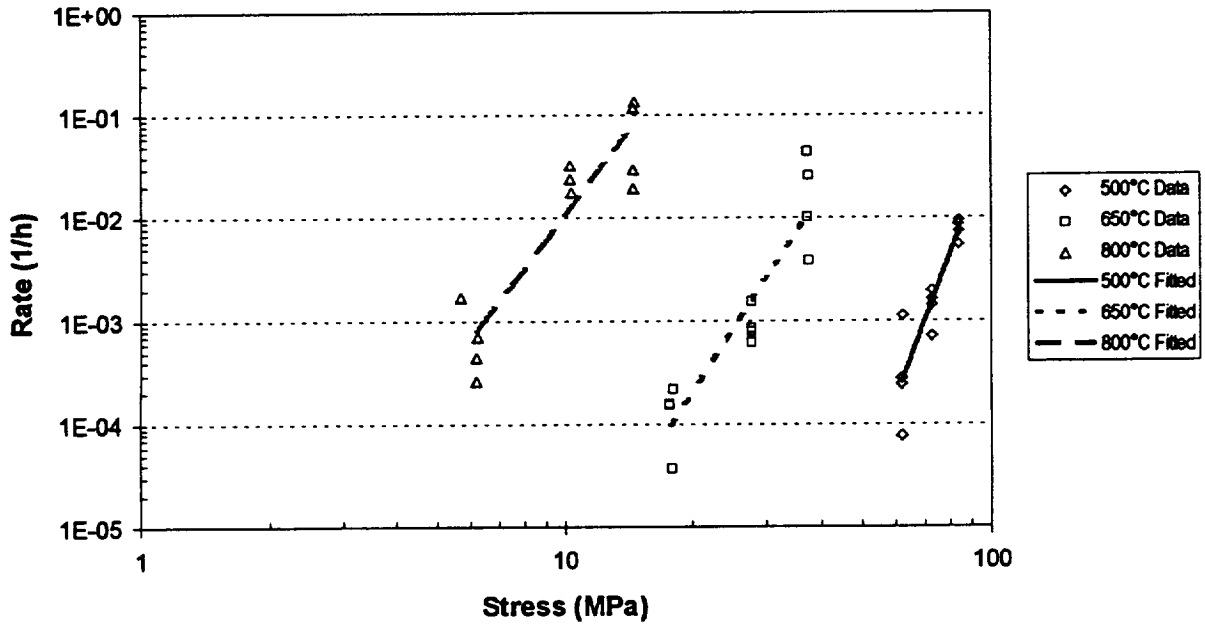


Figure 16 -
Steady-State Creep Rates Of NARloy-Z

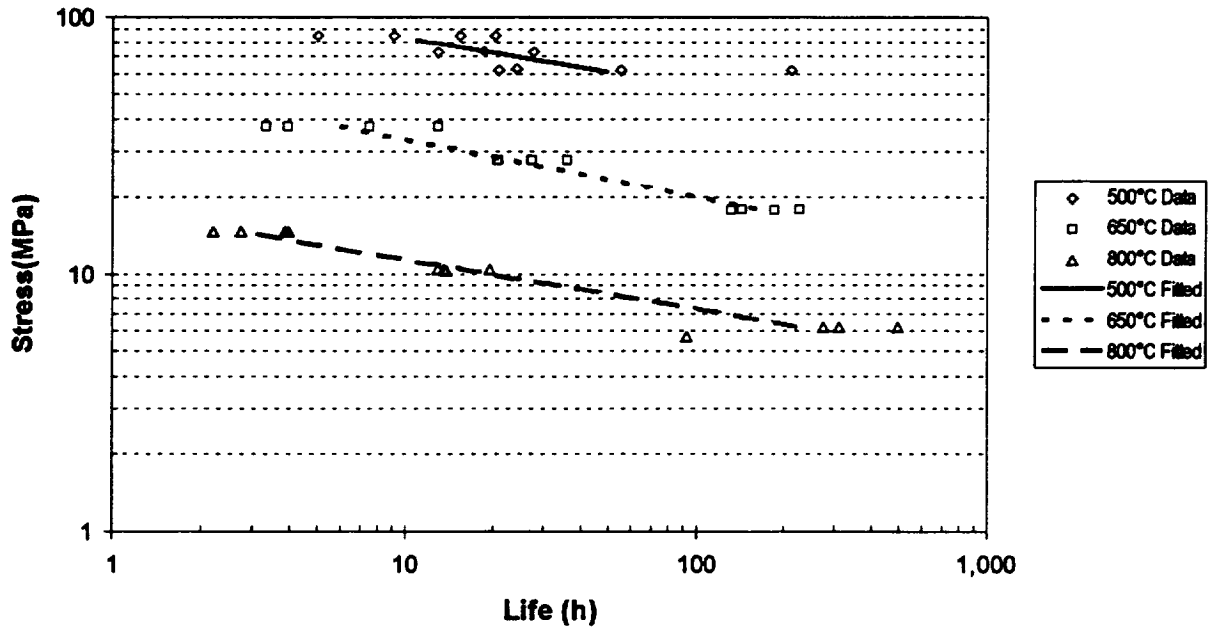


Figure 17 -
Creep Rupture Lives Of NARloy-Z

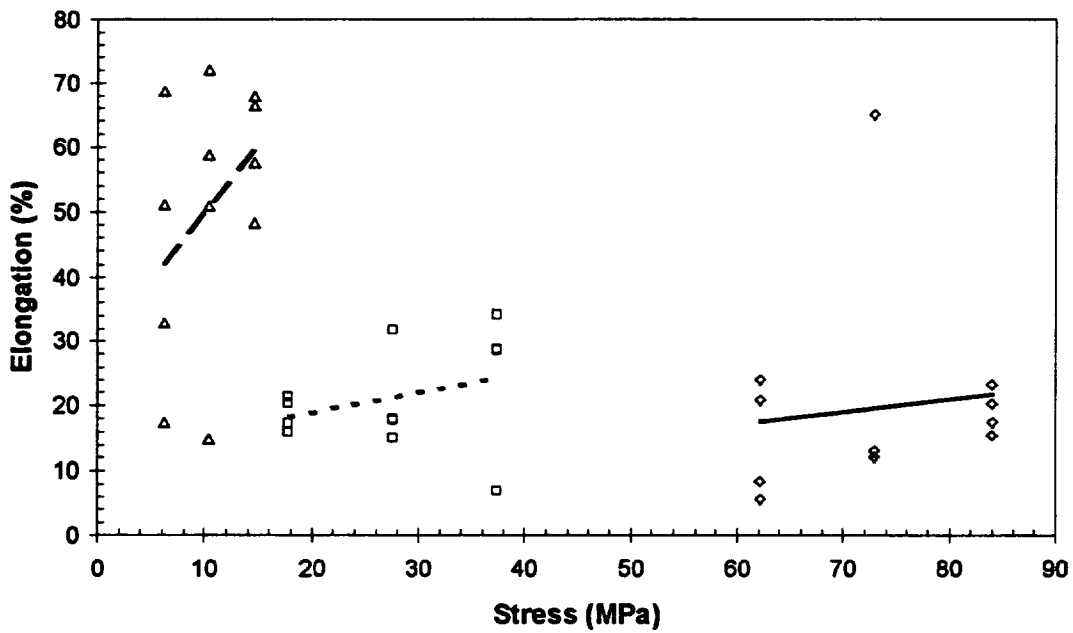


Figure 18 -
Creep Elongations Of NARloy-Z

Creep Fracture Surfaces

The creep fracture surfaces were examined using a Hitachi Field Emission SEM and a JEOL SEM. Typical fracture surfaces for the Cu-Cr-Nb and NARloy-Z creep specimens are shown in Figure 19. The Cu-Cr-Nb samples show a very rough surface with many faceted precipitates visible (Figure 19b). The NARloy-Z samples show a much smoother surface with little evidence of precipitates on the surfaces. The NARloy-Z also shows more striations on the fracture surface.

From examination of the fracture surfaces it was evident that the NARloy-Z samples failed by microvoid coalescence and growth. Large "pipes" could be seen extending deep into the material from the surfaces. Large, sharp ridges were also observed.

The mechanism for the Cu-Cr-Nb alloy failure is not as easily distinguished, but careful examination reveals that the samples failed by microvoid coalescence and growth. In this case, the precipitates appeared to limit the growth of the voids. Hence the scale of the dimples was much smaller than that for NARloy-Z.

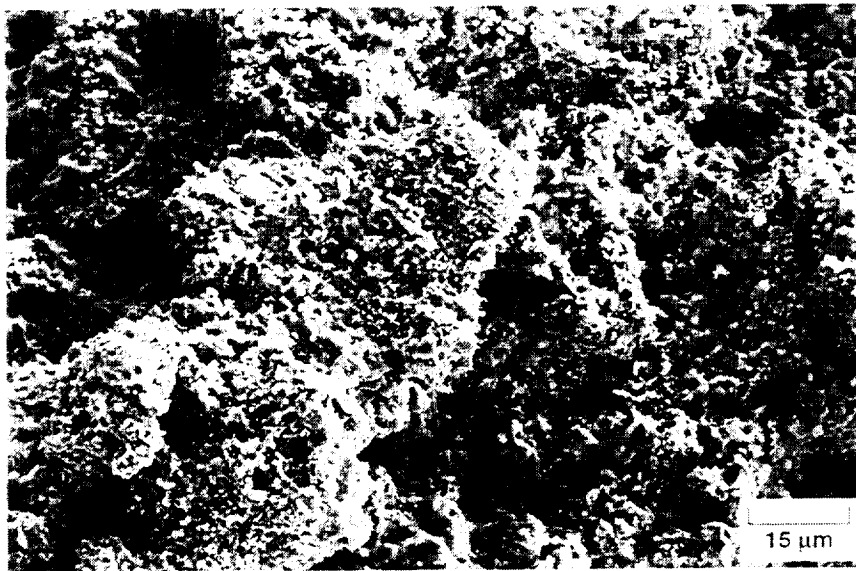


Figure 19a -
Typical Fracture Surface Of Cu-8 Cr-4 Nb Creep Samples
(Extrusion L-3107 Tested At 500°C/84.0 MPa)



Figure 19b -
Detail Of Cu-8 Cr-4 Nb Fracture Surface
(Extrusion L-3107 Tested At 500°C/84.0 MPa)

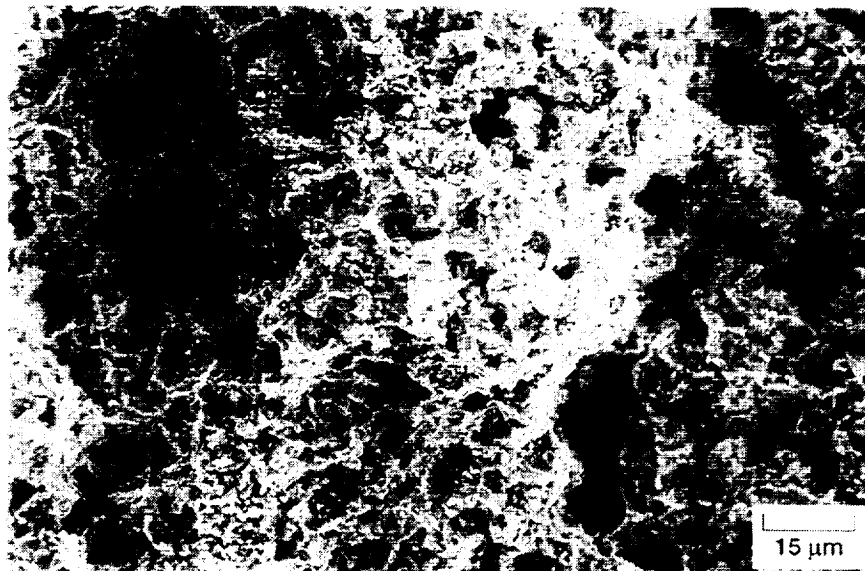


Figure 19c -
Typical Fracture Surface Of Cu-4 Cr-2 Nb Creep Samples
(Extrusion L-3297 Tested At 650°C/37.4 MPa)



Figure 19d -
 Typical Fracture Surface Of NARloy-Z Creep Samples
 (Plate 3 Tested At 800°C/10.4 MPa)

Modeling of Creep Properties

The creep rate and creep life of the alloys were modeled with the help of Dennis Keller of Real World Quality Systems, Inc. using the RS/1 Explore² computer program. Due to range of the data, the values were scaled so that the scaled values would fall between -1 and 1. The general equations used to describe the creep properties are

$$\ln(Y) = \beta_0 + \beta_1 \ln(T)_{scaled} + \beta_2 \ln(\sigma)_{scaled} + \beta_{11} [\ln(T)_{scaled}]^2 \quad [4]$$

$$\ln(Y) = \beta_0 + \beta_1 \ln(T)_{scaled} + \beta_2 \ln(\sigma)_{scaled} + \beta_{12} [\ln(T)_{scaled} \ln(\sigma)_{scaled}] \quad [5]$$

$$\ln(Y) = \beta_0 + \beta_1 \ln(T)_{scaled} + \beta_2 \ln(\sigma)_{scaled} \quad [6]$$

where Y is either the creep rate, time to 1% creep or creep life, β_x are the model coefficients, and $\ln(T)_{scaled}$ and $\ln(\sigma)_{scaled}$ are the scaled temperatures and stresses defined by the equations

$$\ln(T)_{scaled} = \frac{\ln(T) - 0.5[\ln(T_{Max}) + \ln(T_{Min})]}{0.5[\ln(T_{Max}) + \ln(T_{Min})]} \quad [7]$$

²RS/1 Explore produced by BBN Software Products, A Division of Bolt Beranek and Newman, Inc., Cambridge, MA

$$\ln(\sigma)_{\text{scaled}} = \frac{\ln(\sigma) - 0.5[\ln(\sigma_{\text{Max}}) + \ln(\sigma_{\text{Min}})]}{0.5[\ln(\sigma_{\text{Max}}) + \ln(\sigma_{\text{Min}})]} \quad [8]$$

The analysis of the data indicated that there was a need for a second order variable in most cases. In the case of Cu-8 Cr-4 Nb, there were no data points that appeared to be outliers from the analysis of the data. Testing of the various models using the time to 1% creep data did not reveal a clear choice for the model. The model given in Equation [4] was chosen since it made the most metallurgical sense and the $S_{\text{inv.lnx}}$ value was the smallest. For the Cu-8 Cr-4 Nb data, there were no apparent outliers, and all 54 data points were used in the analyses.

In the case of NARloy-Z, there were no apparent outliers for the creep rate. However, analysis of the time to 1% creep and creep life data indicated that one data point from each data set could be considered an outlier. The effect is most apparent in the model for creep life where the second order term changes from a stress-temperature interaction to a T^2 term. Both the model for the complete data set and the data set without the suspected outliers are presented in Table 6. The models are differentiated by the number of data points used in the analysis.

The largest number of outliers occurred in the Cu-4 Cr-2 Nb data set. In addition to one data point which was lost, the analysis indicated that two data points for the creep rate and three data points for the creep life were potential outliers. For the creep rate model, the exclusion of the three data points did not change the model but did increase the fit considerably. For the creep life model, the exclusion of the three potential outliers changes the model by requiring the addition of a temperature-stress interaction term while the model with all data points can be fit without the second order term.

The analyses showed that the samples tested at higher than desired stresses produced valid results. The only drawback was the time to 1% creep and creep lives were quite short. The creep rates also were much higher than other samples.

Table 6 -
Creep Model Coefficients

Alloy	Y	Points	β_0	β_1	β_2	β_{12}	β_{11}	$S_{inv,lnx}$
Cu - 8 Cr - 4 Nb	Creep Life	54	4.836	-5.756	-5.383		-0.4578	0.697
	1% Creep	54	2.678	-5.825	-5.265		-1.150	0.971
	Creep Rate	54	-1.399	6.240	5.725		0.7509	0.822
Cu - 4 Cr - 2 Nb	Creep Life	28	4.044	-6.186	-5.982			0.818
		25	4.551	-6.822	-6.496	0.4294		0.442
	1% Creep	27	2.048	-6.154	-5.672	1.788		0.937
	Creep Rate	28	-8.053	8.098	8.138	-1.001		0.835
		26	-8.091	8.205	7.986	-0.7612		0.556
NARloy-Z	Creep Life	36	4.464	-5.175	-6.683	0.7220		0.551
		35	4.461	-4.671	-6.228		-0.7156	0.448
	1% Creep	36	2.894	-6.794	-7.266	1.713		0.902
		35	3.344	-7.511	-8.127	2.177		0.729
	Creep Rate	36	-8.465	8.261	9.175	-2.290		0.800

There is some concern in choosing to call some points outliers given the scatter of the data. For the most conservative applications where the response is mission critical, the models with all data points should probably be preferred. For applications where minor deviations are not critical, i.e., welding electrodes, the better fit models with the outliers removed give an adequate model of the materials.

The value of any model is its predictive capabilities. It must be pointed out that the design space for the testing was non-standard in that it was not rectangular (Figure 20). Rather, because of the nature of creep, the maximum stress of the lowest temperature creep test was not the same as the maximum stress of the highest temperature creep test. When predicting the response of the alloys one *must* stay within the polygons defined by the design spaces.

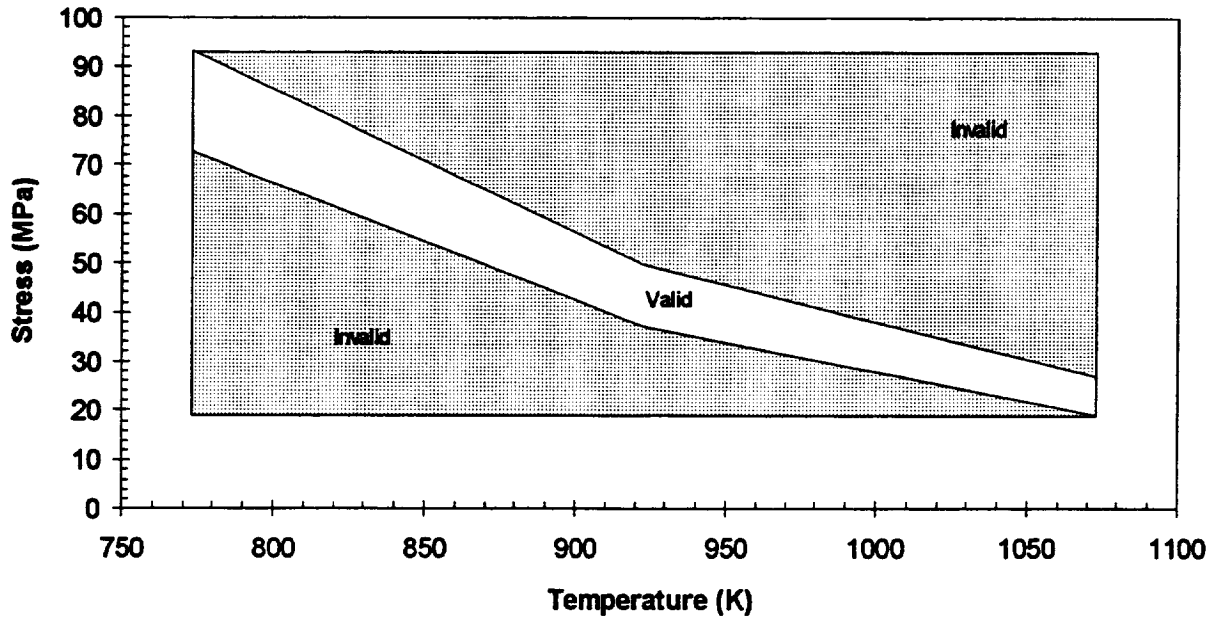


Figure 20a -
Design Space for Cu-8 Cr-4 Nb

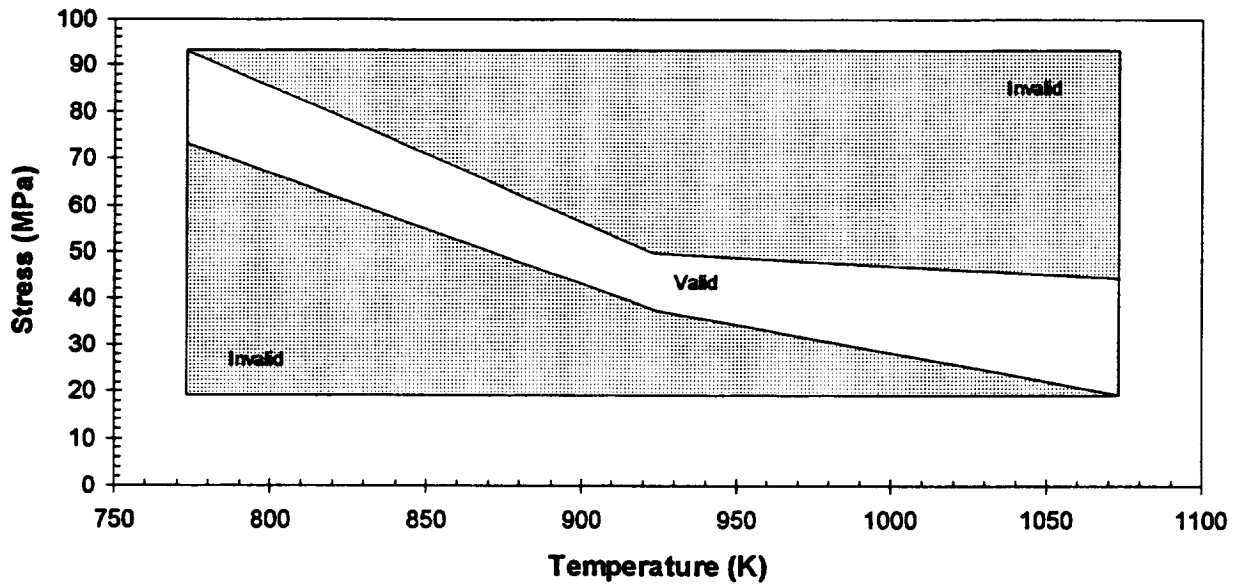


Figure 20b -
Design Space for Cu-4 Cr-2 Nb

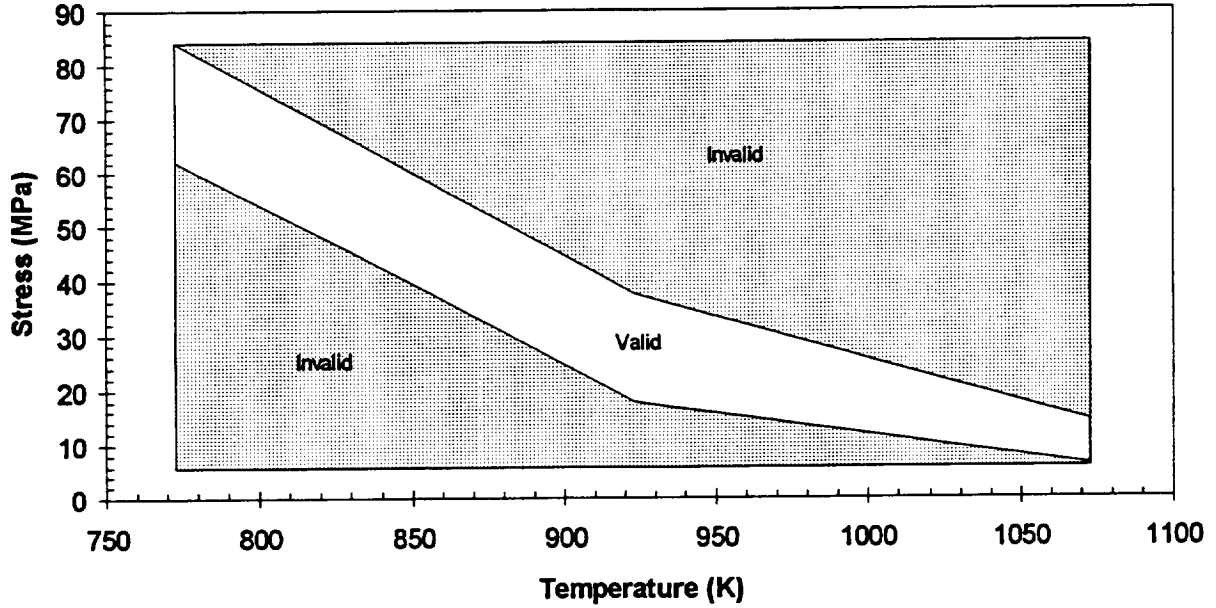


Figure 20c -
Design Space for NARloy-Z

There is no easy way to predict 95% confidence interval limits for the untransformed creep rate and life. However, a good approximation can be arrived at by using the standard errors of regression ($S_{\ln y, \ln x}$) listed in Table 6. The value for Y is given by the equation

$$\exp(\ln(Y)) = \exp \left\{ \begin{array}{l} \beta_0 + \beta_1 \ln(T)_{scaled} + \beta_2 \ln(\sigma)_{scaled} \\ + \beta_{12} [\ln(T)_{scaled} \ln(\sigma)_{scaled}] + \beta_{11} [\ln(T)_{scaled}]^2 \end{array} \right\} \quad [9]$$

The approximate 95% confidence intervals for a given Y at a specified temperature and stress combination are given by the equation

$$\exp[\ln(Y) \pm 2S_{\ln y, \ln x}] = \exp \left\{ \begin{array}{l} \beta_0 + \beta_1 \ln(T)_{scaled} + \beta_2 \ln(\sigma)_{scaled} \\ + \beta_{12} [\ln(T)_{scaled} \ln(\sigma)_{scaled}] + \beta_{11} \ln(T)_{scaled}^2 \pm 2S_{\ln y, \ln x} \end{array} \right\} \quad [10]$$

To back calculate the stress that the alloy can withstand at a given temperature for a specified time, the equation

$$\sigma = \exp \left\{ \frac{-[\ln(Y) - \beta_0 - \beta_1 \ln(T)_{scaled} - \beta_{11} [\ln(T)_{scaled}]^2]}{-\beta_2 - \beta_{12} \ln(T)_{scaled}} \right\} \quad [11]$$

can be used. Once again the 95% confidence intervals must be approximated using the equation

$$\sigma \pm 2S_{\ln Y, \ln X} = \exp \left\{ \frac{-[\ln(Y) \pm 2S_{\ln Y, \ln X} - \beta_0 - \beta_1 \ln(T)_{scaled} - \beta_{11} [\ln(T)_{scaled}]^2]}{-\beta_2 - \beta_{12} \ln(T)_{scaled}} \right\} \quad [12]$$

Examination of the results shows that within the limits of the design space these approximation of the 95% confidence intervals are valid and meaningful. For other confidence intervals, i.e., a 99% confidence interval, $2S_{\ln Y, \ln X}$ should be replaced by $xS_{\ln Y, \ln X}$ where x is the appropriate t-test value for the confidence interval given the degrees of freedom for the tests.

Examples of the calculated -2σ stresses for the creep lives of the alloys are presented in Table 7. The points column refers to the number of data points used in the model. The trends generally follow the data. However, in some cases the models can predict that NARloy-Z is superior to the Cu-Cr-Nb alloys. Examination of the data and the models indicates this is because of the $S_{\ln Y, \ln X}$ term in the equations for predicting the stresses. Since the NARloy-Z values of $S_{\ln Y, \ln X}$ are smaller than the Cu-Cr-Nb values, the decrease from the average value when calculating the lower 95% confidence limit is smaller. The two cases for Cu-4 Cr-2 Nb also show this phenomena. For other properties where the value of $S_{\ln Y, \ln X}$ for the NARloy-Z data is comparable to the Cu-Cr-Nb values, the expected result of the NARloy-Z being inferior does occur.

Table -7 -
95% Confidence Minimum Predicted Stresses For 1, 10 and 100 Hour Creep Lives

Alloy	Temperature (°C)	Points	Life (h)		
			1	10	100
Cu-8 Cr-4 Nb	500	54	189.3	108.4	62.1
	650	54	46.8	26.8	15.4
	800	54	11.7	6.7	3.8
Cu-4 Cr-2 Nb	500	28	148.4	89.9	54.4
		25	164.2	106.5	69.1
	650	28	34.5	20.9	12.7
		25	42.7	26.9	16.9
	800	28	10.0	6.1	3.7
		25	11.6	7.1	4.3
NARloy-Z	500	36	147.5	89.2	53.9
		35	110.1	68.0	42.0
	650	36	40.3	25.8	16.5
		35	44.4	27.4	16.9
	800	36	16.6	11.1	7.4
		35	15.6	9.6	5.9

Thermal Conductivity Testing

Cu-8 Cr-4 Nb

The heat capacity of seven Cu-8 Cr-4 Nb samples were measured from 23°C to 702°C. The data was extrapolated to 800°C for the thermal conductivity

calculations. The average heat capacity and 95% confidence limits are presented in Table 8 and Figure 21. The heat capacity was well described by the equation

$$c_p = 2.58 \times 10^{-8} T^2 + 5.42 \times 10^{-5} T + 0.379 \quad [13]$$

where c_p is the heat capacity (J/gK) and T is temperature (K). Analysis did indicate that the temperature squared term was sufficiently important to include in the fitting of the data.

Table 8 also contains the thermal diffusivity of the alloy as measured by the laser flash technique. Figure 22 graphically presents the values. The thermal diffusivity decreased slowly with increasing temperature. Between 700°C and 800°C the thermal diffusivity decreased more rapidly, probably because of the dissolution of Cr₂Nb into the Cu matrix. Statistical analysis indicated that a good fit of the data could still be obtained for all the data. The data for the thermal diffusivity between 23°C and 800°C was fitted to the equation

$$\alpha = -2.57 \times 10^{-7} T^2 + 170 \times 10^{-5} T + 0.834 \quad [14]$$

where α is the thermal diffusivity (cm²/s). This representation does not take into account the decrease in thermal diffusivity between 700°C and 800°C.

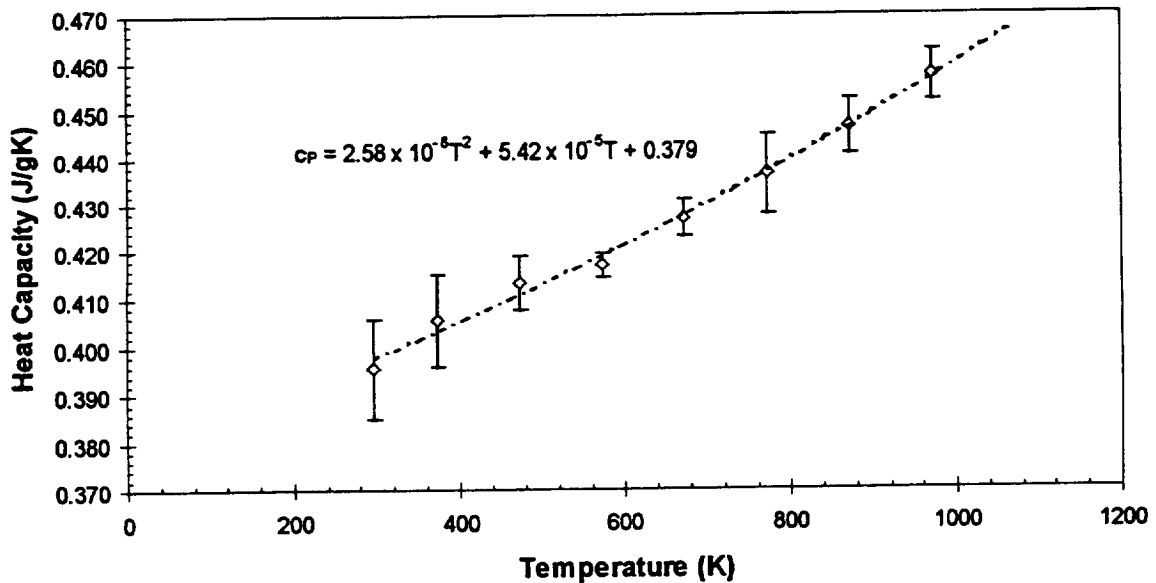
The value for the thermal conductivity was calculated as previously explained in the Experimental Procedure. The average room temperature density of the alloy was 8.304 g/cm³. The calculated thermal conductivities are presented in Table 8 and Figure 23. The thermal conductivity decreases between 700°C and 800°C, probably due to dissolution of the small amount of elemental Cr precipitates into the matrix. The 95% confidence intervals were approximately 10% of the value of the thermal conductivities.

The Cu-8 Cr-4 Nb alloy frequently will be used at temperatures less than or equal to 700°C. Between 23°C and 700°C the thermal conductivity is accurately modeled by the simple linear equation

$$\lambda = 9.35 \times 10^{-3} T + 286 \quad [15]$$

Table 8 -
Average Thermal Properties Of Cu-8 Cr-4 Nb

Temperature (K)	Heat Capacity (J/gK)		Thermal Diffusivity (cm ² /s)		Thermal Conductivity (W/mK)	
	Average	95% Confidence Interval	Average	95% Confidence Interval	Average	95% Confidence Interval
296	0.395	±0.010	0.870	±0.059	286	±24.788
373	0.406	0.010	0.855	0.065	290	22.772
473	0.413	0.005	0.852	0.060	293	20.575
573	0.417	0.003	0.851	0.047	293	17.958
673	0.427	0.004	0.830	0.051	295	19.255
773	0.436	0.008	0.805	0.066	293	26.785
873	0.446	0.006	0.789	0.073	293	27.800
973	0.457	0.005	0.777	0.056	294	23.292
1073			0.706	0.094	277	22.305



Error Bars represent 95% Confidence Intervals on 7 tests

Figure 21 -
Average Heat Capacity Of Cu-8 Cr-4 Nb

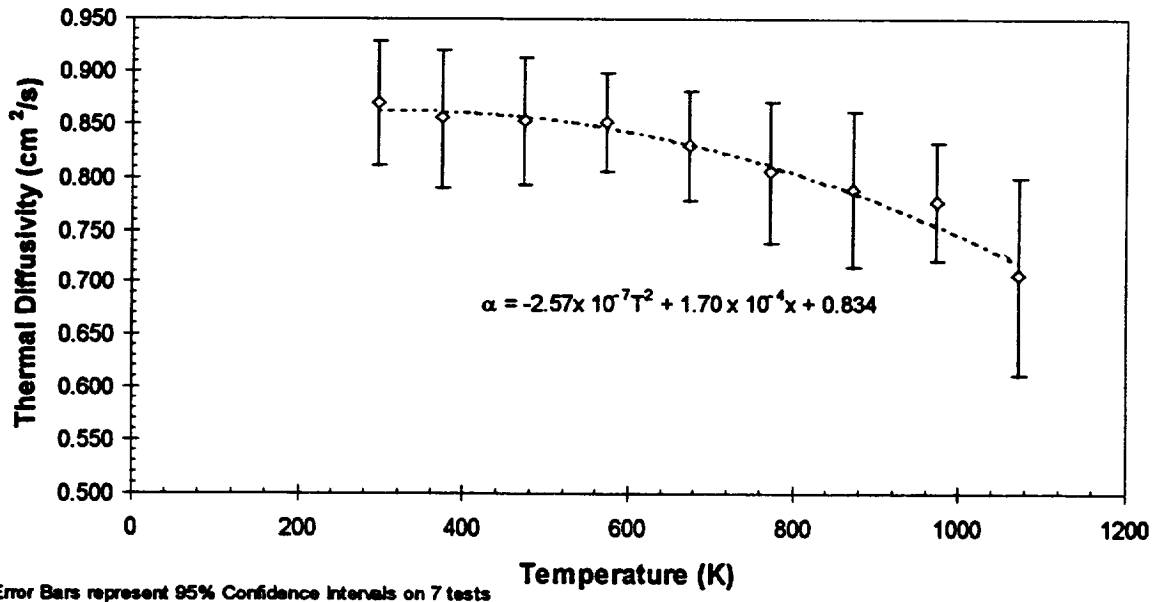


Figure 22 -
Average Thermal Diffusivity Of Cu-8 Cr-4 Nb

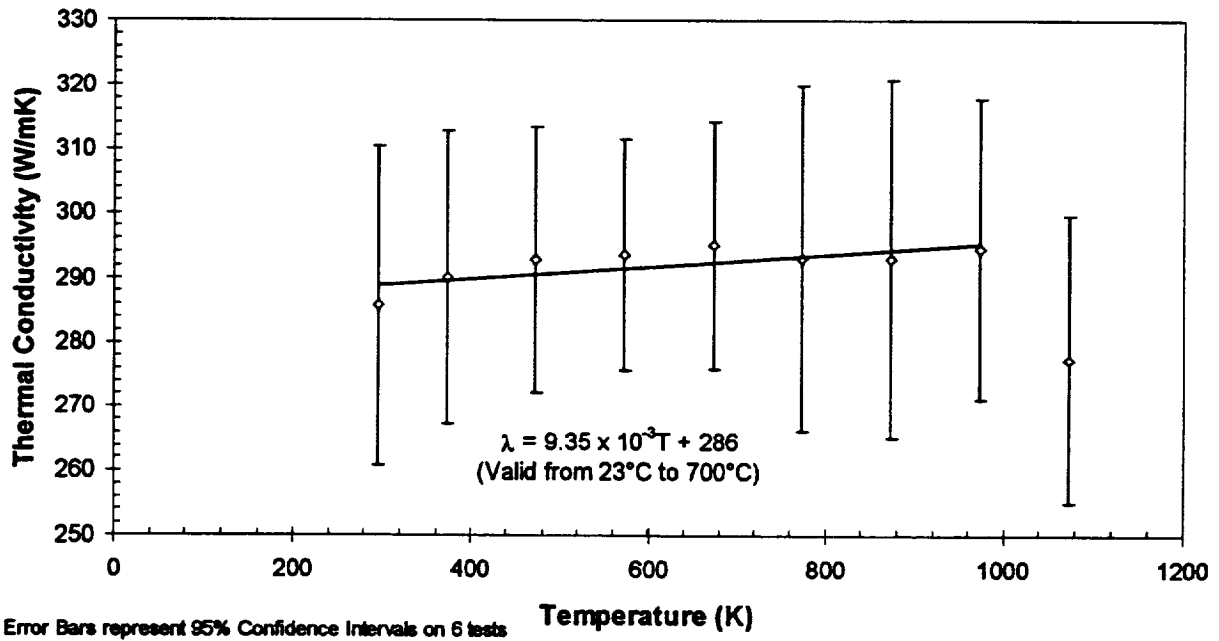


Figure 23 -
Average Thermal Conductivity Of Cu-8 Cr-4 Nb

Cu-4 Cr-2 Nb

The heat capacity of the Cu-4 Cr-2 Nb alloy is presented in Figure 24 and tabulated in Table 9. Since only one sample was tested, there are no confidence intervals assigned to the data points. A curve with the equation

$$c_p = -6.97 \times 10^{-8}T^2 + 1.71 \times 10^{-4}T + 0.338 \quad [16]$$

where c_p is the heat capacity (J/gK) and T is temperature (K) was fitted to the heat capacity data.

The thermal diffusivity for Cu-4 Cr-2 Nb is presented in Figure 25 and Table 9. A curve with the equation

$$\alpha = -3.69 \times 10^{-8}T^2 - 2.16 \times 10^{-4}T + 1.10 \quad [17]$$

where α is the thermal diffusivity (cm²/s) was fitted to the data.

Using the density of 8.799 g/cm³ obtained experimentally from the diffusivity sample, the thermal conductivity was calculated as explained in the Experimental Procedure. The resulting values are presented in Table 9 and plotted in Figure 26. A curve with the equation

$$\lambda = -8.95 \times 10^{-5}T^2 + 8.71 \times 10^{-2}T + 329 \quad [18]$$

where λ is the thermal conductivity (W/m•K) was fitted to the data. The parabolic shape of the curve comes from the competing phenomena of increasing heat capacity and decreasing thermal diffusivity. Most likely the decrease in thermal diffusivity is caused by the gradually dissolution of Cr back into the Cu matrix. With a slightly higher Cr:Nb ratio than the Cu-8 Cr-4 Nb samples, there is more Cr readily available for this.

Table 9 -
Thermal Properties Of Cu-4 Cr-2 Nb

Temperature (K)	Heat Capacity (J/gK)	Thermal Diffusivity (cm²/s)	Thermal Conductivity (W/mK)
296	0.381	1.032	345
373	0.394	1.012	350
473	0.405	0.985	351
573	0.414	0.962	350
673	0.422	0.936	347
773	0.428	0.907	341
873	0.434	0.885	337
973	0.438	0.853	328
1073	0.443	0.822	320

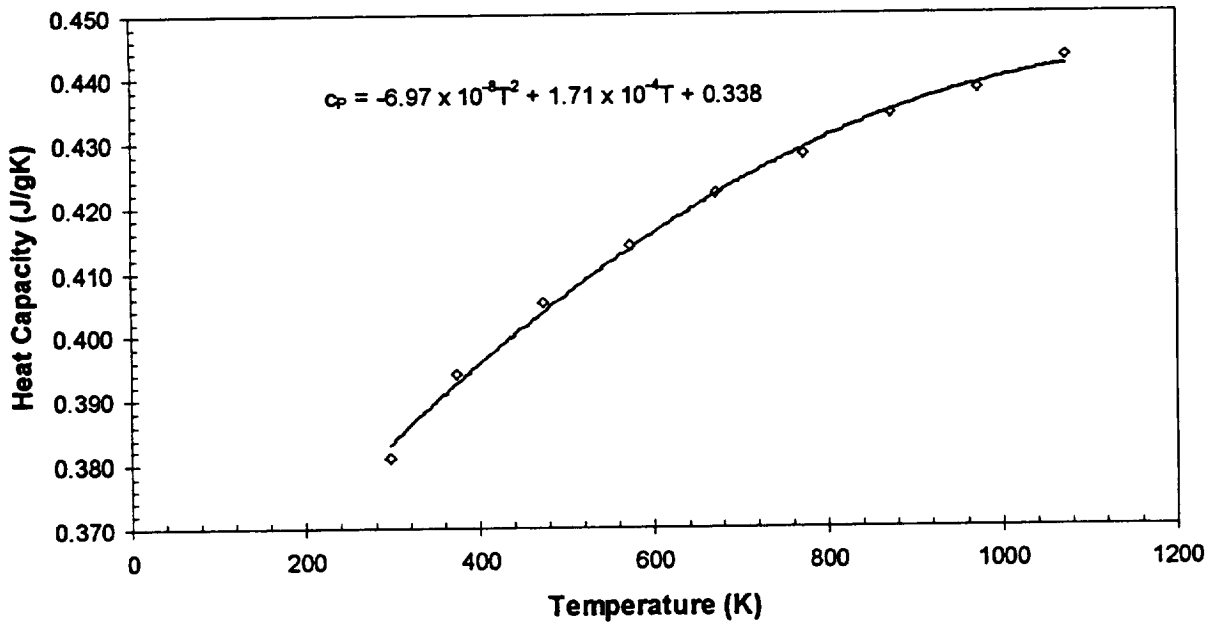


Figure 24 -
Heat Capacity Of Cu-4 Cr-2 Nb

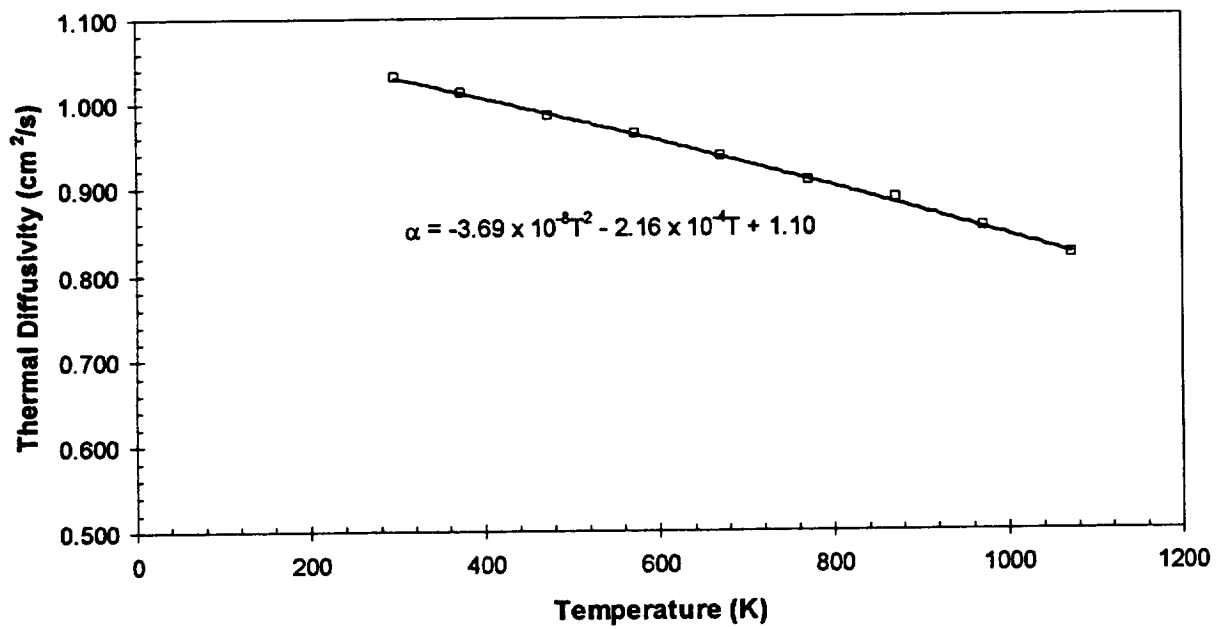


Figure 25 -
Thermal Diffusivity Of Cu-4 Cr-2 Nb

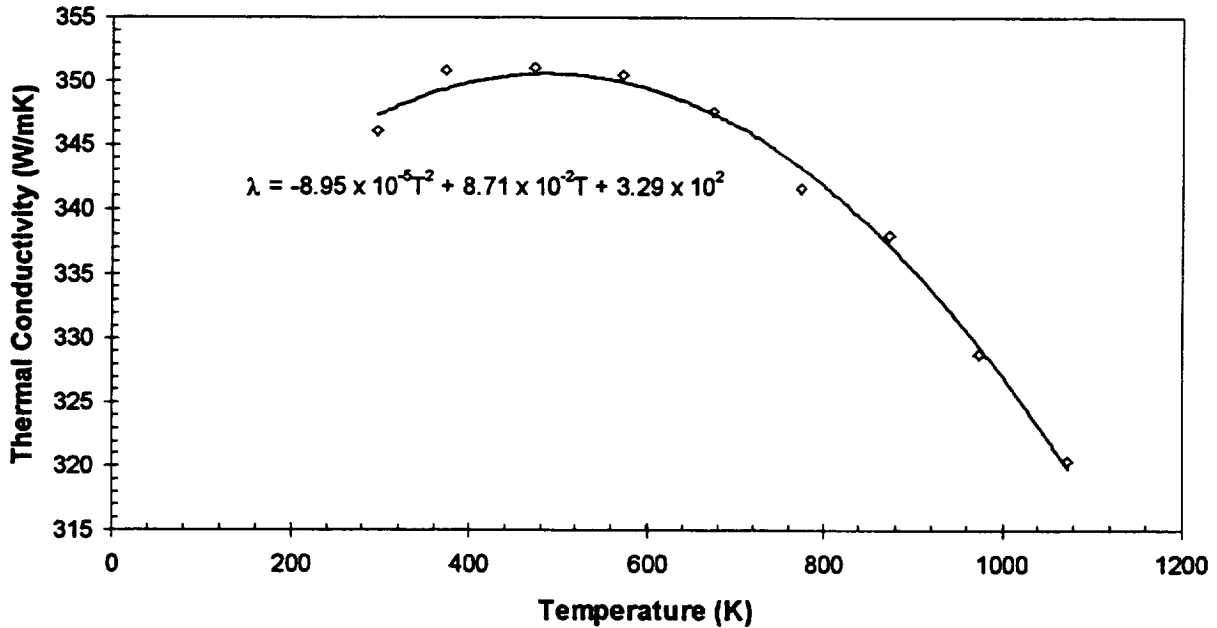


Figure 26 -
Thermal Conductivity Of Cu-4 Cr-2 Nb

Low Cycle Fatigue

Typical Cu-8 Cr-4 Nb low cycle fatigue (LCF) loops are presented in Figure 27. Data were collected for many cycles, and representative cycles are presented in the figure. Representative loops for all Cu-8 Cr-4 Nb samples are presented in Appendix D.

The LCF lives of the specimens are presented in Figure 28. Additional data on the inelastic strain and stress at half life are presented in Table 10. Data for NARloy-Z in the solution heat treated and aged condition are also presented where available for comparison.

The results show that the Cu-8 Cr-4 Nb possess superior LCF capability. At room temperature and a 2.0% strain range, the worst case, Cu-8 Cr-4 Nb has a life comparable to NARloy-Z. The data are also very reproducible. At lower strain ranges the life of the Cu-8 Cr-4 Nb is significantly higher than that of NARloy-Z.

The best LCF lives relative to NARloy-Z, though, are obtained at higher temperatures. At 538°C, the average life of Cu-8 Cr-4 Nb is approximately 50% greater at a 2.0% strain range and 200% greater at a 0.7% strain range compared to NARloy-Z. Even if the temperature is increased to 650°C, the lives of the Cu-8 Cr-4 Nb specimens are approximately 100% greater at both 0.7%

and 2.0% strain ranges than NARloy-Z tested at the lower temperature of 538°C.

Table 10 -
Low Cycle Fatigue Results

T (°C)	$\Delta\epsilon_{\text{Total}}$ (%)	$\Delta\epsilon_{\text{Inelastic}}$ (%)	N_f (Cycles)	$\Delta\sigma$ at $\frac{1}{2}N_f$ (MPa)
Cu-8 Cr-4 Nb				
25	0.7	N.A.	4,647	N.A.
25	0.8	N.A.	15,641	N.A.
25	2.0	1.279	442	659.0
25	2.0	1.394	435	647.5
538	0.7	0.306	12,032	393.7
538	0.7	0.335	10,990	437.1
538	1.2	0.810	1,731	493.4
538	1.2	0.787	1,810	461.5
650	0.7	0.342	10,393	378.5
650	0.7	0.359	7,131	390.0
650	1.2	0.782	2,260	399.2
650	1.2	0.801	2,391	381.5
NARloy-Z (Refs. 9, 12)				
25	0.8	N.A.	3,800	N.A.
25	1.2	N.A.	500	N.A.
538	0.7	0.46	3,601	231.8
538	1.2	0.92	1,126	253.0

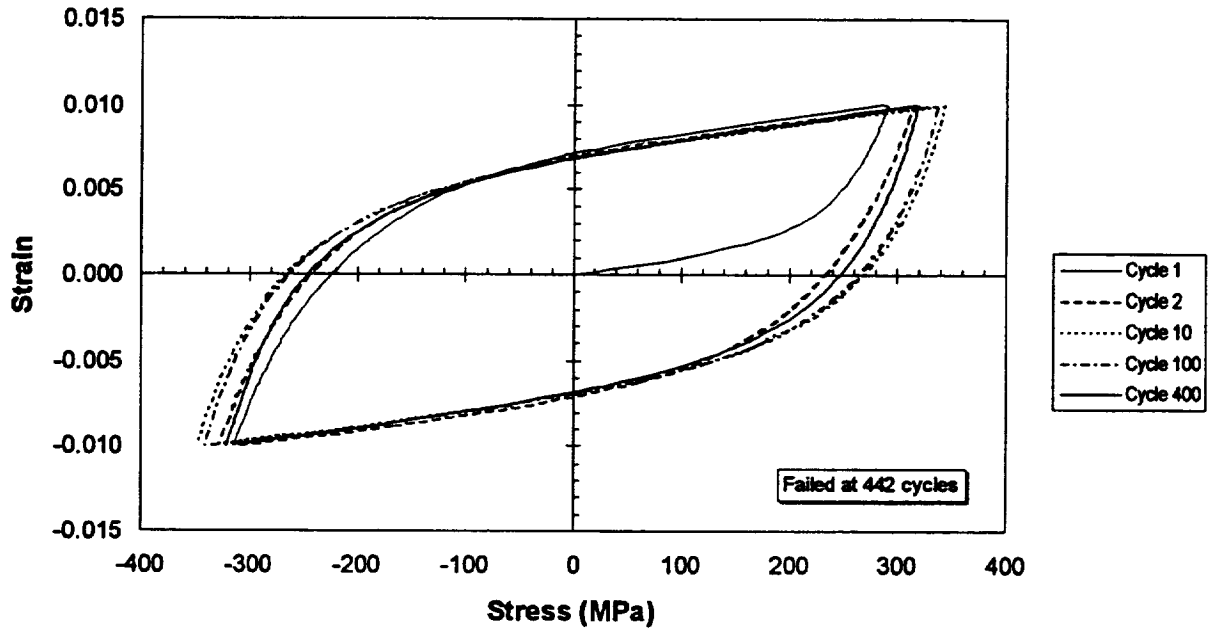


Figure 27 -
Typical LCF Loops For Cu-8 Cr-4 Nb
(Sample 1-1 Tested At Room Temperature)

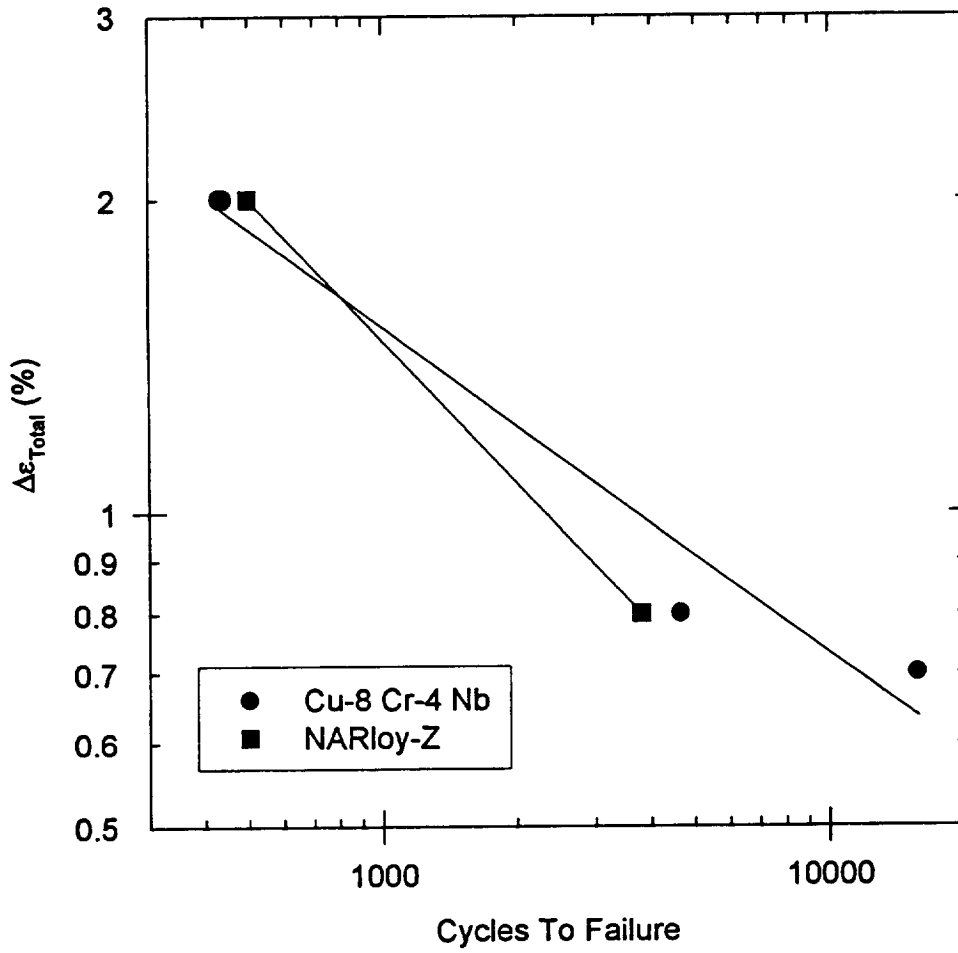


Figure 28a -
Room Temperature Low Cycle Fatigue Lives Of Cu-8 Cr-4 Nb and NARloy-Z

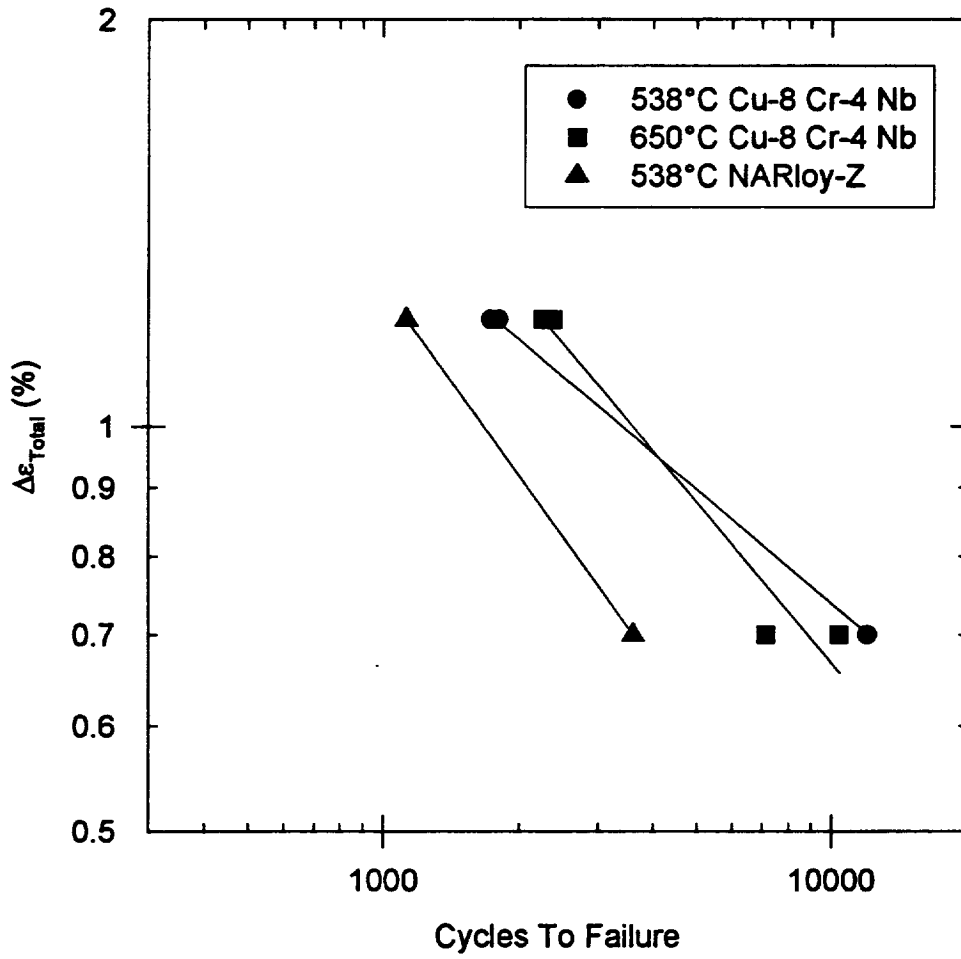


Figure 28b -
Elevated Temperature Low Cycle Fatigue Lives Of Cu-8 Cr-4 Nb and NARloy-Z

Discussion

Creep

The creep resistance of Cu-8 Cr-4 Nb, Cu-4 Cr-2 Nb and NARloy-Z were measured between 500°C and 800°C at a variety of stresses. It was possible to use the same stresses for the Cu-8 Cr-4 Nb and Cu-4 Cr-2 Nb samples, but the NARloy-Z samples were not capable of supporting as high a load.

The NARloy-Z data was compared to the published values (9). The reference source gives the minimum design levels or -3σ values. Unfortunately, the value for the standard deviation was not provided. However, all results do fall above the line for the minimum design curve.

One observation that was confirmed in talks with Don Ulmer at Rocketdyne (13) was the propensity of NARloy-Z to go into third stage creep quite early and stay in third stage creep a significant portion of the test. While it did not occur in all cases (see Appendix C), the long time in third stage creep resulted in significantly greater creep elongations.

In comparison, the Cu-Cr-Nb show only a little third stage behavior before fracture (see Appendices A and B). Of the two alloys examined, the Cu-4 Cr-2 Nb is more likely to exhibit third stage creep behavior. It was interesting to note that the data from the Cu-4 Cr-2 Nb samples tested at 800°C/44.3 MPa were consistent with the other 800°C data at lower stresses. Even though the stress was much higher than the other 800°C tests, the data still fall on the regression lines calculated with and without the 44.3 MPa data points. This indicates that the material is well behaved, and the possibility exists to extrapolate data to points outside the design spaces. It is important to remember that care must be used in the extrapolations. The confidence intervals increase extremely fast outside of the design space.

The results of the time to 1% creep, creep rates and creep lives for the Cu-Cr-Nb alloys were very similar. The Cu-4 Cr-2 Nb alloy is clearly inferior to the Cu-8 Cr-4 Nb alloy, but the difference is minimal over the temperature and stress ranges of interest. Given the higher thermal conductivity of the Cu-4 Cr-2 Nb alloy, thermally induced stresses may actually be less than in the Cu-8 Cr-4 Nb alloy because of smaller thermal gradients. A designer should examine both alloys to determine which is superior for a given application.

Both Cu-Cr-Nb alloys showed much greater creep resistance than NARloy-Z. The much higher volume fractions of precipitates for the Cu-Cr-Nb alloys compared to NARloy-Z accounts for the better behavior at lower temperatures, especially 500°C. The stability of the precipitates contributes to the excellent creep resistance at 650°C and 800°C. The NARloy-Z precipitates are rapidly

dissolving at these higher temperatures. Any remaining benefit from working the alloy is also diminishing as the material recovers and recrystallizes. Examination of the various charts also reveals that the slope of the lines for the Cu-Cr-Nb alloys are nearly parallel. The slopes of the NARloy-Z lines are also similar, but tend toward slightly worse values.

The mean times to 1% creep for the Cu-Cr-Nb alloys and NARloy-Z are compared in Figure 29. Compared to NARloy-Z, Cu-8 Cr-4 Nb takes 100% to 200% longer to reach 1% strain at a given stress. The life advantage is smallest at 500°C and very pronounced at 800°C. Cu-4 Cr-2 Nb has intermediate values for the time to 1% creep, but tends to be closer to Cu-8 Cr-4 Nb, especially at the higher temperatures.

The mean steady-state creep rates of the three alloys are presented in Figure 30. The creep rates for the Cu-Cr-Nb alloys were significantly lower than NARloy-Z. Cu-8 Cr-4 Nb creep rates were 1.5 to 3 orders of magnitude lower at a given stress than the corresponding values for NARloy-Z. Cu-4 Cr-2 Nb creep rates were 1.3 to 2.5 orders of magnitude lower than NARloy-Z in the range of temperatures and stresses tested.

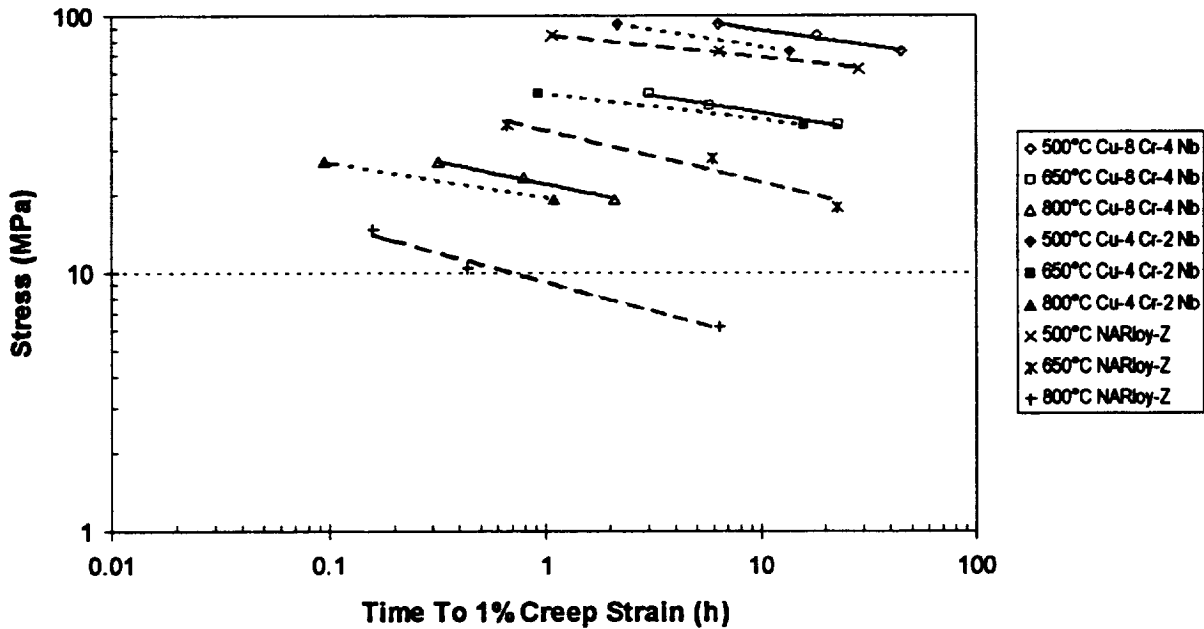


Figure 29 -
Comparison Of Mean Times To 1% Creep

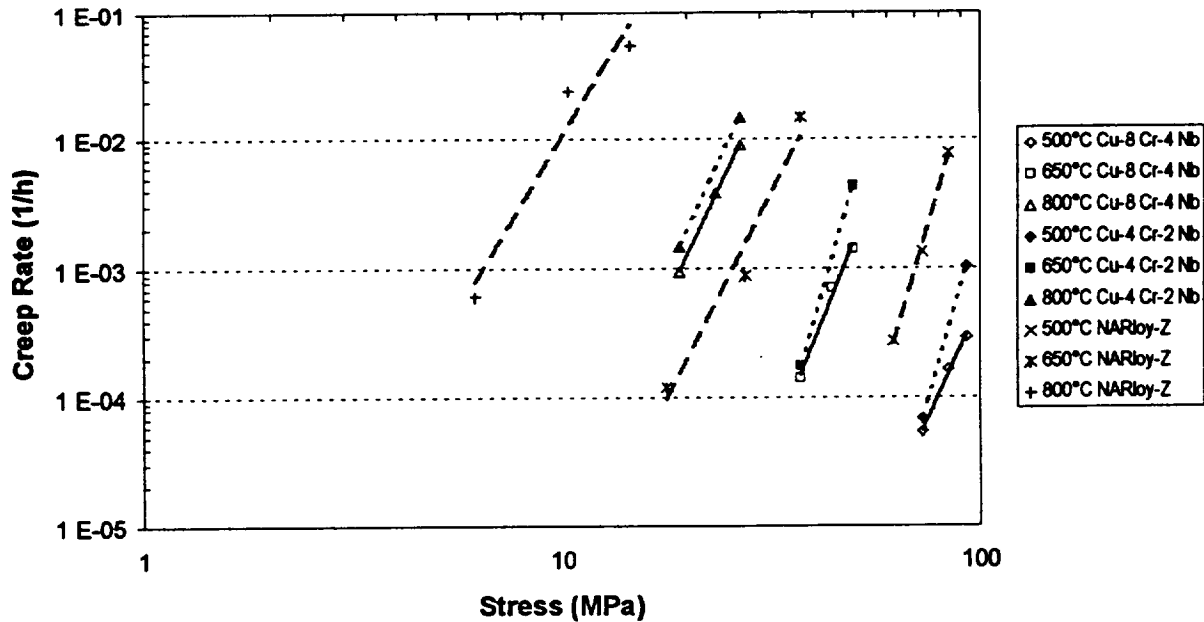


Figure 30 -
Comparison Of Mean Creep Rates

Figure 31 compares the mean creep lives of the Cu-Cr-Nb alloys and NARloy-Z. Cu-8 Cr-4 Nb enjoys an advantage of 150% to 250% longer lives at a constant stress. Cu-4 Cr-2 Nb enjoys an advantage of between 100% and 150% longer lives.

Figure 32 presents the average creep elongations of the three alloys. For NARloy-Z, increasing the temperature can greatly increase the creep elongation. There appears to be a weak correlation between increasing temperature and increasing elongation for the Cu-Cr-Nb alloys, but it is not nearly as strong as for NARloy-Z. For all three alloys, there does not appear to be a good correlation between stress and creep elongation.

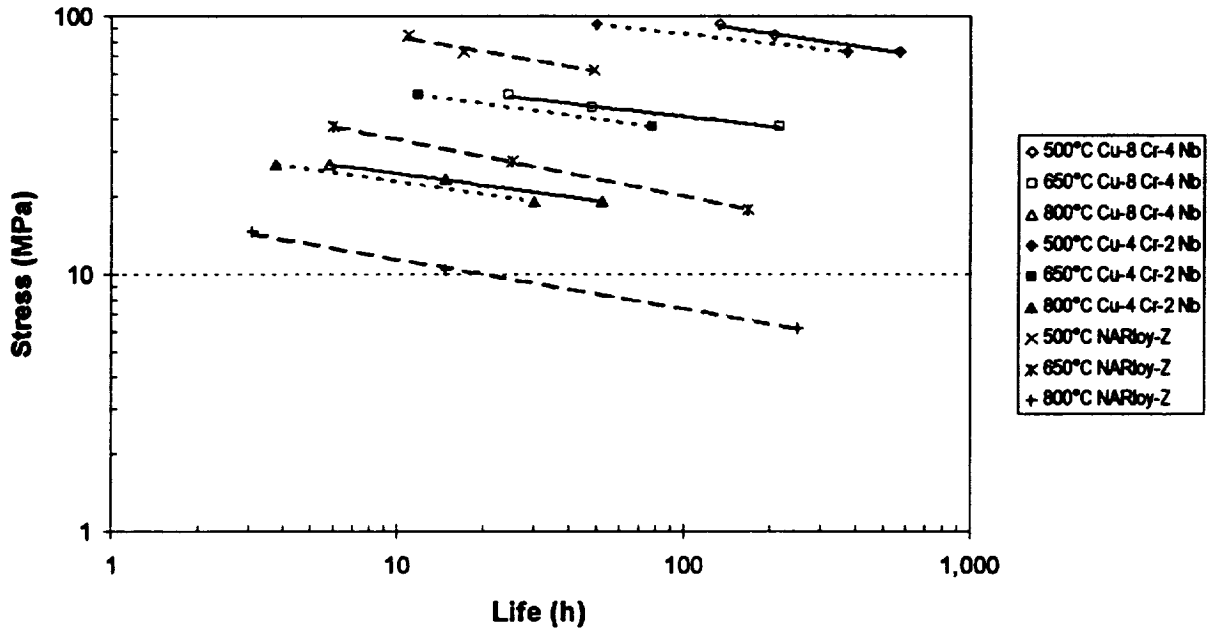


Figure 31 -
Comparison Of Mean Creep Lives

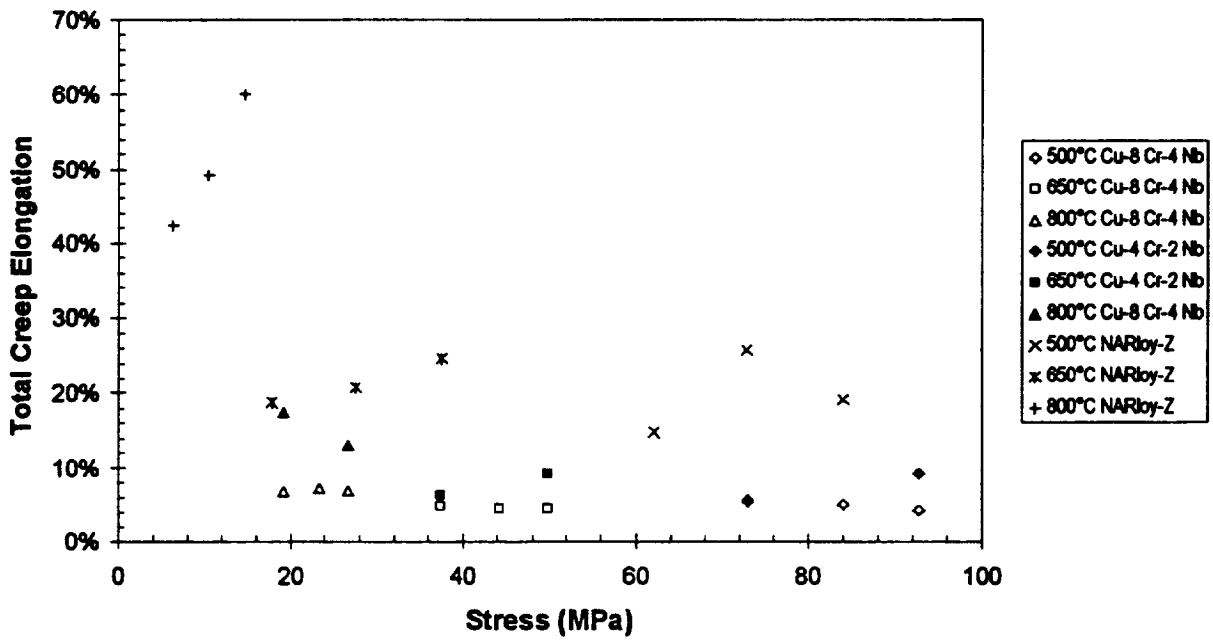


Figure 32 -
Comparison Of Average Creep Elongations

A designer may wish to design for a given life rather than a specific stress. Revisiting Figure 28 and 30, the Cu-Cr-Nb alloys show the ability to support much greater stresses for a given life. Cu-8 Cr-4 Nb enjoys an advantage of 30% to 160% greater stress at a given time to 1% creep compared to NARloy-Z. For a given stress-rupture life, Cu-8 Cr-4 Nb can withstand stresses 80% to 160% more than NARloy-Z. Cu-4 Cr-2 Nb can withstand 10% to 150% greater stress for a specific time to 1% creep and 60% to 150% greater stress for a given stress-rupture life.

Low Cycle Fatigue

Examining the Cu-8 Cr-4 Nb LCF loops, there were some changes in the shape of the loops with increasing cycles, but in general the shape of the loops remained reasonably constant until failure. The magnitude of the stresses were not greatly increased with increasing cycles, indicating minimal work hardening under the test conditions. The stresses at 538°C and 650°C were very close for the 0.7% total strain tests. The 1.2% total strain tests were not as close, but were still similar.

The results of the low cycle fatigue testing show that Cu-8 Cr-4 Nb had a significantly higher LCF lives than NARloy-Z. Detailed microscopy was not conducted on the test specimens. However, the increase in LCF life even though the Cu-8 Cr-4 Nb alloy has a lower ductility is most likely attributable to the large volume fraction of very fine, extremely hard Cr₂Nb precipitates. These precipitates delay or stop the formation of persistent slip bands and extend the life of the alloy in LCF testing.

NARloy-Z, on the other hand, has a much lower volume fraction of Cu_xZr precipitates. These precipitates do not stop the formation of persistent slip bands. The Ag present in the alloy is predominantly present in a Cu solid solution. Even if present as a precipitate, the soft metallic precipitates would not be effective at stopping persistent slip band formation. Because of this, NARloy-Z must rely on its modest strength, high ductility and good toughness for its LCF resistance.

Since both the matrix and precipitate mechanical properties are not significantly affected by changes in temperature over the testing temperature range, the LCF lives are not radically different at the different test temperatures. The increase in life and temperature capability could give Cu-8 Cr-4 Nb a significant advantage over competitive materials.

Thermal Conductivity

Figure 33 compares the thermal conductivities of Cu, NARloy-Z and the Cu-Cr-Nb alloys to each other and pure Cu. In all cases, the relative thermal

conductivity is the alloy thermal conductivity at a given temperature divided by the thermal conductivity of Cu at the same temperature.

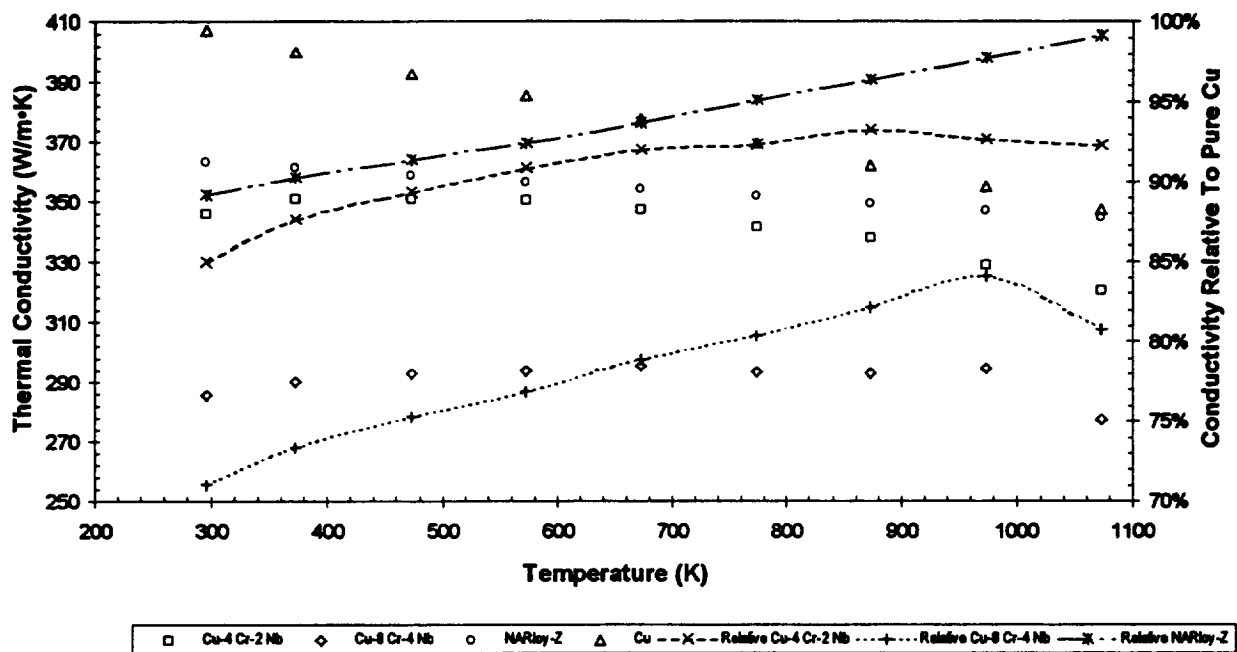


Figure 33 - Comparison of Cu-Cr-Nb, NARloy-Z And Cu Thermal Conductivities

The thermal conductivity of the Cu-8 Cr-4 Nb alloy suffers in comparison to NARloy-Z. This is most likely due to the much higher total alloying content and significantly larger volume fraction of precipitates. The precipitates probably act as scattering sites to lower the thermal diffusivity and hence thermal conductivity. In the case of Cu-4 Cr-2 Nb, the alloying levels have been reduced sufficiently to make the thermal conductivity competitive with NARloy-Z, especially at the intermediate and higher temperatures where the material is expected to be used.

The relative thermal conductivity of NARloy-Z increases steadily as the temperature increases. The dissolving of Ag precipitates into the Cu matrix appears to be the cause of this phenomena (14). The increase in thermal conductivity indicates that the strengthening from the precipitates is decreasing over the temperature range. There is therefore a strong inverse relationship between strength and thermal conductivity that must be considered in a design.

Compared to most materials, i.e., stainless steels and superalloys, the conductivities of the Cu-Cr-Nb alloys are much greater. Typically steels and

other materials with comparable strengths to the Cu-Cr-Nb alloys typically have conductivities in the 25 to 75 W/mK range. This is less than one third the value of the Cu-Cr-Nb alloys.

The higher strengths of the Cu-Cr-Nb alloys also allow for trade-offs resulting in a reduced wall thickness. Ultimately the wall thickness will determine the operating temperatures and thermal gradients. While it would be preferable that the thermal conductivities of the Cu-Cr-Nb alloys were higher, a proper design should eliminate any problems associated with the slightly lower thermal conductivities.

Summary and Conclusions

Two Cu-Cr-Nb alloys have been successfully produced using conventional argon gas atomization and extrusion. The properties of the resulting materials showed a remarkable high temperature creep resistance combined with a good thermal conductivity. The Cu-8 Cr-4 Nb alloy has also been shown to have exceptional LCF capability as well.

The creep resistance of the Cu-Cr-Nb alloys were both considerably greater than NARloy-Z. For a constant rupture life, the stress that Cu-4 Cr-2 Nb can support is between 60% and 150% greater than NARloy-Z. Cu-8 Cr-4 Nb is even better, being able to support 80% to 160% greater stresses. Times to 1% creep are similarly improved. Steady-state creep rates are more than one order of magnitude lower for the Cu-Cr-Nb alloys.

Cu-8 Cr-4 Nb performs well in LCF. The loops tend to be consistent throughout the life of the samples with little deviation in the stress-strain behavior. The loops indicate that Cu-8 Cr-4 Nb does not undergo much work hardening under the test conditions. The lives of the Cu-8 Cr-4 Nb specimens ranged from comparable at room temperature to as much as 200% longer at elevated temperatures. In addition, the LCF lives of Cu-8 Cr-4 Nb are not adversely affected by increasing the temperature from 538°C to 650°C.

The thermal conductivities of the Cu-Cr-Nb alloys are good, but are not as good as NARloy-Z. The Cu-8 Cr-4 Nb alloy which has the higher volume fraction of precipitates ranges from 72% to 82% the thermal conductivity of pure Cu. Cu-4 Cr-2 Nb with its lower loading has a thermal conductivities that range from 85% to 93% of the thermal conductivity of Cu. In comparison, most materials with similar strengths such as stainless steels have conductivities less than 25% that of Cu. NARloy-Z has somewhat higher thermal conductivity. It achieves a peak thermal conductivity almost equal to pure Cu at 800°C. However, NARloy-Z has minimal strength at these temperatures. A careful design taking advantage of the excellent high temperature strength of the Cu-Cr-Nb alloys can easily circumvent the slightly lower thermal conductivities.

The combination of excellent high temperature strength, good LCF resistance and high thermal conductivity make the Cu-Cr-Nb alloys excellent choices for high temperature applications.

Future Work

Testing is currently underway to determine the tensile strengths of the Cu-8 Cr-4 Nb, Cu-4 Cr-2 Nb and NARloy-Z at room and elevated temperatures. A design level test matrix is also being used for that testing program.

Additional tensile and creep testing is planned on material that has been extruded into a bar form and hot and cold rolled various reductions.

Finally, Cu-8 Cr-4 Nb powder has been supplied to the Rocketdyne Division of Rockwell International for the fabrication of combustion chamber liners under the Air Force Thrust Cell Initiative Program. Results will be forthcoming on the performance of the alloy.

Acknowledgments

The author would like to acknowledge the considerable help given by the personnel at NASA LeRC. In particular, Robert Dreshfield, Robert Miner and Michael Nathal of the Advanced Metallics Branch, Hugh Gray of the Materials Division, and Thomas Glasgow of the Processing Science and Technology Branch. In addition, a special thanks is extended to Michael Verrilli of the Structures Division for the low cycle fatigue testing and Ron Phillips and Peter Eichele of Gilcrest for performing the creep testing.

References

- (1) D.L. Ellis and G.M. Michal, "Precipitation Strengthened High Strength, High Conductivity Cu-Cr-Nb Alloys Produced by Chill Block Melt Spinning," NASA CR-185144, NASA LeRC, Cleveland, OH (Sept. 1989)
- (2) K.R. Anderson, J.R. Groza, R.L. Dreshfield, and D.L. Ellis, "Microstructural Evaluation of Precipitation-Strengthened Cu-8 Cr-4 Nb Alloy," *Materials Science and Engineering*, A169, (1993), pp. 167-175
- (3) K.R. Anderson, J.R. Groza, R.L. Dreshfield, and D.L. Ellis, "High Performance Dispersion Strengthened Cu-8 Cr-4 Nb Alloy," *Met. Trans A*, Vol. 26A, (Sept. 1995), pp. 2197-2206
- (4) K. Kuo, "Ternary Laves and Sigma-Phases of Transition Metals," *Acta Metall.*, Vol. 1, (Nov. 1953), pp. 720-724
- (5) D.L. Ellis and G.M. Michal, "Formation of Cr and Cr₂Nb Precipitates in Rapidly Solidified Cu-Cr-Nb Ribbon," *Ultramicroscopy*, Vol. 30, Nos. 1/2, pp. 210-216
- (6) D.L. Ellis and R.L. Dreshfield, "Preliminary Evaluation of a Powder Metal Copper-8 Cr-4 Nb Alloy," *Proc. of the Advanced Earth-to-Orbit Conference 1992*, Vol. 1, CP-3174, NASA MSFC, Huntsville, AL, (May 19-21, 1992), pp. 18-27
- (7) D.L. Ellis, R.L. Dreshfield, M.J. Verrilli, and D.G. Ulmer, "Mechanical Properties of a Cu-8 Cr-4 Nb Alloy," *Proc. of the Earth-to-Orbit Conference 1994*, Vol. 1, CP-3282, NASA MSFC, Huntsville, AL (May 1994), pp. 32-41
- (8) *1992 Annual Book of ASTM Standards*, Vol. 03.01, ASTM, Philadelphia, PA, 1992, pp. 130-149
- (9) *Materials Properties Manual*, 4th Ed., Rockwell International, Rocketdyne Div., (Oct. 30, 1987)
- (10) D.L. Ellis, A.K. Misra, and R.L. Dreshfield, "Effect of Hydrogen on Cr₂Nb and Cu-Cr-Nb Alloys," *Hydrogen Effects On Material Behavior*, *Proc. of Fifth International Conference*, Moran, WY (Sept. 1994)
- (11) *Smithells Metals Reference Book*, Sixth Ed., Editor E.A. Brandes, Butterworths, London, England, (1983), p. 14-16

- (12) Conway, J.B., Stentz, R.H., and Berling, J.T., NASA CR-134908, NASA LeRC, Cleveland, OH (Nov. 1975)
- (13) Don Ulmer, Rocketdyne, Westlake Facility, private communications
- (14) P.A. Wycliffe, "Literature Search On High Conductivity Copper Based Alloys," Final Report IDWA No. 6458-2, Rockwell International Science Center, Los Angeles, CA (March 1984)

Appendices

Appendix A - Creep Of Cu-8 Cr-4 Nb

Appendix B - Creep Of Cu-4 Cr-2 Nb

Appendix C - Creep Of NARloy-Z

Appendix D - Low Cycle Fatigue (LCF) Loops For Cu-8 Cr-4 Nb

Appendix A - Creep Of Cu-8 Cr-4 Nb

**Table A - 1
Results of Cu-8 Cr-4 Nb Creep Testing**

Temperature (°C)	Nominal Stress (MPa)	Extrusion	Test Order	Actual Stress (MPa)	Rate (1/h)	Time In			Time To 1% Strain (h)	Life (h)	Total Elongation (%)
						Stage 1 (h)	Stage 2 (h)	Stage 3 (h)			
500	72.9	L-3097	10	72.9	3.63E-05	250.26	349.88	59.98	82.82	660.12	3.64
500	72.9	L-3104	47	72.9	8.37E-05	50.20	349.76	46.49	52.70	446.44	5.00
500	72.9	L-3105	39	72.9	6.71E-05	40.29	359.93	128.45	17.30	528.67	4.25
500	72.9	L-3106	36	72.9	1.07E-04	49.76	200.43	21.99	33.76	272.18	3.93
500	72.9	L-3107	29	72.9	1.07E-04	25.03	249.65	100.47	33.71	375.15	5.32
500	72.9	L-3108	28	72.9	1.31E-05	199.95	900.01	169.26	95.67	1269.22	2.59
500	84.0	L-3097	5	84.0	4.41E-05	80.09	399.47	76.47	70.59	556.03	3.68
500	84.0	L-3104	43	84.0	8.76E-05	50.10	275.06	32.12	43.60	357.28	4.07
500	84.0	L-3105	25	84.0	3.44E-04	36.04	51.98	31.49	11.67	119.51	6.03
500	84.0	L-3106	45	84.0	1.92E-04	10.28	89.97	87.97	8.28	188.23	5.97
500	84.0	L-3107	49	84.0	3.19E-04	15.98	99.62	8.50	21.63	124.09	4.64
500	84.0	L-3108	6	84.0	2.71E-04	12.14	107.46	28.99	5.64	148.59	5.75

Table A - 1
Results of Cu-8 Cr-4 Nb Creep Testing (Cont.)

Temperature (°C)	Nominal Stress (MPa)	Extrusion	Test Order	Actual Stress (MPa)	Rate (1/h)	Time In			Time To 1% Strain (h)	Life (h)	Total Elongation (%)
						Stage 1 (h)	Stage 2 (h)	Stage 3 (h)			
500	92.8	L-3097	19	92.8	4.50E-05	250.15	369.64	51.85	33.51	671.65	4.49
500	92.8	L-3104	20	92.8	1.66E-03	2.87	25.02	5.00	0.87	32.89	6.99
500	92.8	L-3105	18	92.8	6.21E-04	3.91	48.48	17.99	4.91	70.39	6.36
500	92.8	L-3106	41	92.8	8.20E-04	4.06	33.39	6.00	0.63	43.45	5.19
500	92.8	L-3107	3	92.8	7.04E-05	60.17	400.02	117.84	60.17	578.03	5.07
500	92.8	L-3108	50	92.8	2.33E-04	20.05	99.97	22.99	11.56	143.02	4.60
650	37.4	L-3097	46	37.4	3.48E-05	149.66	450.48	49.48	125.67	649.63	3.67
650	37.4	L-3104	24	37.4	2.13E-04	40.12	51.48	43.49	7.77	135.08	5.87
650	37.4	L-3105	40	37.4	2.85E-04	16.44	83.47	8.50	17.69	108.41	4.17
650	37.4	L-3106	48	37.4	1.81E-04	20.14	160.31	8.00	14.15	188.45	4.71
650	37.4	L-3107	35	37.4	3.31E-04	7.22	92.86	11.50	7.72	111.57	4.85
650	37.4	L-3108	11	37.4	5.94E-05	150.06	309.89	70.48	78.58	530.43	4.11
650	44.3	L-3097	38	44.3	2.22E-04	15.68	88.76	10.50	11.84	114.93	3.71

Table A - 1
Results of Cu-8 Cr-4 Nb Creep Testing (Cont.)

Temperature (°C)	Nominal Stress (MPa)	Extrusion	Test Order	Actual Stress (MPa)	Rate (1/h)	Time In			Time To 1% Strain (h)	Life (h)	Total Elongation (%)
						Stage 1 (h)	Stage 2 (h)	Stage 3 (h)			
650	44.3	L-3104	26	44.3	1.61E-03	2.95	15.99	5.00	2.94	23.94	4.92
650	44.3	L-3105	12	44.3	1.04E-03	3.02	23.92	5.50	2.81	32.43	4.51
650	44.3	L-3106	7	44.3	8.84E-04	4.94	33.99	6.50	3.64	45.42	5.05
650	44.3	L-3107	1	44.3	4.25E-04	15.22	44.48	15.49	15.72	75.20	4.04
650	44.3	L-3108	13	44.3	8.76E-04	5.04	32.49	2.75	5.96	40.28	4.37
650	49.8	L-3097	27	49.8	3.51E-04	6.01	68.48	2.50	15.51	76.99	3.68
650	49.8	L-3104	17	49.8	1.74E-03	2.34	14.00	3.00	0.95	19.33	5.39
650	49.8	L-3105	4	49.8	2.07E-03	2.99	12.03	6.16	2.57	21.19	5.72
650	49.8	L-3106	37	49.8	2.69E-03	1.60	6.41	4.50	2.35	12.50	4.57
650	49.8	L-3107	23	49.8	2.81E-03	2.00	7.55	4.58	1.79	14.13	5.21
650	49.8	L-3108	2	49.8	7.83E-04	9.82	20.49	9.00	4.45	39.32	4.24
800	19.2	L-3097	54	19.2	3.67E-04	30.09	34.99	24.49	7.60	89.57	5.25
800	19.2	L-3104	9	19.2	8.46E-04	9.79	31.99	20.49	2.80	62.28	7.07

Table A - 1
Results of Cu-8 Cr-4 Nb Creep Testing (Cont.)

Temperature (°C)	Nominal Stress (MPa)	Extrusion	Test Order	Actual Stress (MPa)	Rate (1/h)	Time In			Time To 1% Strain (h)	Life (h)	Total Elongation (%)
						Stage 1 (h)	Stage 2 (h)	Stage 3 (h)			
800	19.2	L-3105	31	19.2	1.10E-03	4.97	29.99	14.00	1.26	48.95	7.51
800	19.2	L-3106	51	19.2	1.19E-03	5.19	34.49	10.00	2.19	49.68	7.63
800	19.2	L-3107	15	19.2	1.42E-03	4.01	27.51	7.00	0.94	38.52	7.36
800	19.2	L-3108	16	19.2	1.23E-03	4.71	24.99	9.00	1.56	38.70	6.96
800	23.3	L-3097	32	23.3	1.13E-03	5.02	27.46	7.50	2.27	39.97	5.91
800	23.3	L-3104	14	23.3	7.23E-03	0.95	6.01	1.58	0.38	8.55	7.88
800	23.3	L-3105	30	23.3	3.32E-03	1.98	14.04	2.50	1.30	18.52	8.53
800	23.3	L-3106	52	23.3	6.39E-03	0.96	5.75	2.00	0.91	8.70	6.61
800	23.3	L-3107	8	23.3	7.46E-03	0.65	7.25	1.50	0.46	9.40	8.60
800	23.3	L-3108	42	23.3	2.02E-03	3.98	13.40	2.75	0.54	20.13	6.03
800	26.8	L-3097	34	26.8	3.84E-03	1.99	7.98	3.00	0.72	12.97	6.87
800	26.8	L-3104	44	26.8	8.81E-03	0.75	4.20	0.00	0.63	4.96	4.97
800	26.8	L-3105	33	26.8	1.05E-02	0.97	2.94	1.50	0.14	5.41	8.07

Table A - 1
Results of Cu-8 Cr-4 Nb Creep Testing (Cont.)

Temperature (°C)	Nominal Stress (MPa)	Extrusion	Test Order	Actual Stress (MPa)	Rate (1/h)	Time In			Time To 1% Strain (h)	Life (h)	Total Elongation (%)
						Stage 1 (h)	Stage 2 (h)	Stage 3 (h)			
800	26.8	L-3106	21	26.8	1.79E-02	0.45	2.15	0.50	0.20	3.10	6.68
800	26.8	L-3107	53	26.8	7.37E-03	0.47	4.50	2.00	0.23	6.97	6.87
800	26.8	L-3108	22	26.8	9.92E-03	0.75	2.89	1.67	0.38	5.30	7.01

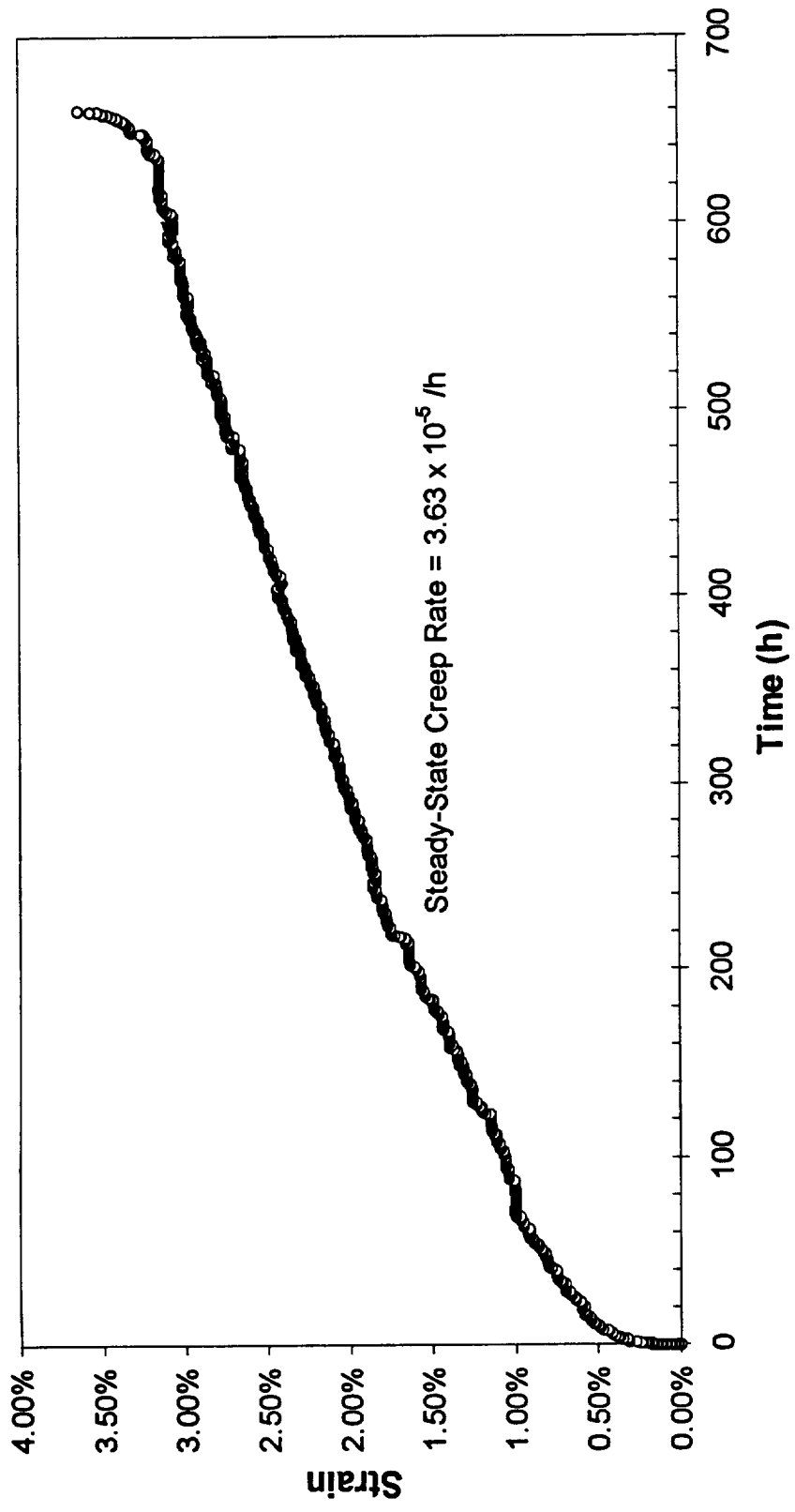


Figure A - 1 -
Extrusion L-3097 Tested At 500°C/72.9 MPa

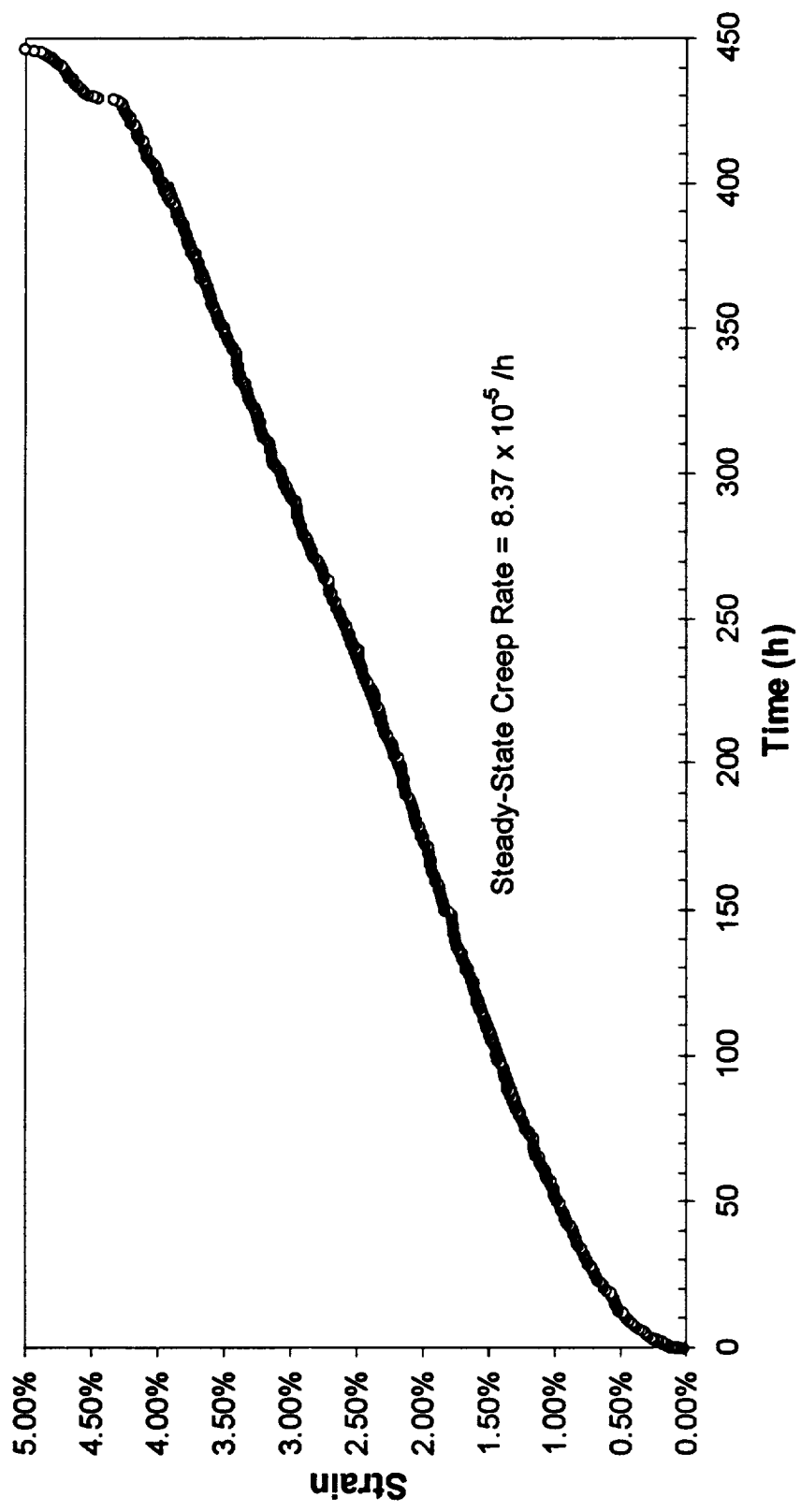


Figure A - 2 -
Extrusion L-3104 Tested At 500°C/72.9 MPa

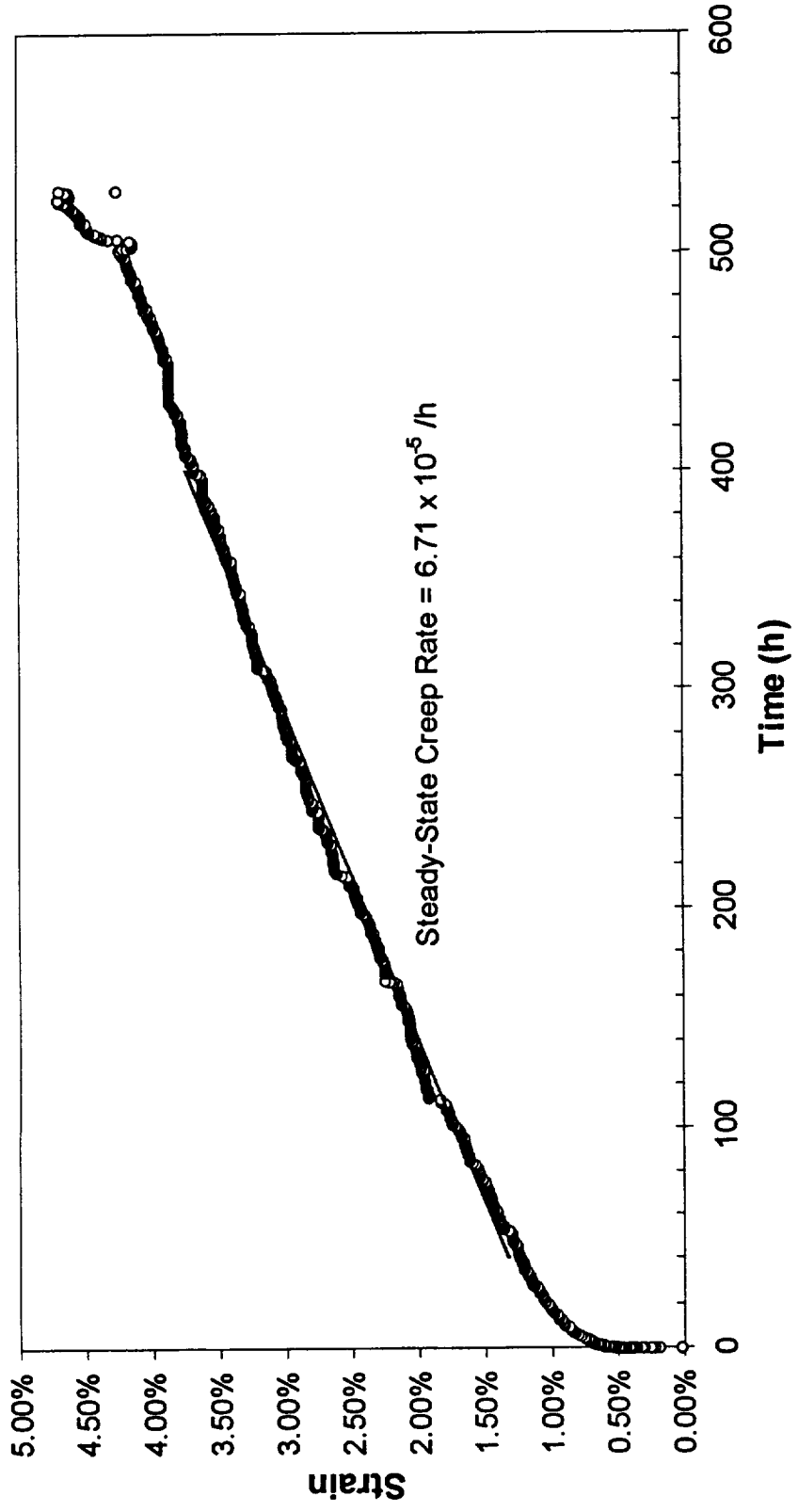


Figure A - 3 -
Extrusion L-3105 Tested At 500°C/72.9 MPa

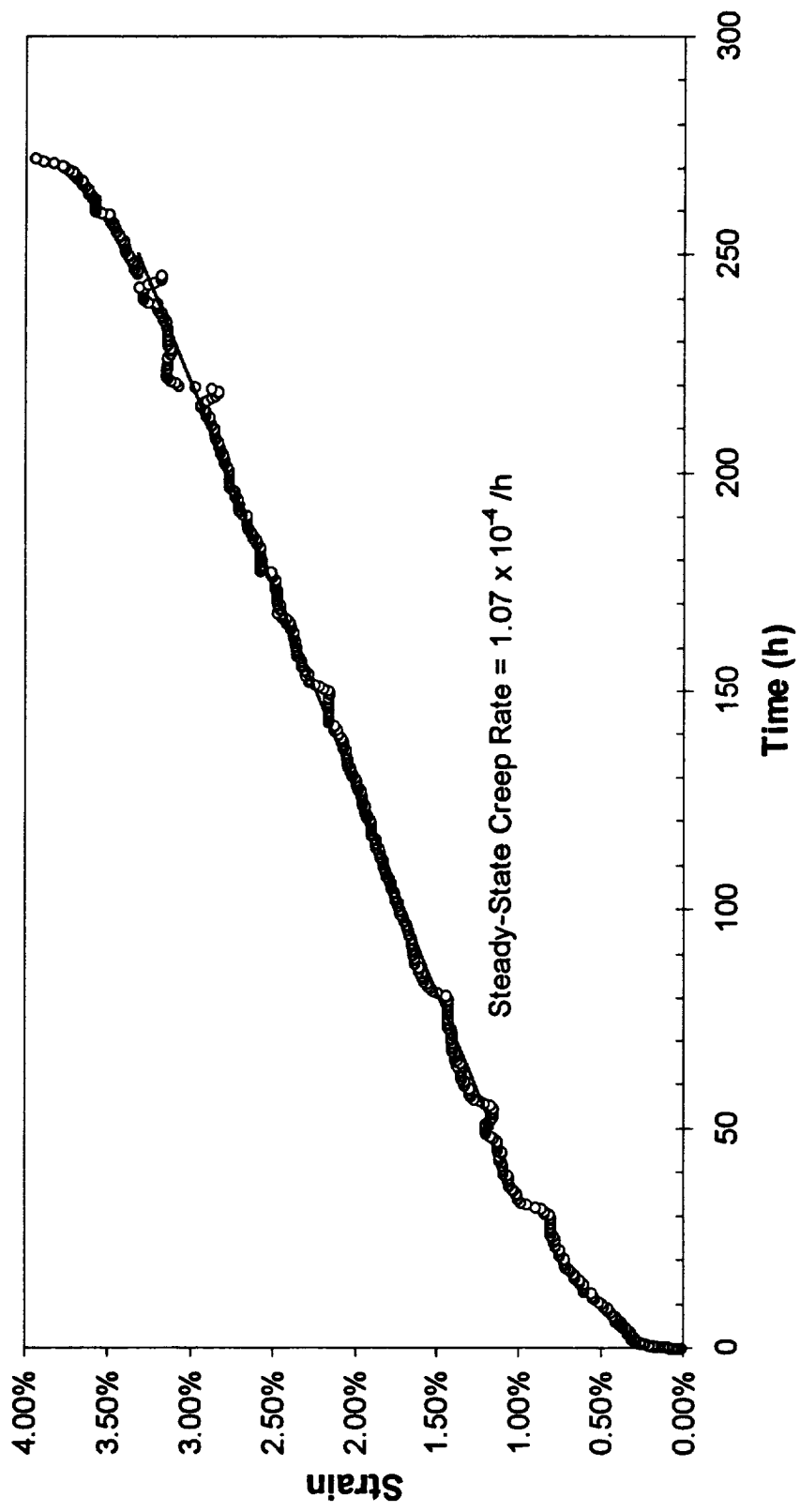


Figure A - 4 -
Extrusion L-3106 Tested At 500°C/72.9 MPa

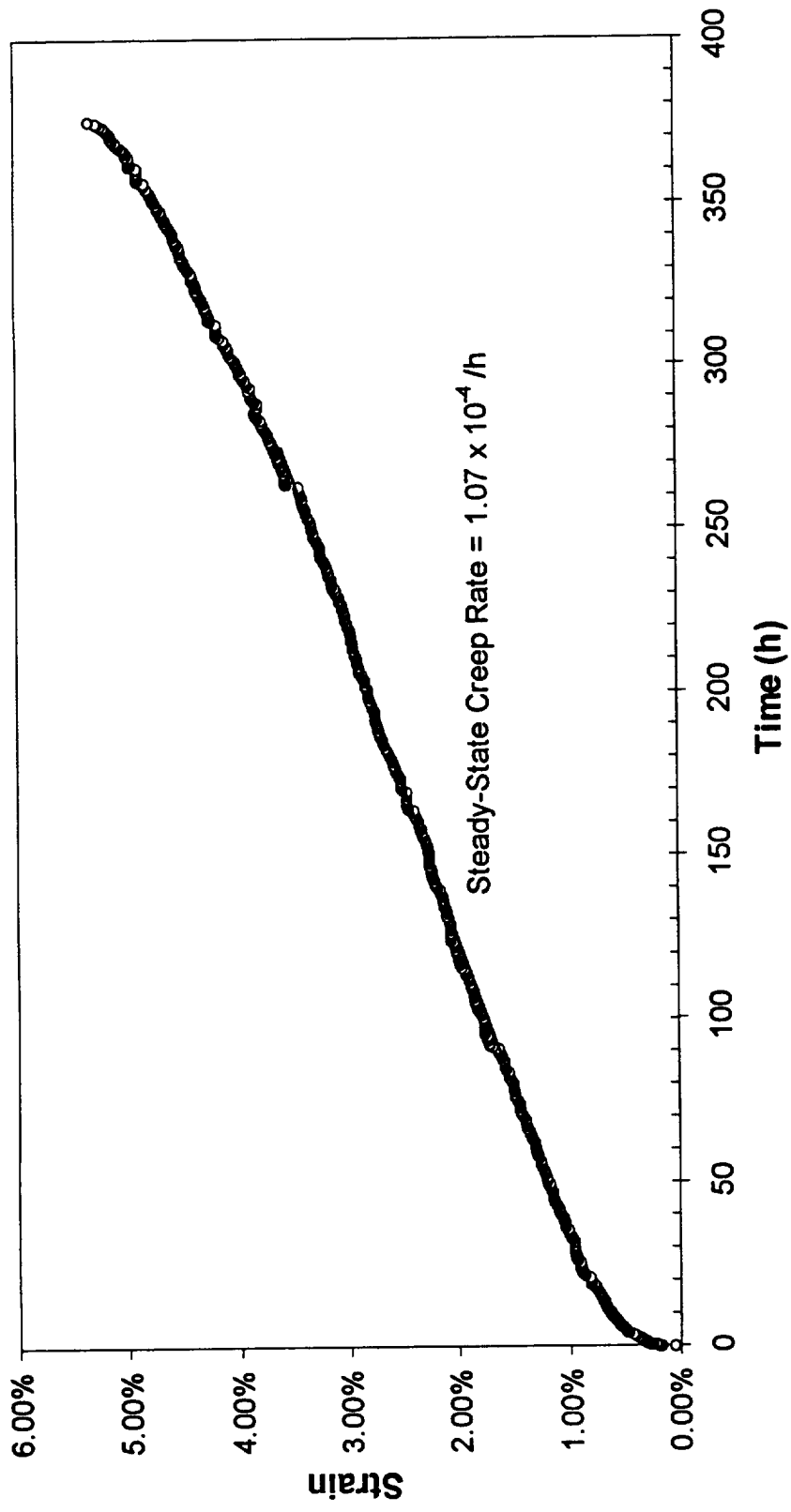


Figure A - 5 -
Extrusion L-3107 Tested At 500°C/72.9 MPa

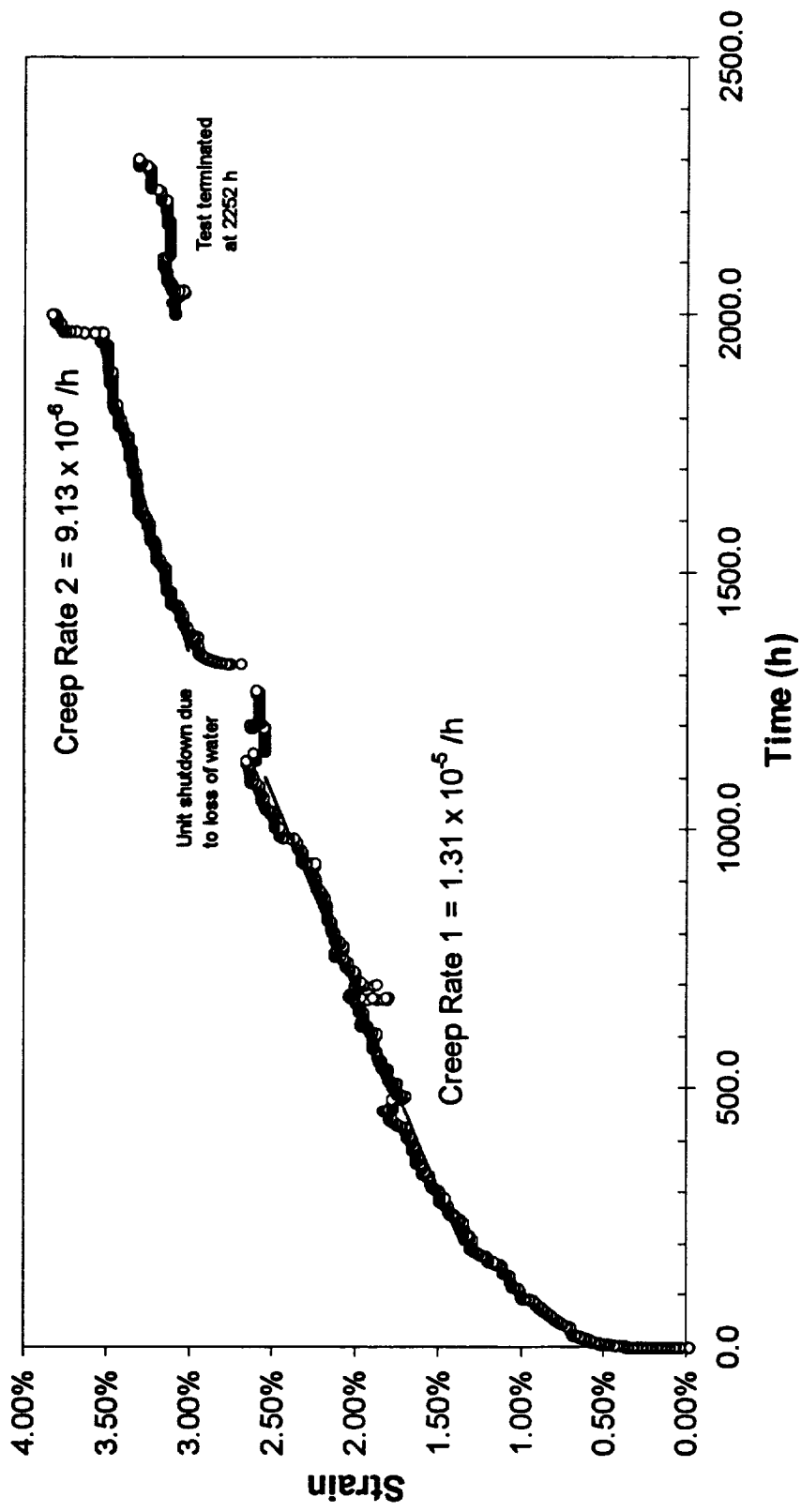


Figure A - 6 -
Extrusion L-3108 Tested At 500°C/72.9 MPa

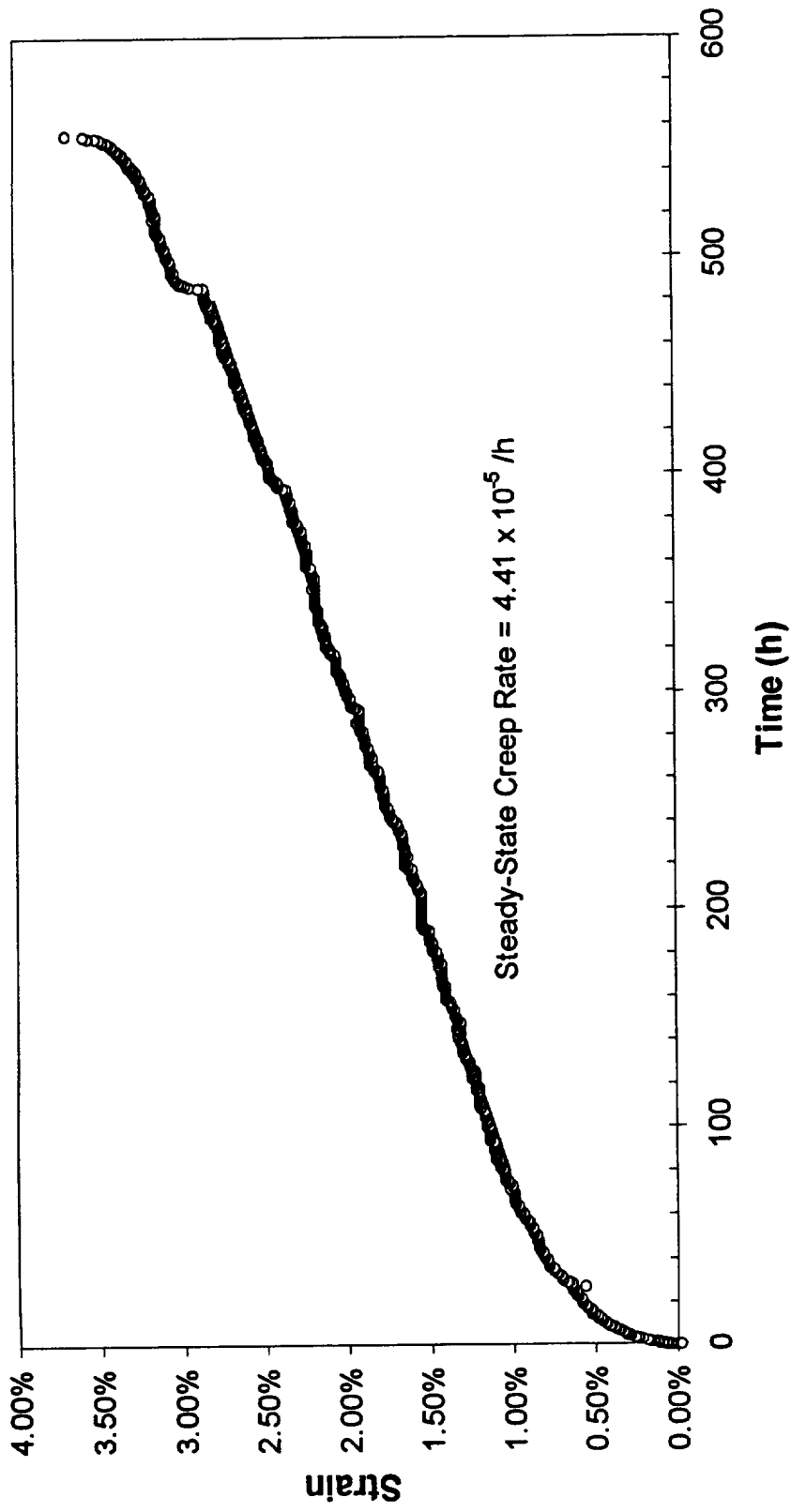


Figure A - 7 -
Extrusion L-3097 Tested At 500°C/84.0 MPa

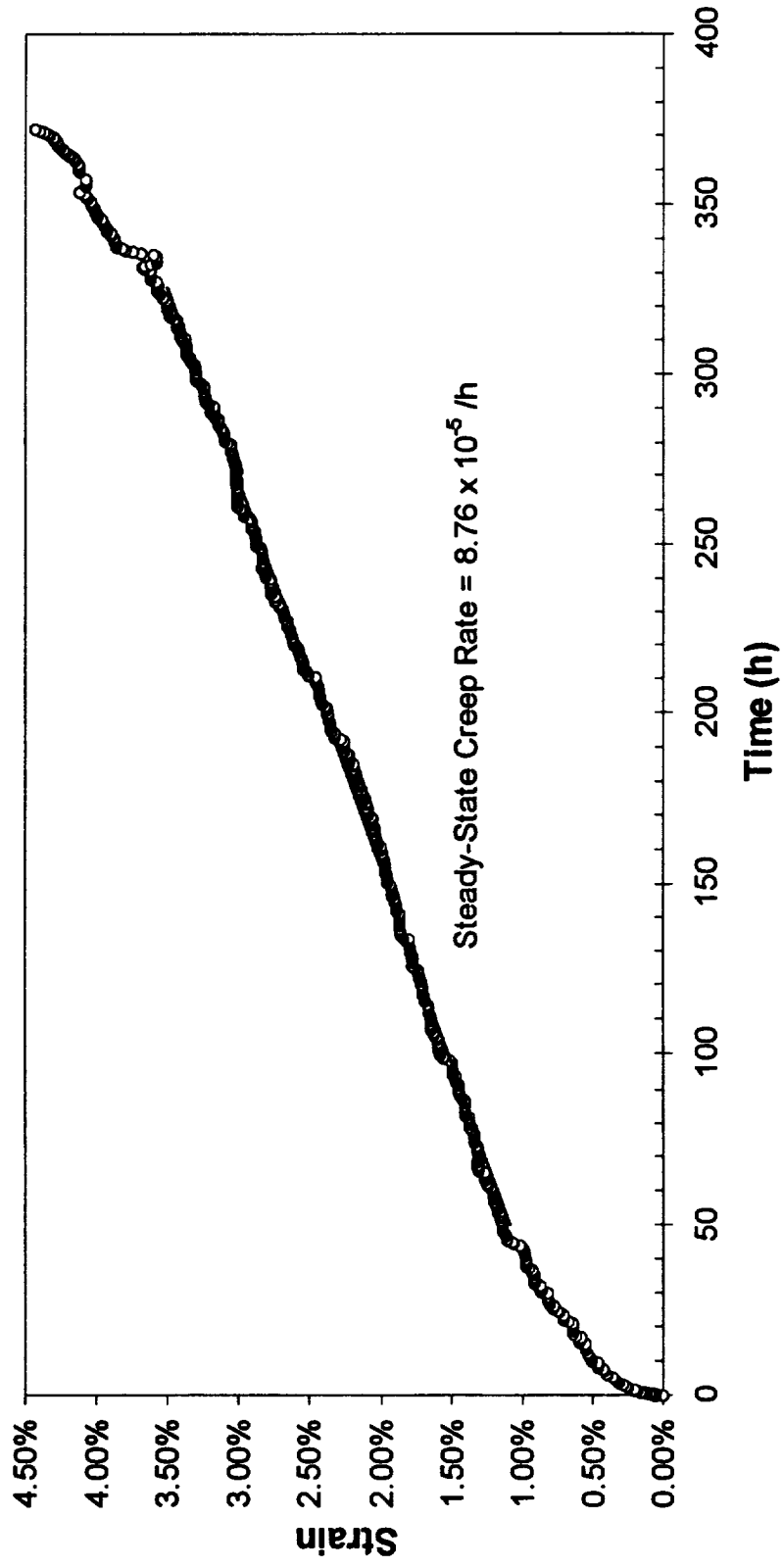


Figure A - 8 -
Extrusion L-3104 Tested At 500°C/84.0 MPa

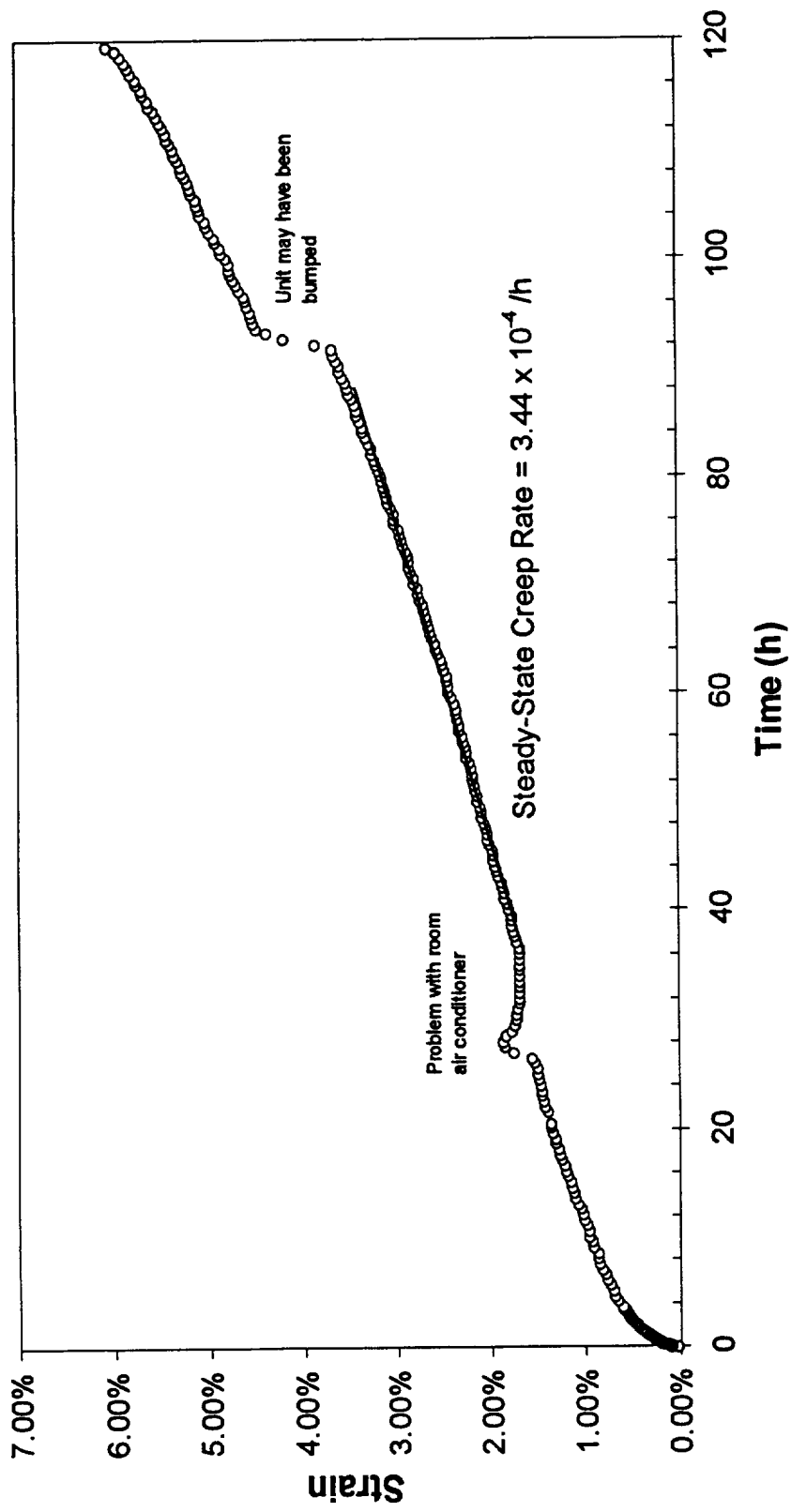


Figure A - 9 -
Extrusion L-3105 Tested At 500°C/84.0 MPa

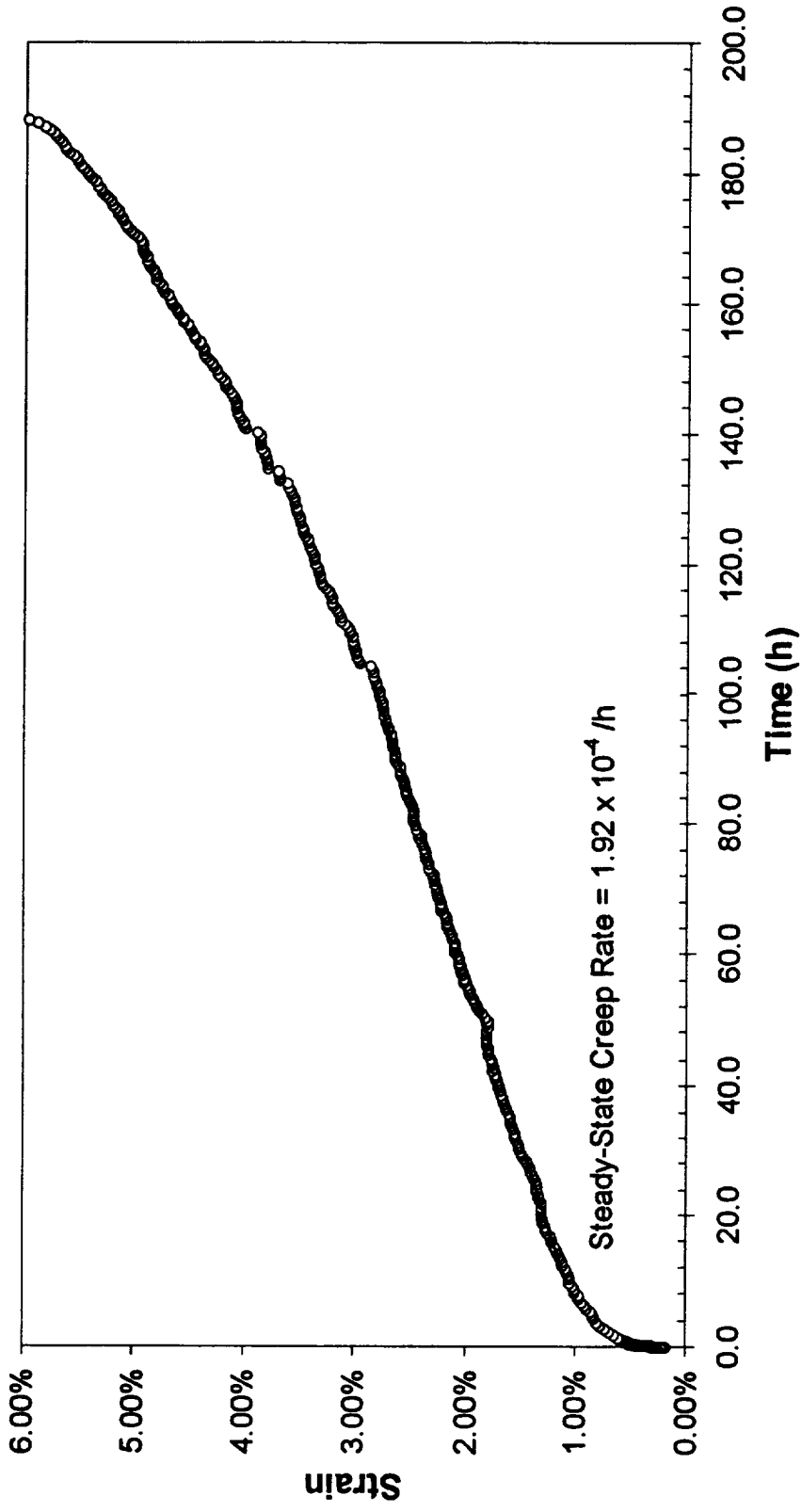


Figure A - 10 -
Extrusion L-3106 Tested At 500°C/84.0 MPa

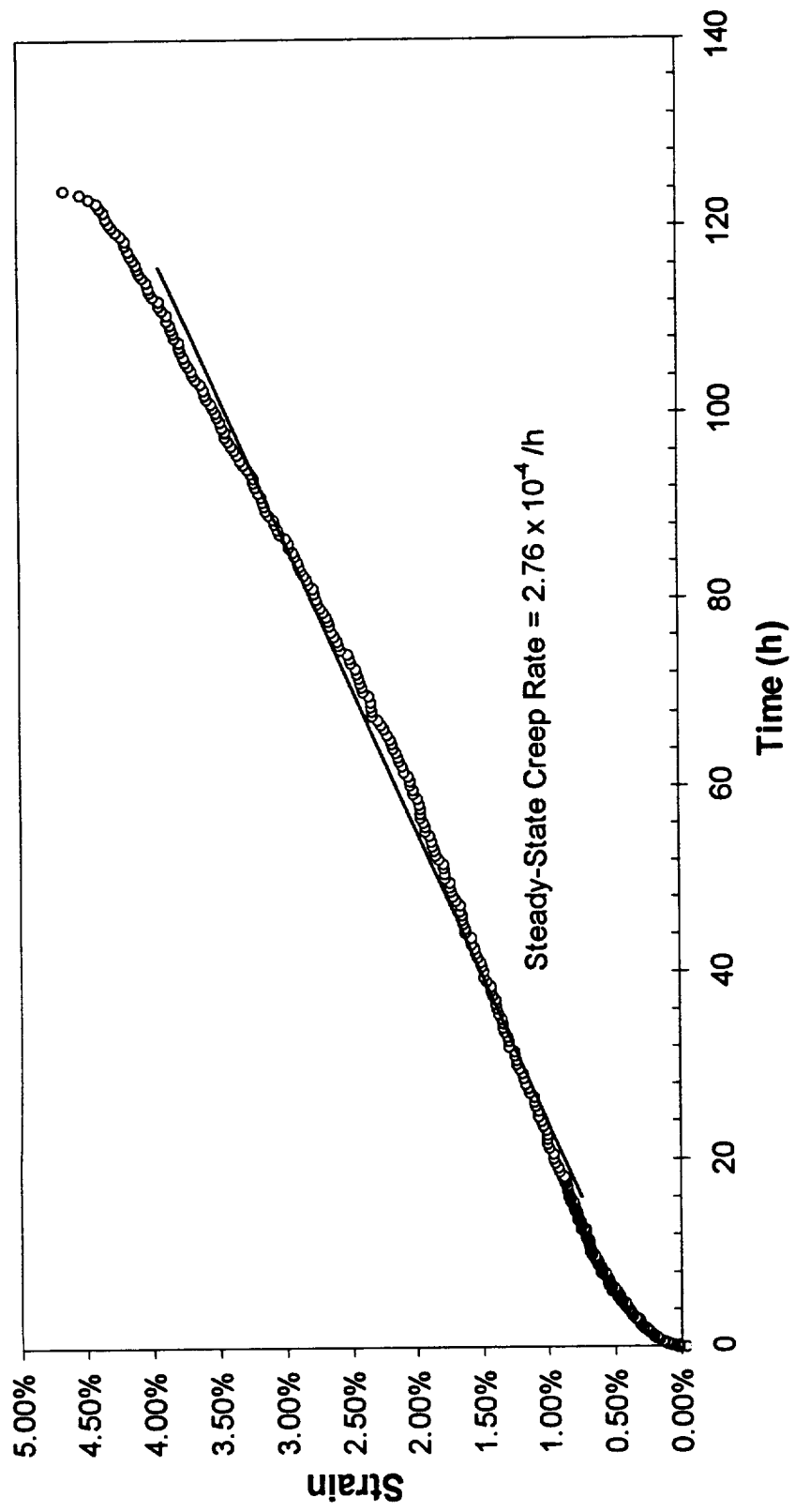


Figure A - 11 -
Extrusion L-3107 Tested At 500°C/84.0 MPa

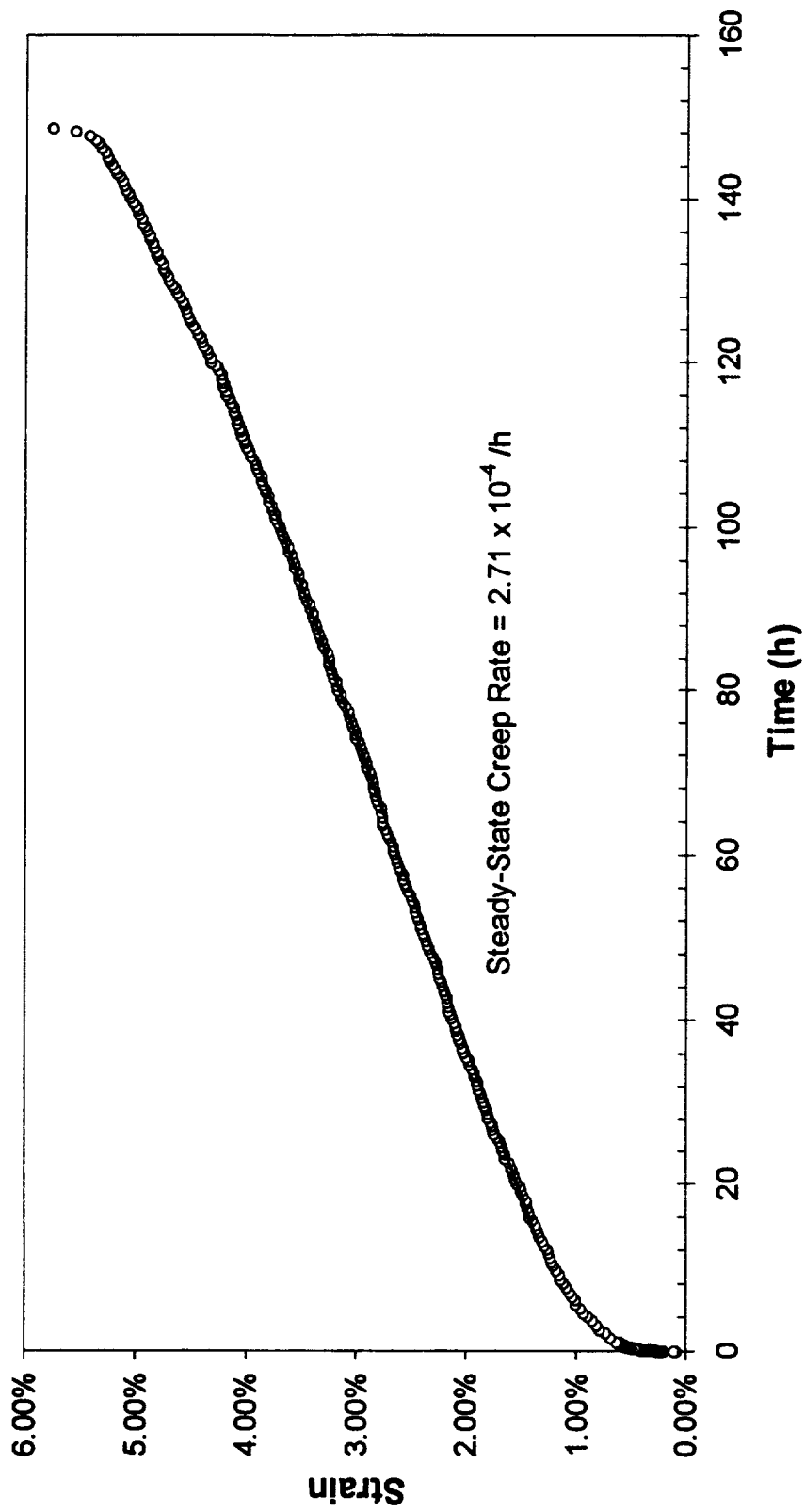


Figure A - 12 -
Extrusion L-3108 Tested At 500°C/84.0 MPa

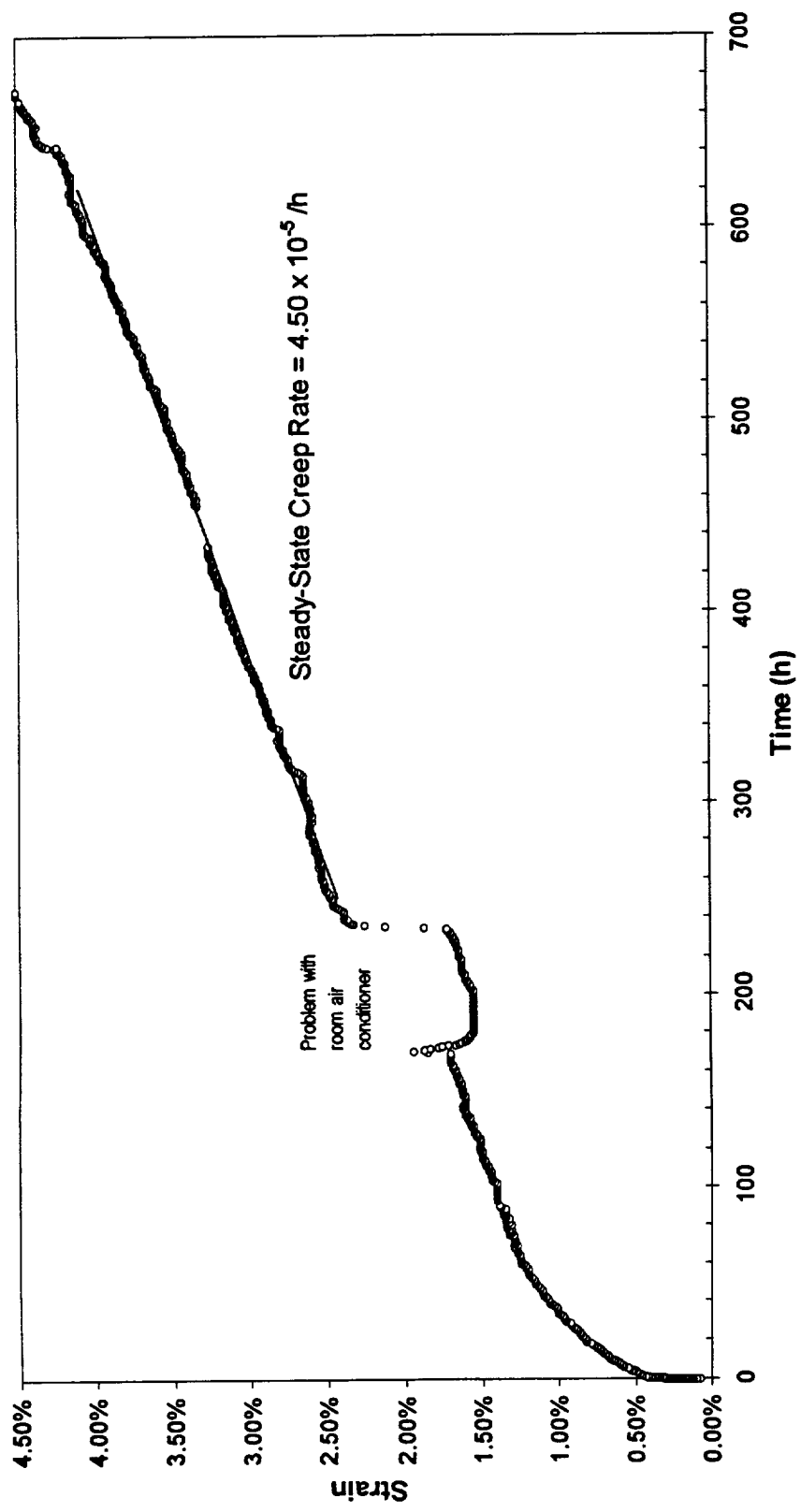


Figure A - 13 -
Extrusion L-3097 Tested At 500°C/92.8 MPa

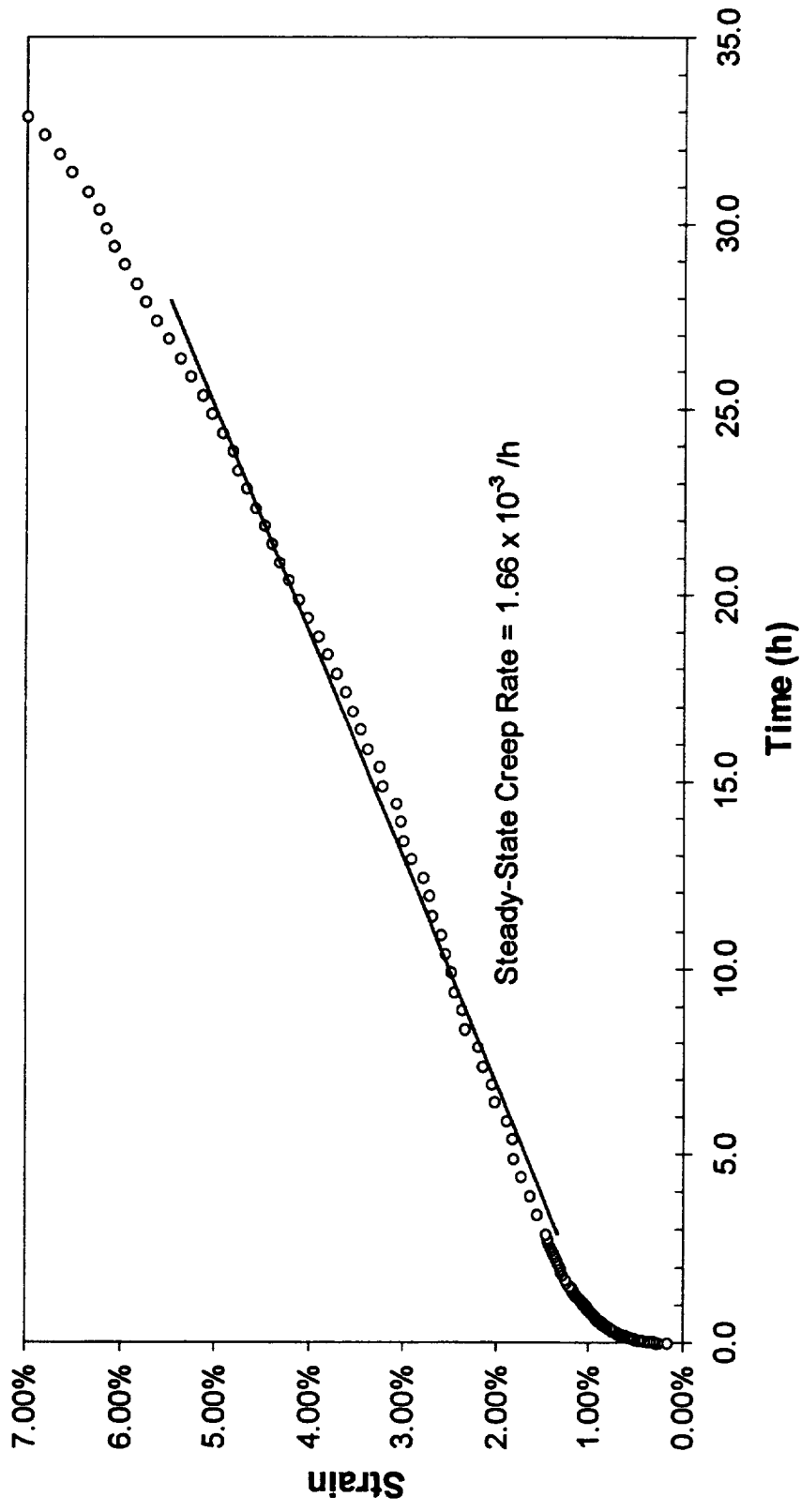


Figure A - 14 -
Extrusion L-3104 Tested At 500°C/92.8 MPa

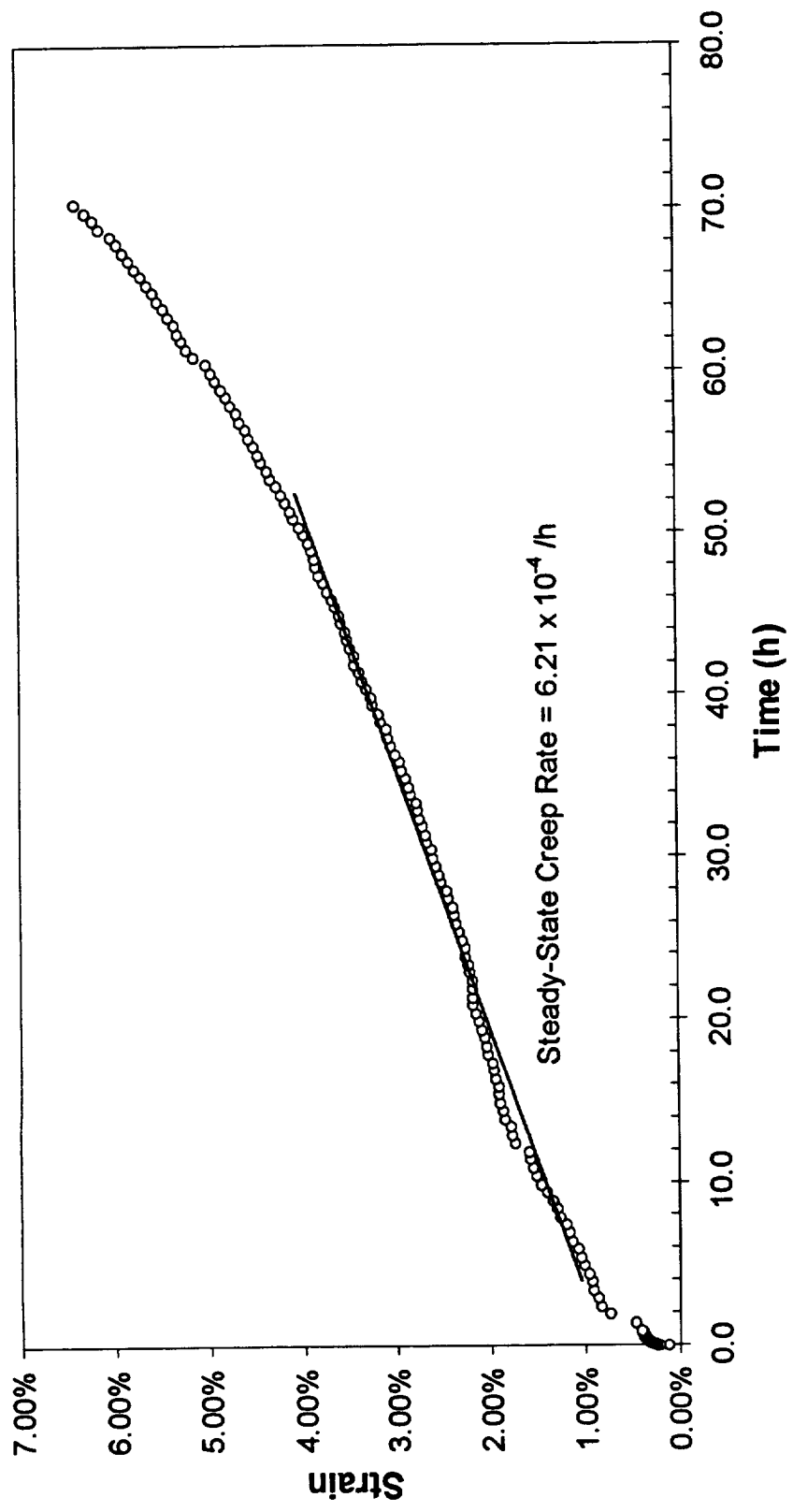


Figure A - 15 -
Extrusion L-3105 Tested At 500°C/92.8 MPa

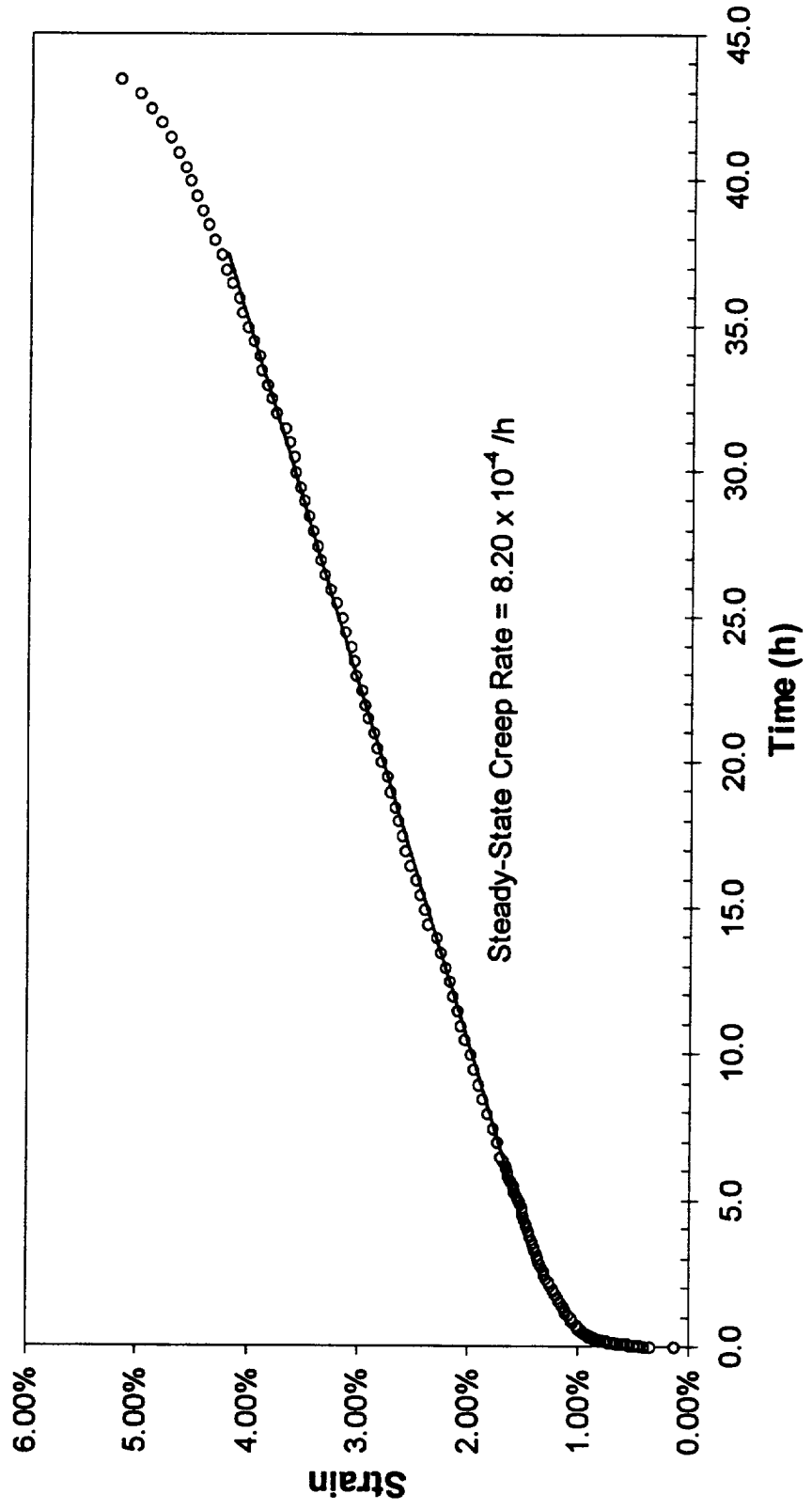


Figure A - 16 -
Extrusion L-3106 Tested At 500°C/92.8 MPa

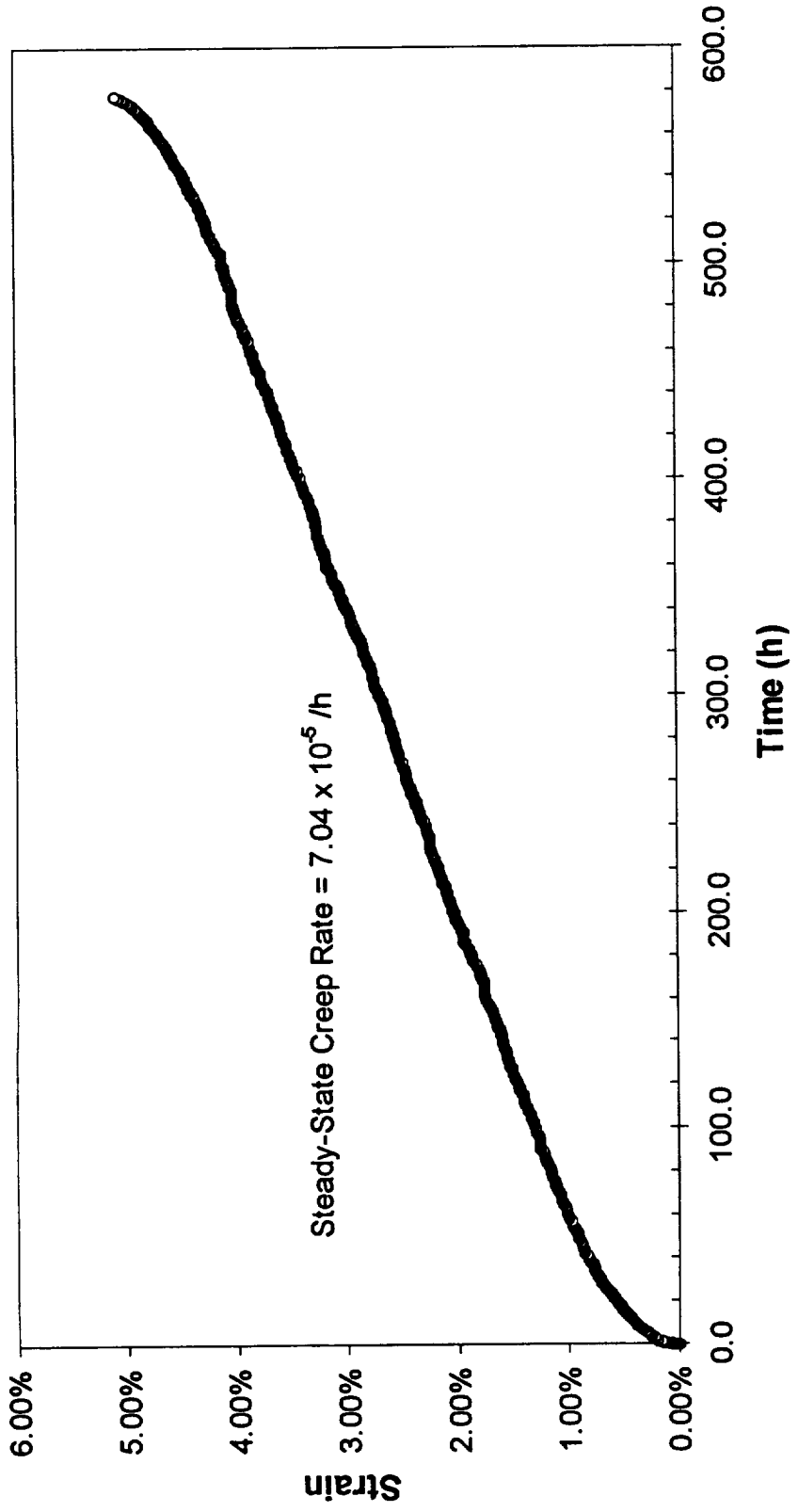


Figure A - 17 -
Extrusion L-3107 Tested At 500°C/92.8 MPa

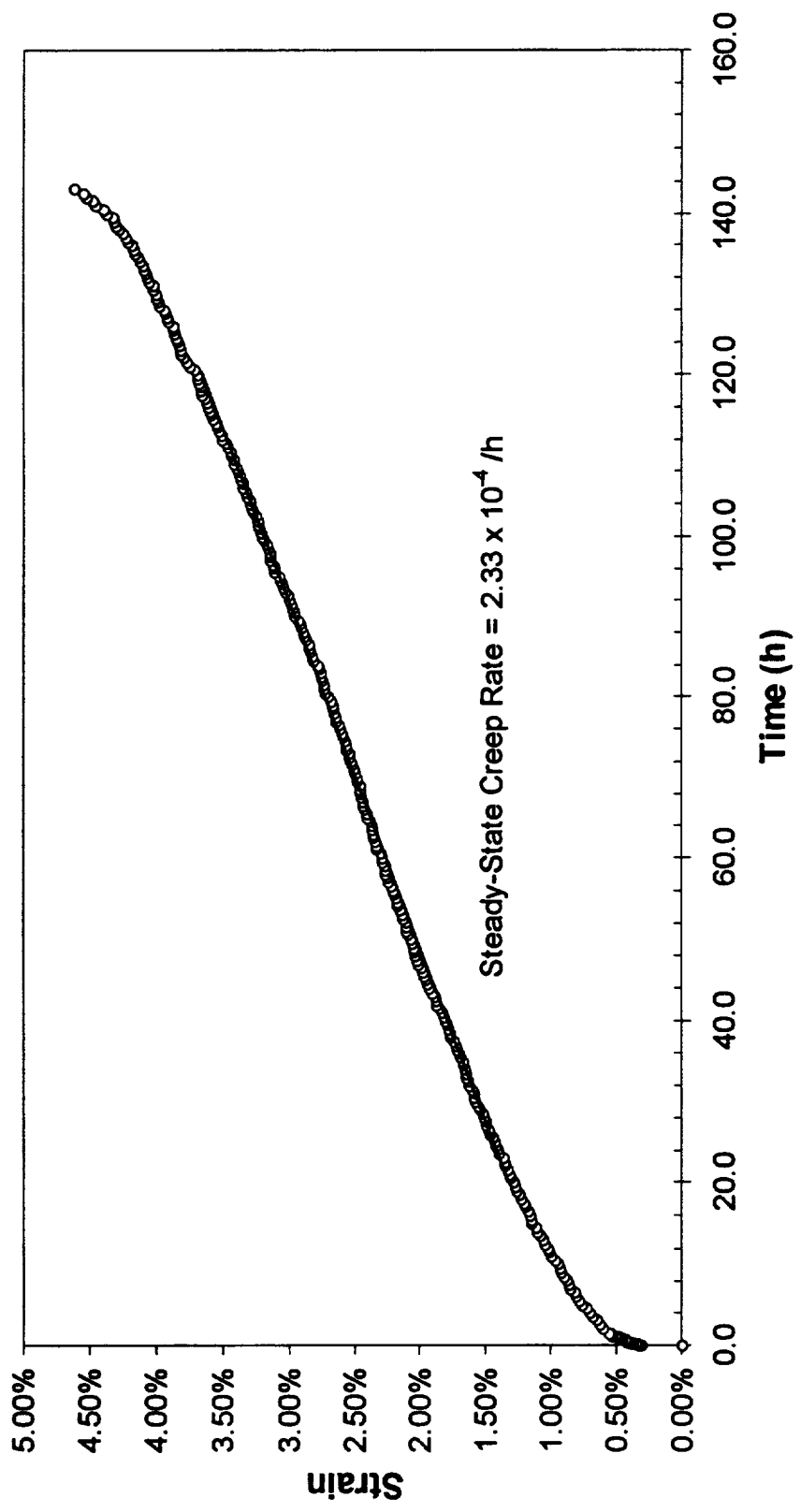


Figure A - 18 -
Extrusion L-3108 Tested At 500°C/92.8 MPa

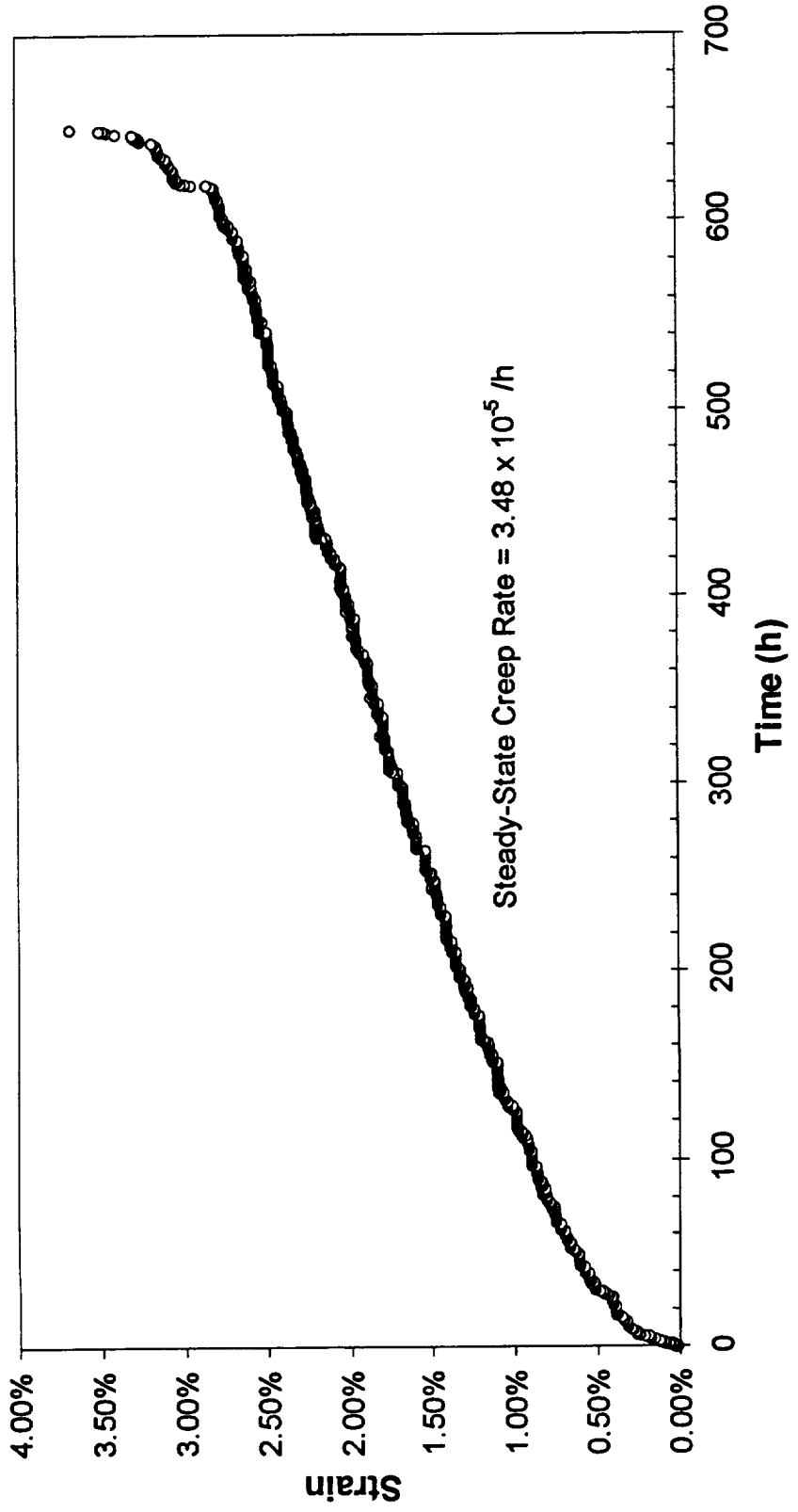


Figure A - 19 -
Extrusion L-3097 Tested At 650°C/37.4 MPa

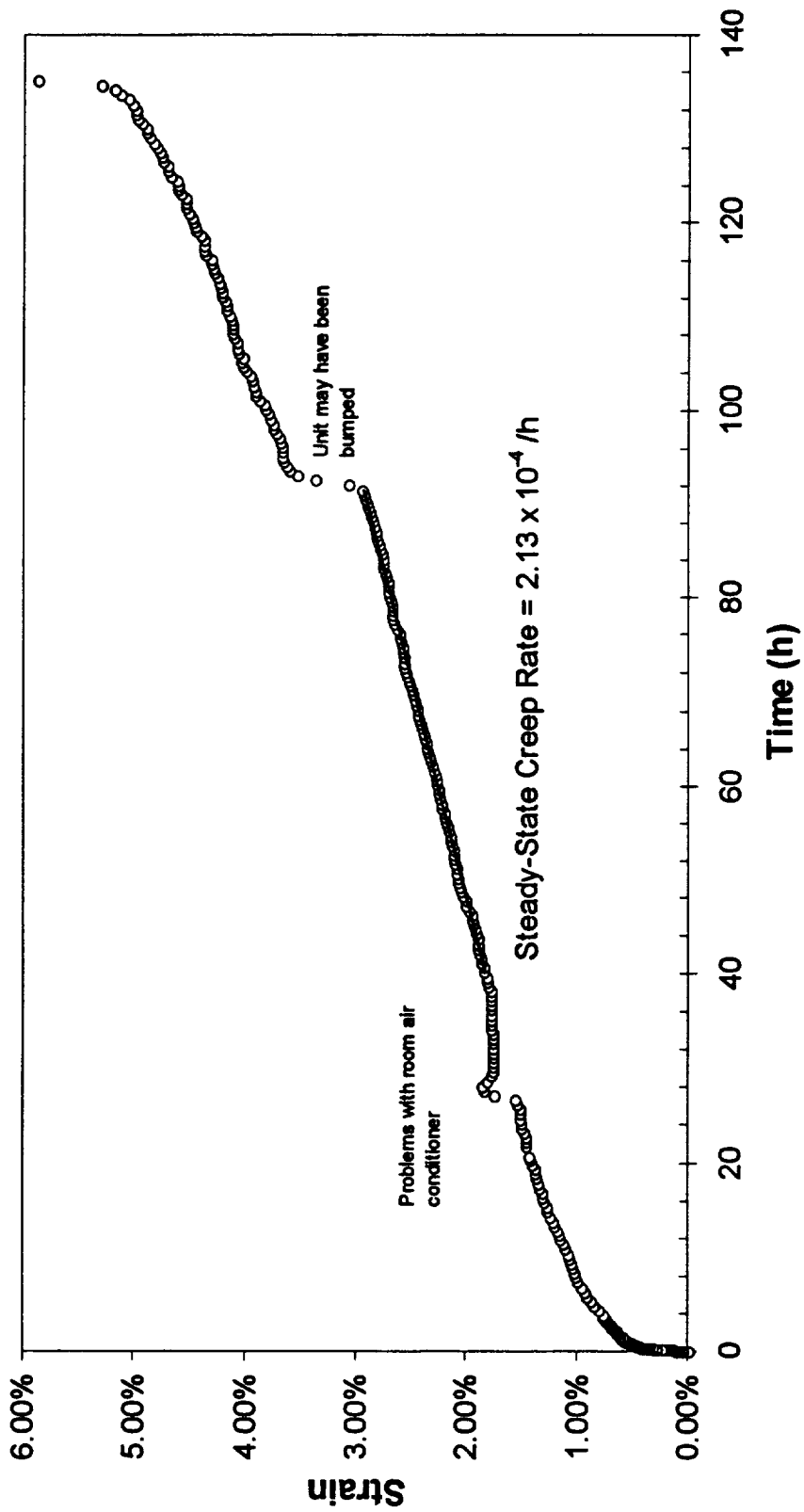


Figure A - 20 -
Extrusion L-3104 Tested At 650°C/37.4 MPa

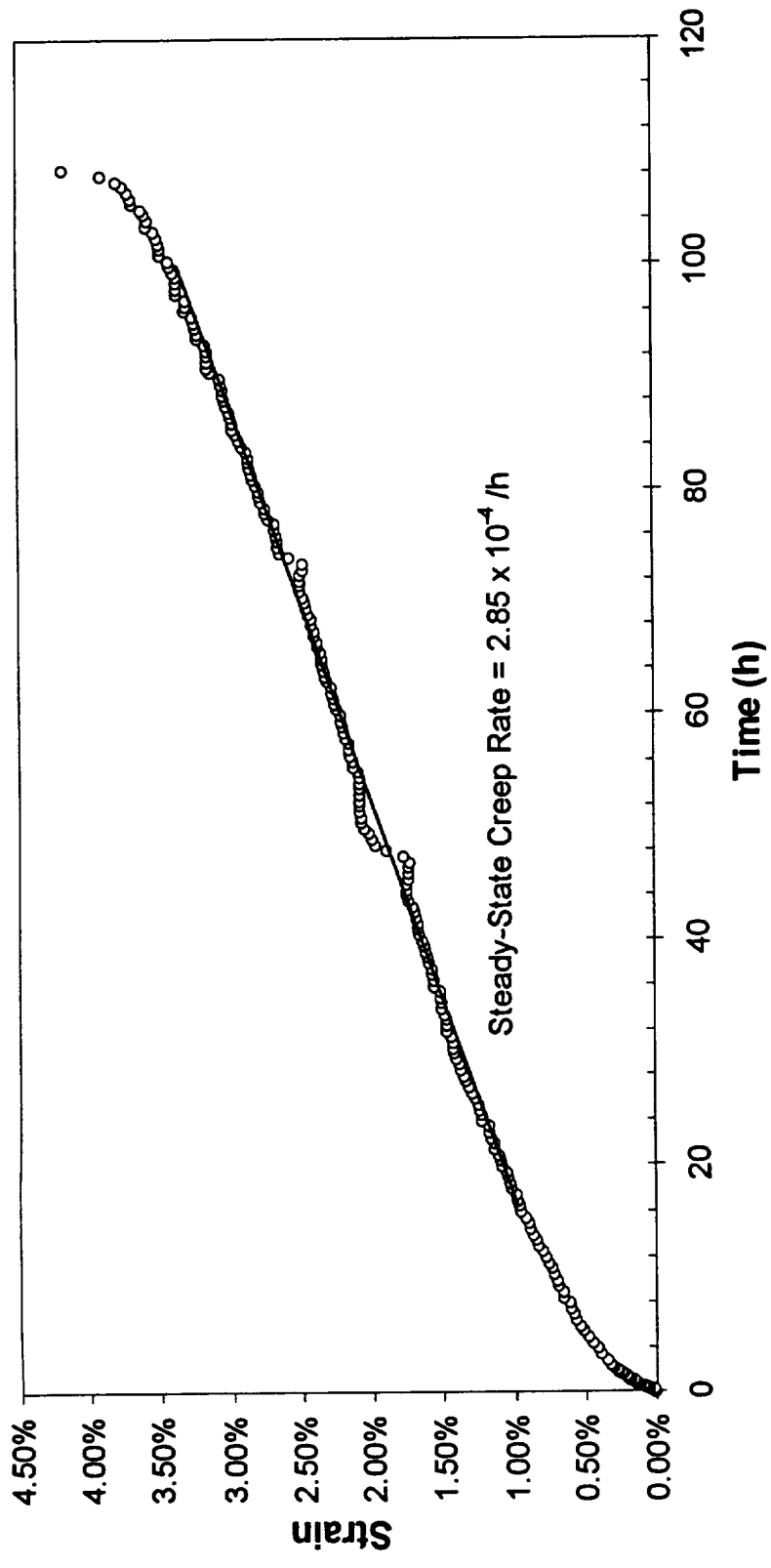


Figure A - 21 -
Extrusion L-3105 Tested At 650°C/37.4 MPa

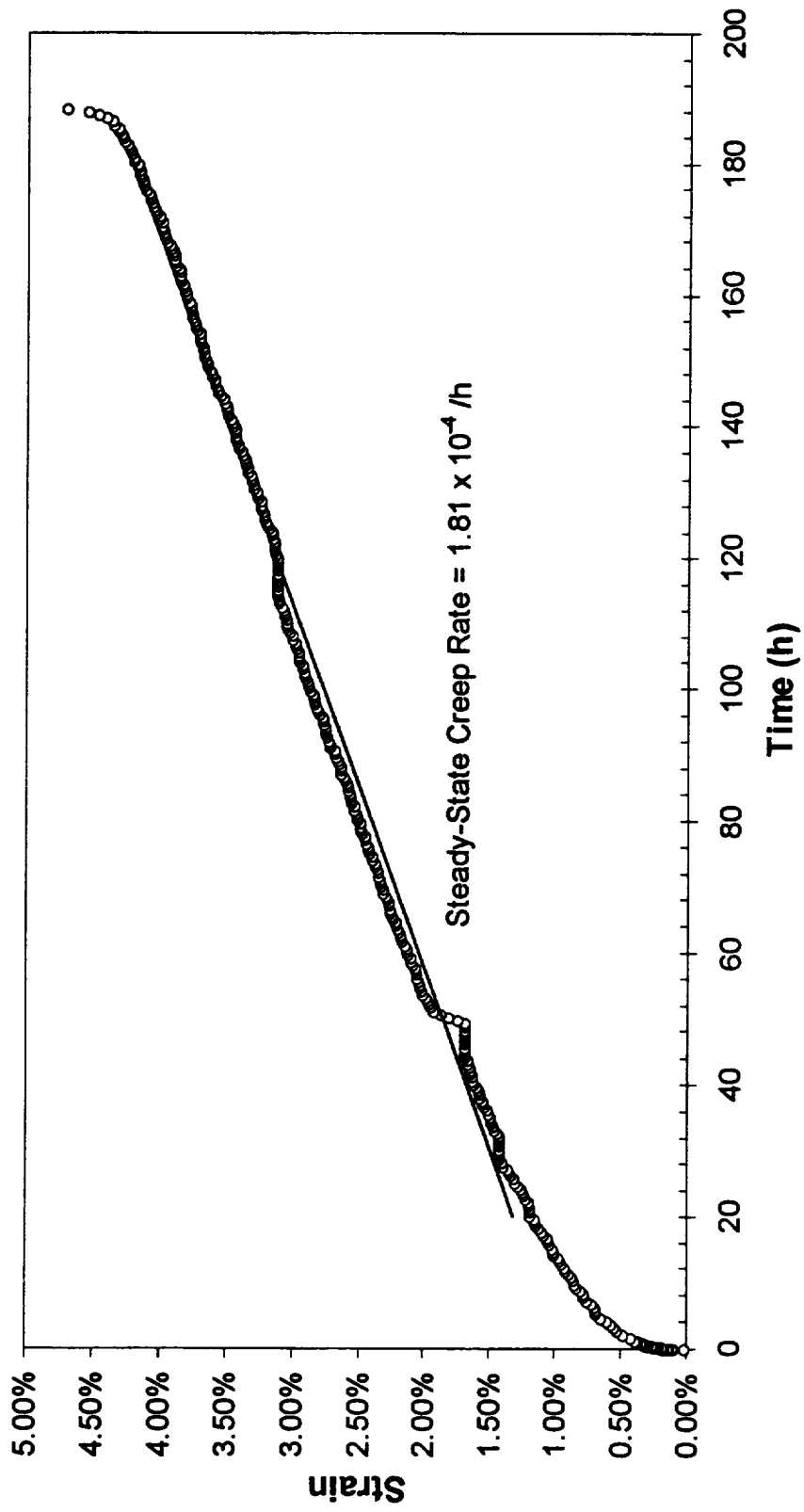


Figure A - 22 -
Extrusion L-3106 Tested At 650°C/37.4 MPa

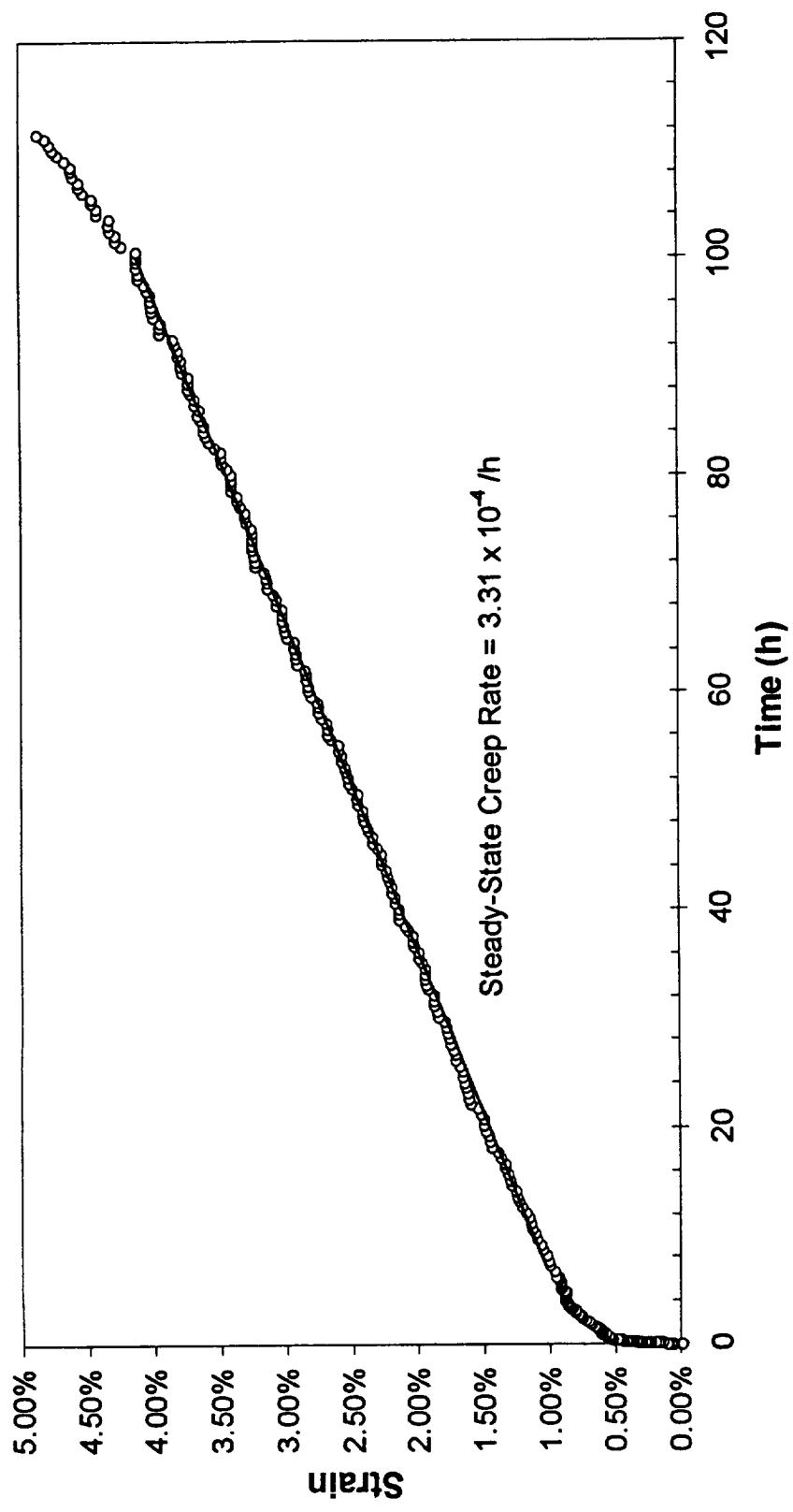


Figure A - 23 -
 Extrusion L-3107 Tested At 650°C/37.4 MPa

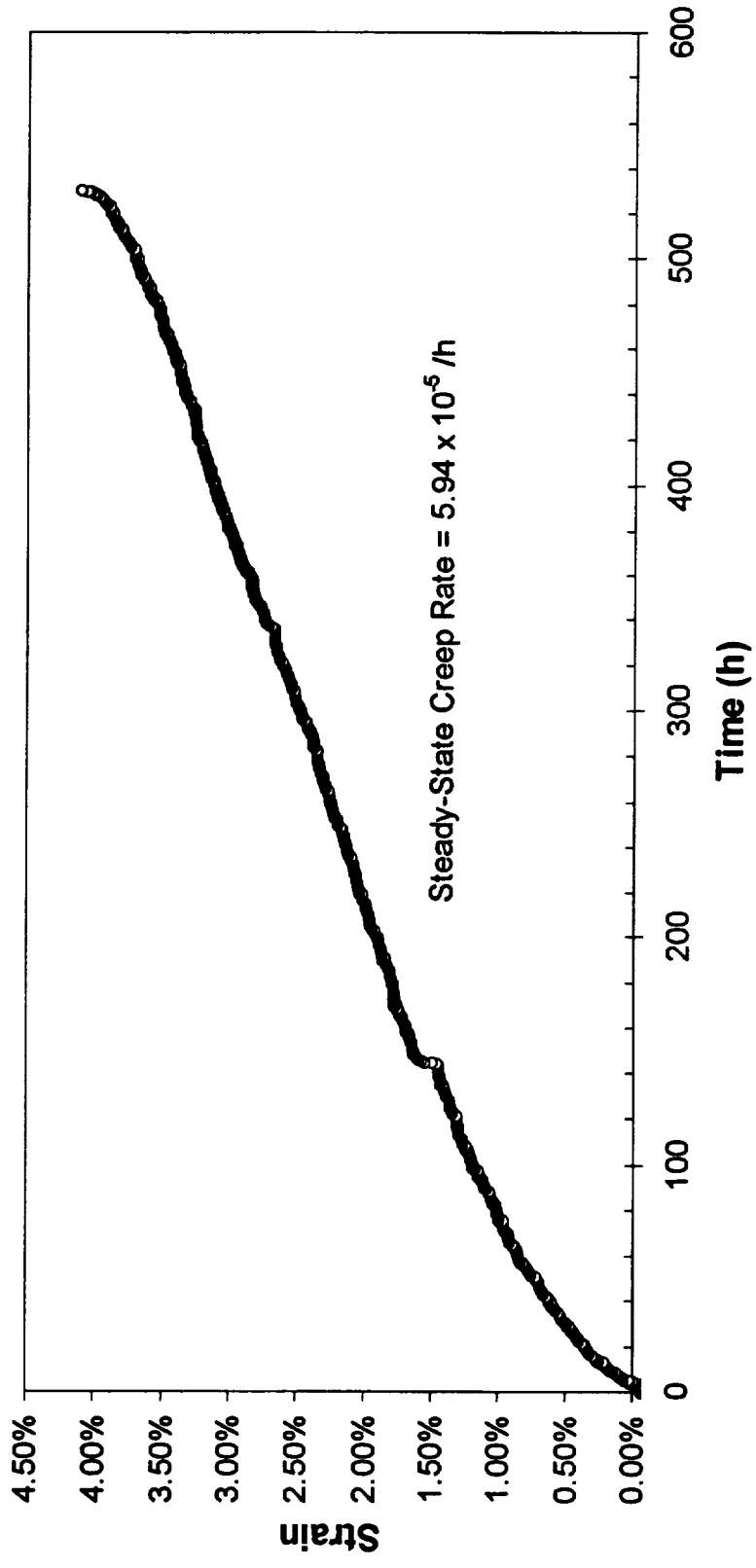


Figure A - 24 -
Extrusion L-3108 Tested At 650°C/37.4 MPa

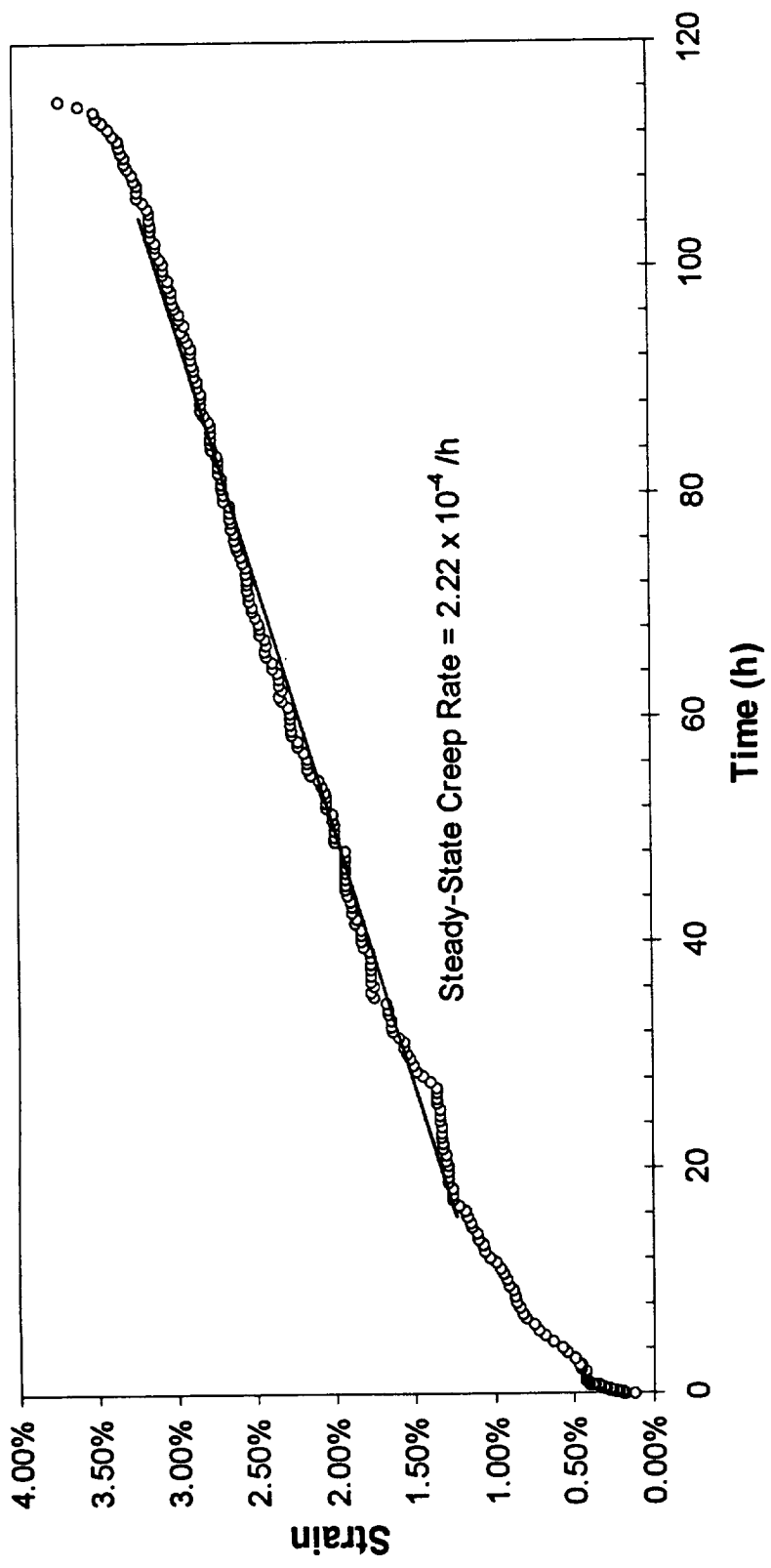


Figure A - 25 -
Extrusion L-3097 Tested At 650°C/44.3 MPa

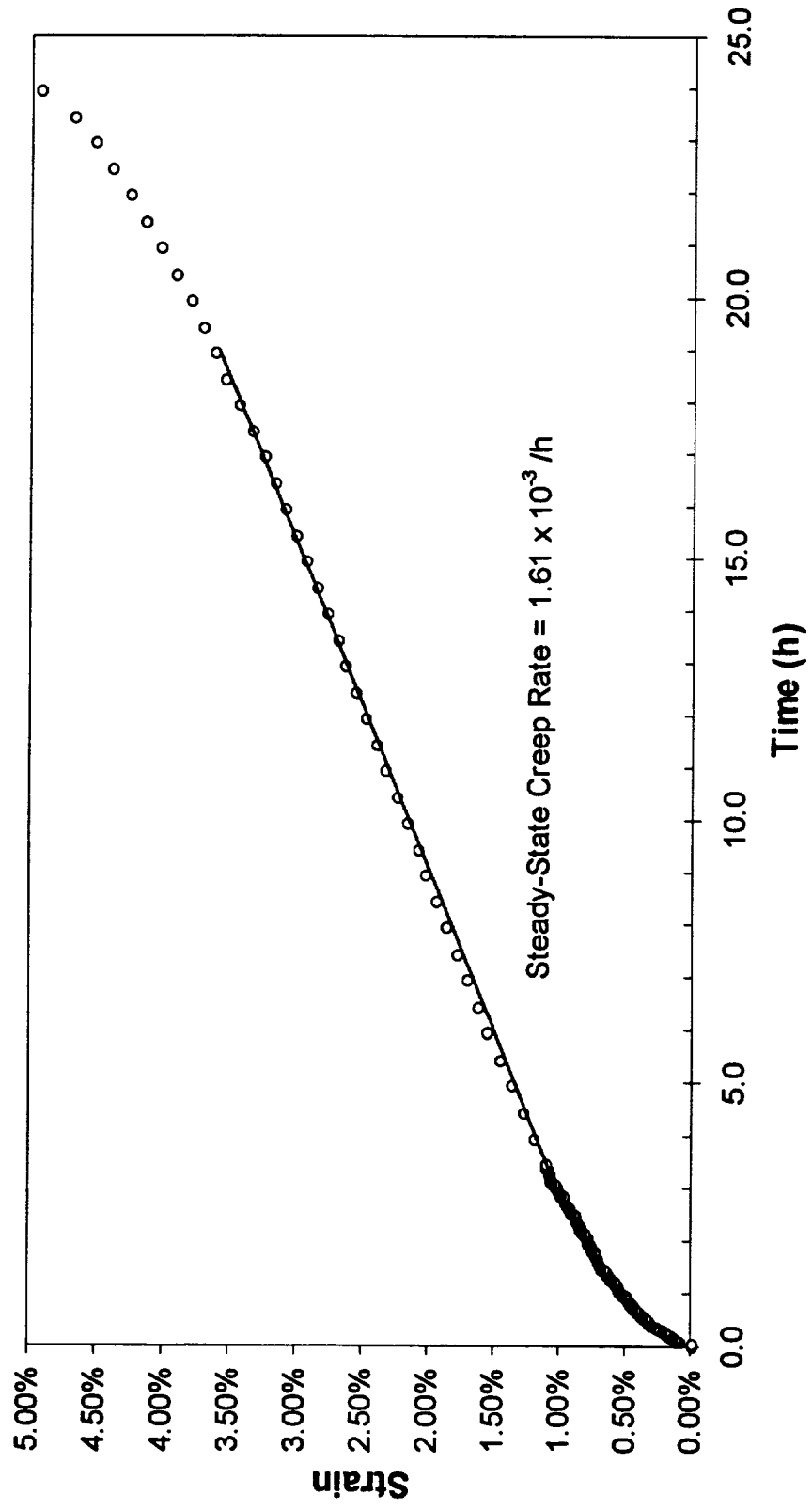


Figure A - 26 -
 Extrusion L-3104 Tested At 650°C/44.3 MPa

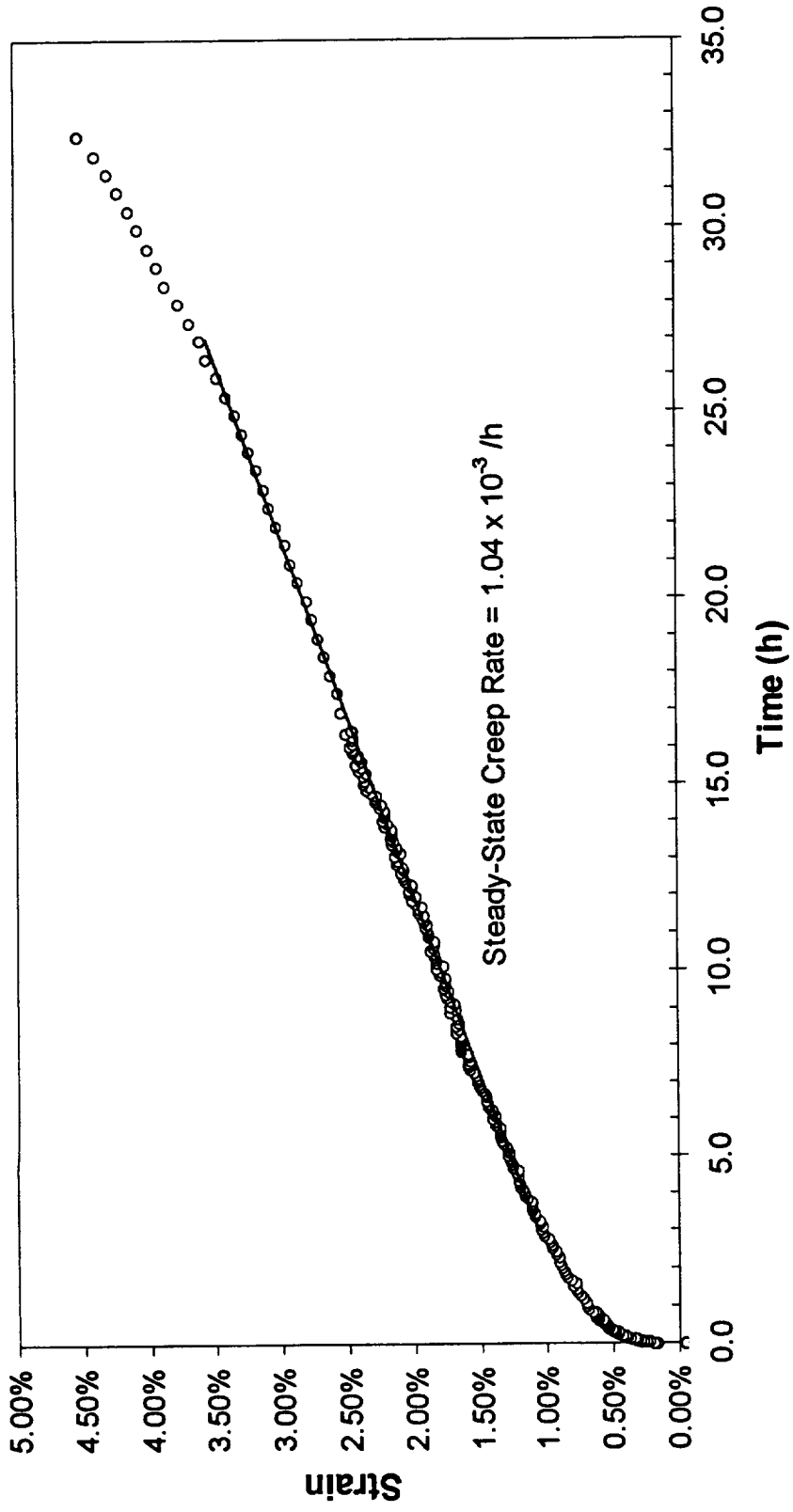


Figure A - 27 -
Extrusion L-3105 Tested At 650°C/44.3 MPa

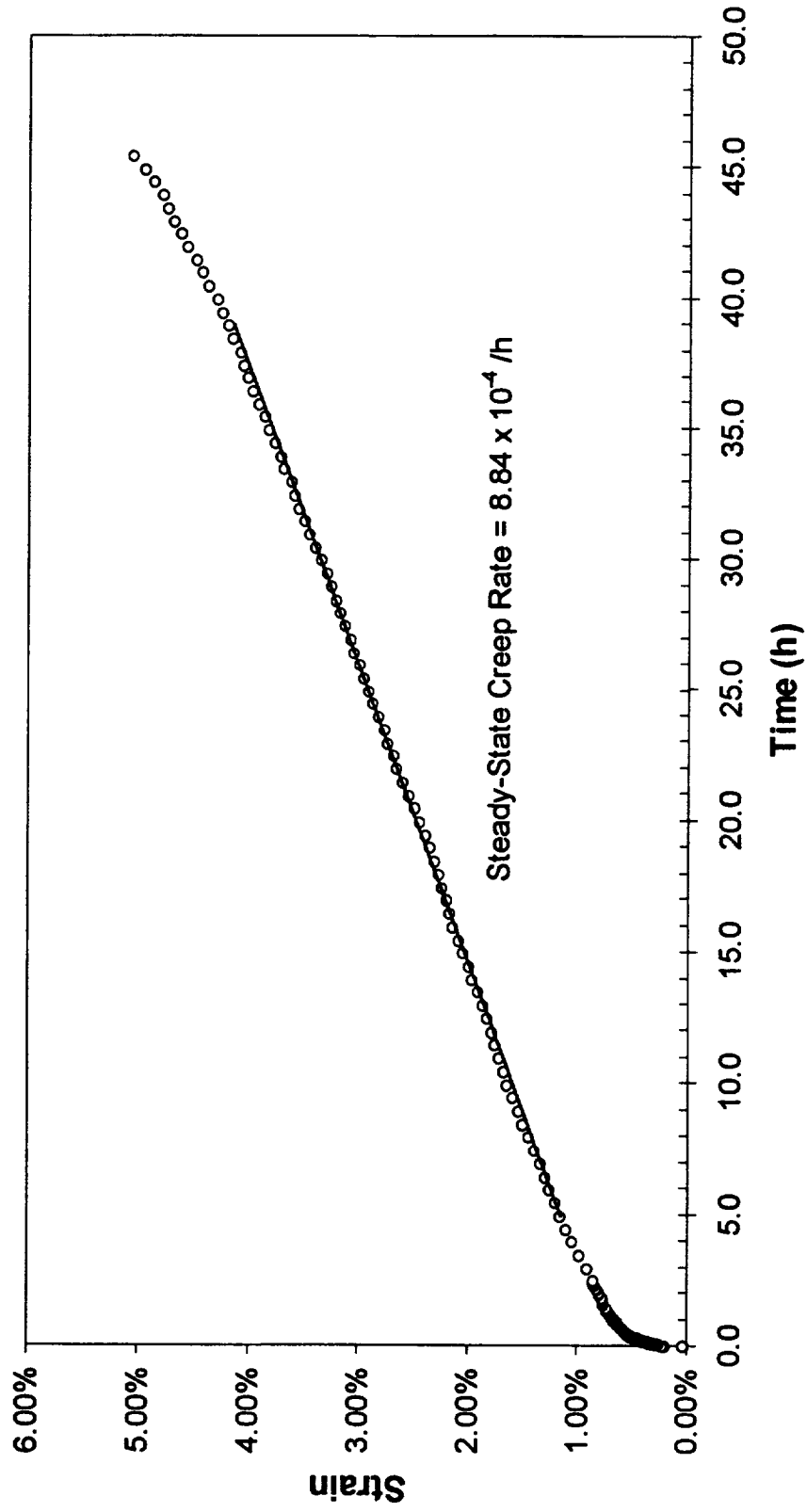


Figure A - 28 -
Extrusion L-3106 Tested At 650°C/44.3 MPa

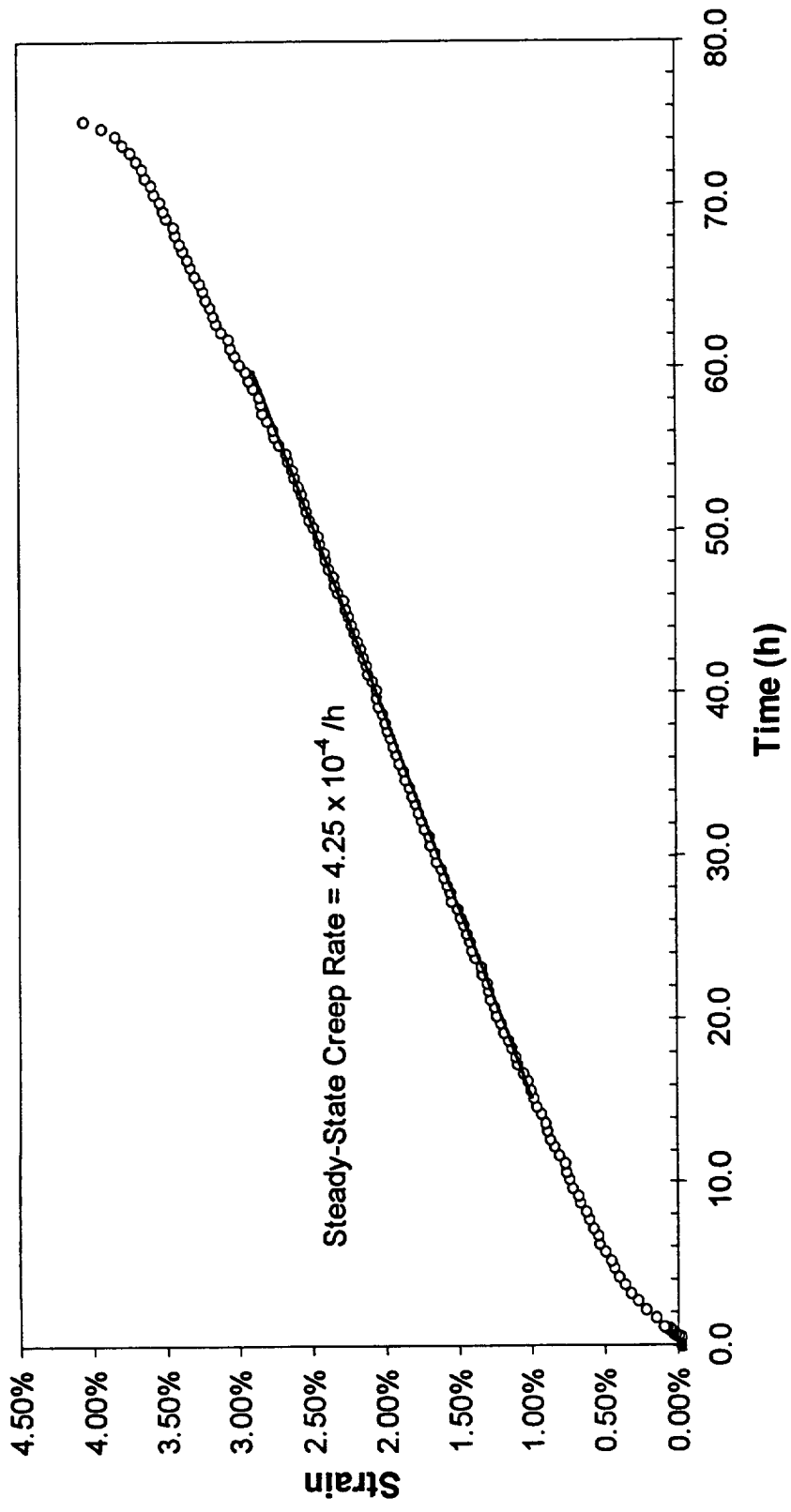


Figure A - 29 -
Extrusion L-3107 Tested At 650°C/44.3 MPa

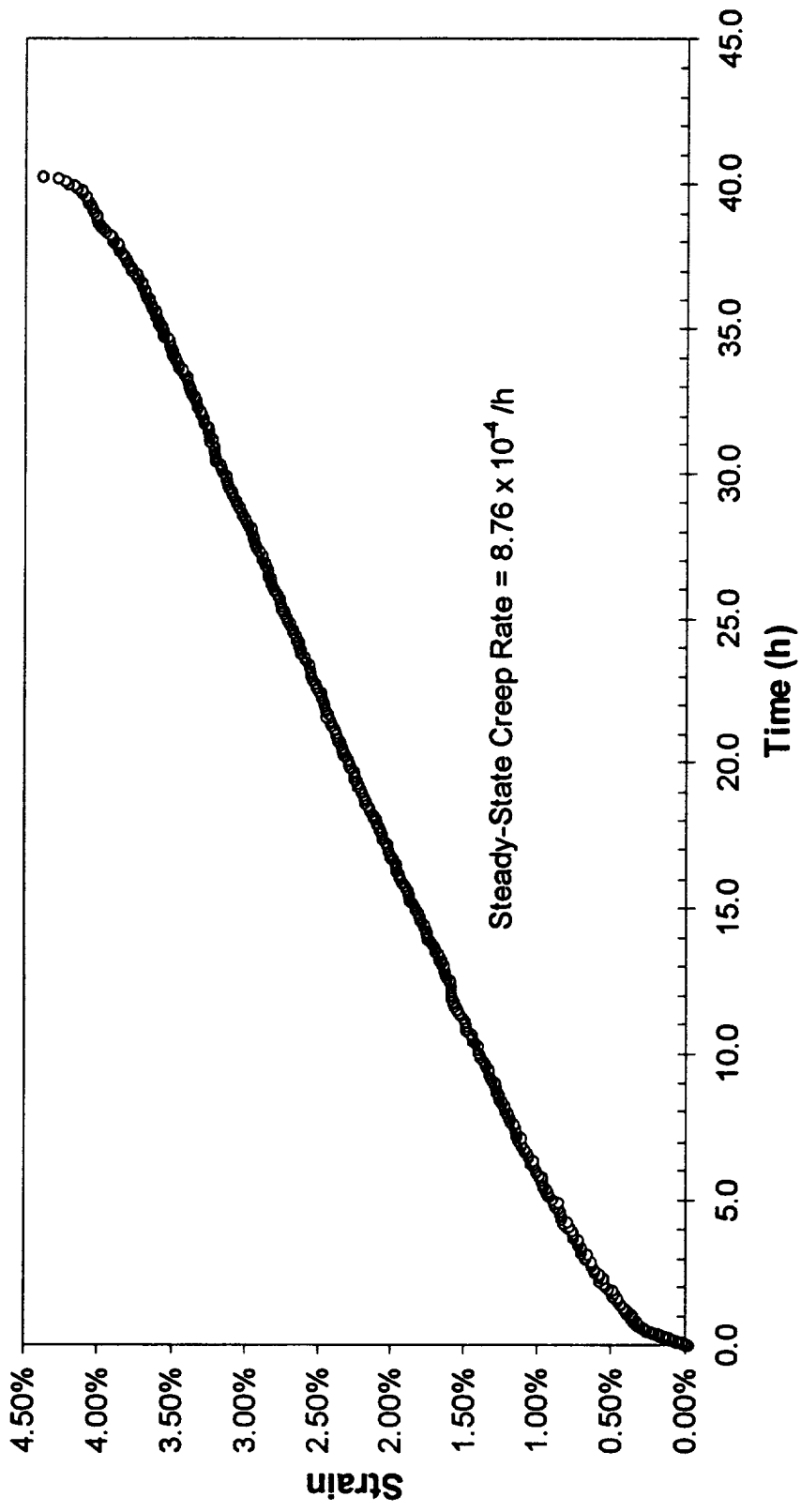


Figure A - 30 -
Extrusion L-3108 Tested At 650°C/44.3 MPa

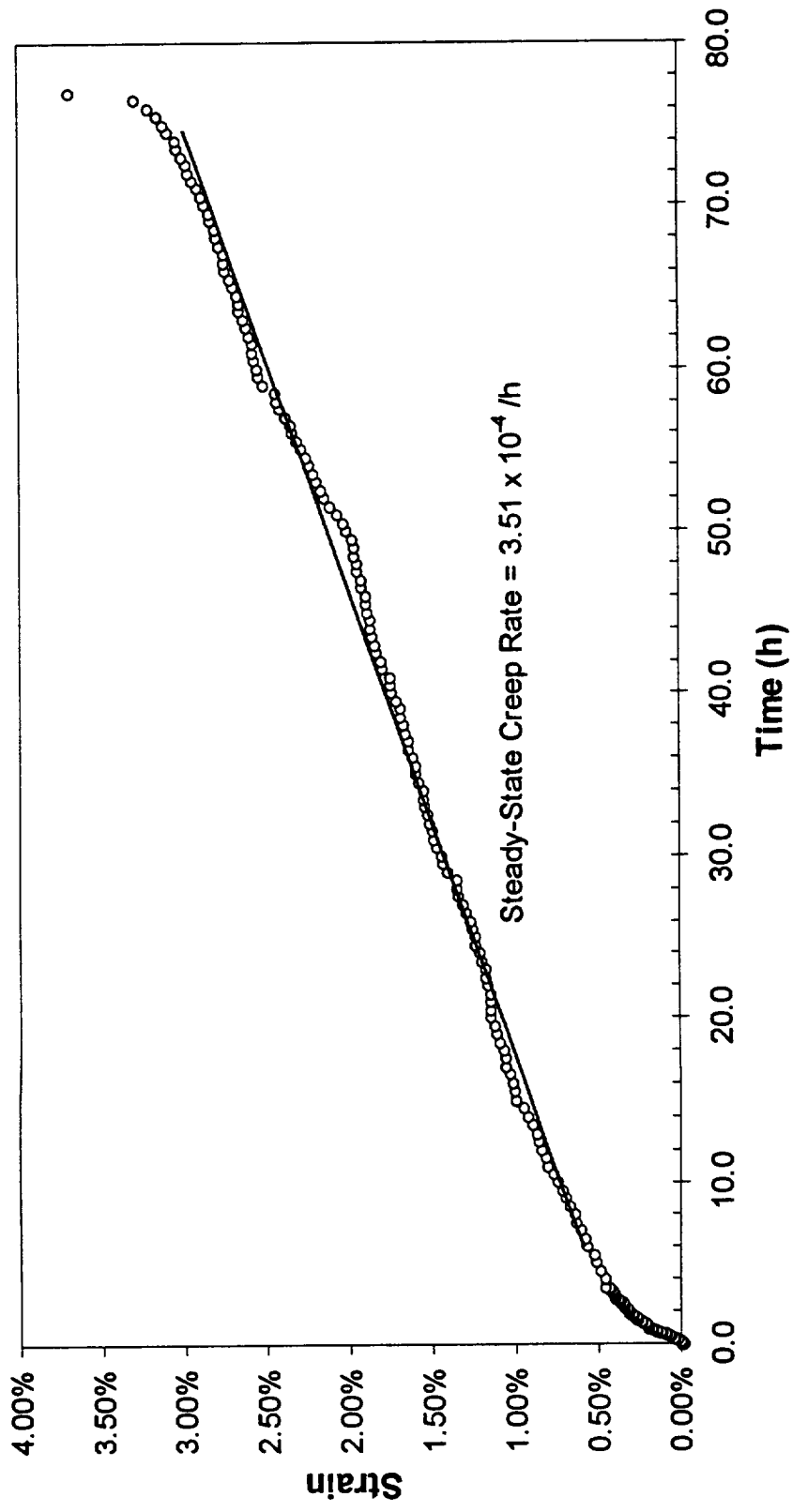


Figure A - 31 -
Extrusion L-3097 Tested At 650°C/49.8 MPa

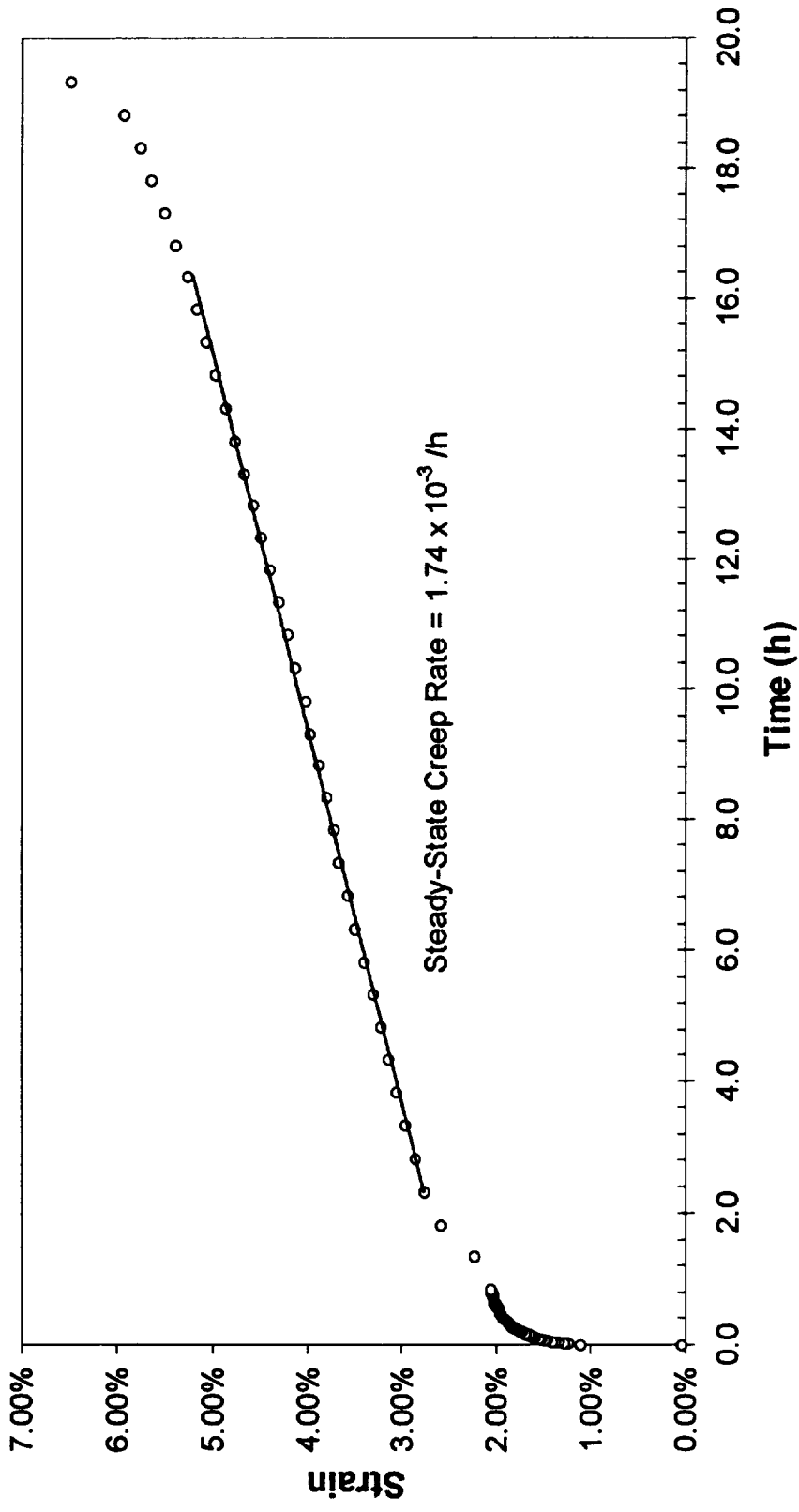


Figure A - 32 -
Extrusion L-3104 Tested At 650°C/49.8 MPa

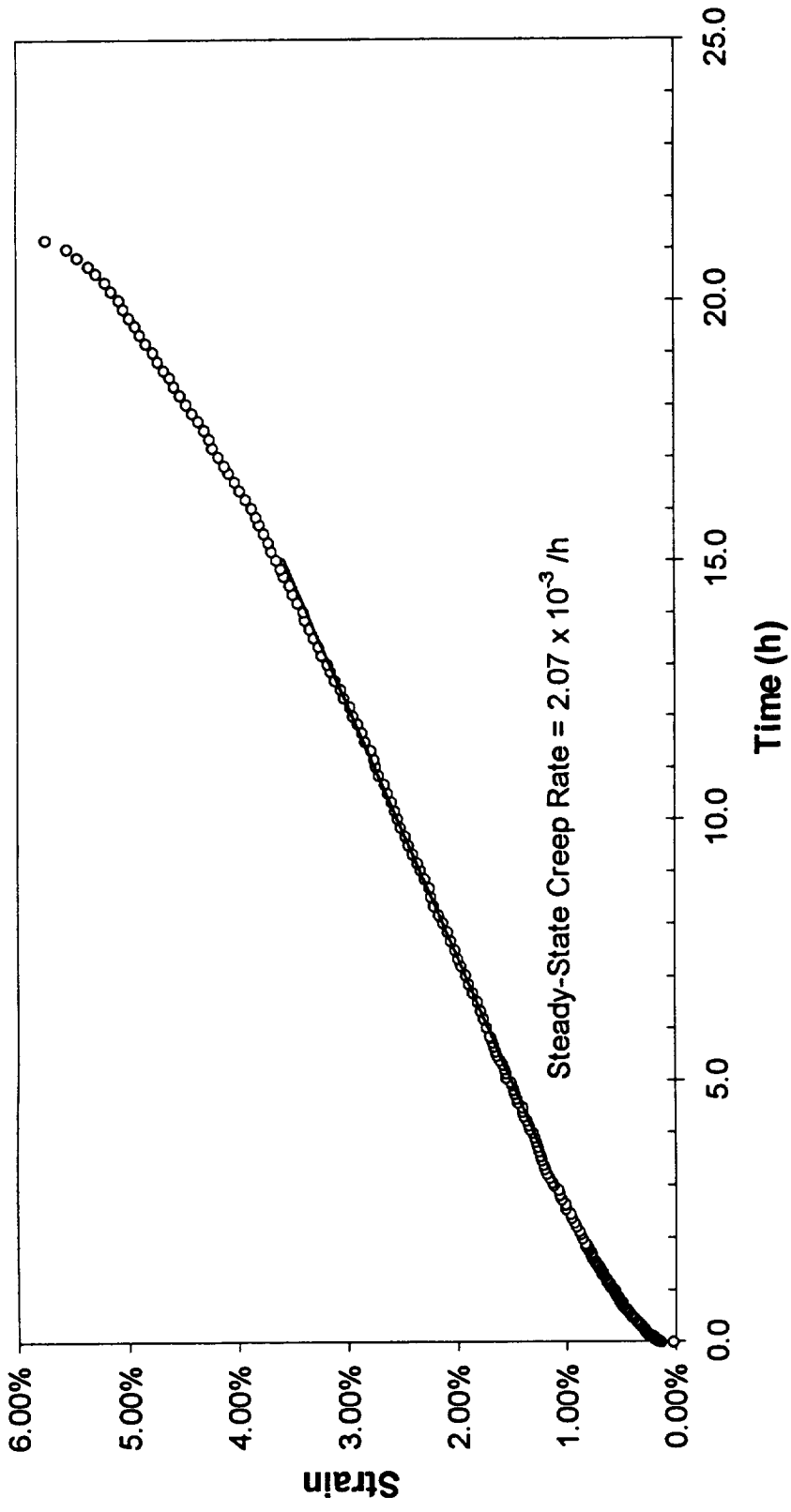


Figure A - 33 -
Extrusion L-3105 Tested At 650°C/49.8 MPa

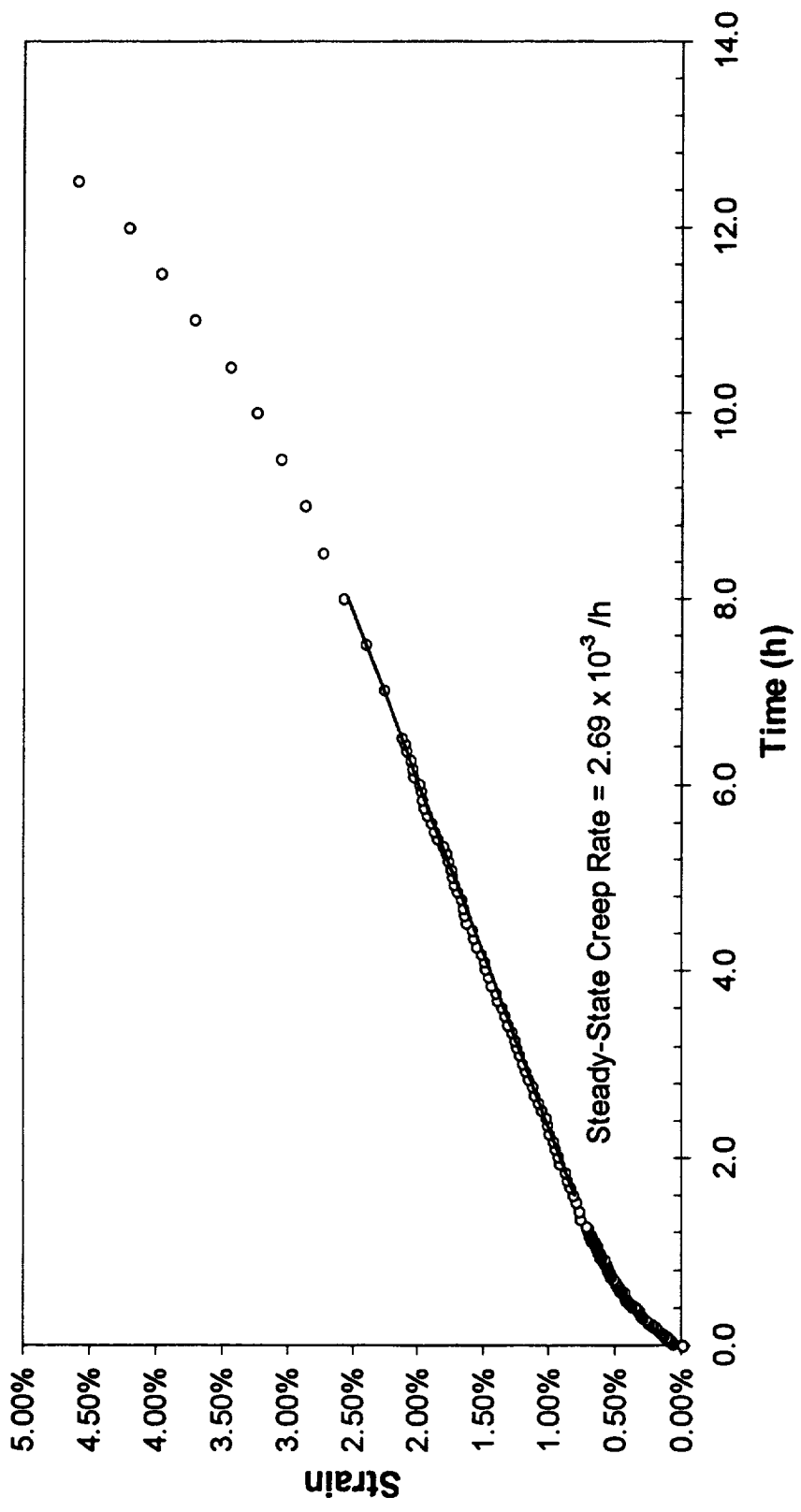


Figure A - 34 -
Extrusion L-3106 Tested At 650°C/49.8 MPa

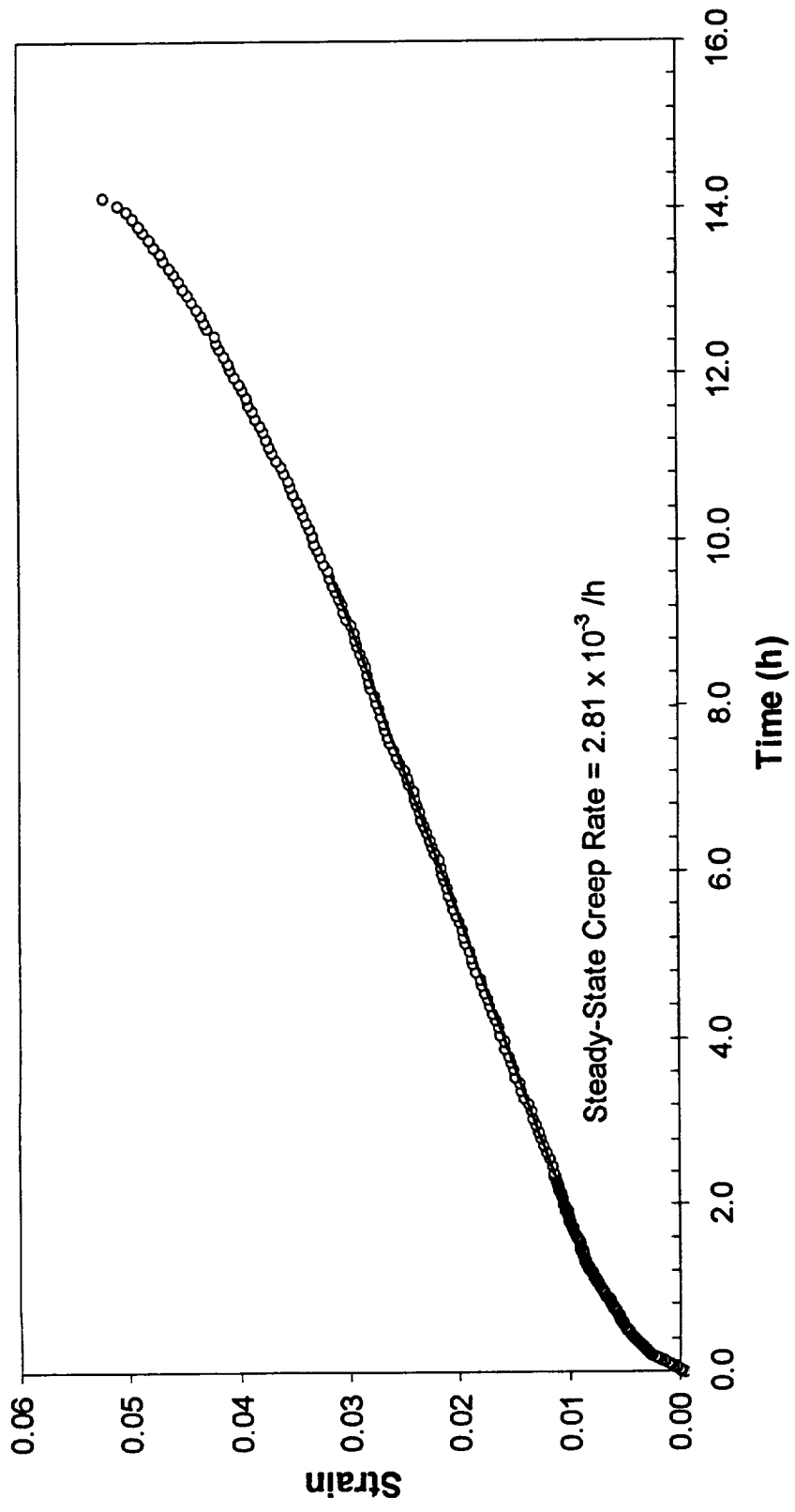


Figure A - 35 -
Extrusion L-3107 Tested At 650°C/49.8 MPa

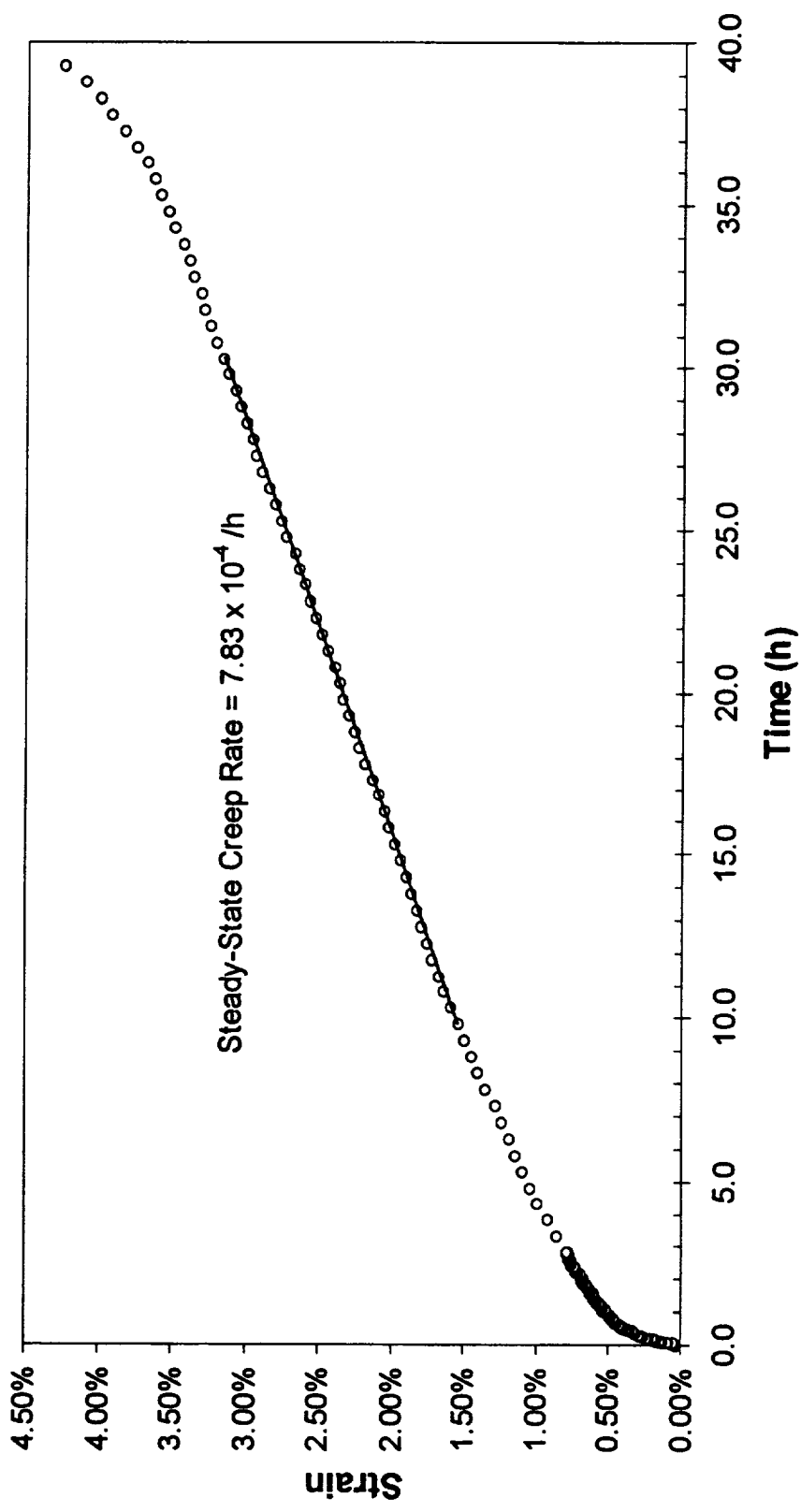


Figure A - 36 -
Extrusion L-3108 Tested At 650°C/49.8 MPa

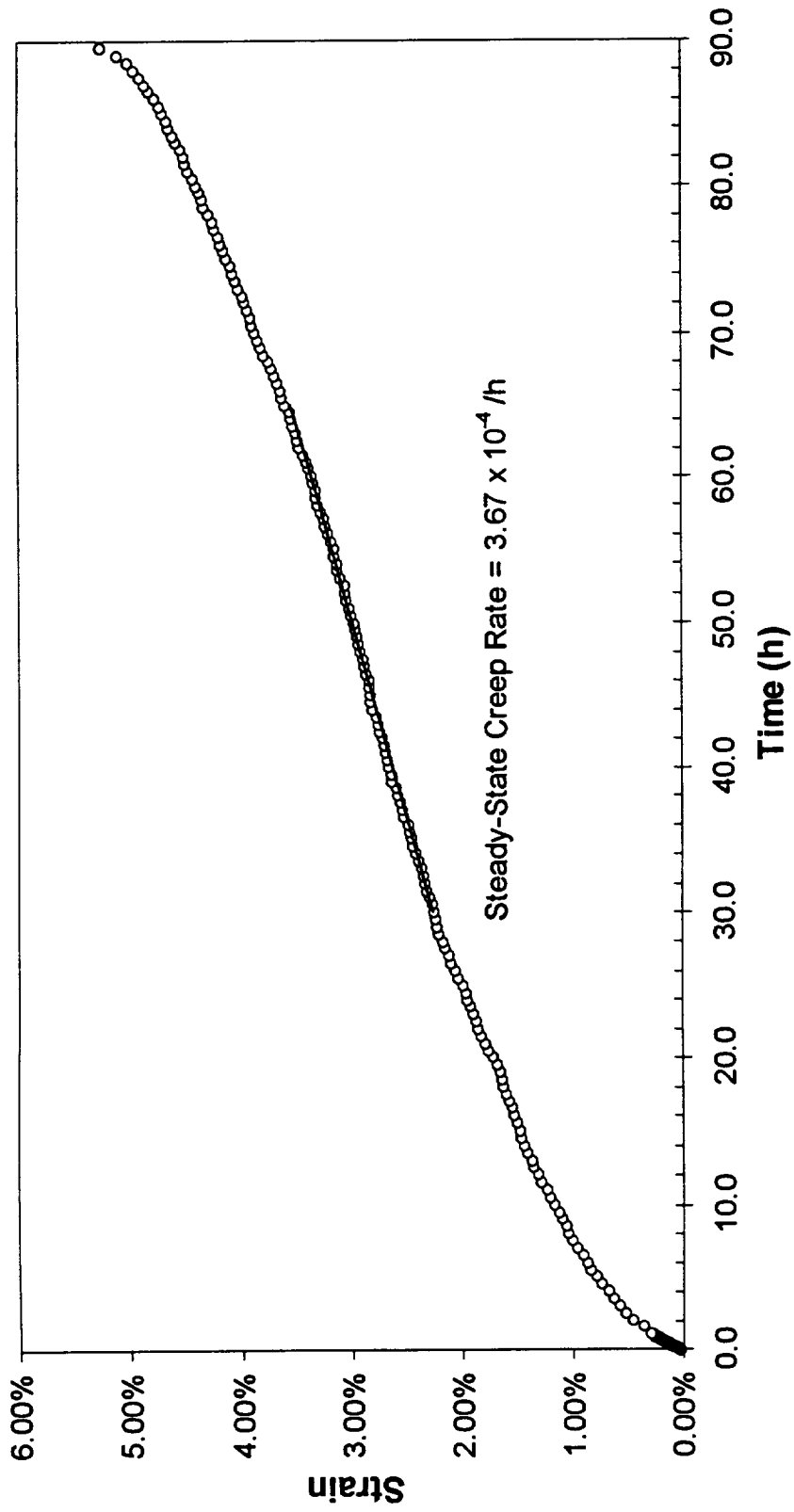


Figure A - 37 -
Extrusion L-3097 Tested At 800°C/19.2 MPa

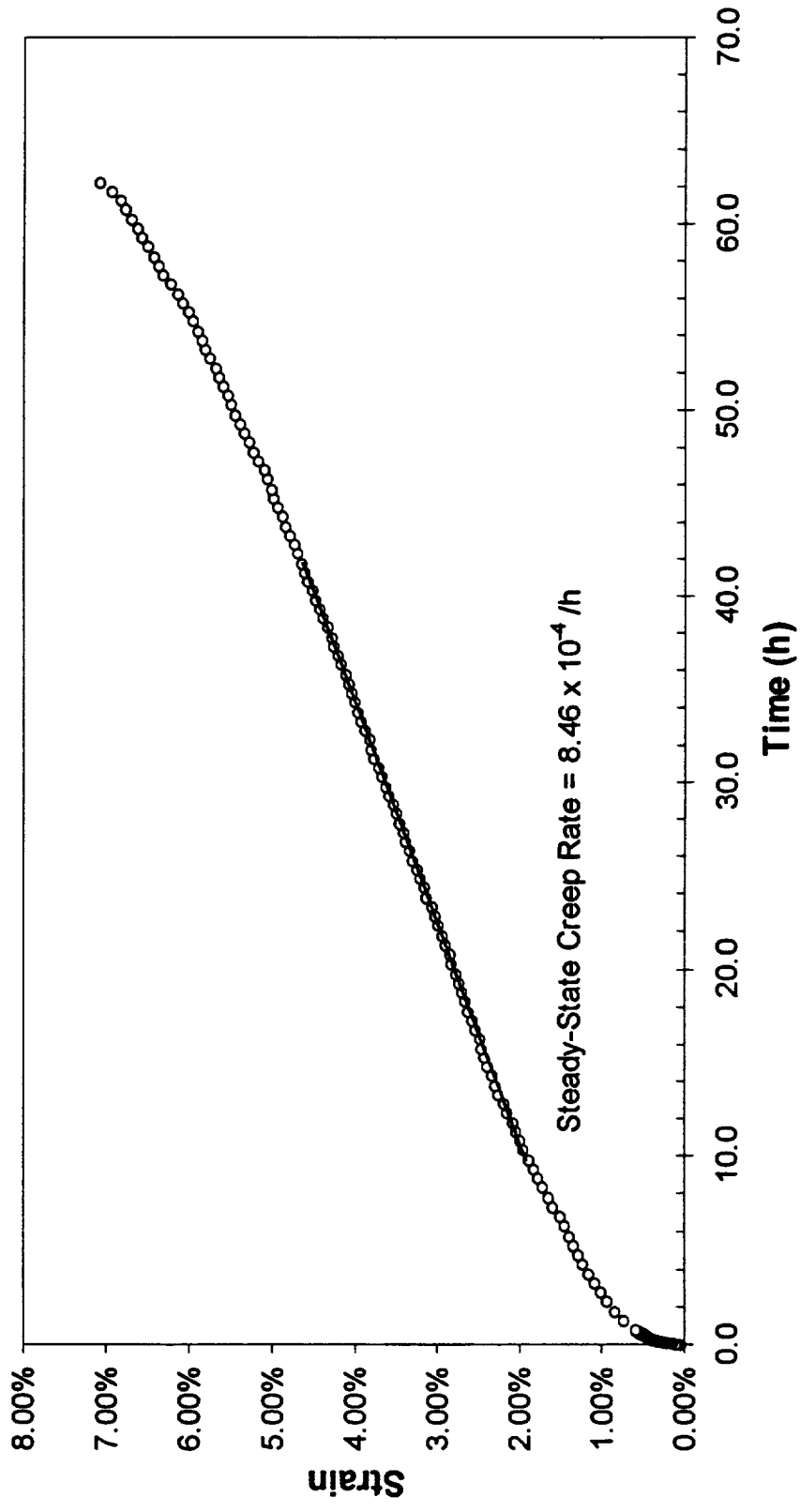


Figure A - 38 -
Extrusion L-3104 Tested At 800°C/19.2 MPa

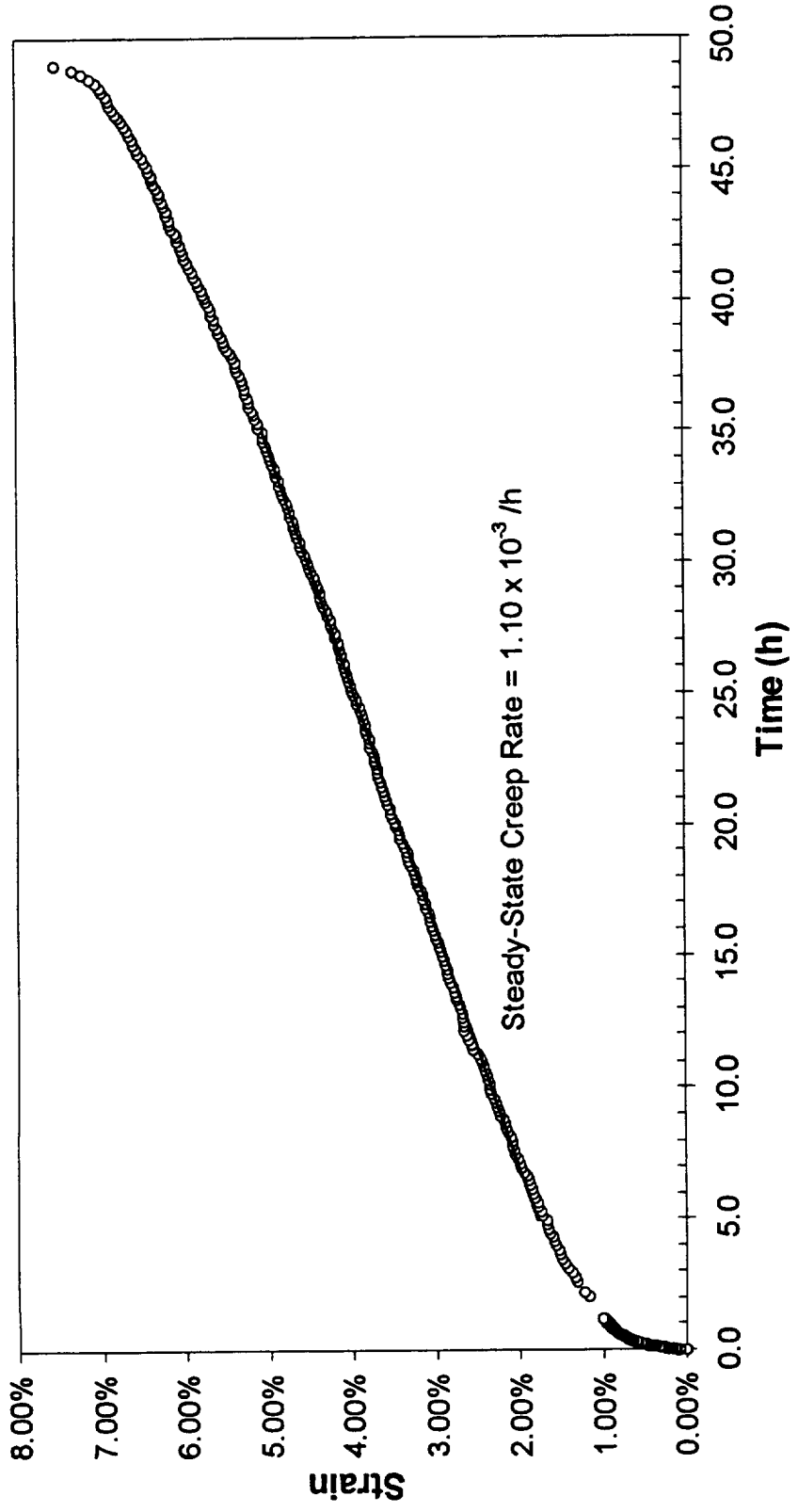


Figure A - 39 -
Extrusion L-3105 Tested At 800°C/19.2 MPa

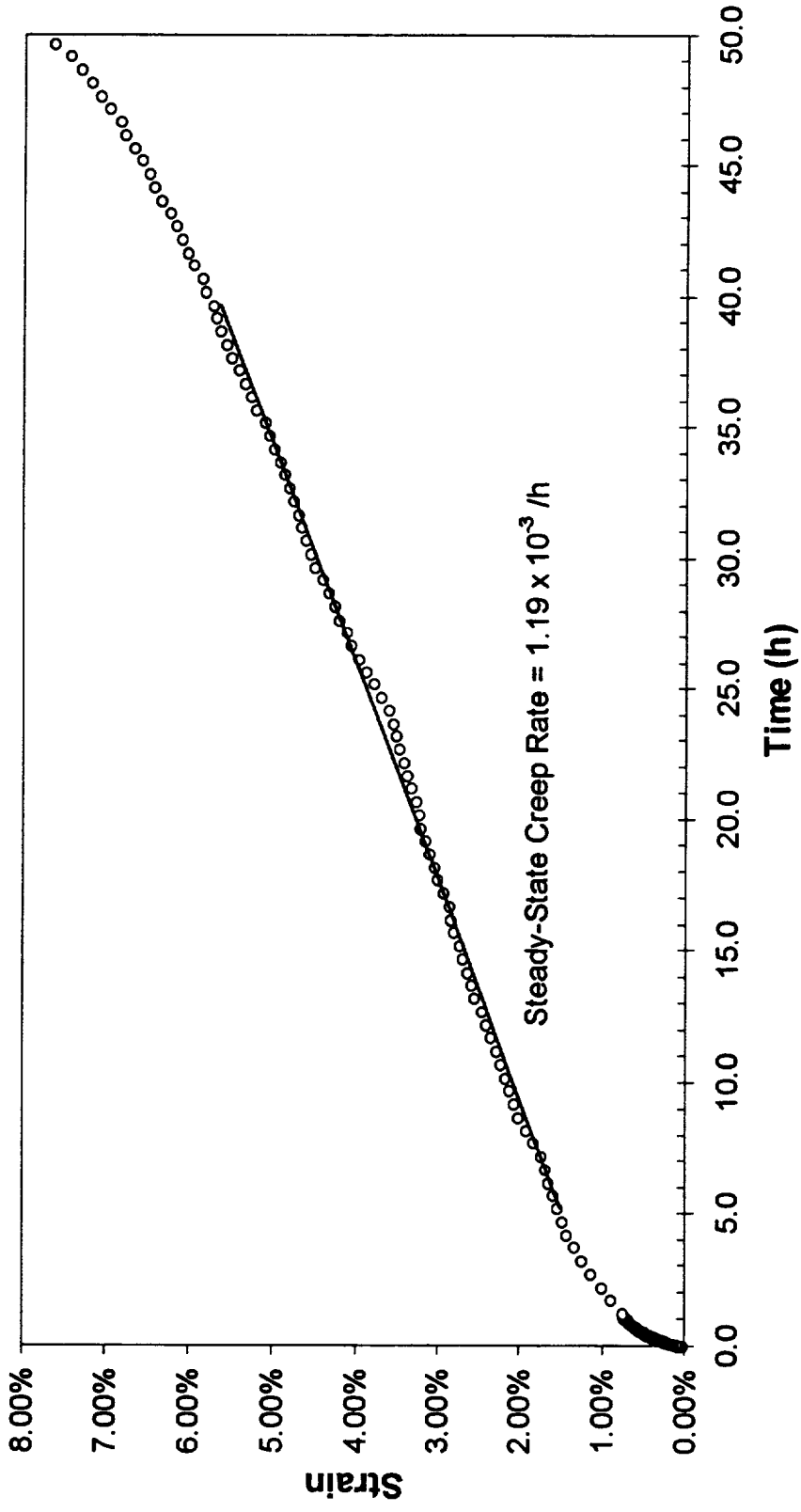


Figure A - 40 -
Extrusion L-3106 Tested At 800°C/19.2 MPa

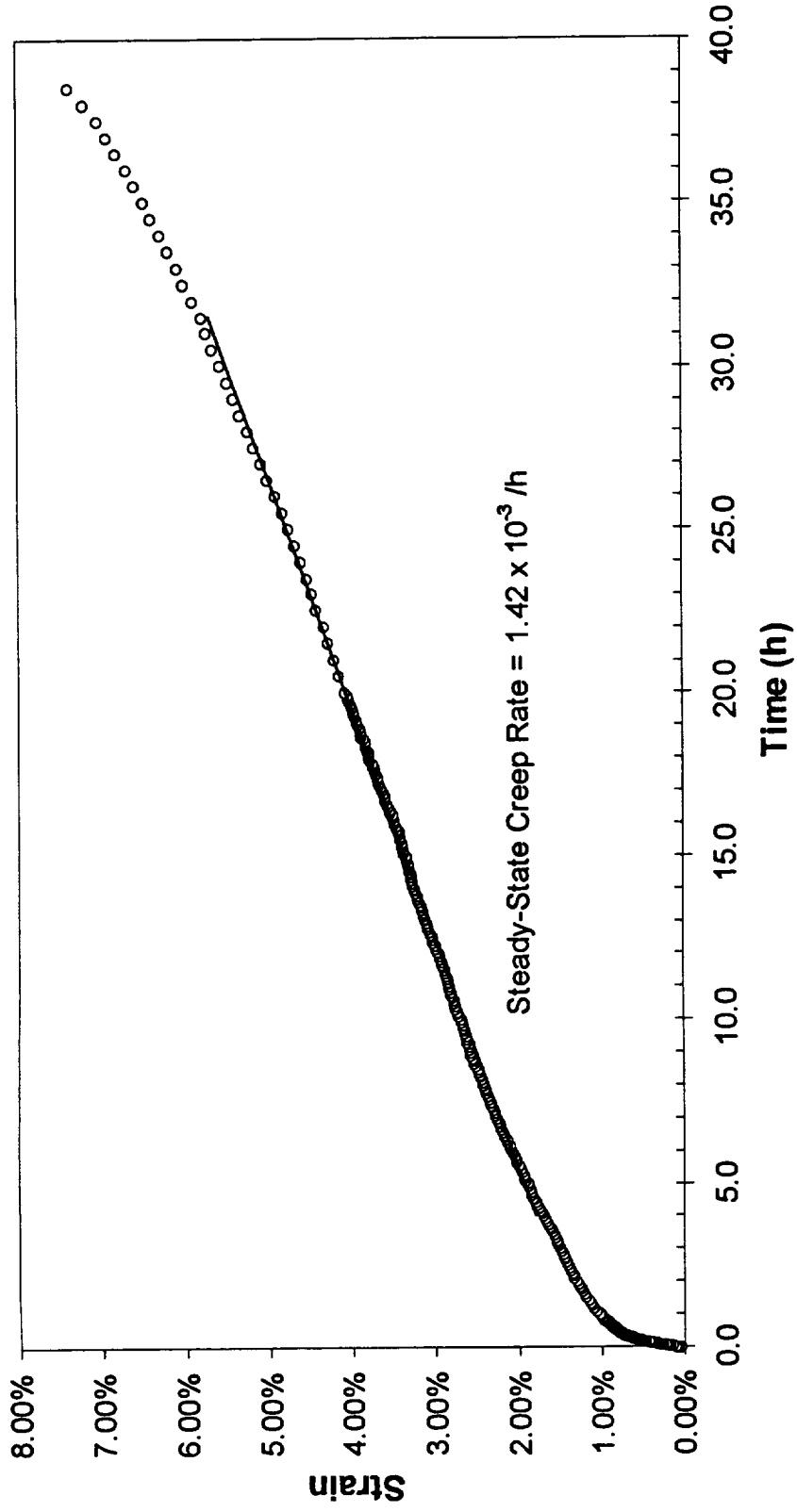


Figure A - 41 -
Extrusion L-3107 Tested At 800°C/19.2 MPa

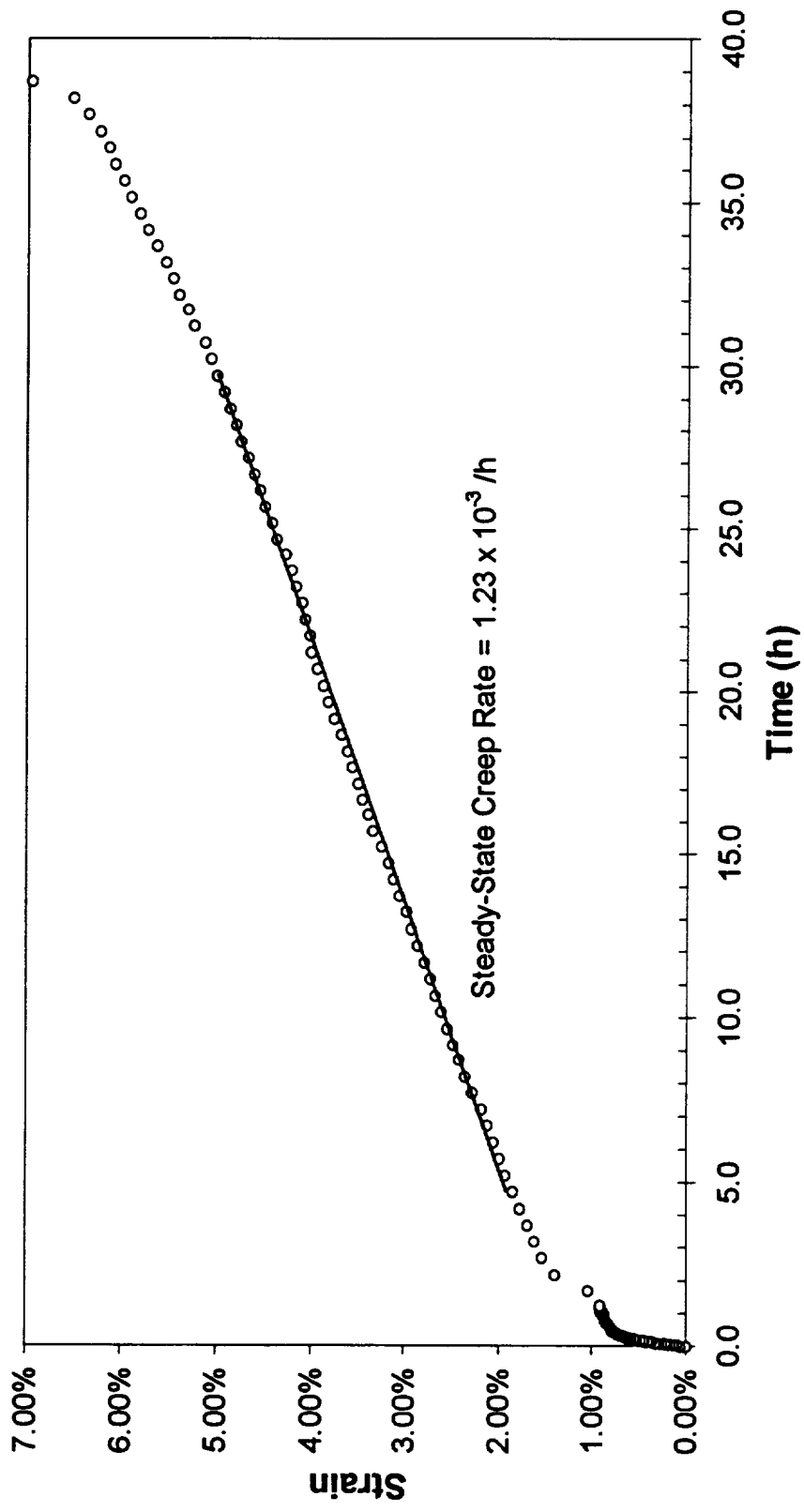


Figure A - 42 -
Extrusion L-3108 Tested At 800°C/19.2 MPa

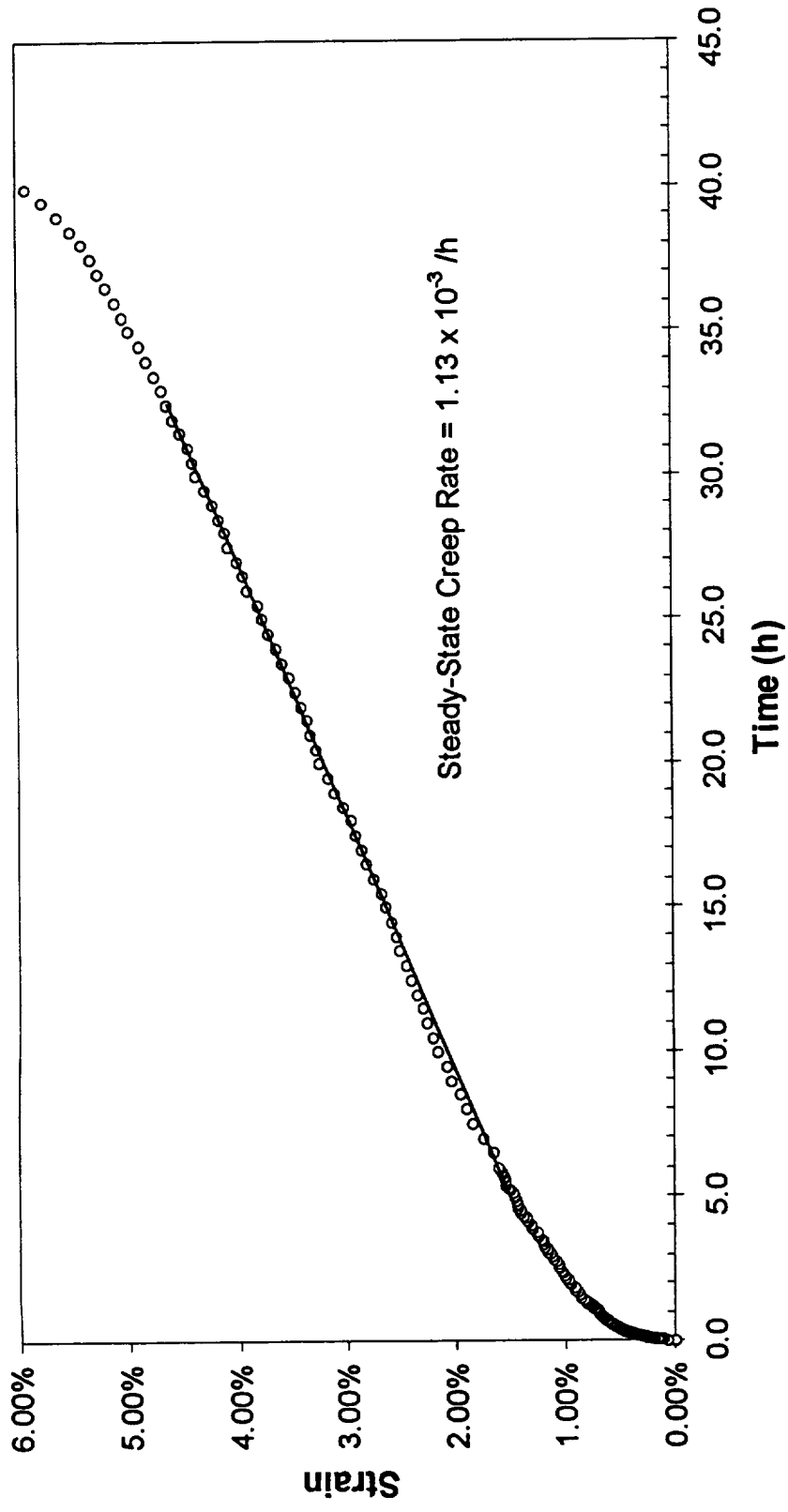


Figure A - 43 -
Extrusion L-3097 Tested At 800°C/23.3 MPa

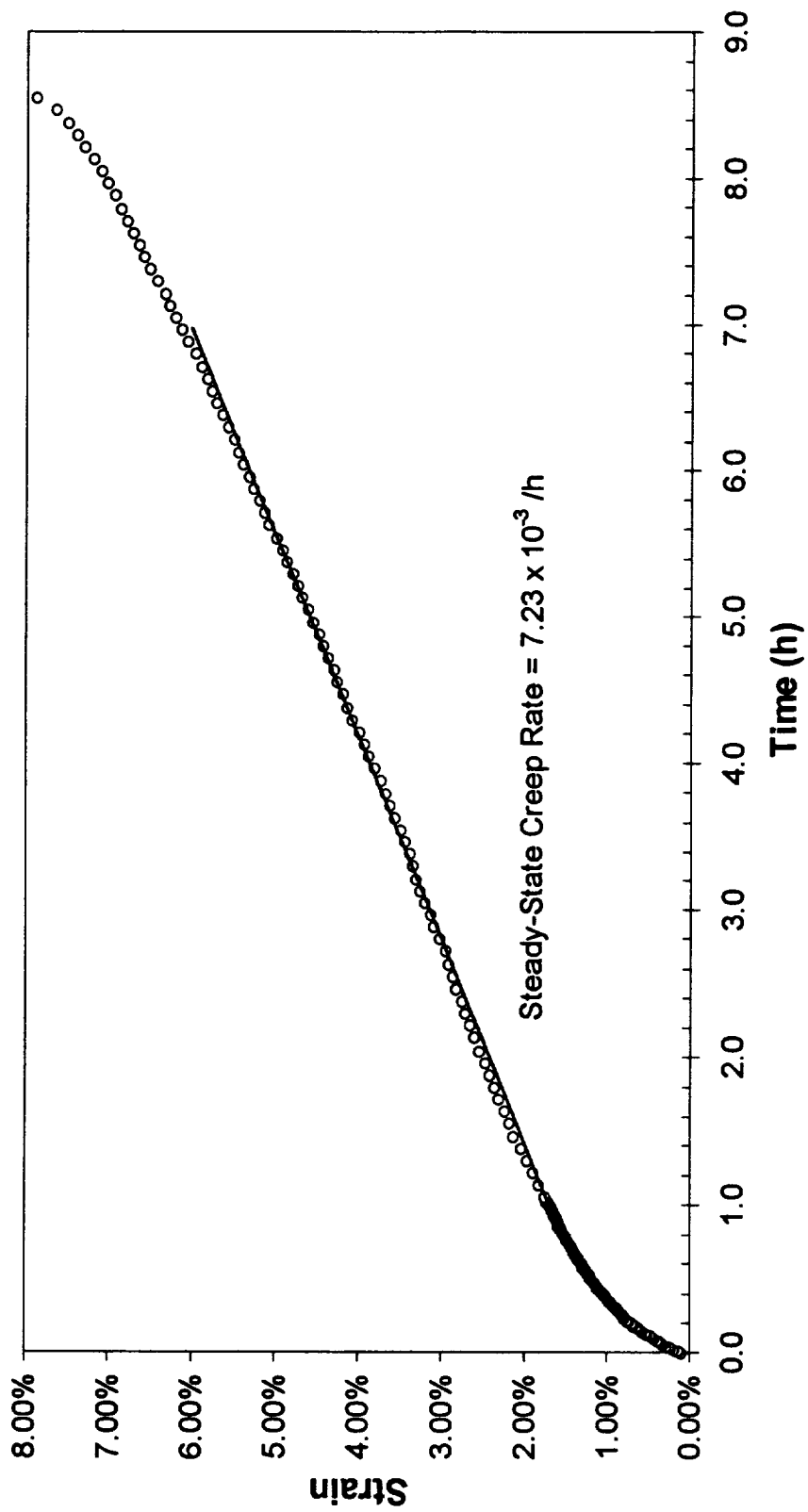


Figure A - 44 -
Extrusion L-3104 Tested At 800°C/23.3 MPa

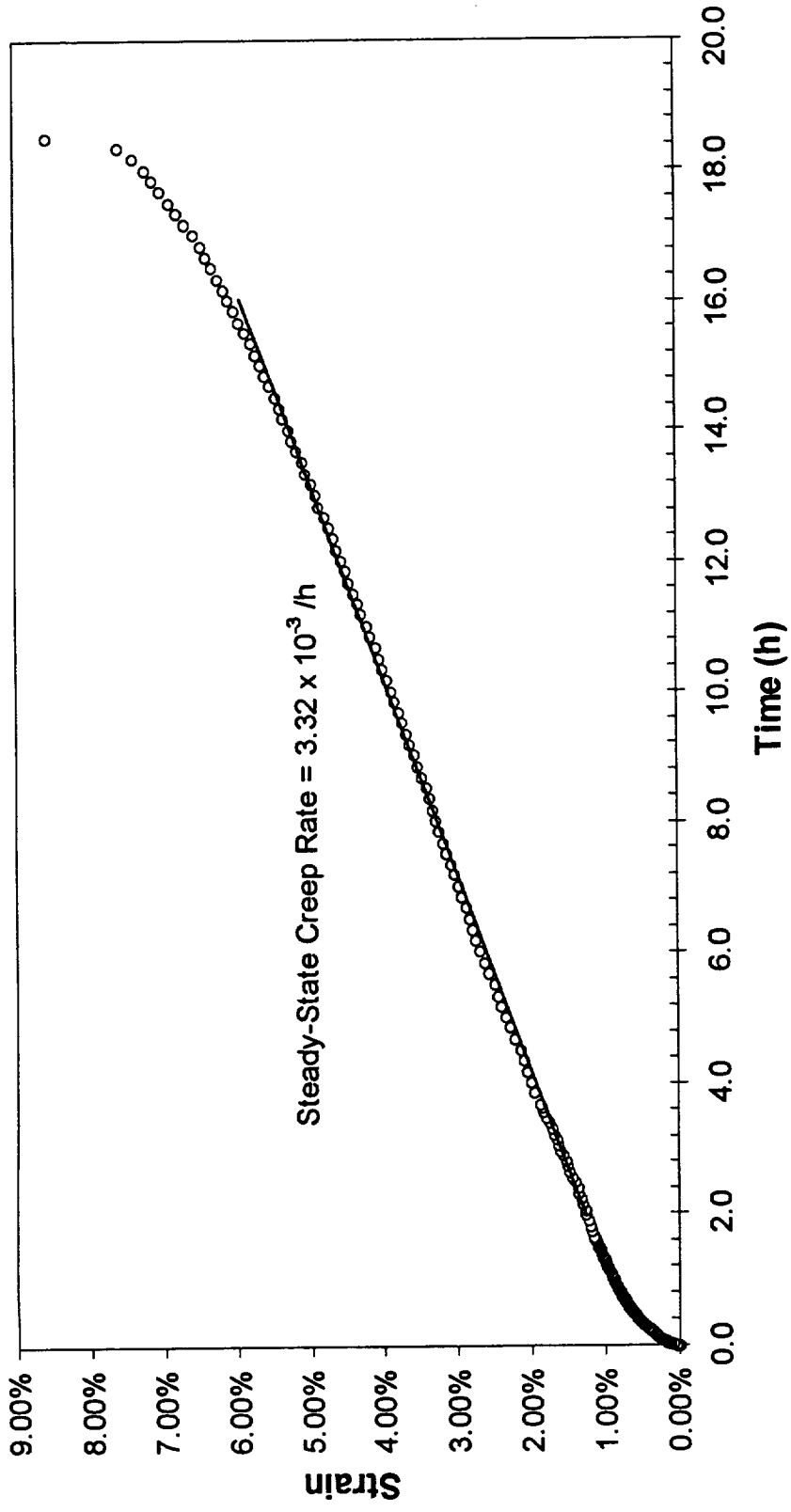


Figure A - 45 -
Extrusion L-3105 Tested At 800°C/23.3 MPa

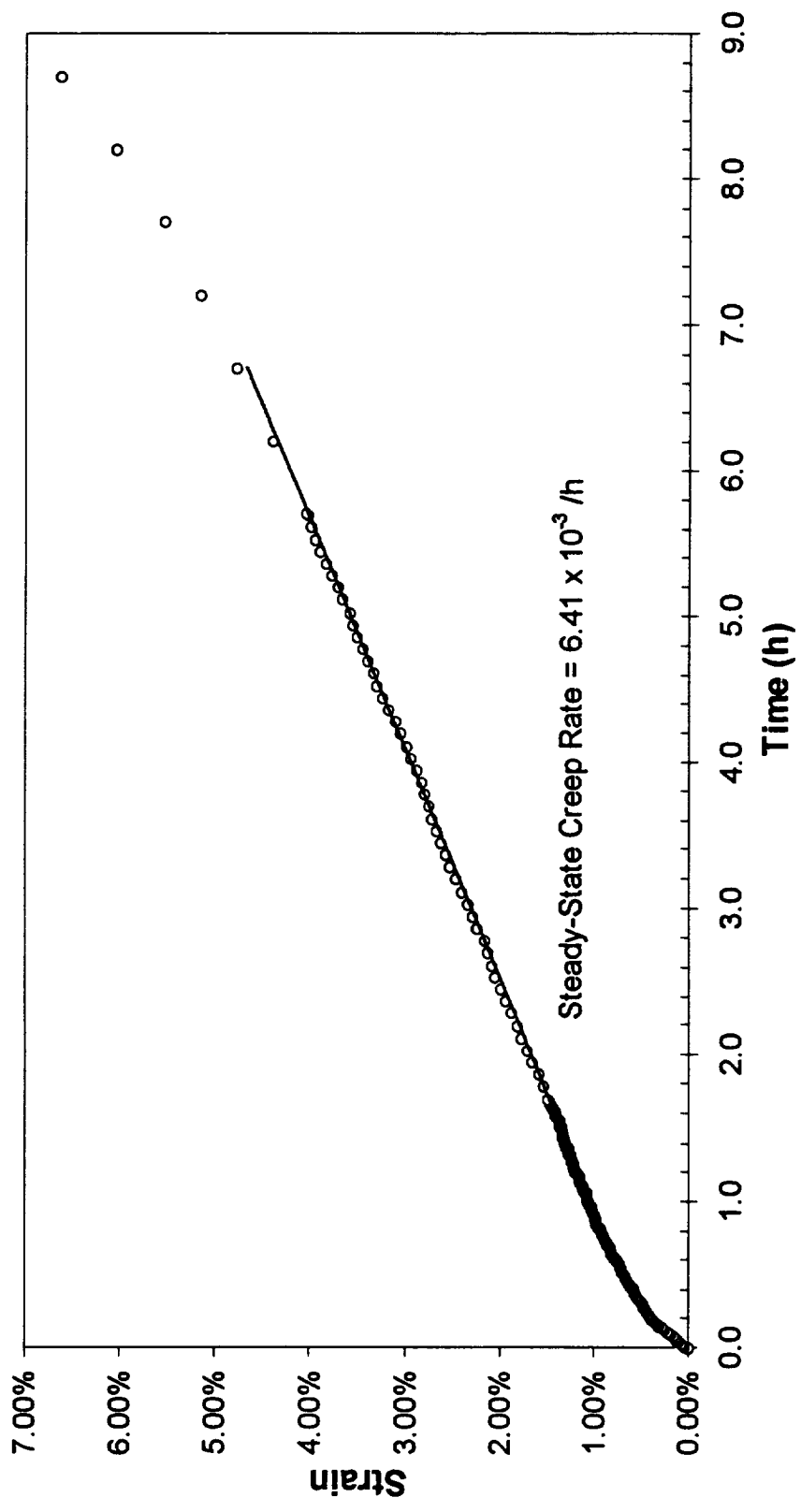


Figure A - 46 -
Extrusion L-3106 Tested At 800°C/23.3 MPa

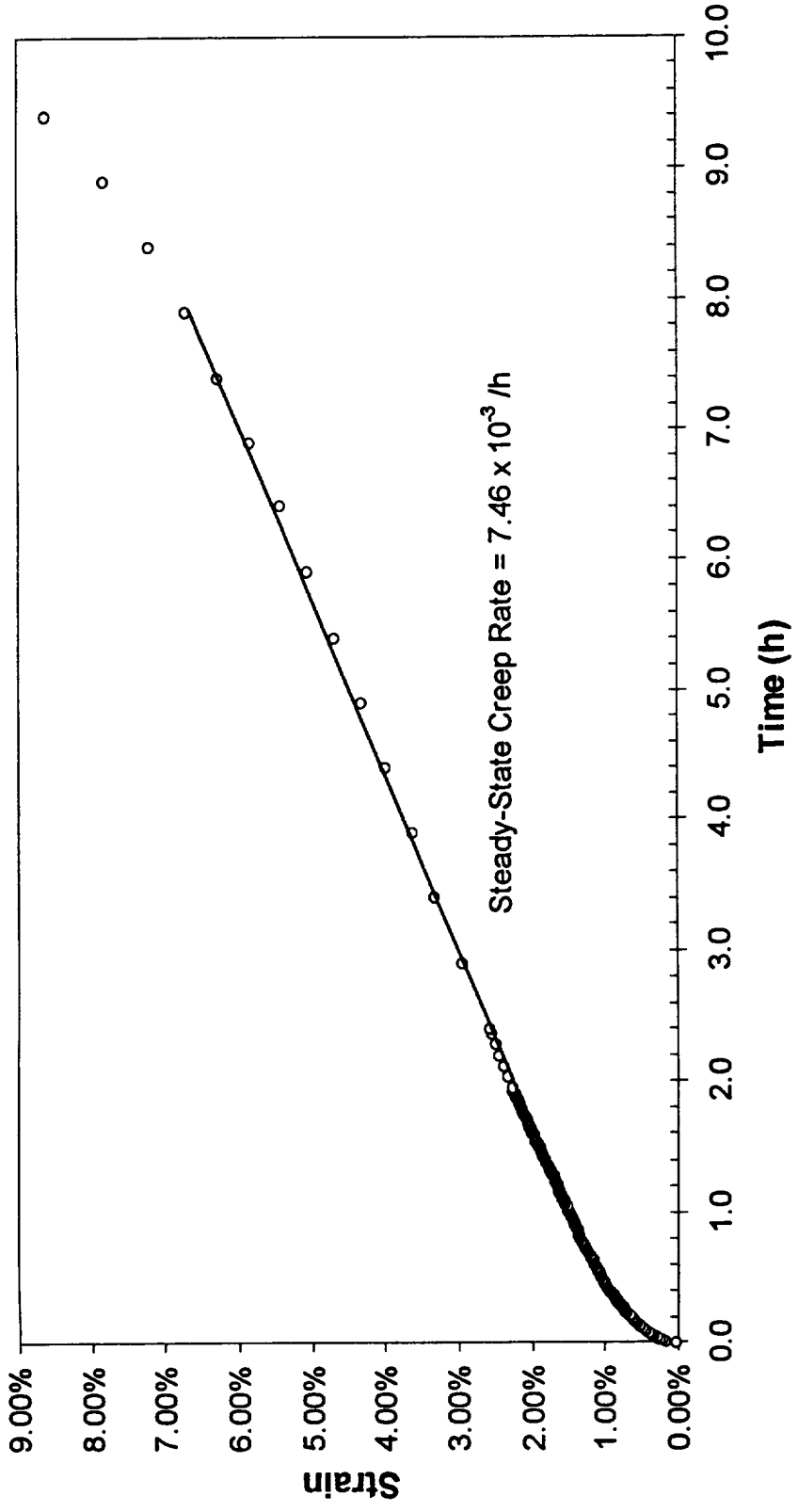


Figure A - 47 -
Extrusion L-3107 Tested At 800°C/23.3 MPa

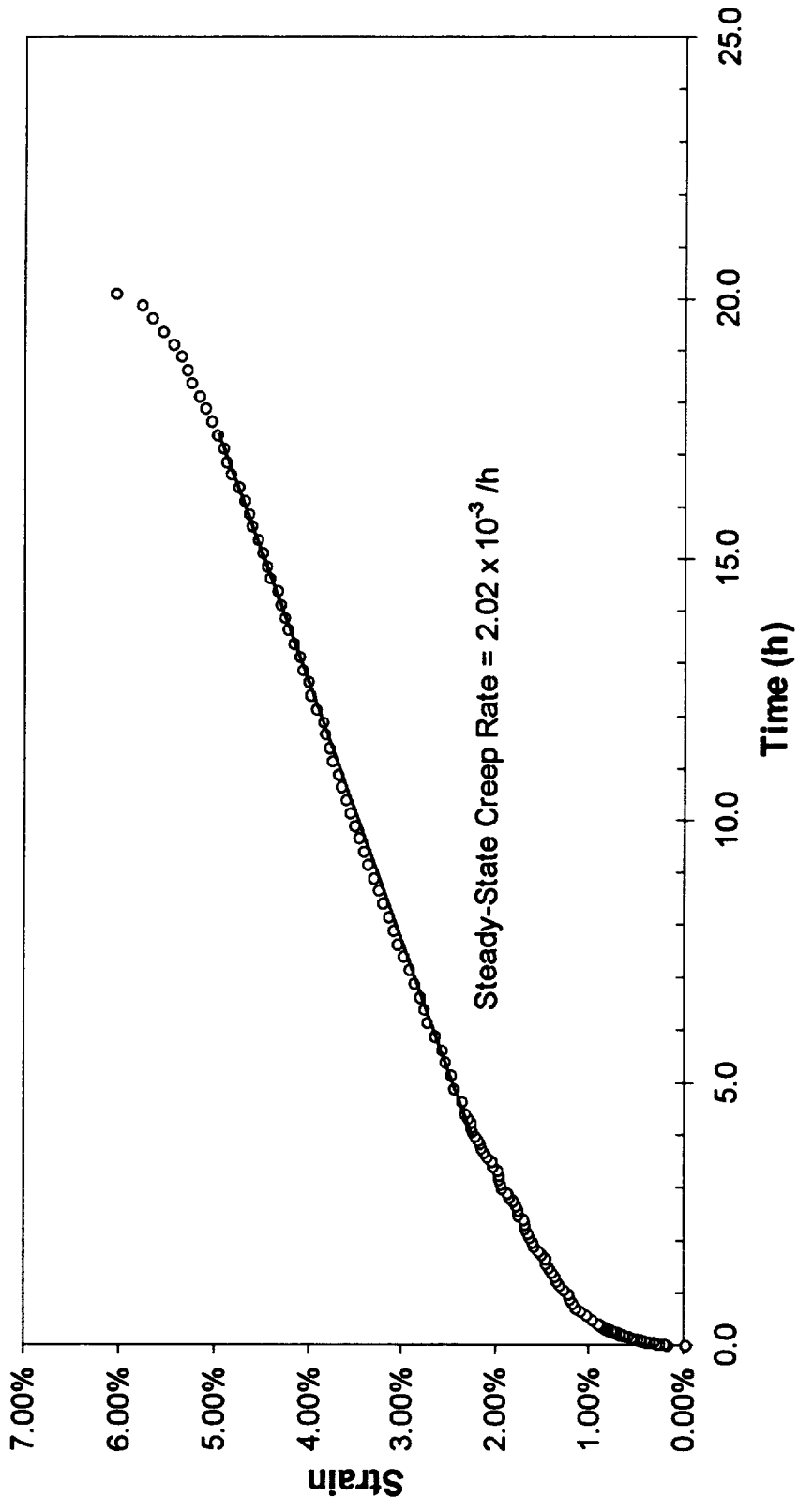


Figure A - 48 -
Extrusion L-3108 Tested At 800°C/23.3 MPa

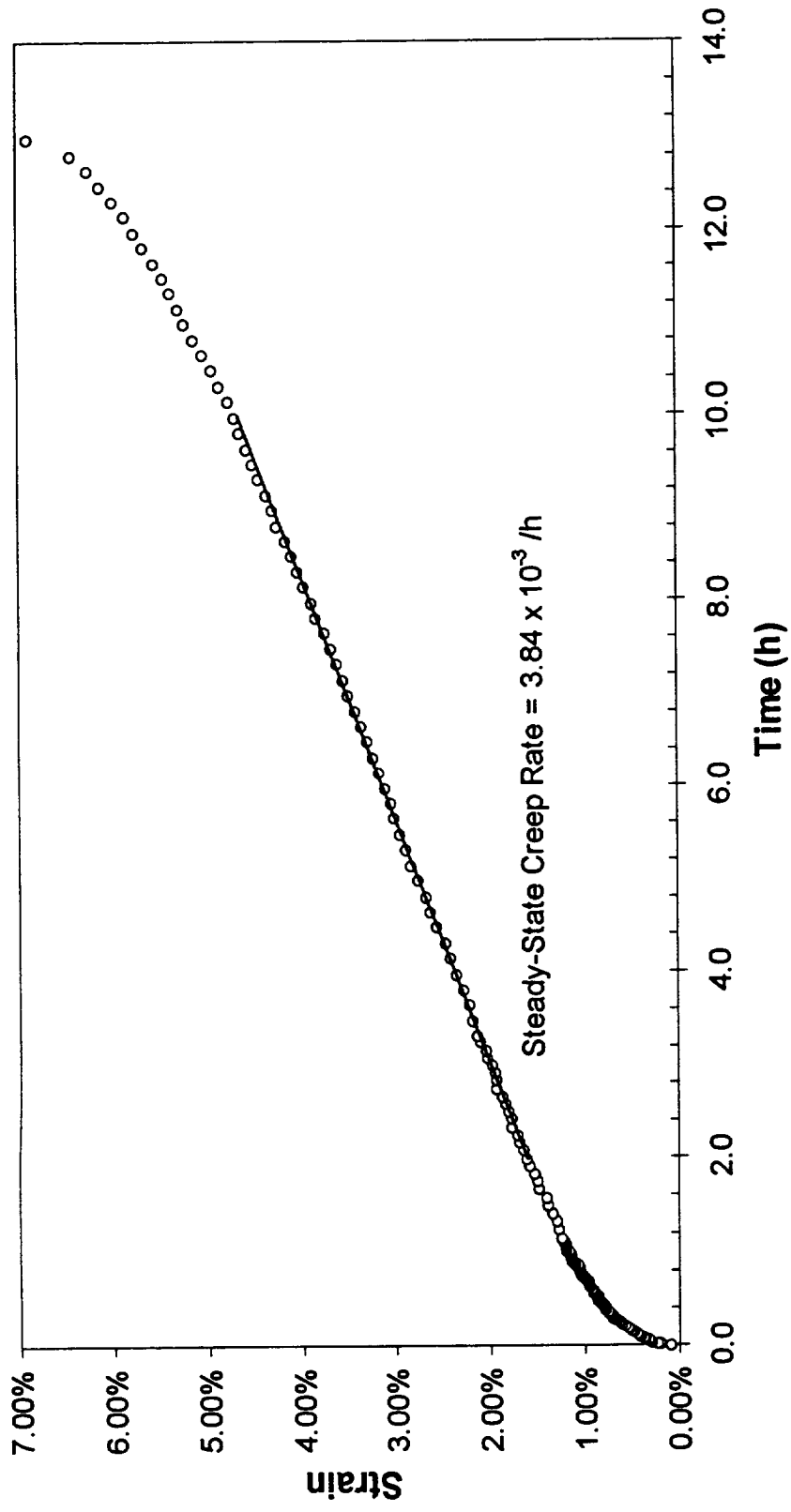


Figure A - 49 -
Extrusion L-3097 Tested At 800°C/26.8 MPa

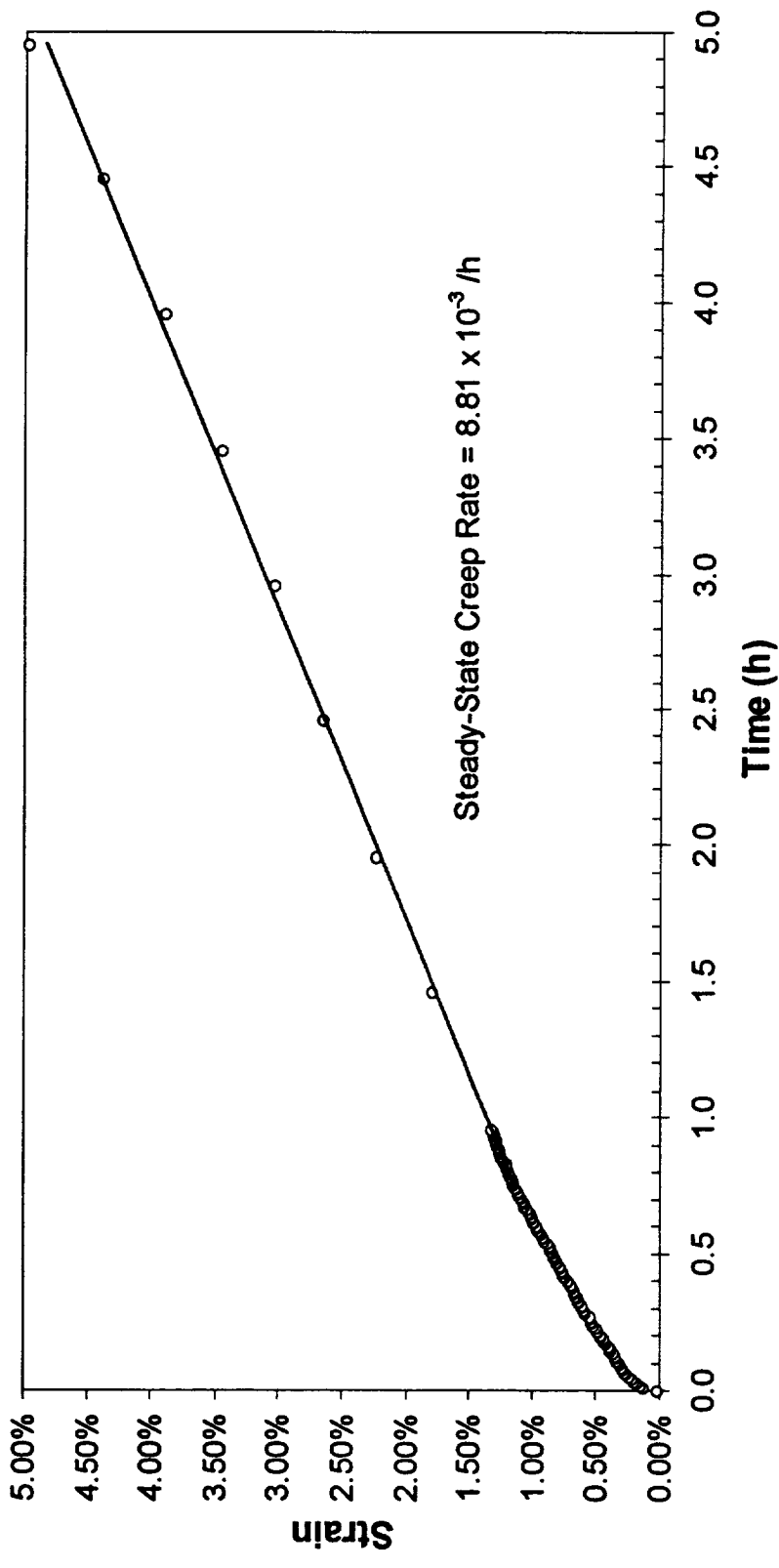


Figure A - 50 -
Extrusion L-3104 Tested At 800°C/26.8 MPa

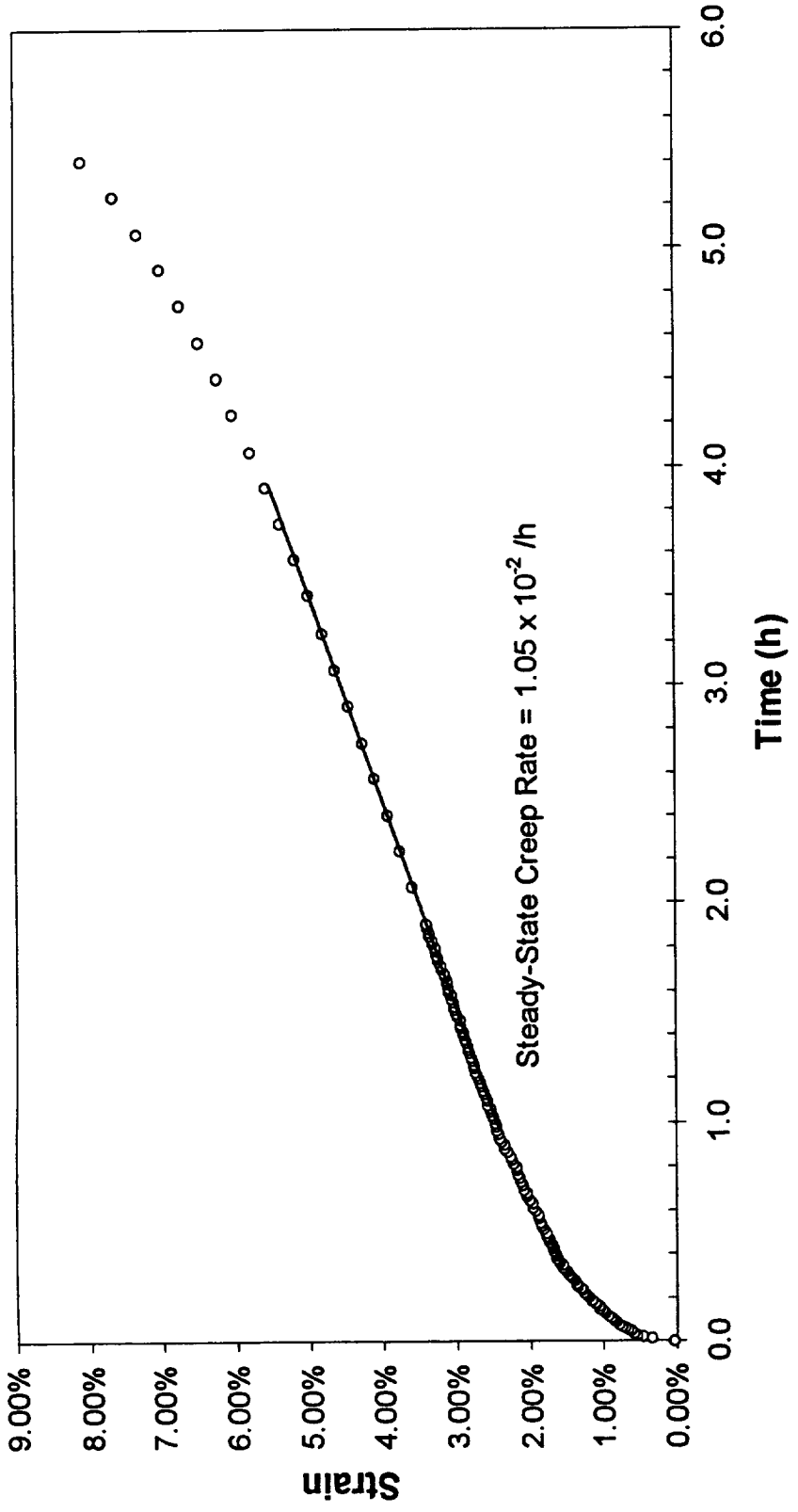


Figure A - 51 -
Extrusion L-3105 Tested At 800°C/26.8 MPa

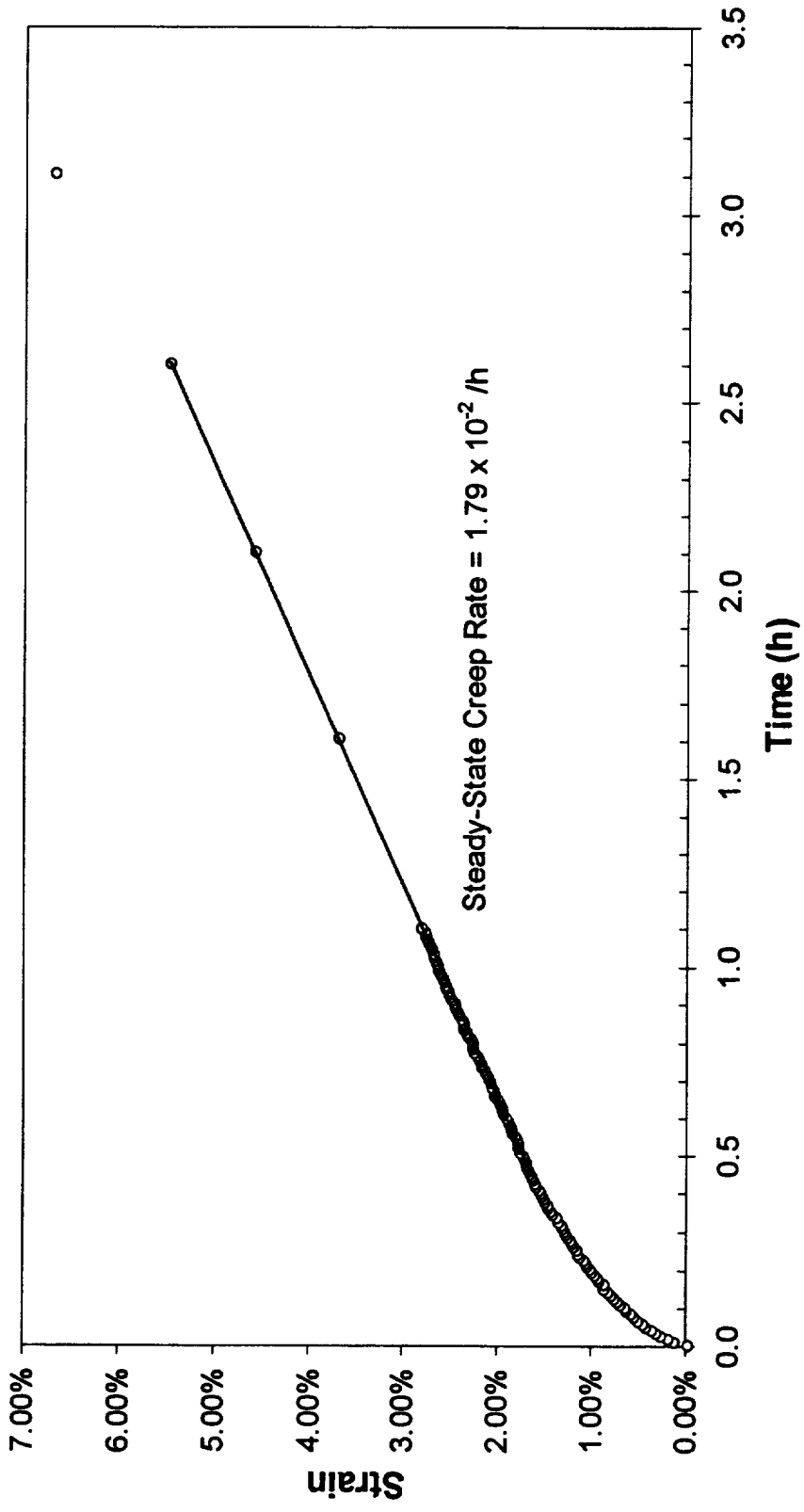


Figure A - 52 -
Extrusion L-3106 Tested At 800°C/26.8 MPa

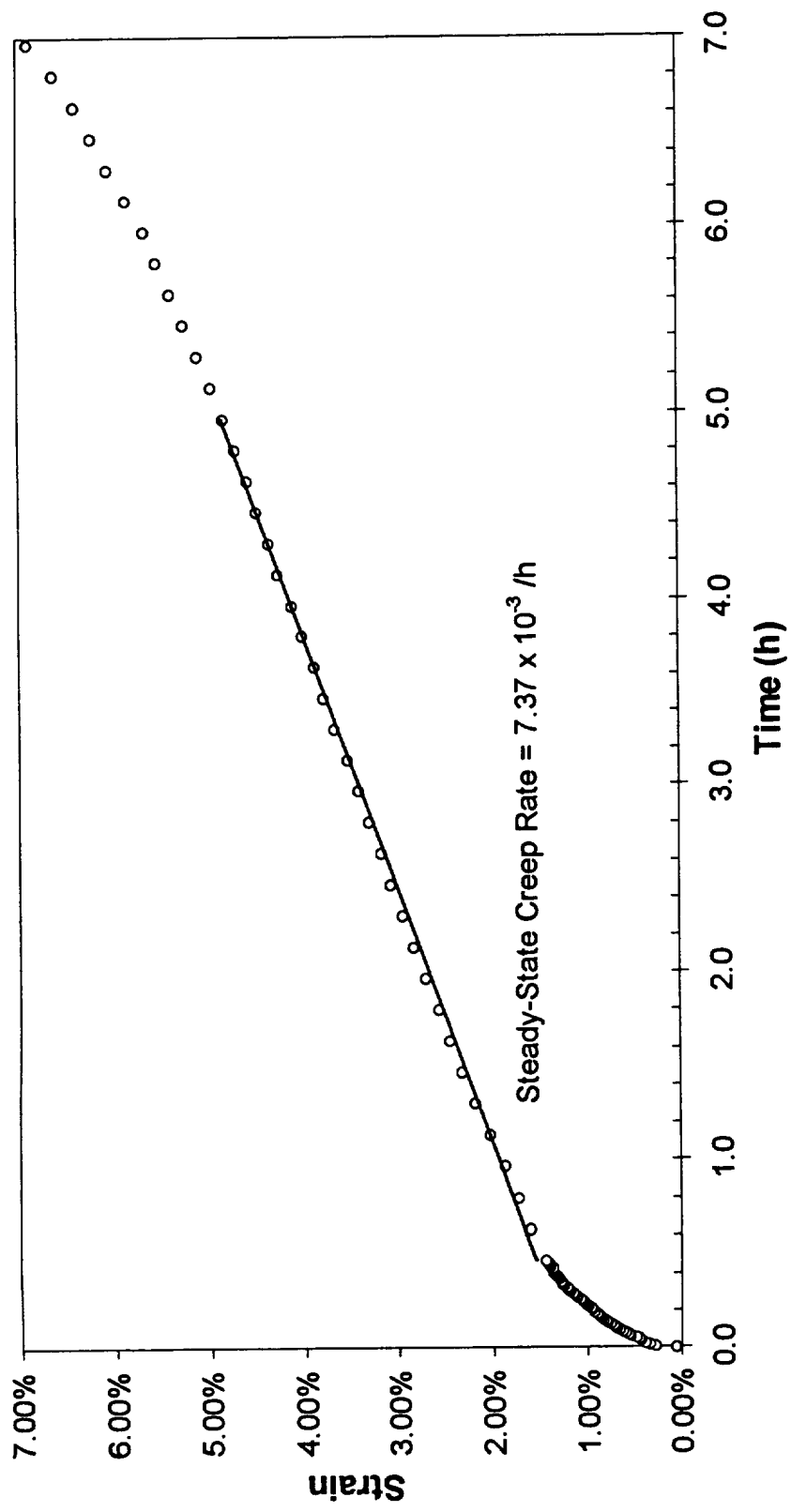


Figure A - 53 -
Extrusion L-3107 Tested At 800°C/26.8 MPa

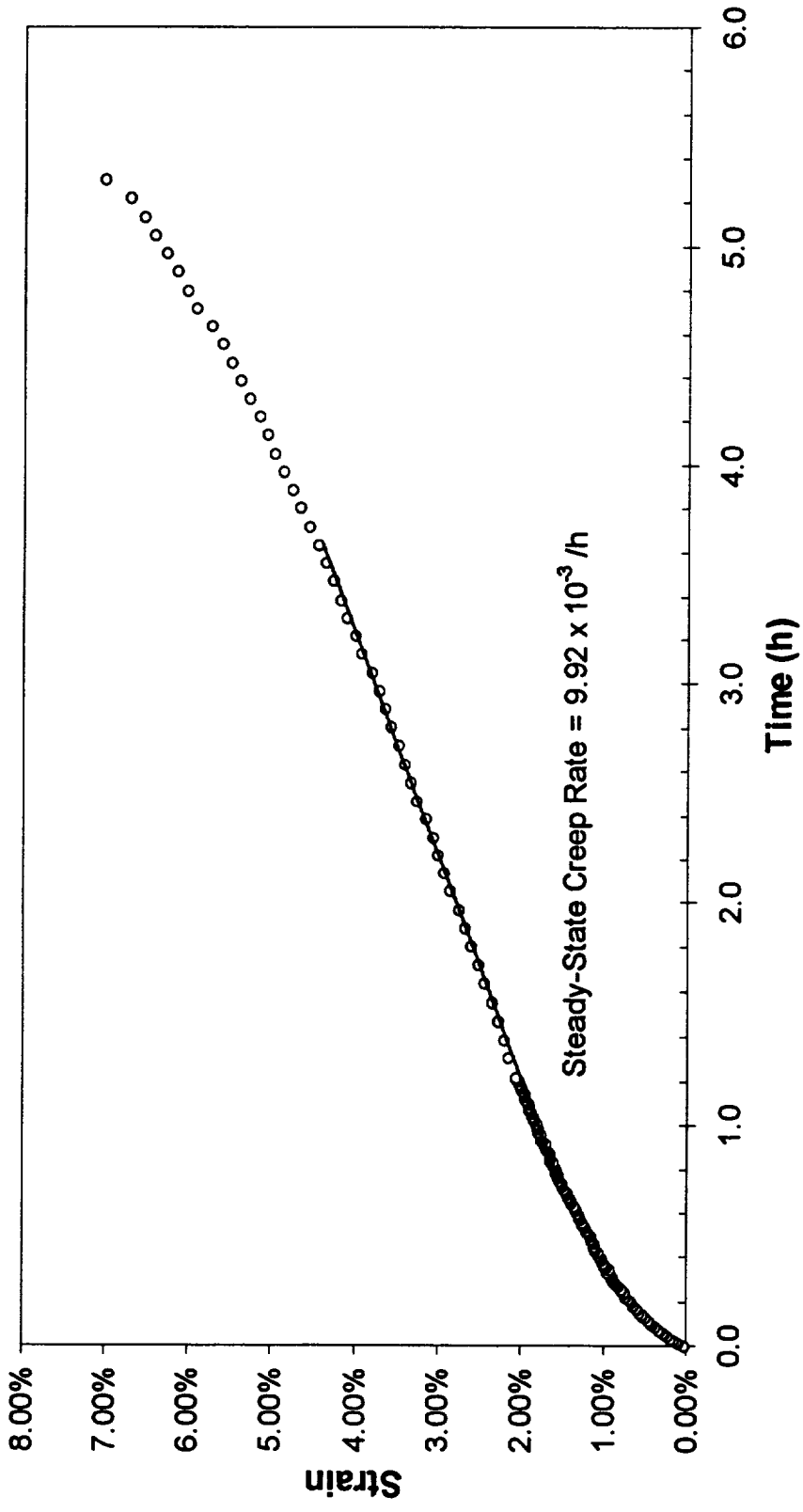


Figure A - 54 -
Extrusion L-3108 Tested At 800°C/26.8 MPa

Appendix B - Creep Of Cu-4 Cr-2 Nb

**Table B - 1
Results of Cu-4 Cr-2 Nb Creep Testing**

Temperature (°C)	Nominal Stress (MPa)	Extrusion	Test Order	Actual Stress (MPa)	Rate (1/h)	Time In			Time To 1% Strain (h)	Life (h)	Total Elongation (%)
						Stage 1 (h)	Stage 2 (h)	Stage 3 (h)			
500	72.9	L-3284	8	73.1	4.22E-04	4.38	42.99	57.98	7.38	105.35	8.13
500	72.9	L-3296	30	72.8	4.31E-05	80.34	360.59	365.00	105.83	805.93	5.72
500	72.9	L-3297	23	72.8	1.81E-05	100.17	304.40	0.00	14.45	404.57	1.96
500	72.9	L-3298	1	72.8	6.33E-05	30.46	244.92	284.57	3.06	559.95	6.85
500	84.0	L-3296	17	84.0	1.02E-04	24.92	197.93	143.45	8.92	366.30	6.35
500	84.0	L-3297	15								
Sample Broke On Loading											
500	84.0	L-3298	4	84.1	2.17E-04	18.50	111.46	95.65	14.55	225.61	8.89
500	92.8	L-3284	24	92.9	6.41E-03	0.65	4.44	9.02	1.07	10.59	10.59
500	92.8	L-3296	7	92.9	1.11E-03	2.00	23.95	22.32	4.95	48.26	12.33
500	92.8	L-3297	6	92.9	3.70E-04	4.60	69.99	28.99	3.60	103.58	5.71
500	92.8	L-3298	9	92.8	4.12E-04	8.04	55.98	52.48	1.14	116.50	8.04
650	37.4	L-3284	29	37.4	1.29E-04	0.65	4.44	9.02	42.30	10.59	10.59
650	37.4	L-3296	25	37.3	3.68E-04	7.92	63.90	28.49	10.42	100.31	5.96

Table B - 1
Results of Cu-4 Cr-2 Nb Creep Testing (Cont.)

Temperature (°C)	Nominal Stress (MPa)	Extrusion	Test Order	Actual Stress (MPa)	Rate (1/h)	Time In			Time To 1% Strain (h)	Life (h)	Total Elongation (%)
						Stage 1 (h)	Stage 2 (h)	Stage 3 (h)			
650	37.4	L-3297	13	37.4	1.11E-04	10.03	164.56	53.98	5.78	228.57	4.45
650	37.4	L-3298	16	37.6	1.74E-04	14.31	95.97	37.99	24.81	148.27	4.15
650	44.3	L-3296	11	Missing Sample							
650	44.3	L-3298	3	44.3	4.11E-04	3.75	54.09	20.49	5.37	78.34	5.64
650	49.8	L-3284	27	49.9	3.31E-03	0.80	5.58	7.00	1.67	13.38	8.28
650	49.8	L-3296	19	49.9	4.39E-03	0.34	6.47	5.50	1.28	12.30	10.32
650	49.8	L-3297	20	49.7	5.15E-03	0.44	4.25	4.50	1.06	9.18	6.64
650	49.8	L-3298	5	49.7	4.41E-03	0.65	7.04	5.16	0.33	12.85	11.15
800	19.2	L-3284	10	44.4	2.82E+00	0.00	0.02	0.02	0.00	0.04	28.08
800	19.2	L-3296	2	19.2	1.40E-03	1.91	20.49	10.00	1.14	32.40	9.31
800	19.2	L-3297	12	44.4	1.37E+00	0.03	0.03	0.03	0.03	0.09	20.40
800	19.2	L-3298	26	19.2	1.57E-03	4.60	10.50	12.76	1.06	27.88	11.93
800	23.3	L-3296	21	23.4	3.21E-03	1.00	6.51	5.75	0.49	13.26	8.29
800	23.3	L-3298	18	23.5	2.58E-03	1.47	9.21	5.00	0.19	15.67	7.79

Table B - 1
Results of Cu-4 Cr-2 Nb Creep Testing (Cont.)

Temperature (°C)	Nominal Stress (MPa)	Extrusion	Test Order	Actual Stress (MPa)	Rate (1/h)	Time In			Time To 1% Strain (h)	Life (h)	Total Elongation (%)
						Stage 1 (h)	Stage 2 (h)	Stage 3 (h)			
800	26.8	L-3284	14	26.8	7.59E-03	0.39	3.34	2.50	0.18	6.23	12.44
800	26.8	L-3296	22	26.9	1.21E-02	0.49	2.27	1.76	0.15	4.52	12.69
800	26.8	L-3298	28	26.9	3.47E-02	0.14	0.98	0.75	0.03	1.87	14.11

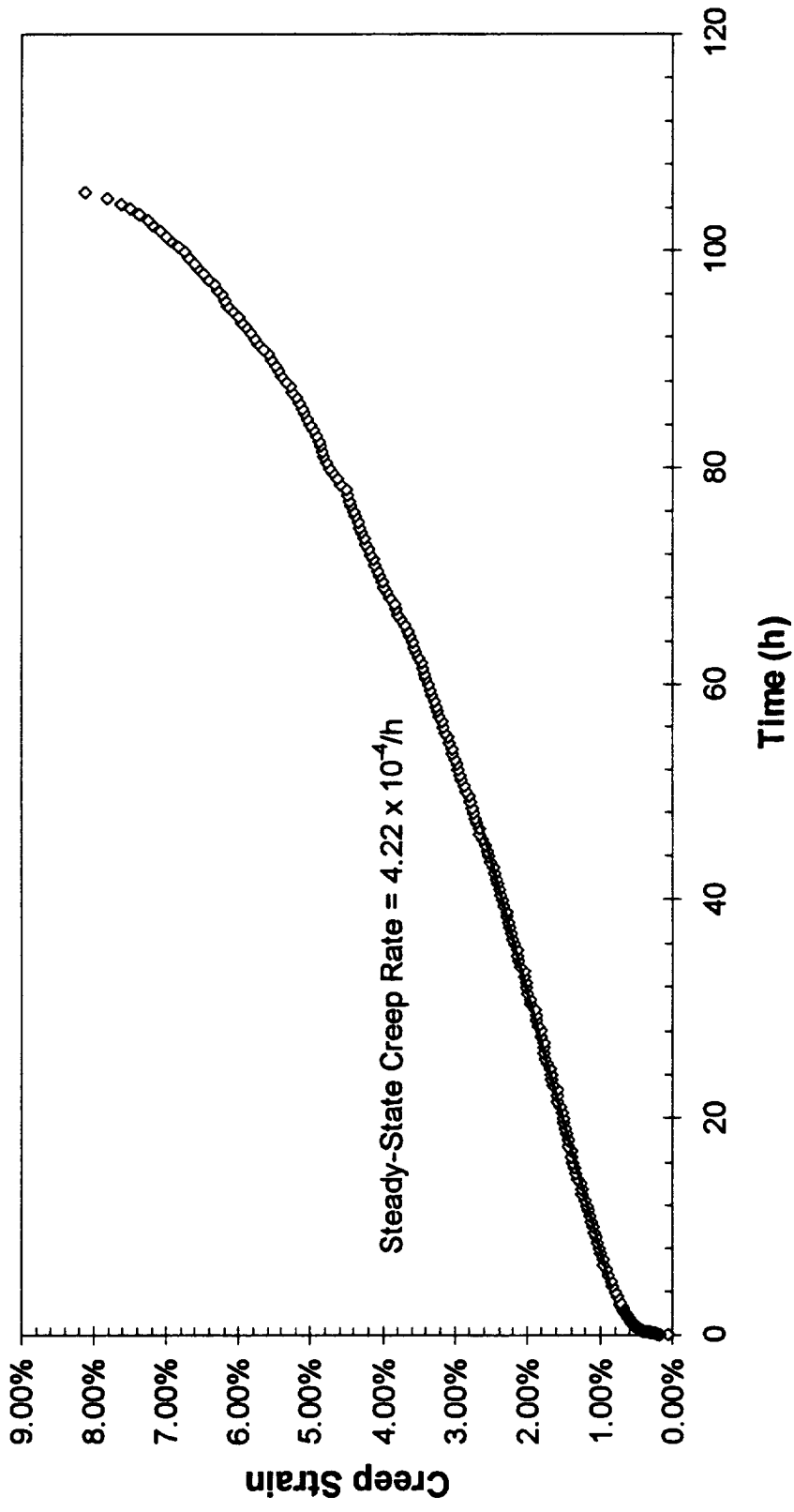


Figure B - 1 -
Extrusion L-3284 Tested At 500°C/72.9 MPa

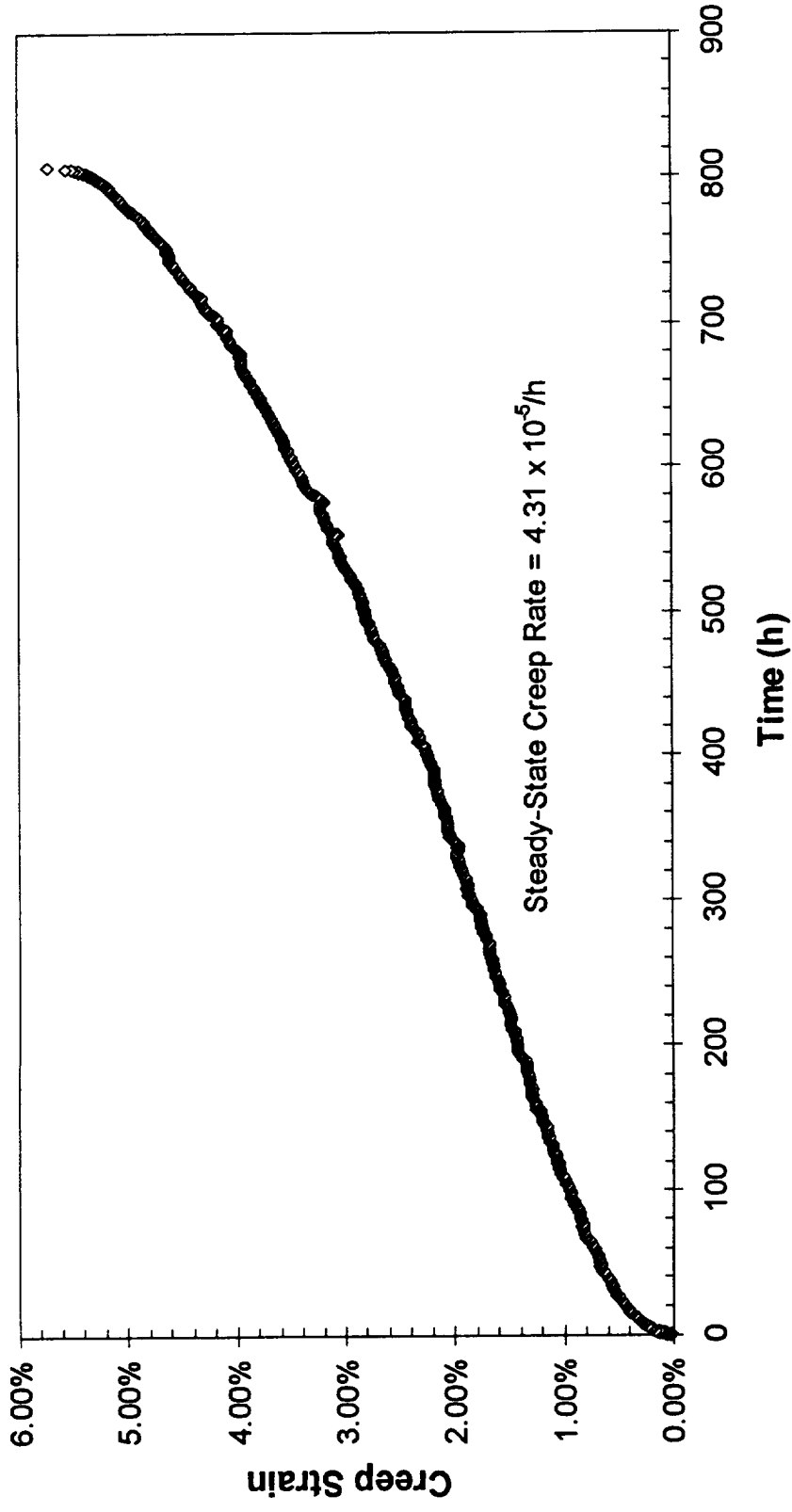


Figure B - 2 -
Extrusion L-3296 Tested At 500°C/72.9 MPa

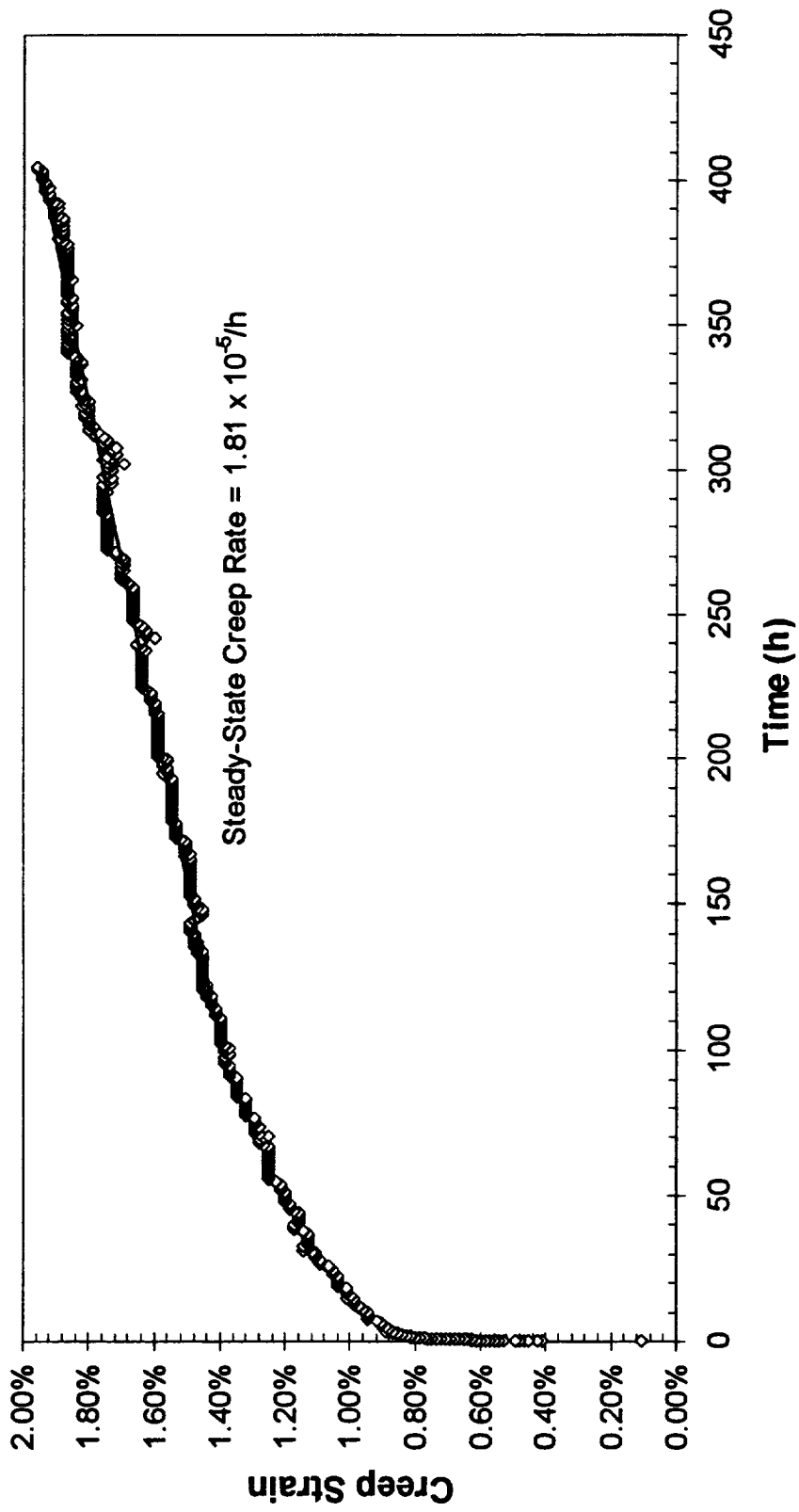


Figure B - 3 -
Extrusion L-3297 Tested At 500°C/72.9 MPa

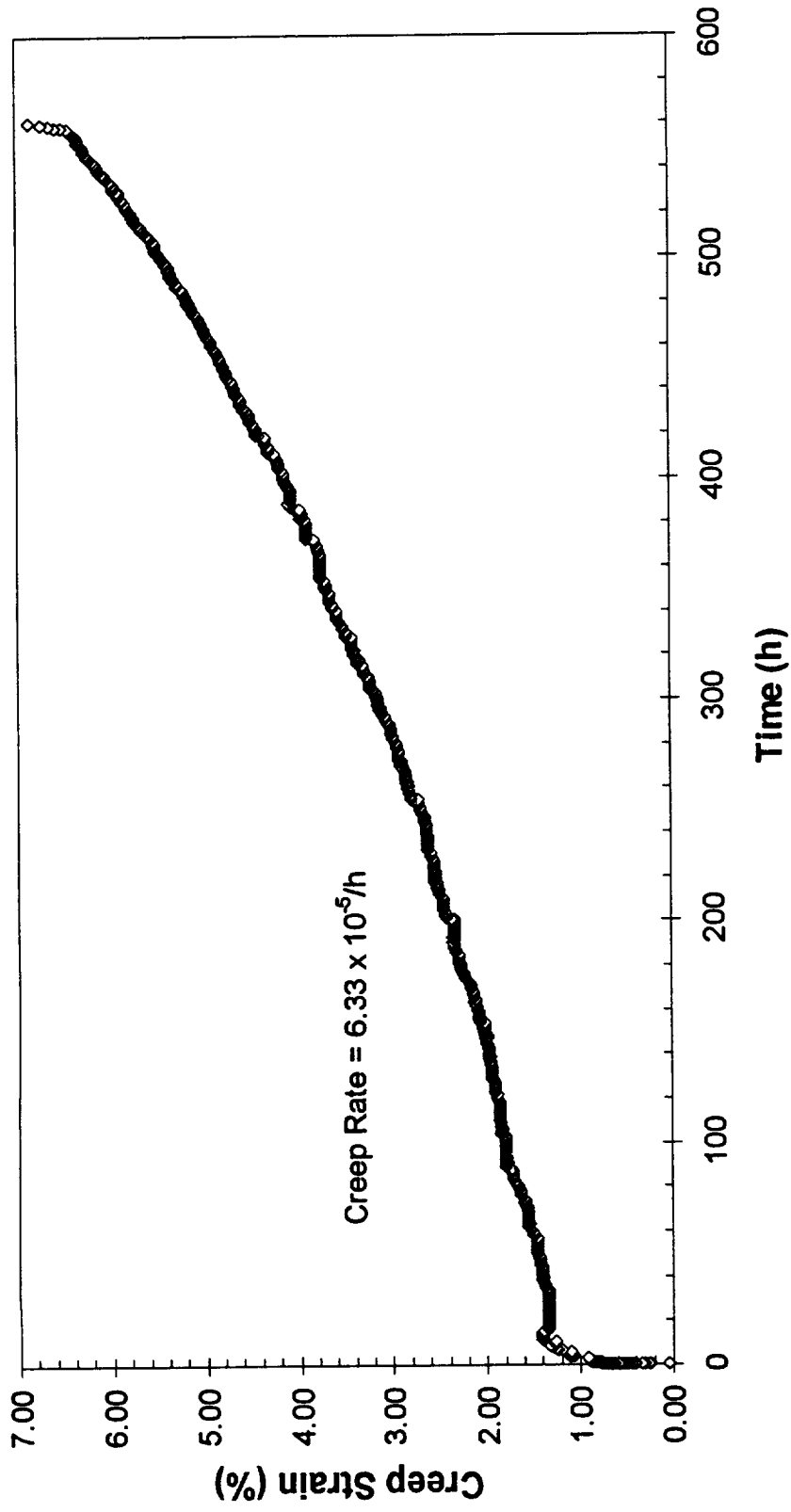


Figure B - 4 -
Extrusion L-3298 Tested At 500°C/72.9 MPa

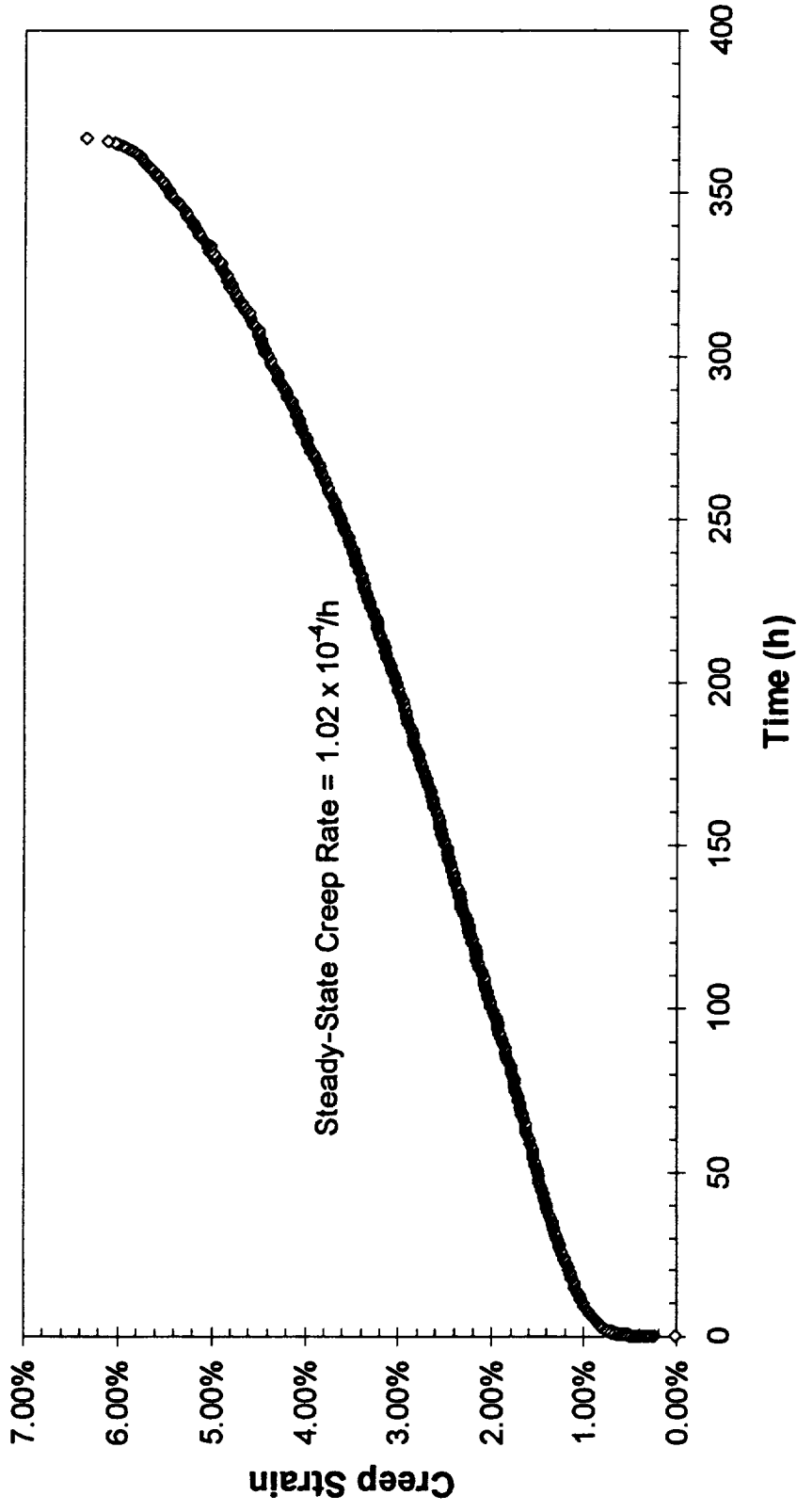


Figure B - 5 -
Extrusion L-3296 Tested At 500°C/84.0 MPa

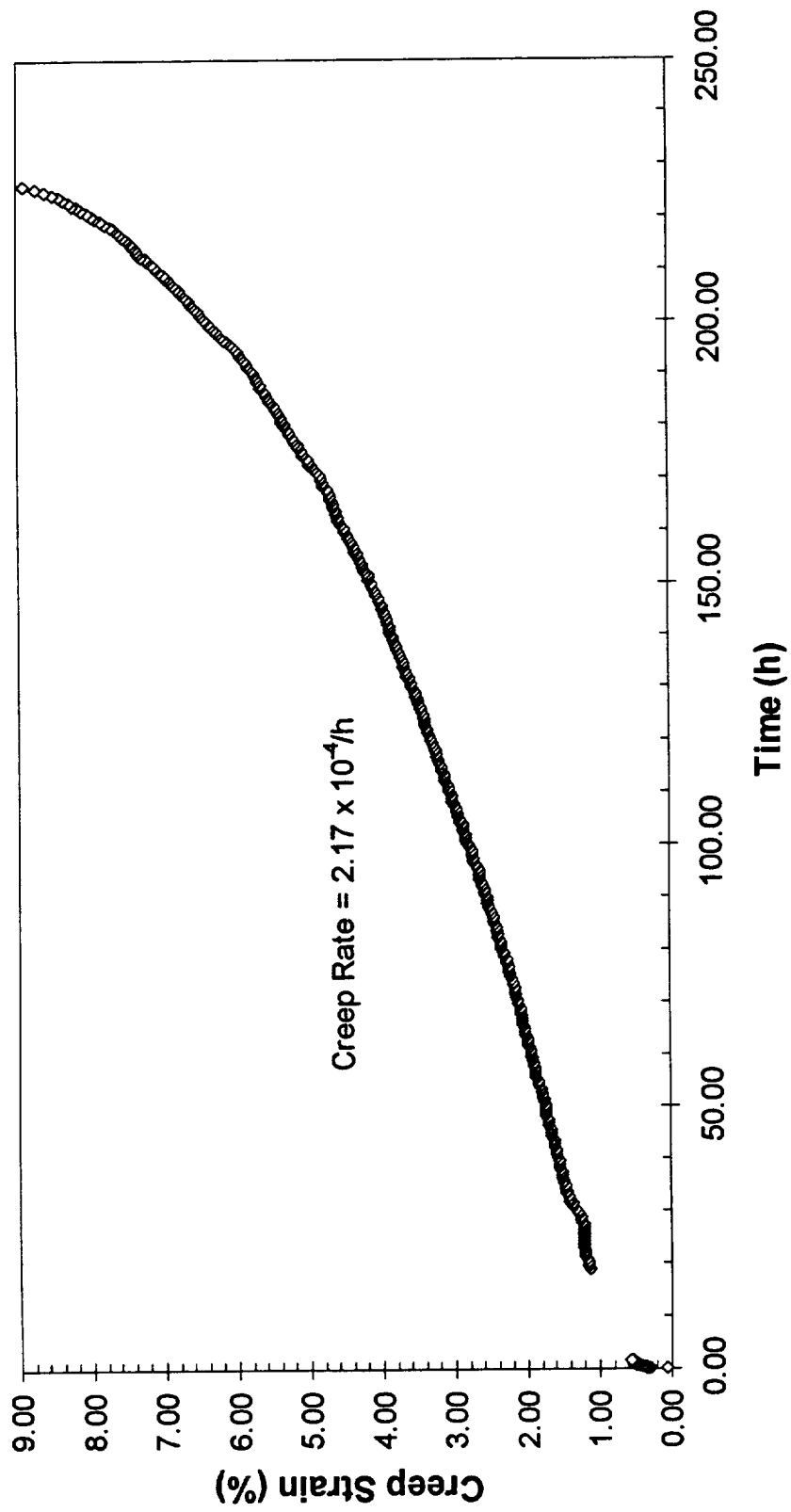


Figure B - 6 -
Extrusion L-3298 Tested At 500°C/84.0 MPa

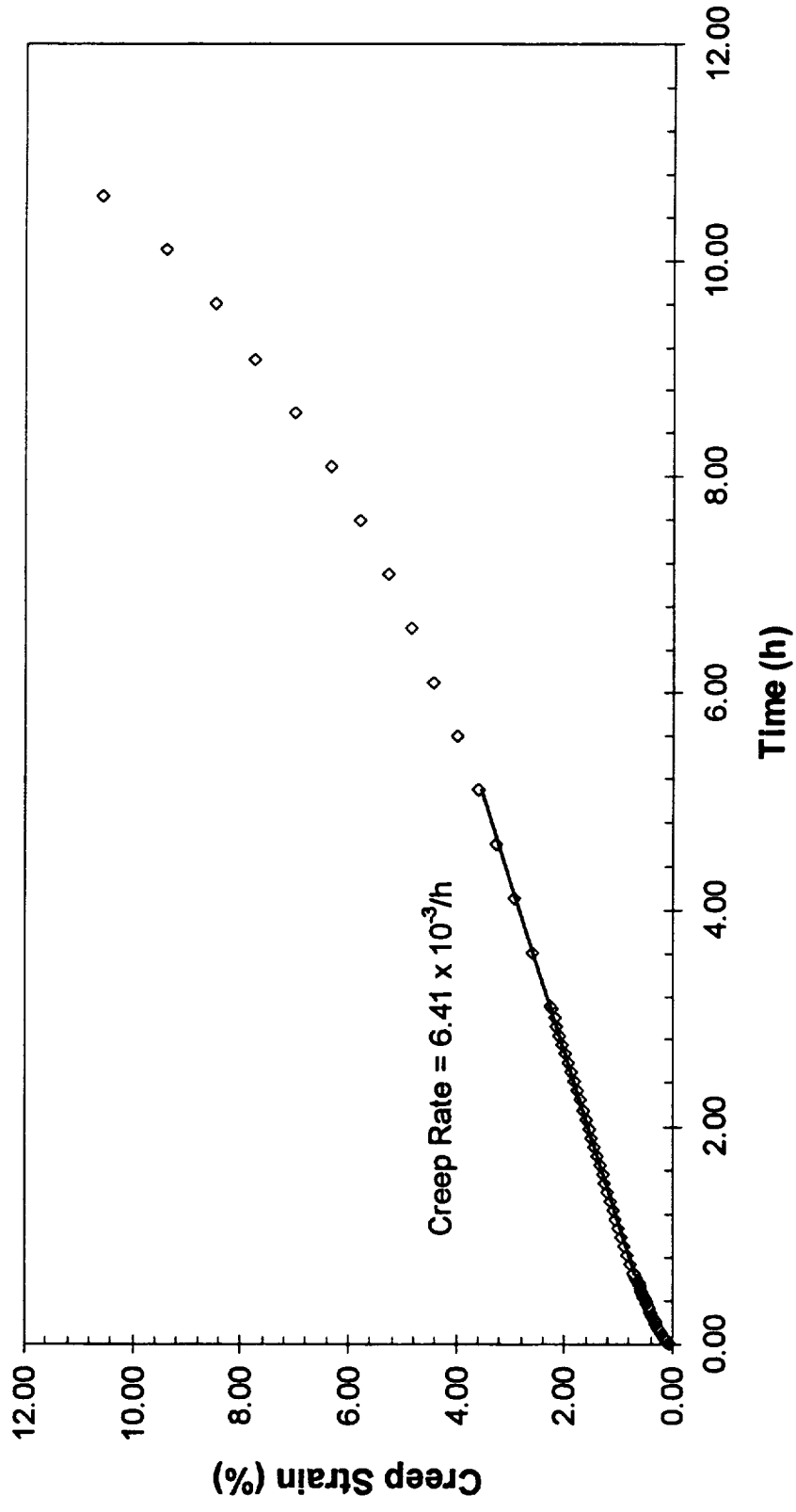


Figure B - 7 -
Extrusion L-3284 Tested At 500°C/92.8 MPa

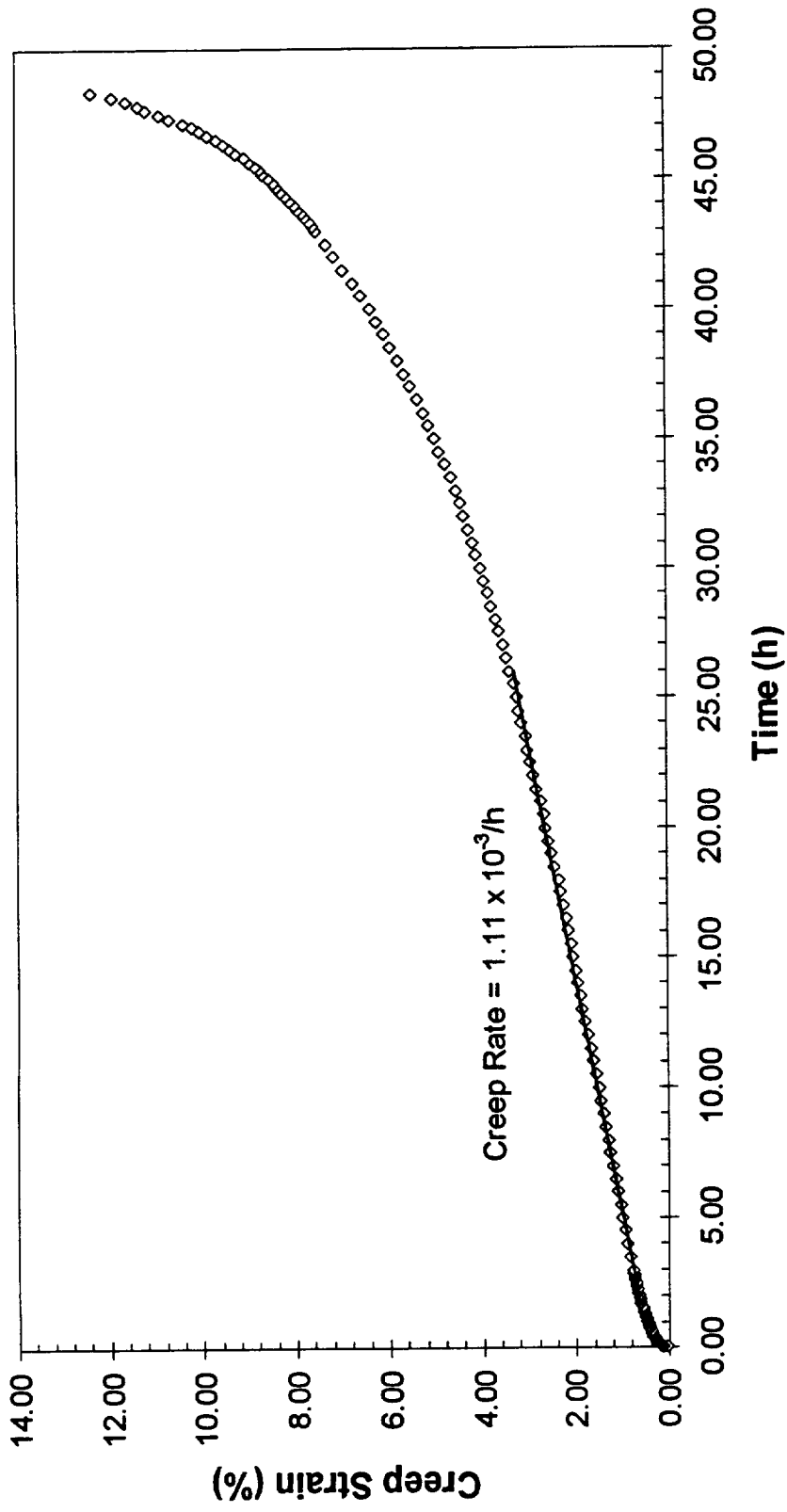


Figure B - 8 -
Extrusion L-3296 Tested At 500°C/92.8 MPa

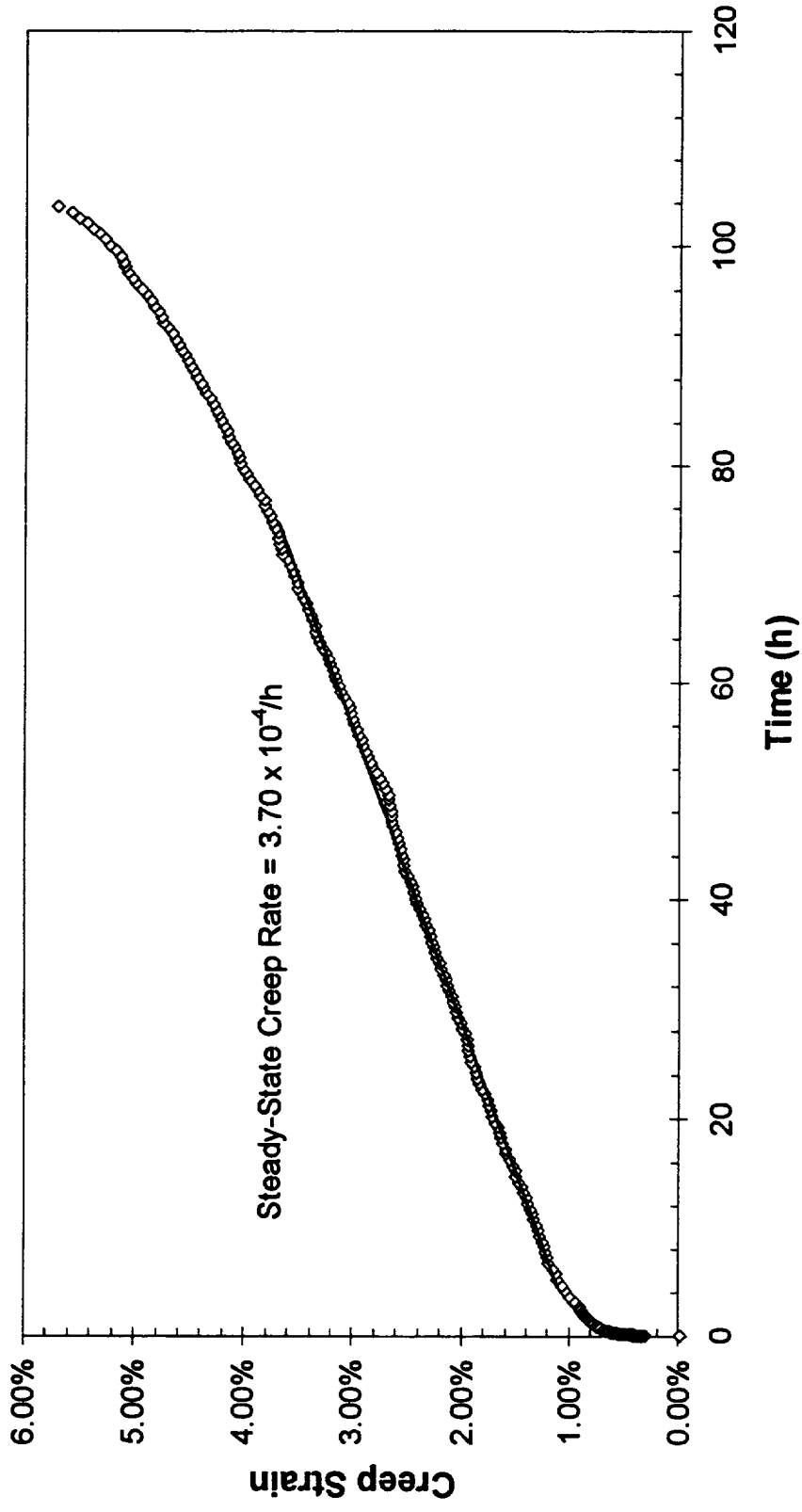


Figure B - 9 -
Extrusion L-3297 Tested At 500°C/92.8 MPa

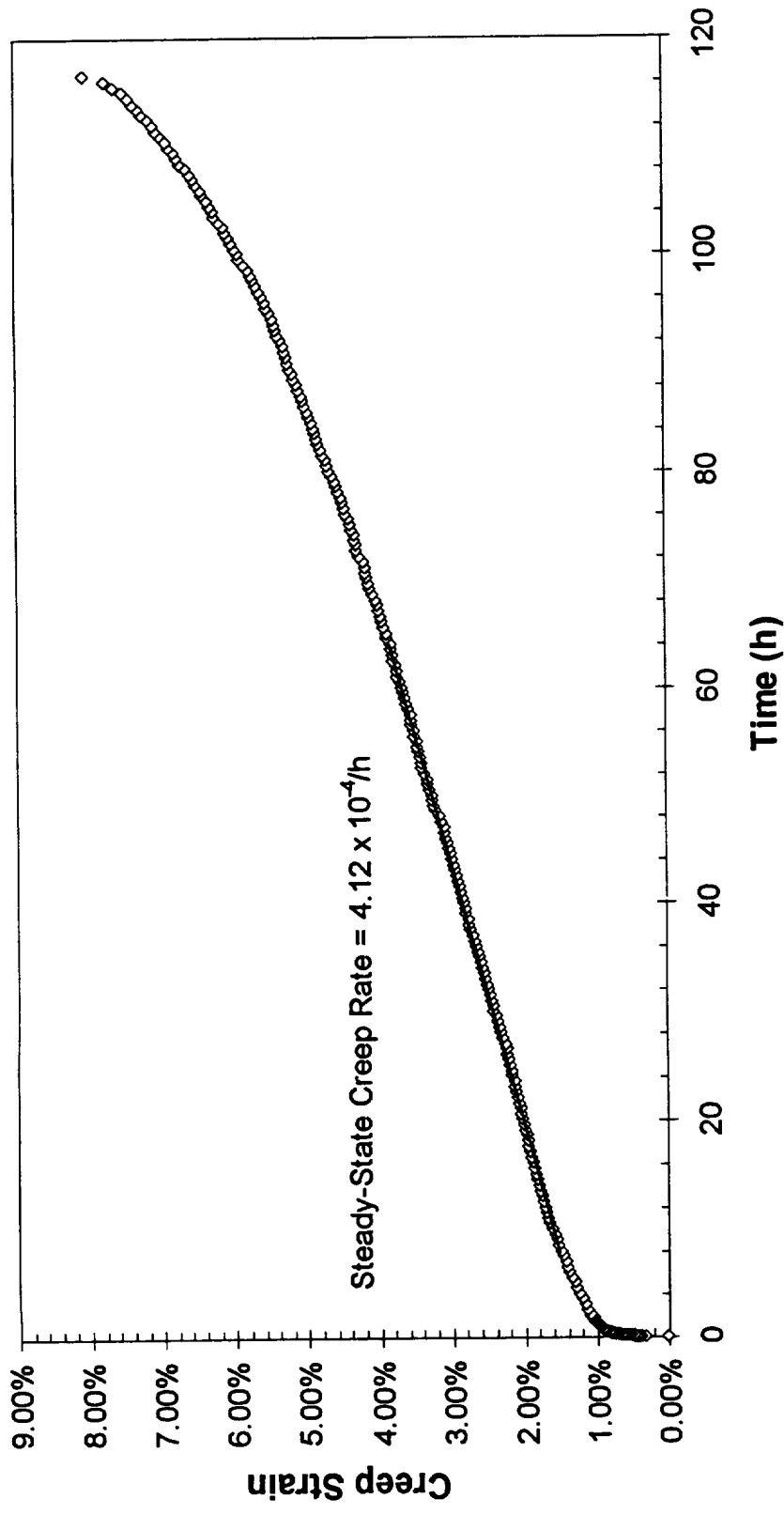


Figure B - 10 -
Extrusion L-3298 Tested At 500°C/92.8 MPa

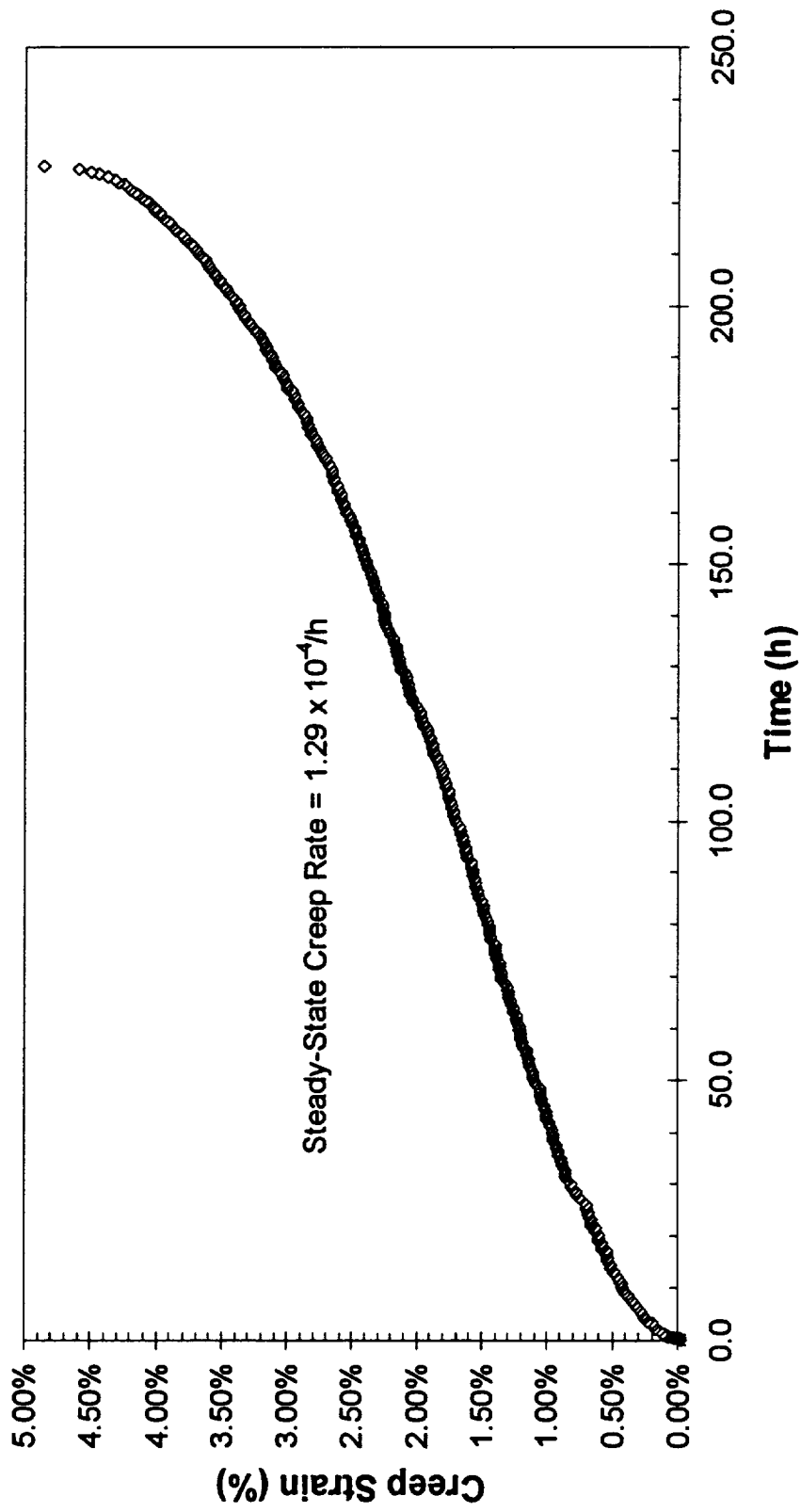


Figure B - 11 -
Extrusion L-3284 Tested At 650°C/37.4 MPa

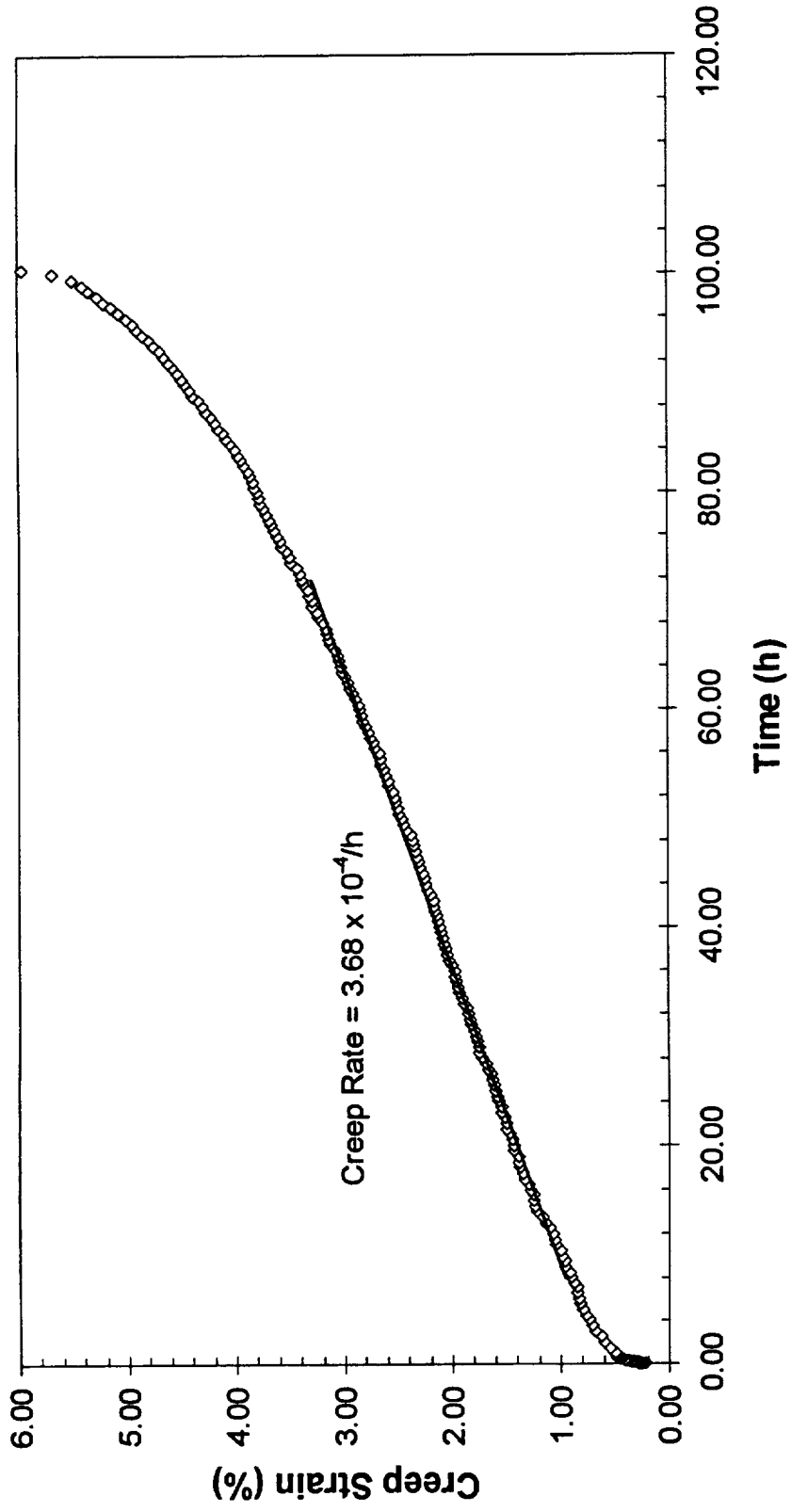


Figure B - 12 -
Extrusion L-3296 Tested At 650°C/37.4 MPa

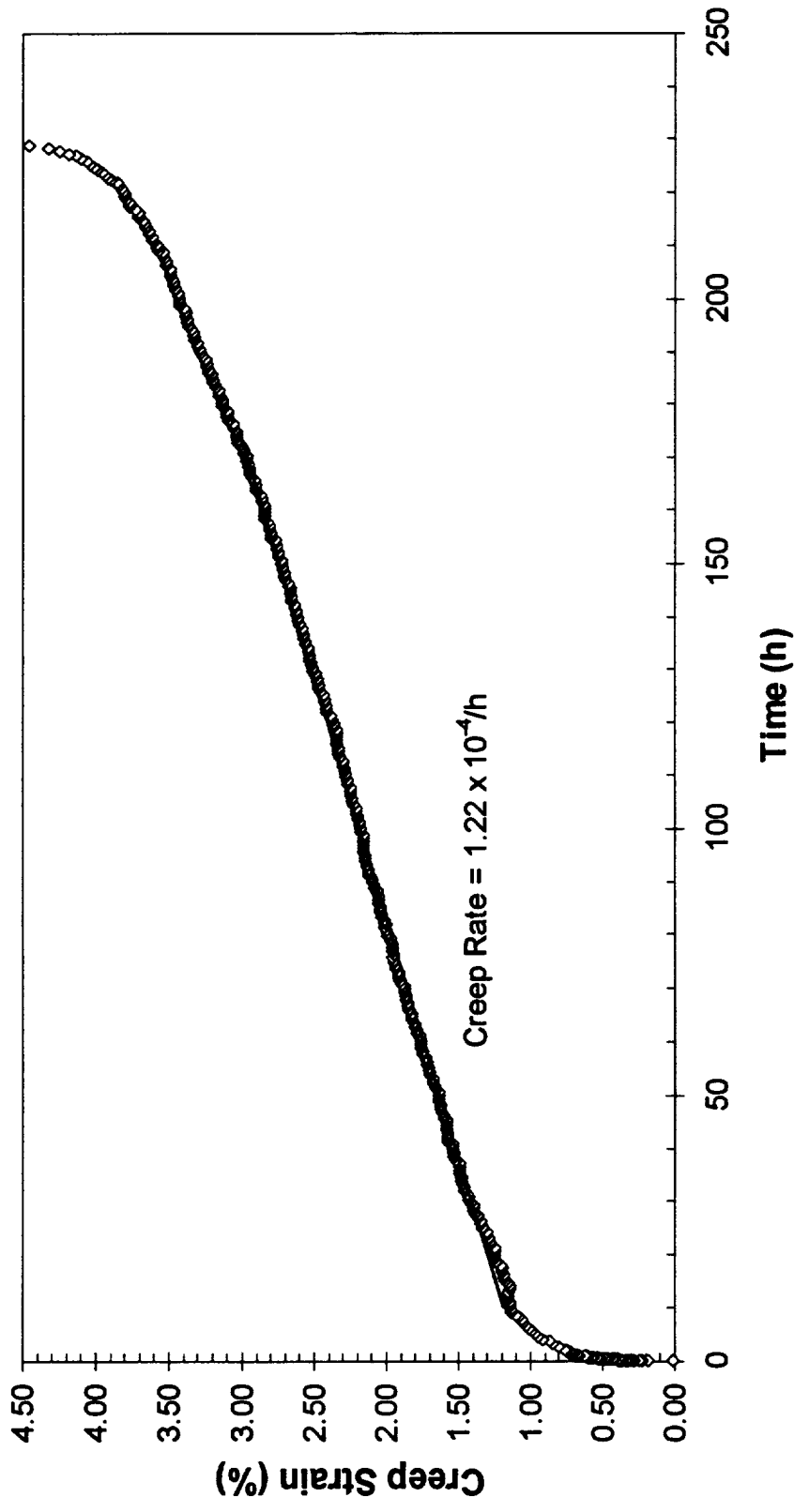


Figure B - 13 -
Extrusion L-3297 Tested At 650°C/37.4 MPa

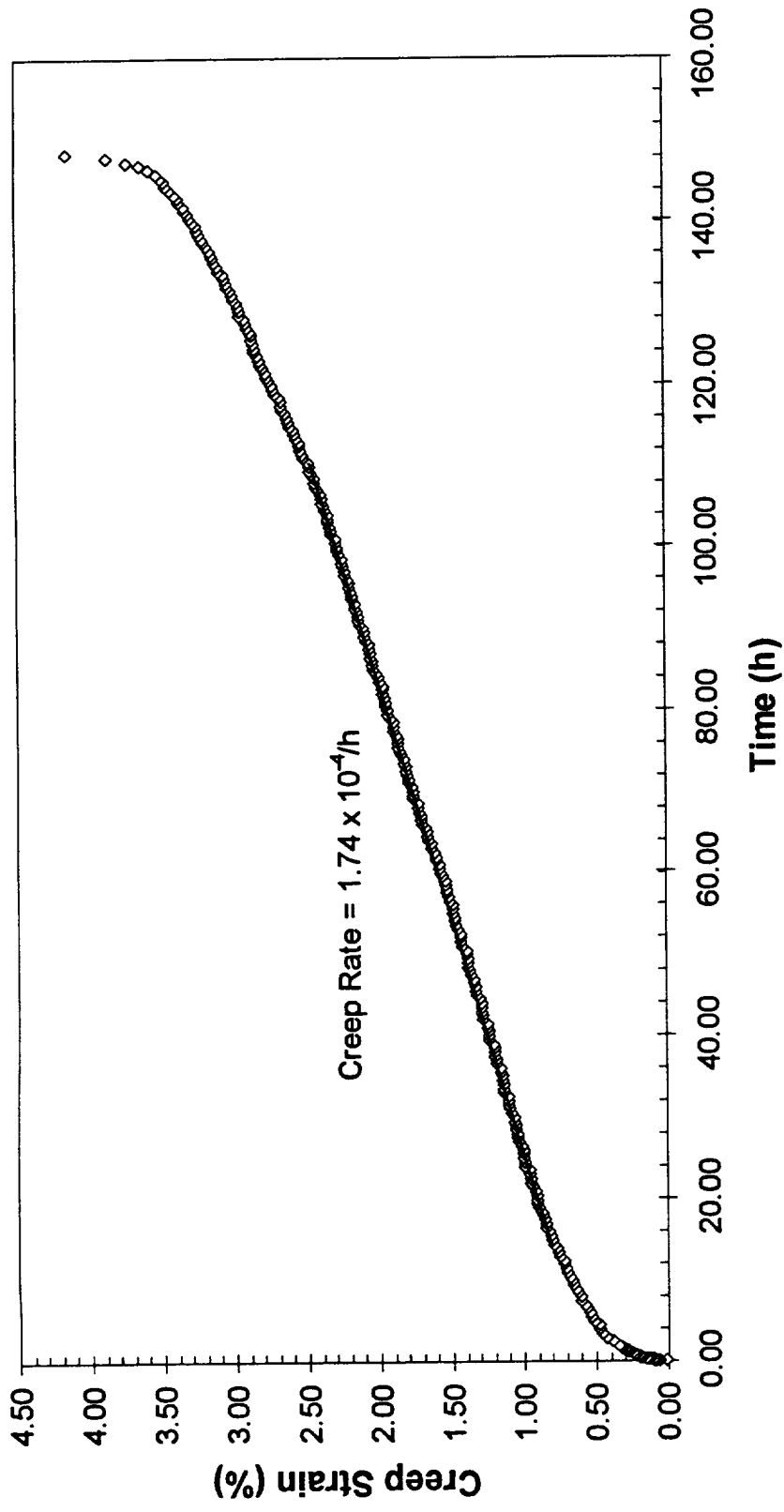


Figure B - 14 -
Extrusion L-3298 Tested At 650°C/37.4 MPa

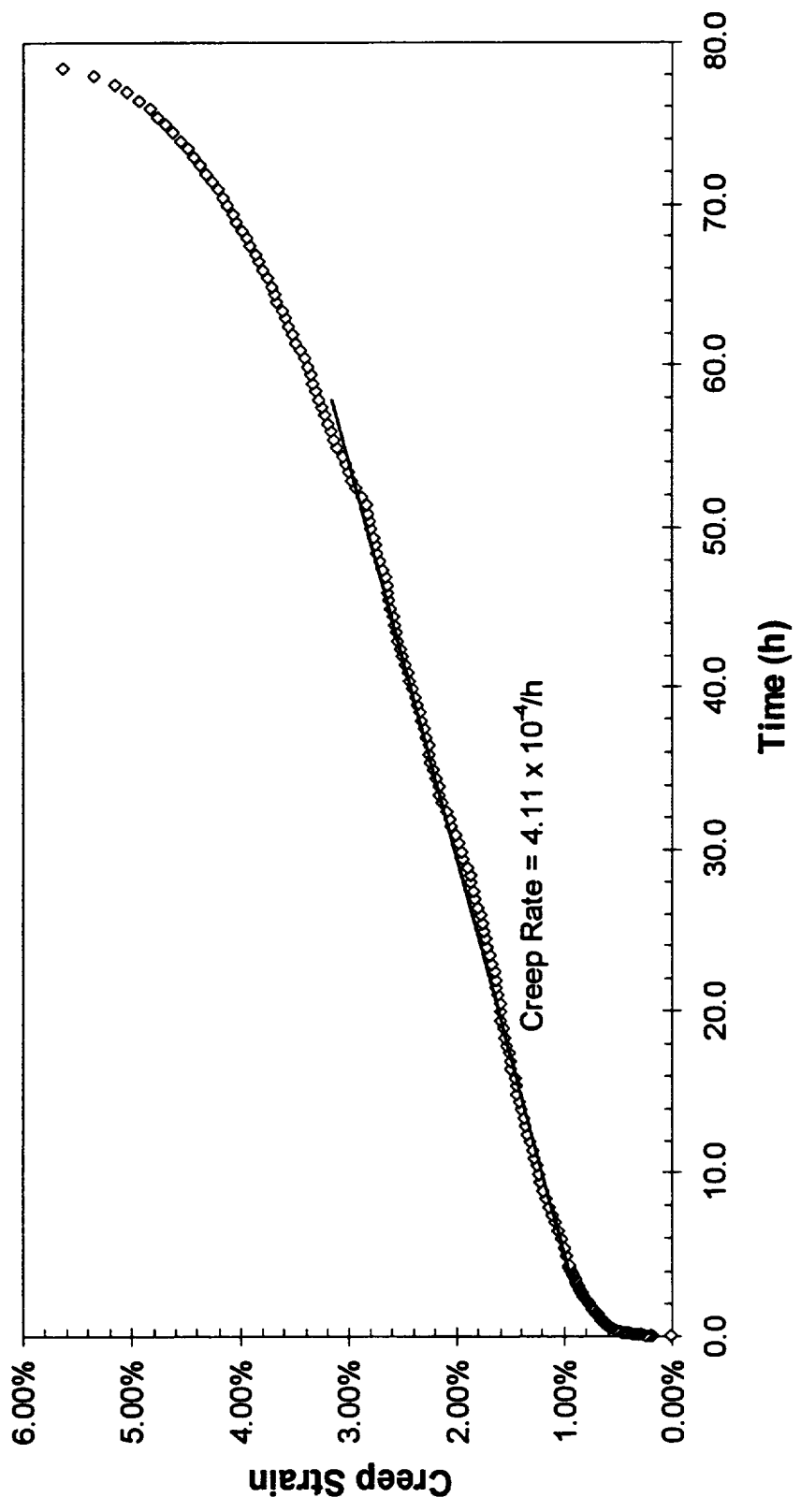


Figure B - 15 -
Extrusion L-3298 Tested At 650°C/44.3 MPa

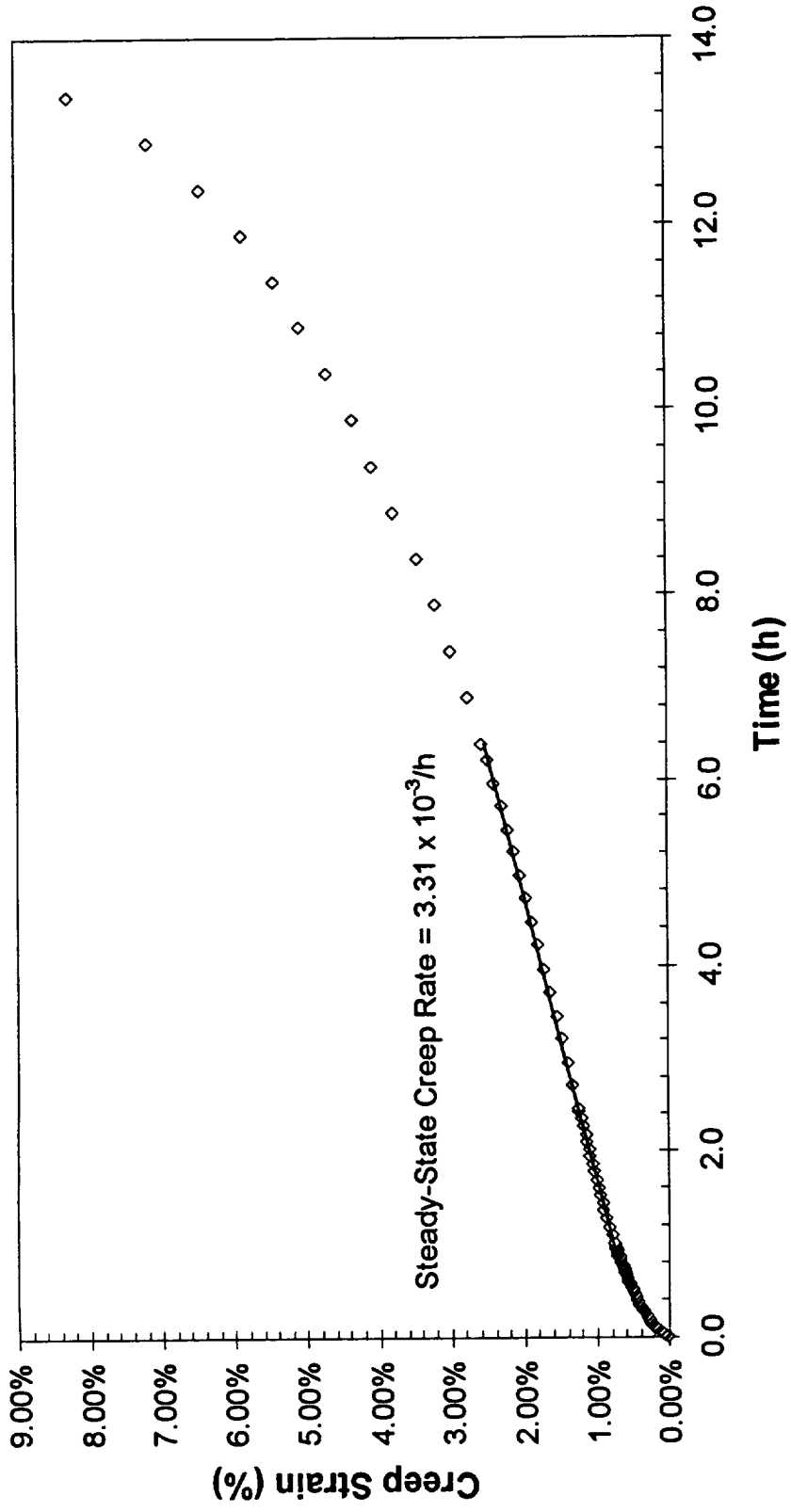


Figure B - 16 -
Extrusion L-3284 Tested At 650°C/49.8 MPa

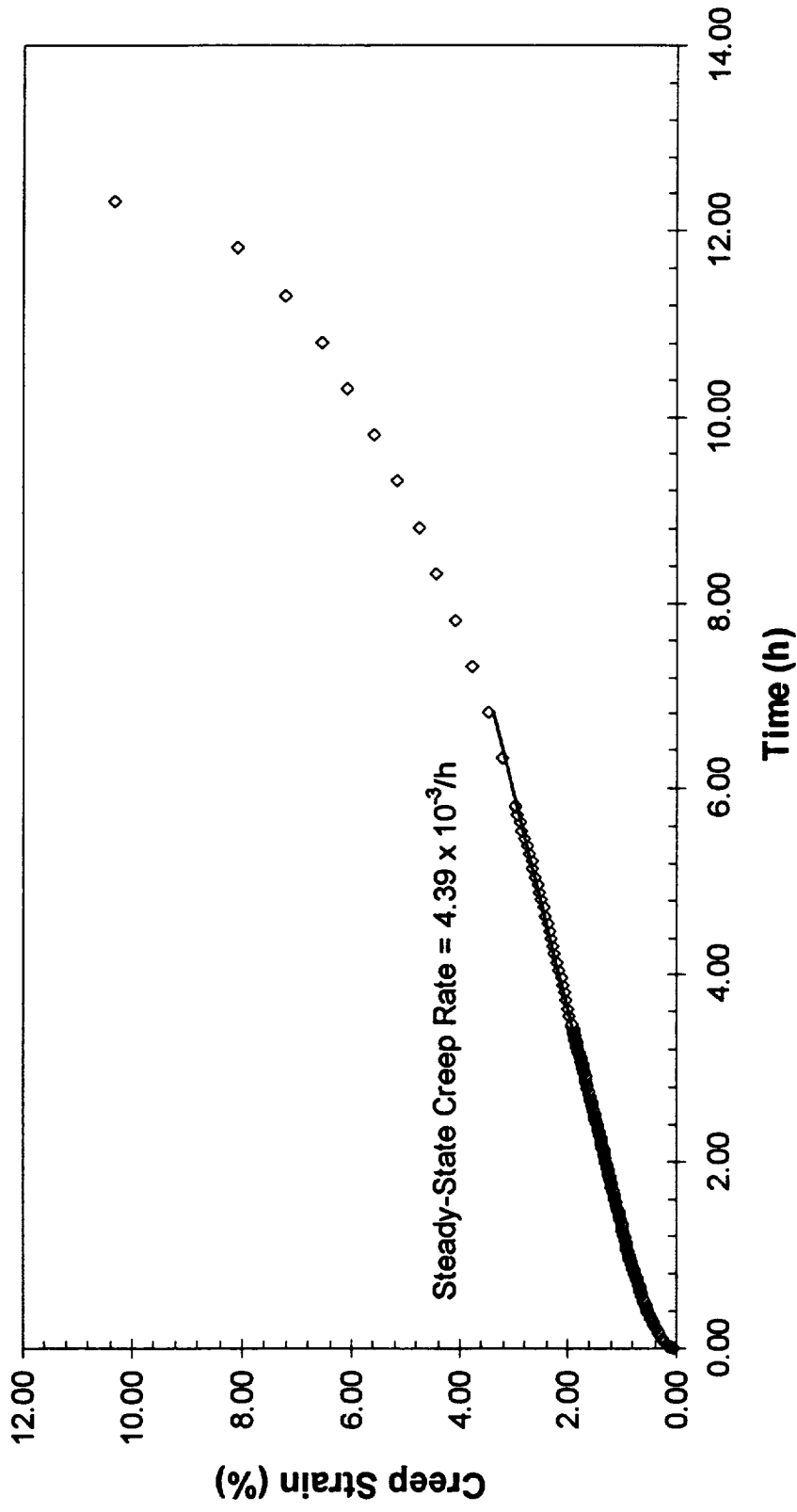


Figure B - 17 -
 Extrusion L-3296 Tested At 650°C/49.8 MPa

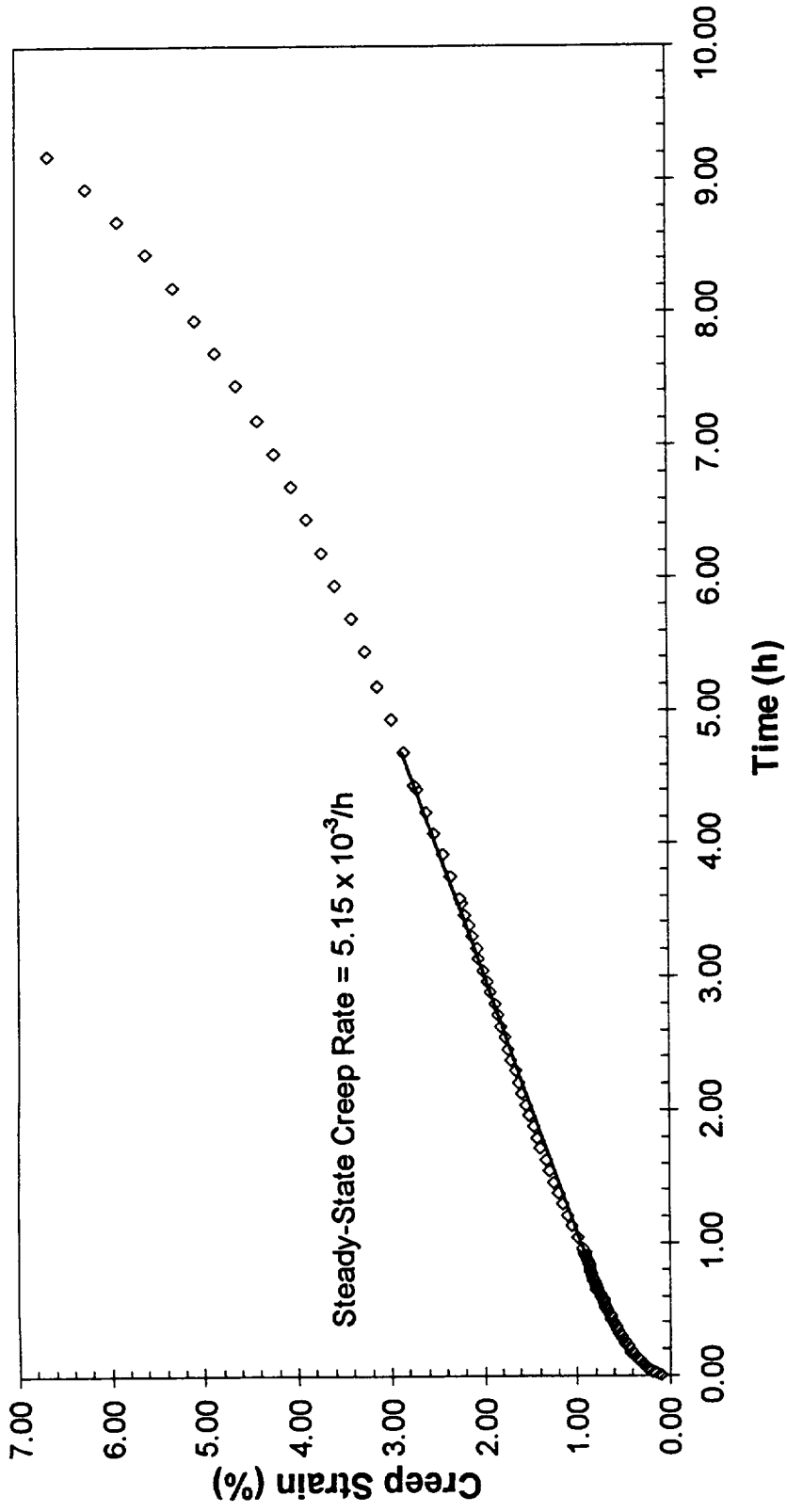


Figure B - 18 -
Extrusion L-3297 Tested At 650°C/49.8 MPa

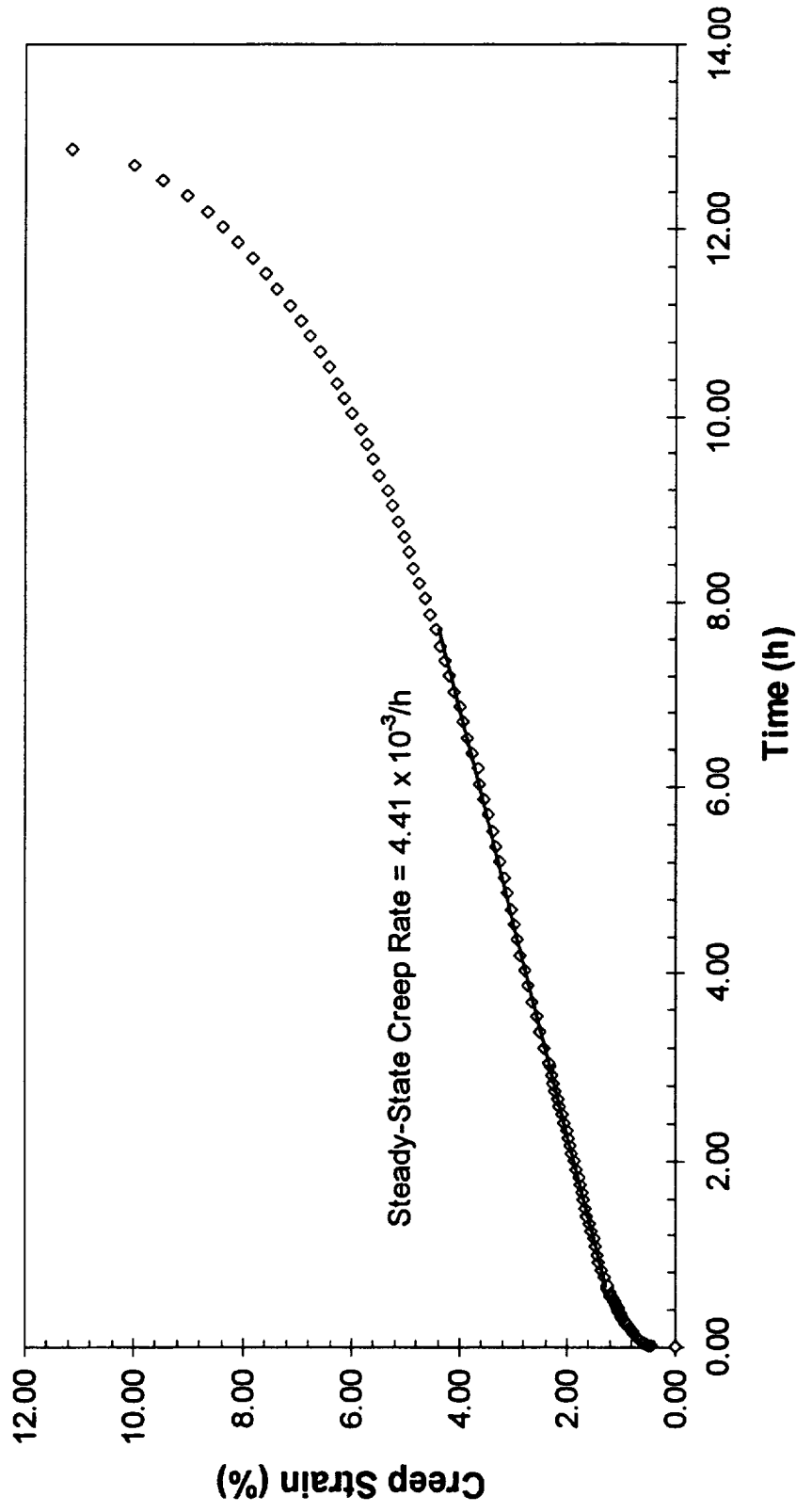


Figure B - 19 -
Extrusion L-3298 Tested At 650°C/49.8 MPa

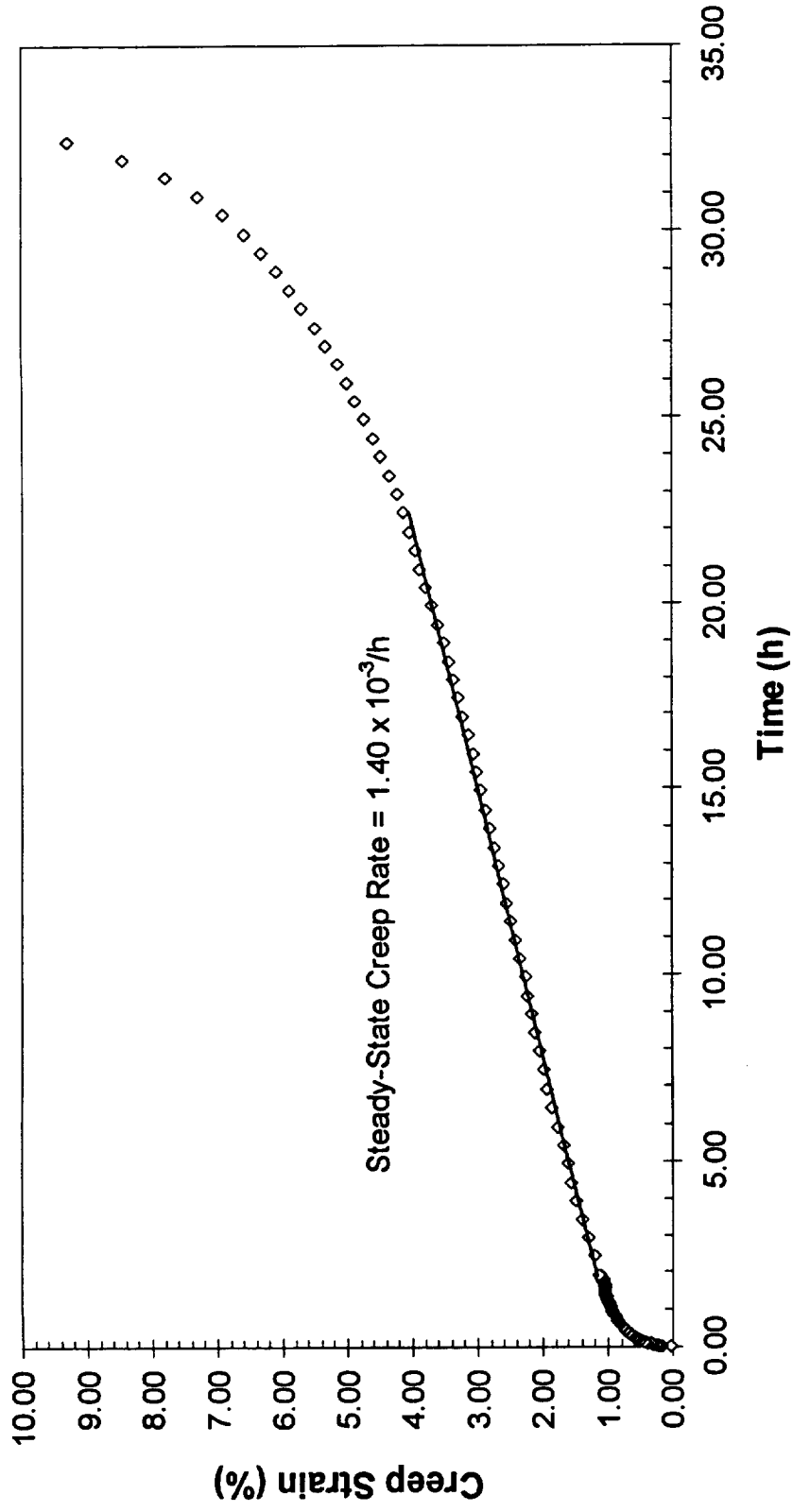


Figure B - 20 -
Extrusion L-3296 Tested At 800°C/19.2 MPa

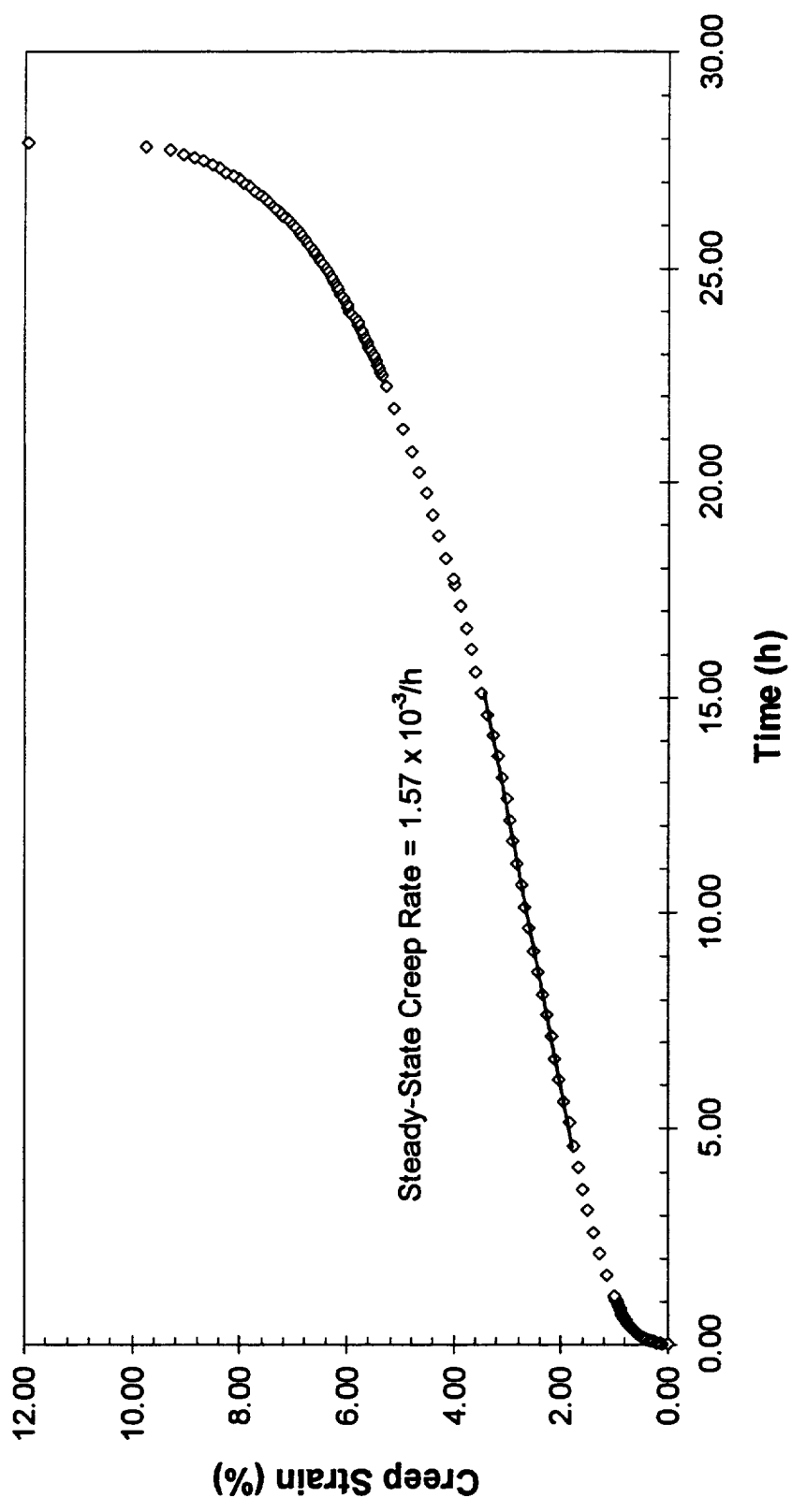


Figure B - 21 -
Extrusion L-3298 Tested At 800°C/19.2 MPa

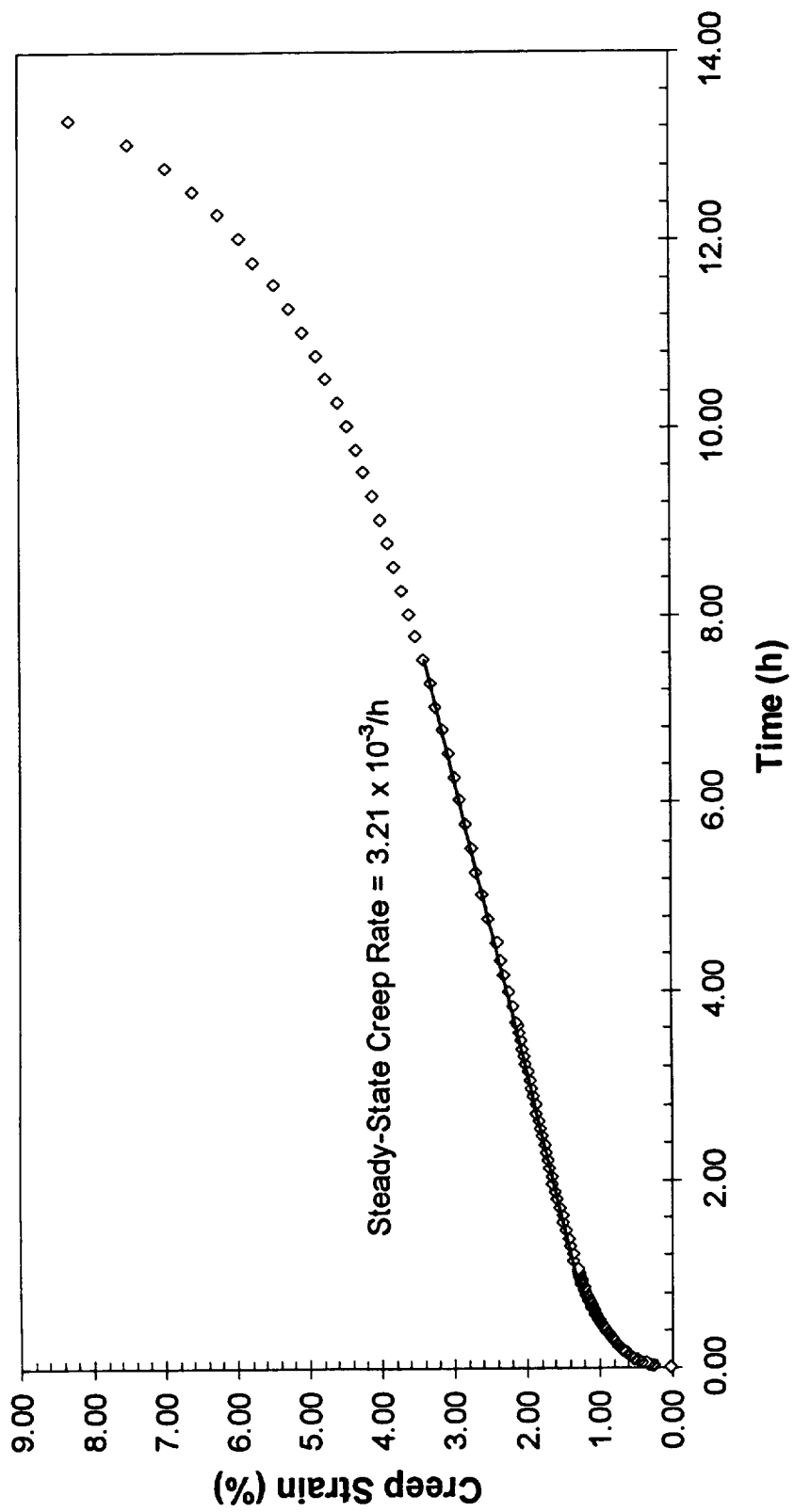


Figure B - 22 -
Extrusion L-3296 Tested At 800°C/23.3 MPa

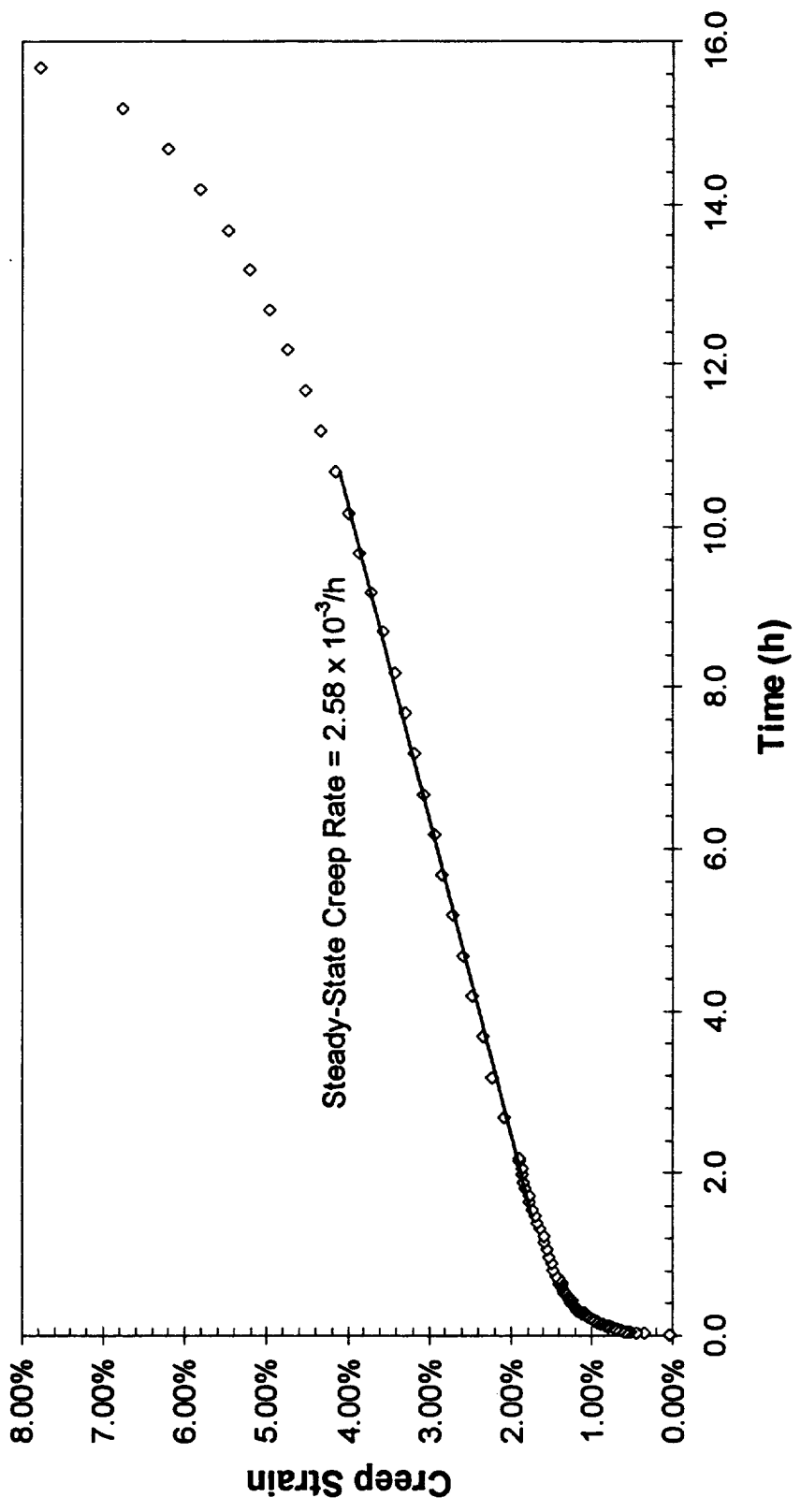


Figure B - 23 -
Extrusion L-3298 Tested At 800°C/23.3 MPa

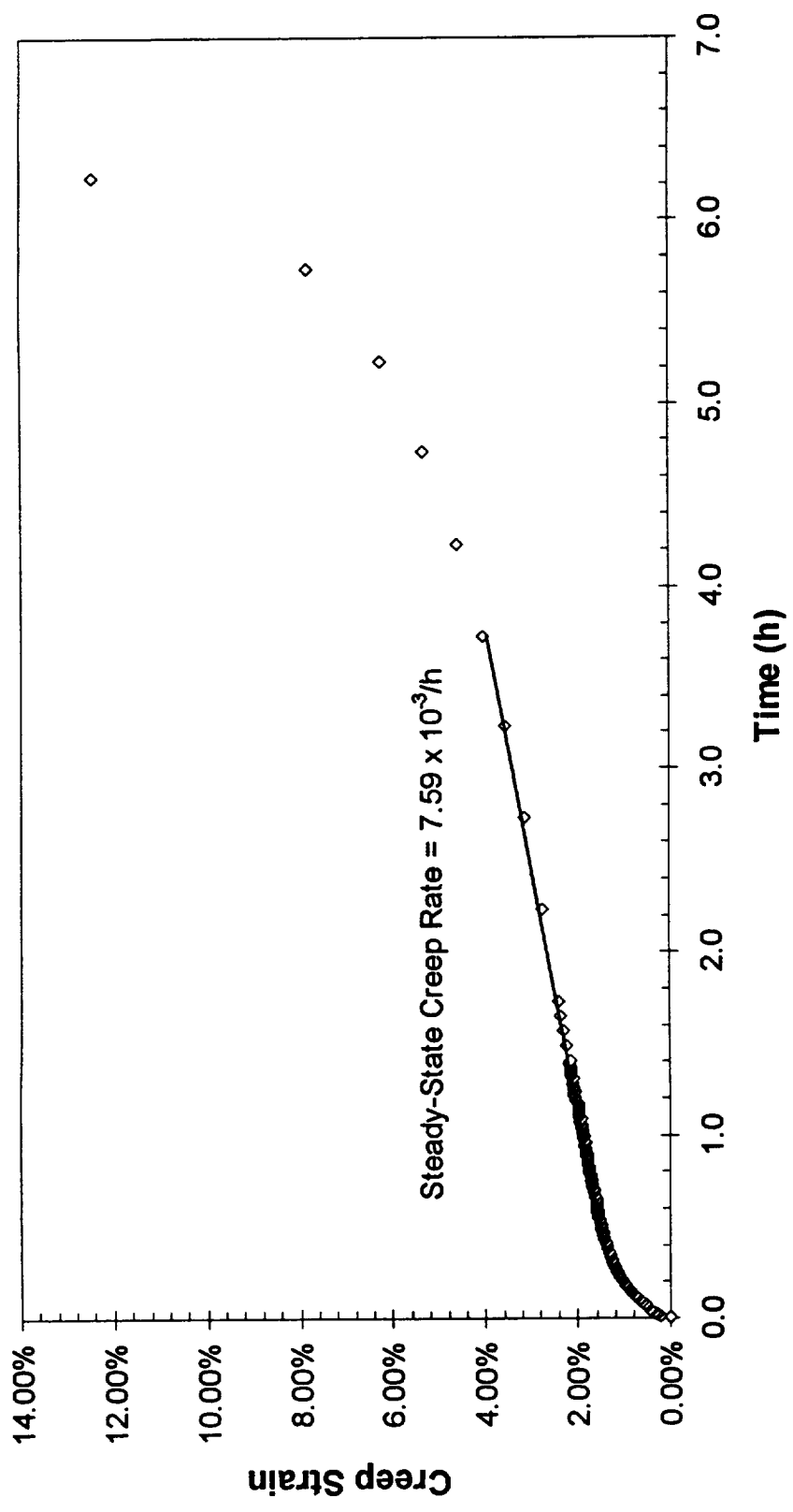


Figure B - 24 -
Extrusion L-3284 Tested At 800°C/26.8 MPa

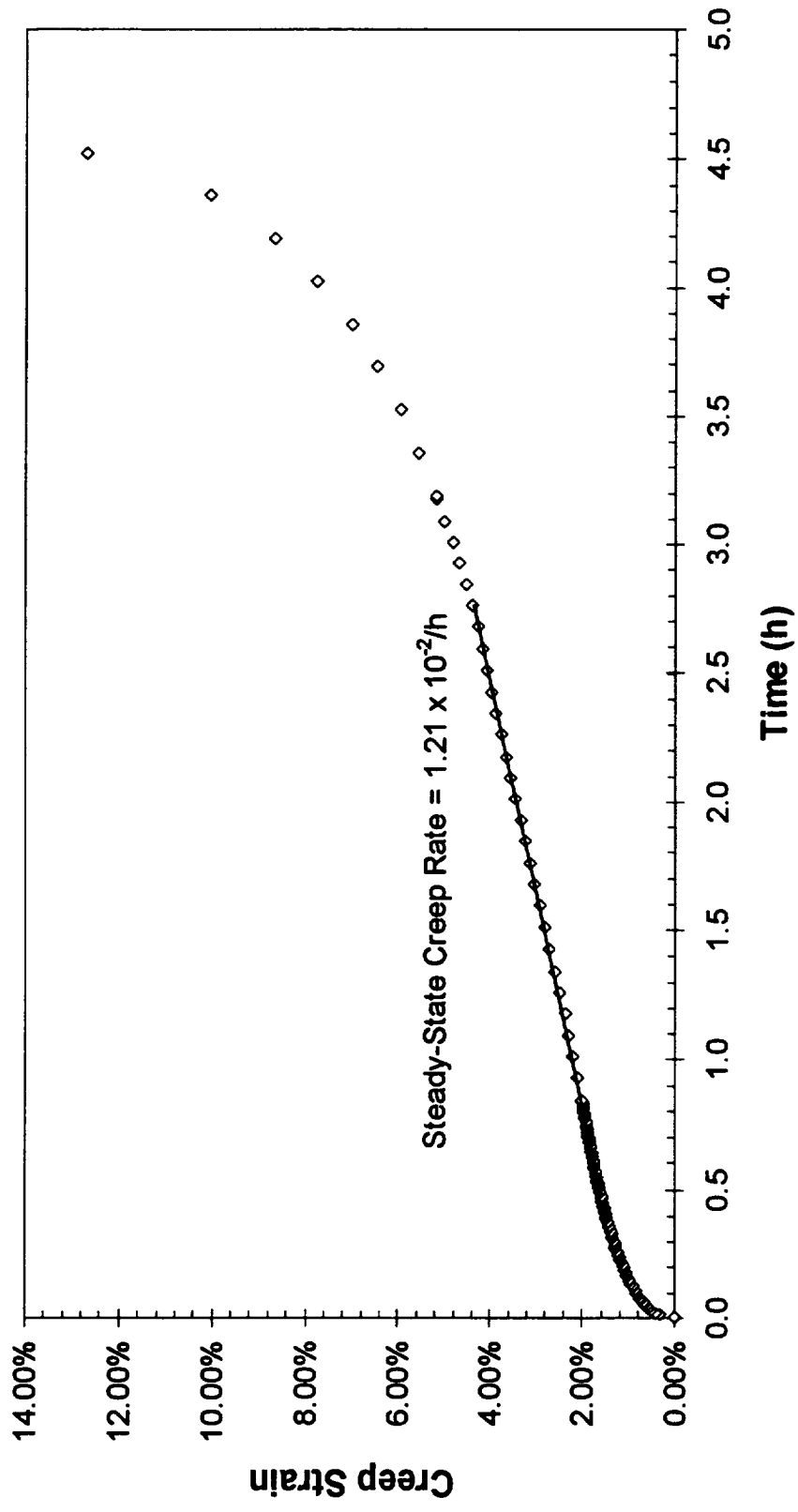


Figure B - 25 -
Extrusion L-3296 Tested At 800°C/26.8 MPa

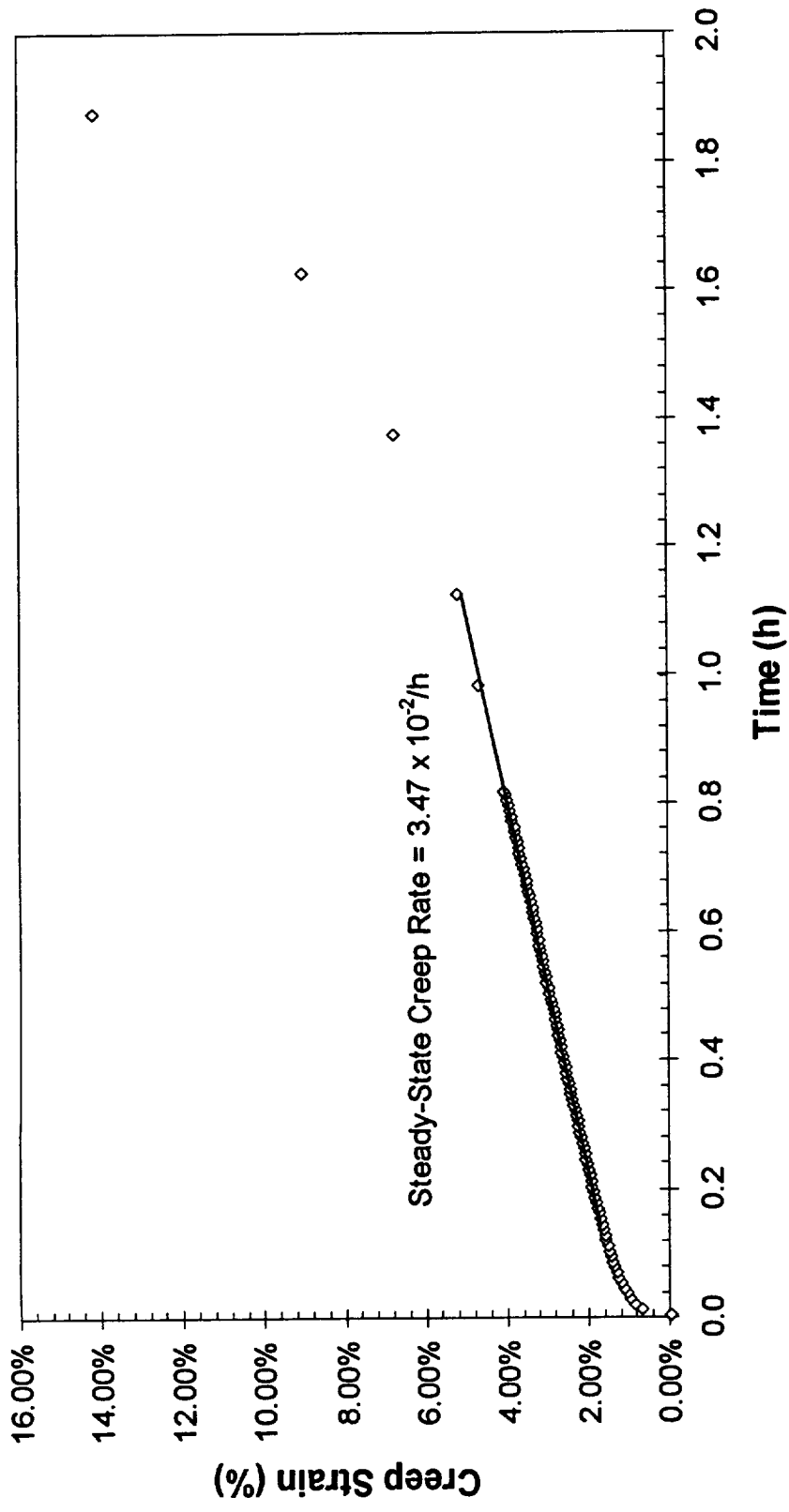


Figure B - 26 -
Extrusion L-3298 Tested At 800°C/26.8 MPa

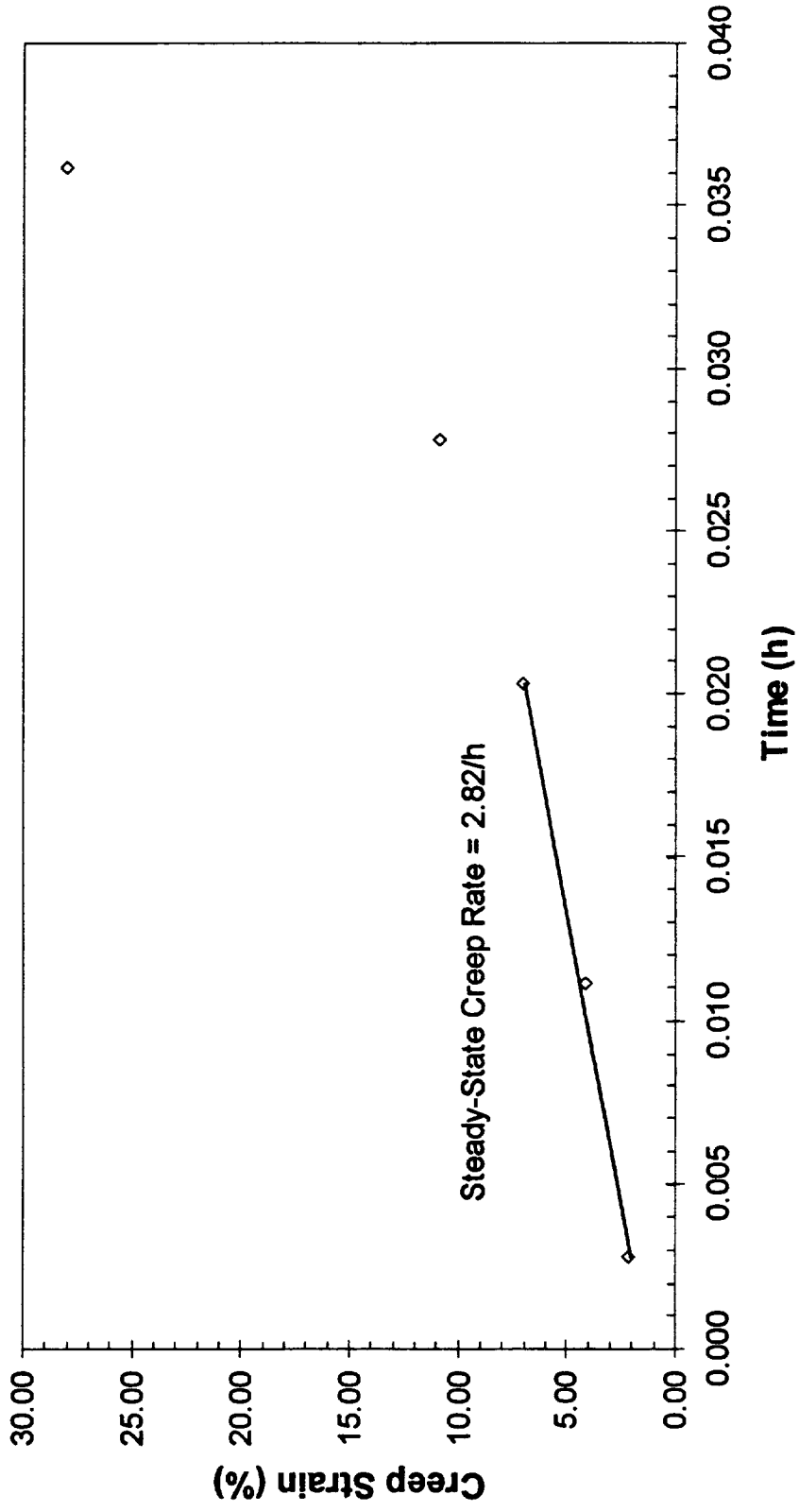


Figure B - 27 -
Extrusion L-3284 Tested At 800°C/44.3 MPa

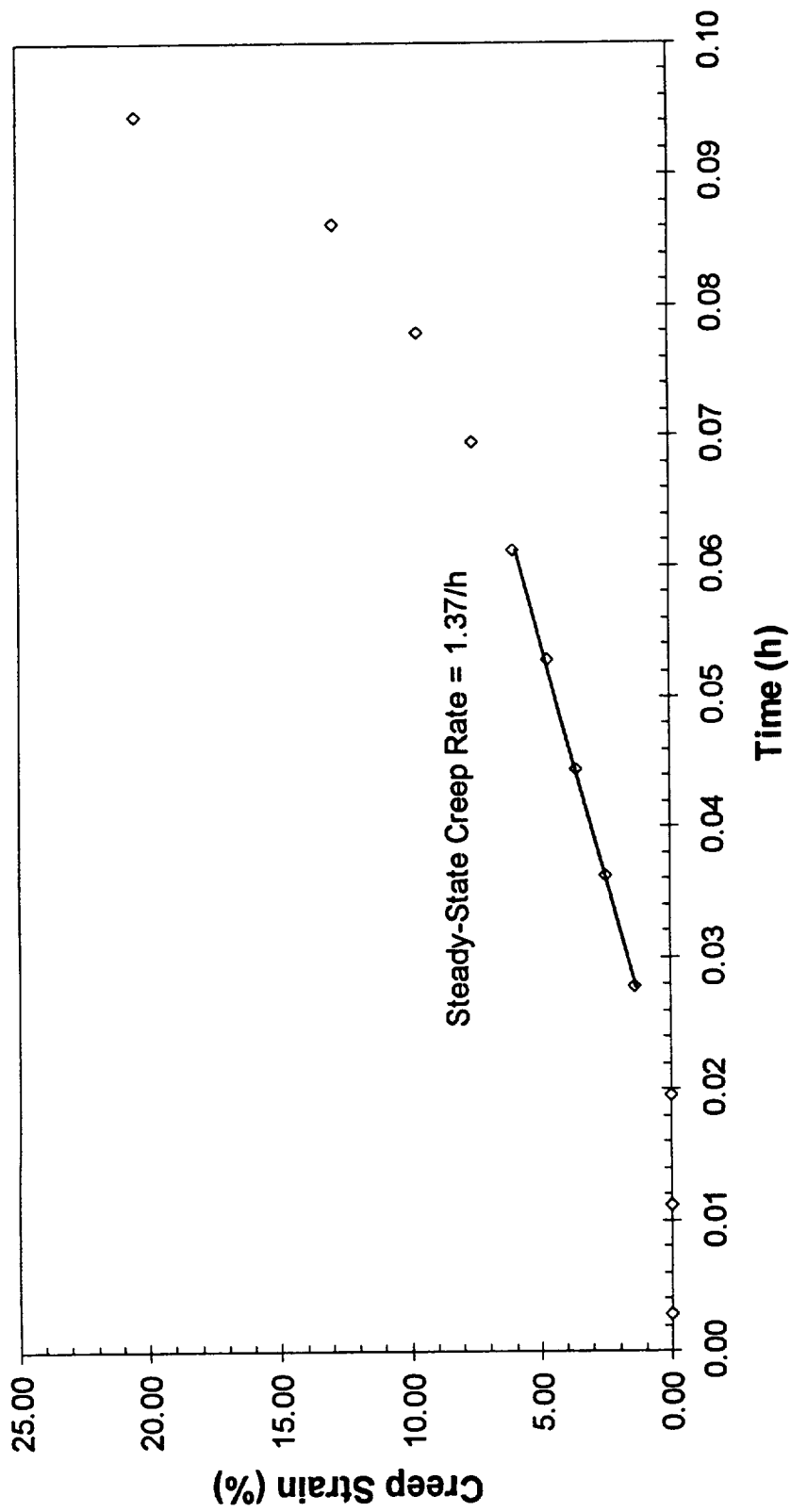


Figure B - 28 -
Extrusion L-3297 Tested At 800°C/44.3 MPa

Appendix C - Creep Of NARloy-Z

**Table C - 1
Results of NARloy-Z Creep Testing**

Temperature (°C)	Nominal Stress (MPa)	Plate	Test Order	Actual Stress (MPa)	Rate (1/h)	Time In			Time To 1% Strain (h)	Life (h)	Total Elongation (%)
						Stage 1 (h)	Stage 2 (h)	Stage 3 (h)			
500	62.1	3	24	62.1	7.65E-05	10.15	154.45	46.48	78.63	211.08	5.64
500	62.1	5	9	62.0	2.71E-04	0.64	49.02	62.98	32.68	112.65	20.75
500	62.1	6	29	62.0	2.43E-04	5.93	26.49	22.24	33.17	54.66	8.43
500	62.1	8	2	62.2	1.09E-03	0.35	10.32	18.70	7.67	29.37	23.96
500	72.9	3	15	72.9	1.42E-03	1.36	10.50	15.50	6.46	27.35	12.08
500	72.9	5	21	72.8	1.93E-03	1.19	4.66	10.50	3.93	16.34	12.95
500	72.9	6	26	73.0	1.62E-03	1.84	5.50	11.21	5.24	18.55	64.99
500	72.9	8	13	72.8	7.06E-04	1.94	16.99	36.49	12.43	43.92	12.92
500	84.0	3	16	84.0	5.46E-03	0.05	3.05	6.00	1.54	9.11	23.29
500	84.0	5	18	84.0	8.66E-03	0.10	1.99	4.11	1.03	6.20	20.15
500	84.0	6	7	84.1	9.32E-03	0.25	1.73	3.00	0.62	4.99	17.39
500	84.0	8	30	83.9	7.43E-03	0.02	1.29	4.50	1.29	5.81	15.40
650	17.8	3	35	17.9	3.72E-05	4.49	105.19	117.30	96.19	226.98	16.04

Table C - 1
Results of NARLOY-Z Creep Testing (Cont.)

Temperature (°C)	Nominal Stress (MPa)	Plate	Test Order	Actual Stress (MPa)	Rate (1/h)	Time In			Time To 1% Strain (h)	Life (h)	Total Elongation (%)
						Stage 1 (h)	Stage 2 (h)	Stage 3 (h)			
650	17.8	5	34	17.7	1.58E-04	1.00	50.62	80.36	29.13	131.98	20.51
650	17.8	6	3	18.0	2.16E-04	2.22	37.78	103.68	2.39	143.69	17.32
650	17.8	8	6	17.8	1.53E-04	4.90	57.09	123.07	38.50	185.06	21.40
650	27.6	3	12	27.7	6.10E-04	0.59	11.50	14.99	8.59	27.08	15.00
650	27.6	5	19	27.6	8.43E-04	1.72	14.99	18.99	7.96	35.70	17.85
650	27.6	6	5	27.7	1.54E-03	0.50	5.47	14.56	1.87	20.53	31.65
650	27.6	8	25	27.7	7.78E-04	1.26	9.25	11.50	9.56	20.74	18.05
650	37.4	3	33	37.3	4.43E-02	0.25	1.18	2.50	0.34	3.93	34.21
650	37.4	5	8	37.4	1.02E-02	0.26	1.24	6.00	0.56	7.50	28.84
650	37.4	6	10	37.6	3.86E-03	1.16	8.98	10.90	2.38	12.97	6.87
650	37.4	8	32	37.4	2.59E-02	0.02	0.63	2.67	0.42	3.32	28.51
800	6.2	3	36	6.2	2.61E-04	6.74	133.84	353.67	18.24	494.25	50.97
800	6.2	5	14	6.2	7.00E-04	0.15	165.14	108.47	3.35	273.76	32.80
800	6.2	6	31	5.7	1.68E-03	0.04	62.26	30.49	4.10	92.79	17.45

Table C - 1
Results of NARloy-Z Creep Testing (Cont.)

Temperature (°C)	Nominal Stress (MPa)	Plate	Test Order	Actual Stress (MPa)	Rate (1/h)	Time In			Time To 1% Strain (h)	Life (h)	Total Elongation (%)
						Stage 1 (h)	Stage 2 (h)	Stage 3 (h)			
800	6.2	8	4	6.2	4.42E-04	0.80	170.77	138.46	6.54	310.03	68.60
800	10.4	3	28	10.3	3.27E-02	1.38	7.50	4.00	0.31	12.88	14.91
800	10.4	5	22	10.3	2.36E-02	0.01	8.25	5.50	0.44	13.76	50.91
800	10.4	6	20	10.3	2.39E-02	1.00	7.55	5.00	0.38	13.55	58.64
800	10.4	8	17	10.4	1.79E-02	0.01	12.48	6.90	0.70	19.39	71.95
800	14.6	3	1	14.7	1.33E-01	0.01	0.95	1.25	0.07	2.20	67.97
800	14.6	5	27	14.6	2.98E-02	0.05	0.35	3.56	0.27	3.97	66.48
800	14.6	6	23	14.6	1.17E-01	0.25	1.17	1.33	0.08	2.75	48.29
800	14.6	8	11	14.6	1.94E-02	0.05	0.48	3.34	0.44	3.87	57.51

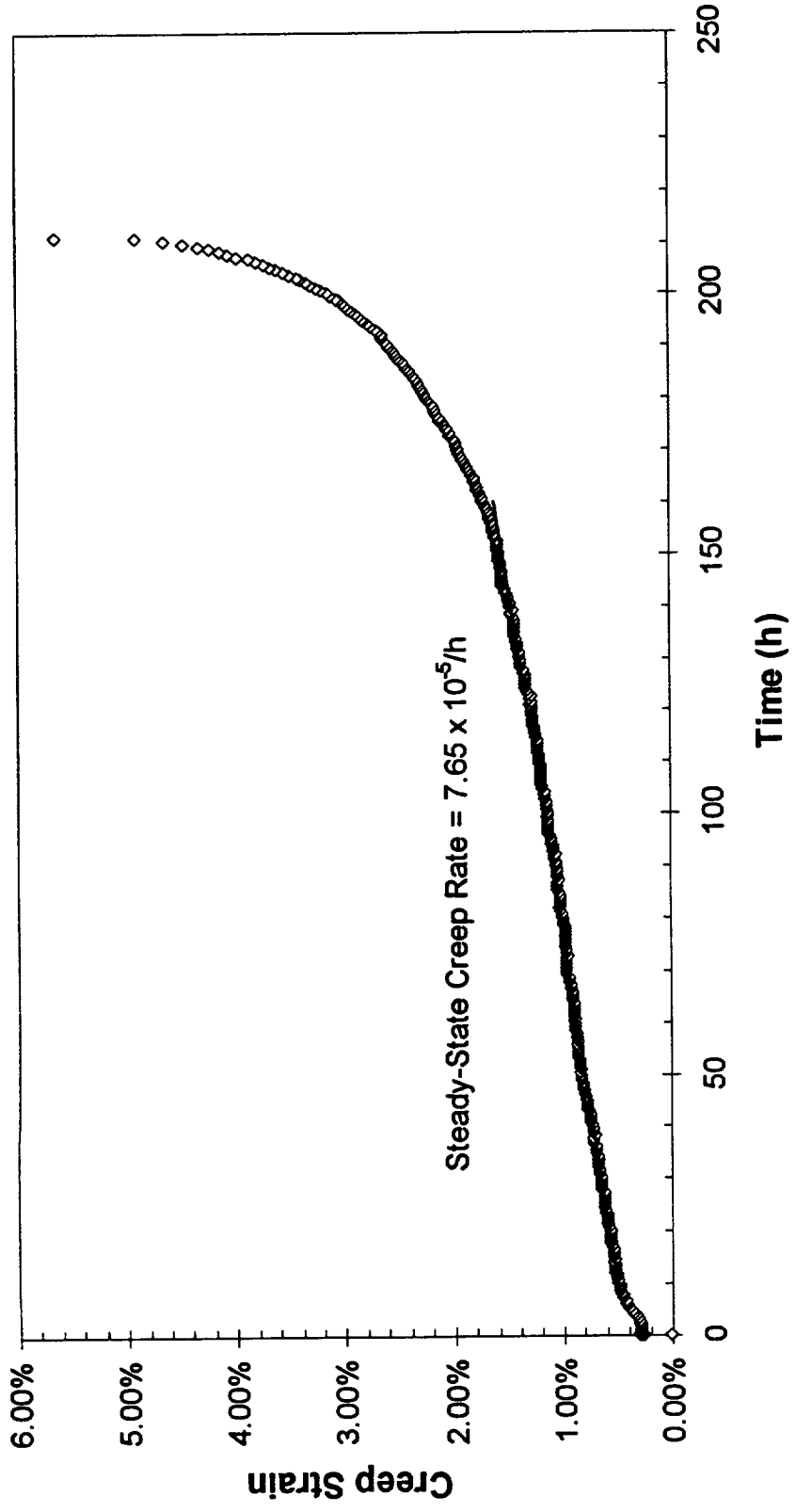


Figure C - 1 -
 Plate 3 Tested At 500°C/62.1 MPa

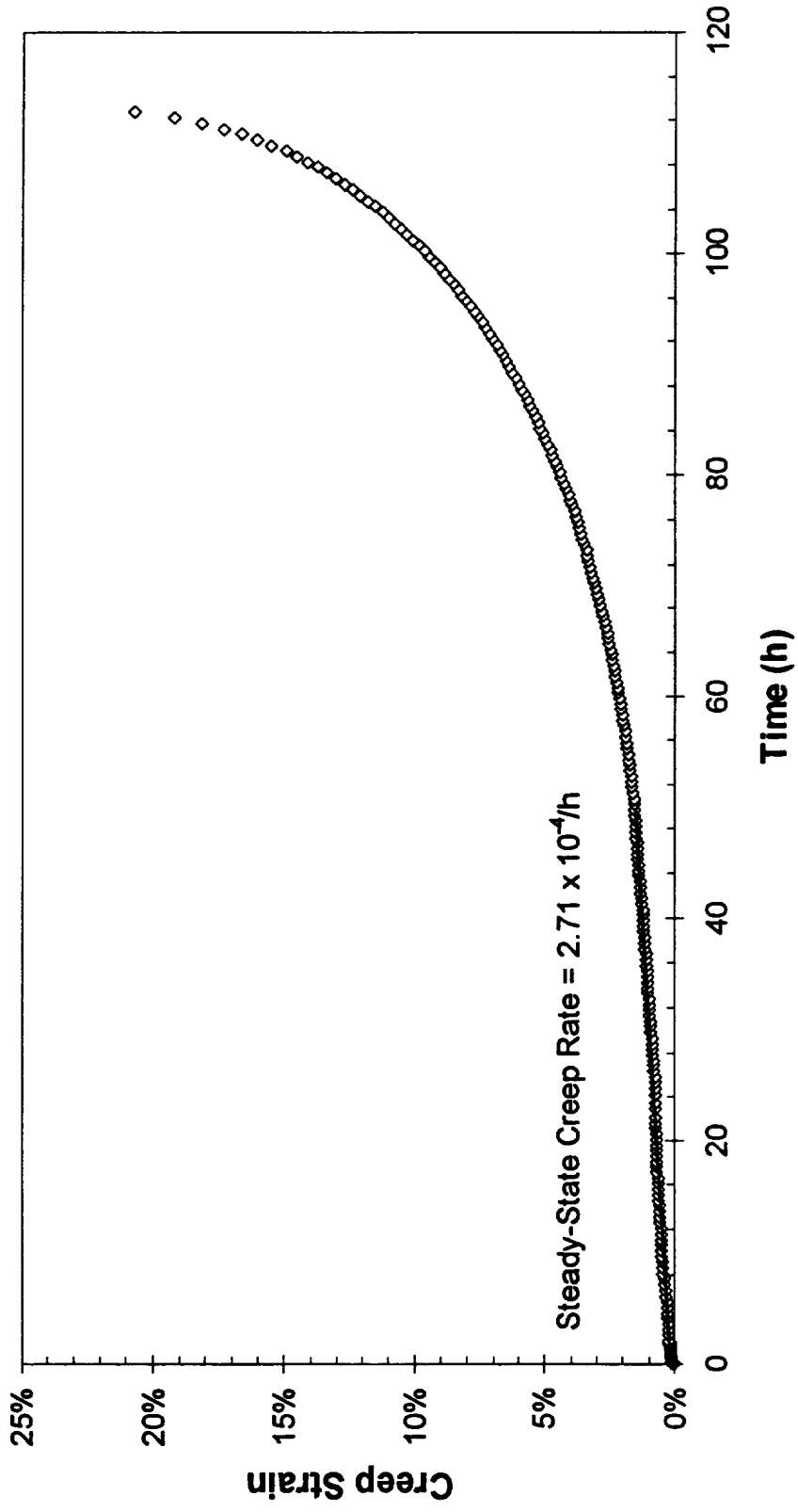


Figure C - 2 -
Plate 5 Tested At 500°C/62.1 MPa

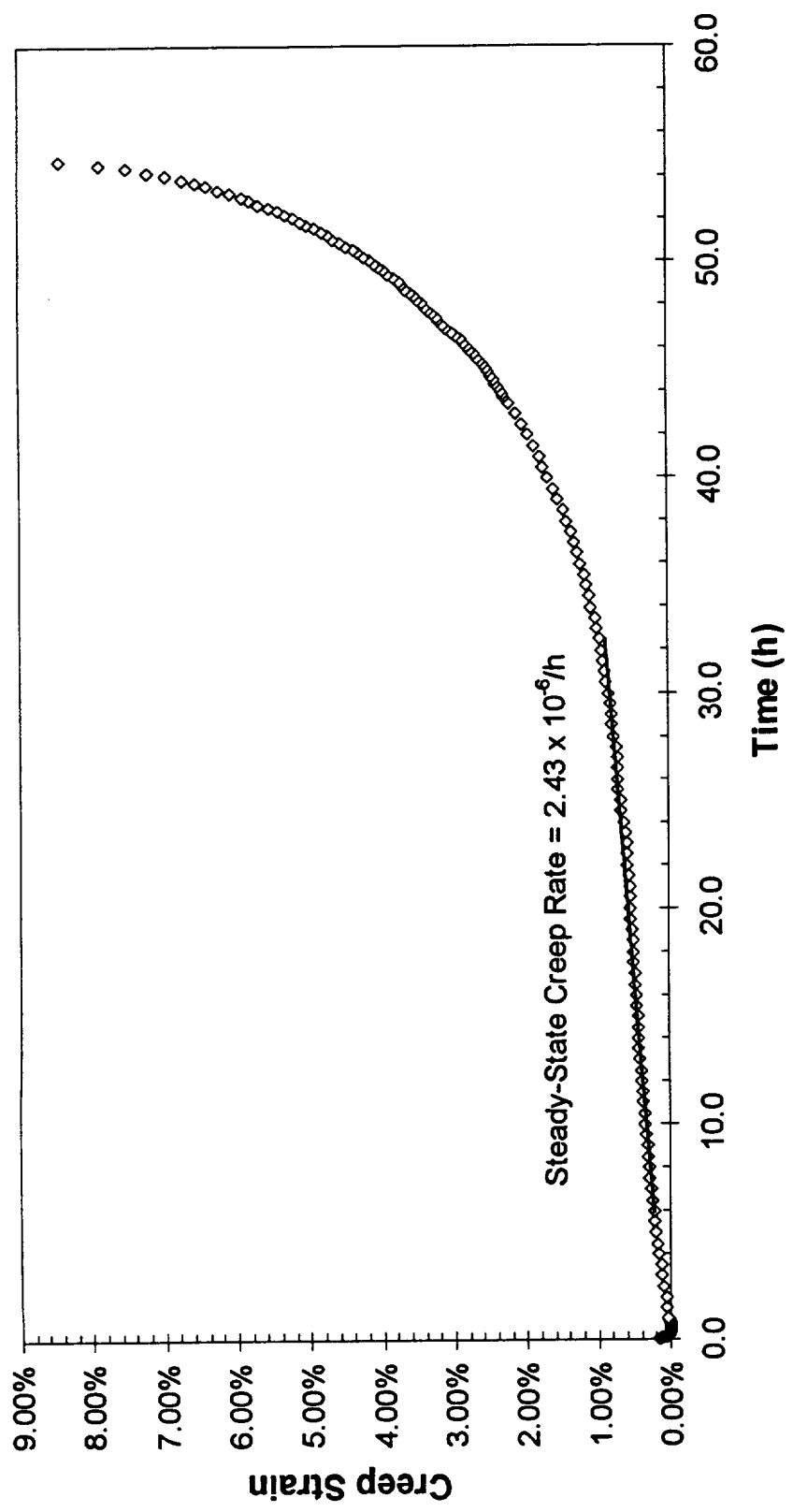


Figure C - 3 -
Plate 6 Tested At 500°C/62.1 MPa

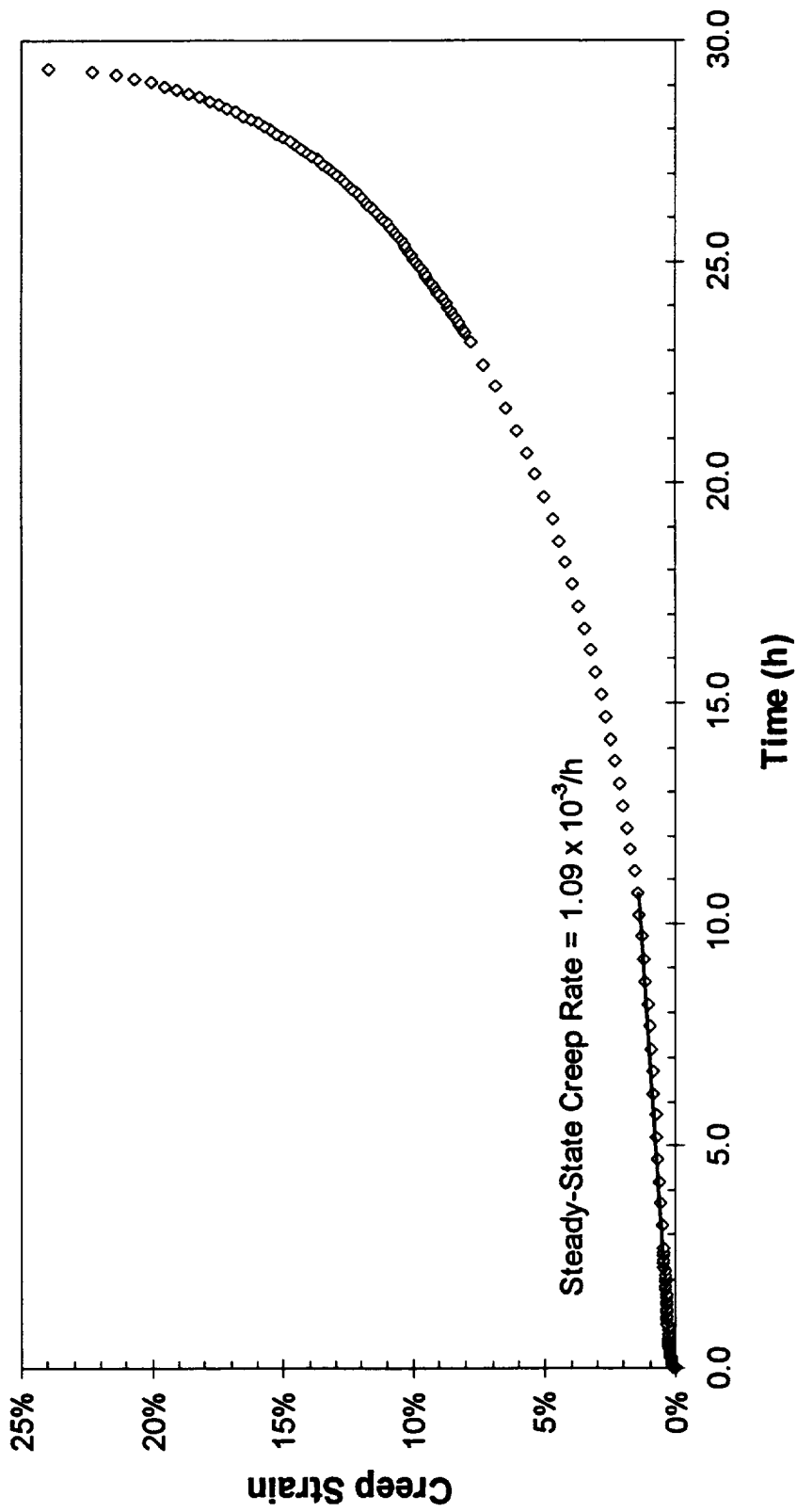


Figure C - 4 -
Plate 8 Tested At 500°C/62.1 MPa

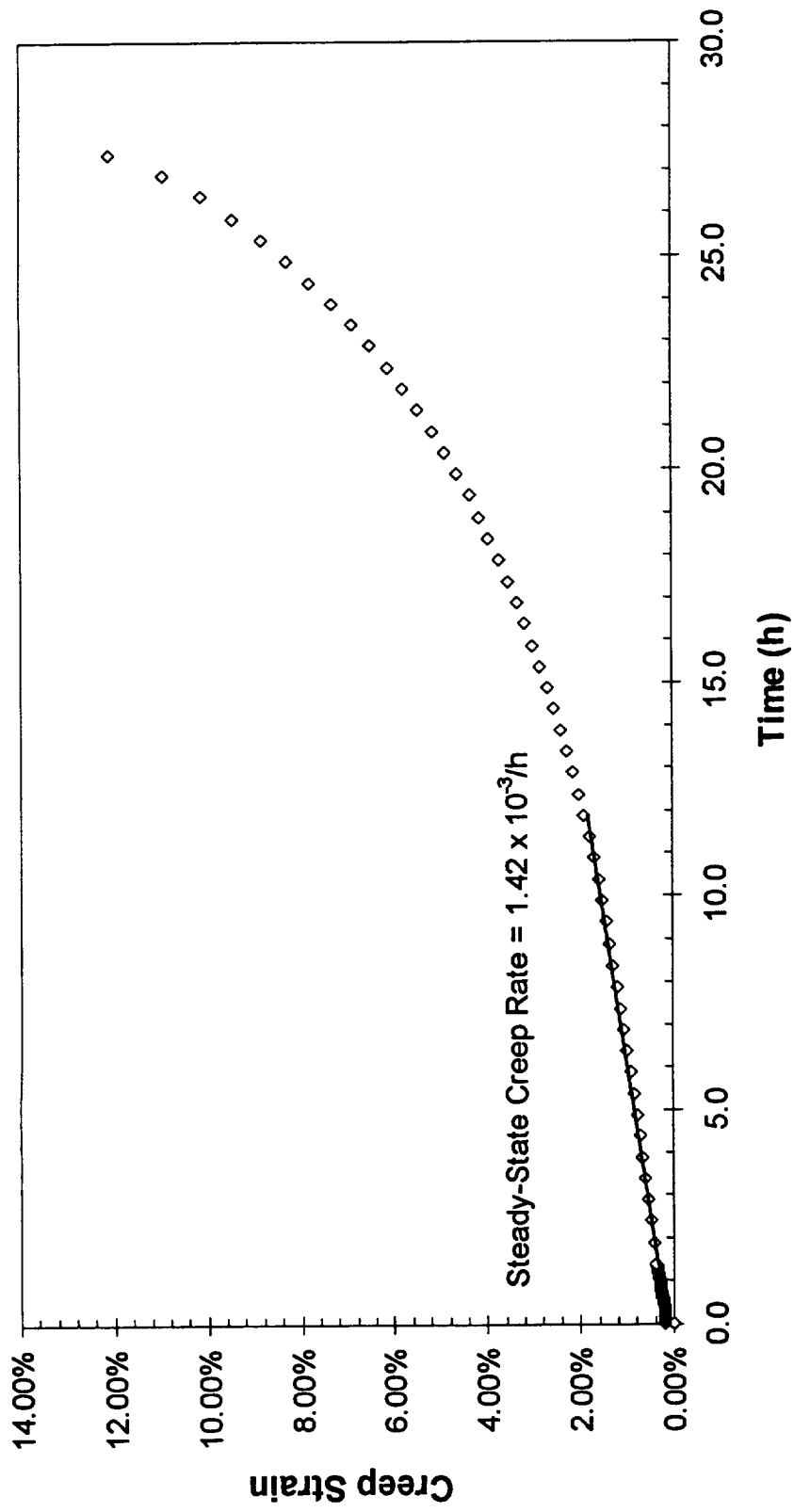


Figure C - 5 -
Plate 3 Tested At 500°C/72.9 MPa

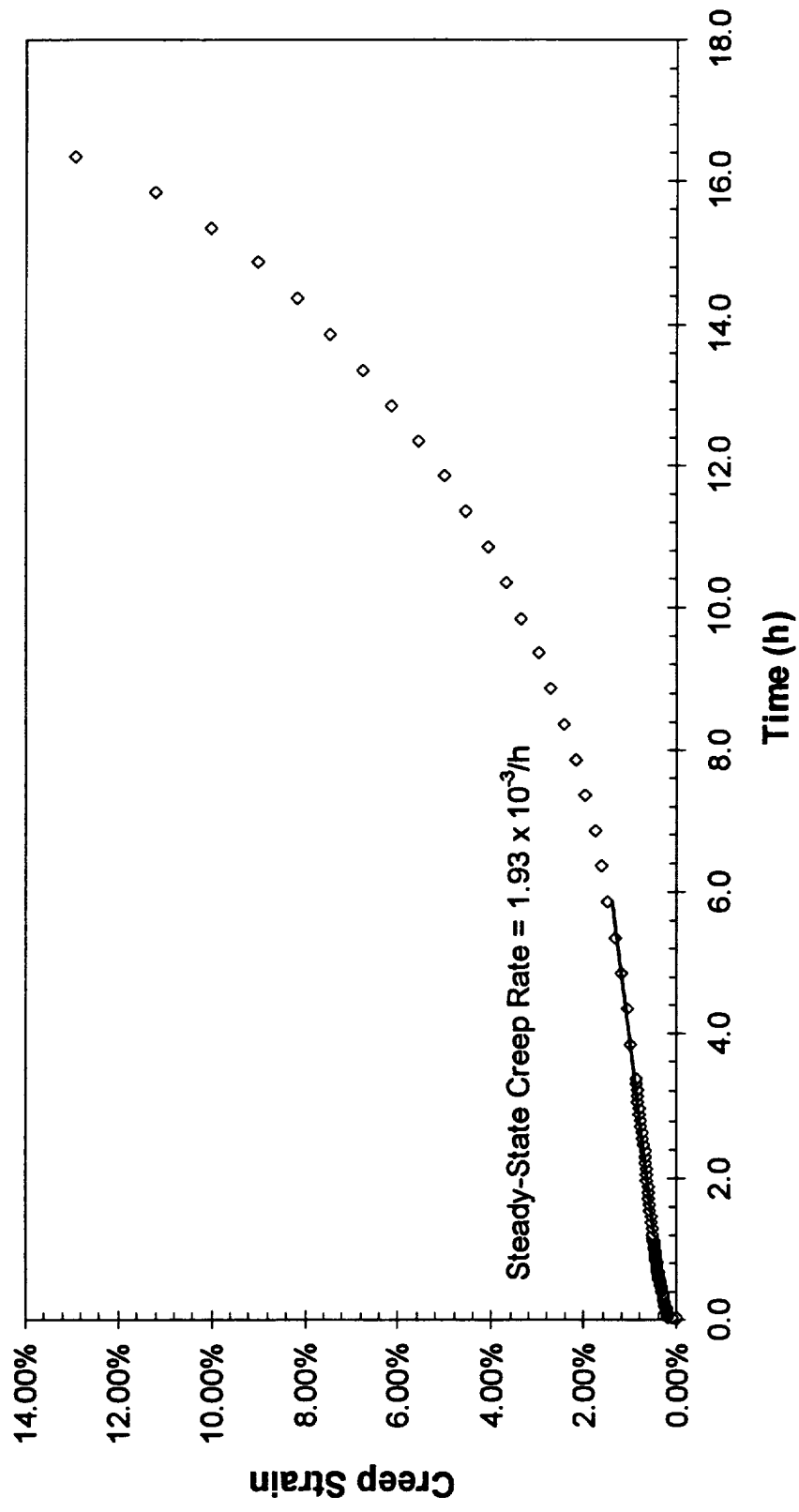


Figure C - 6 -
Plate 5 Tested At 500°C/72.9 MPa

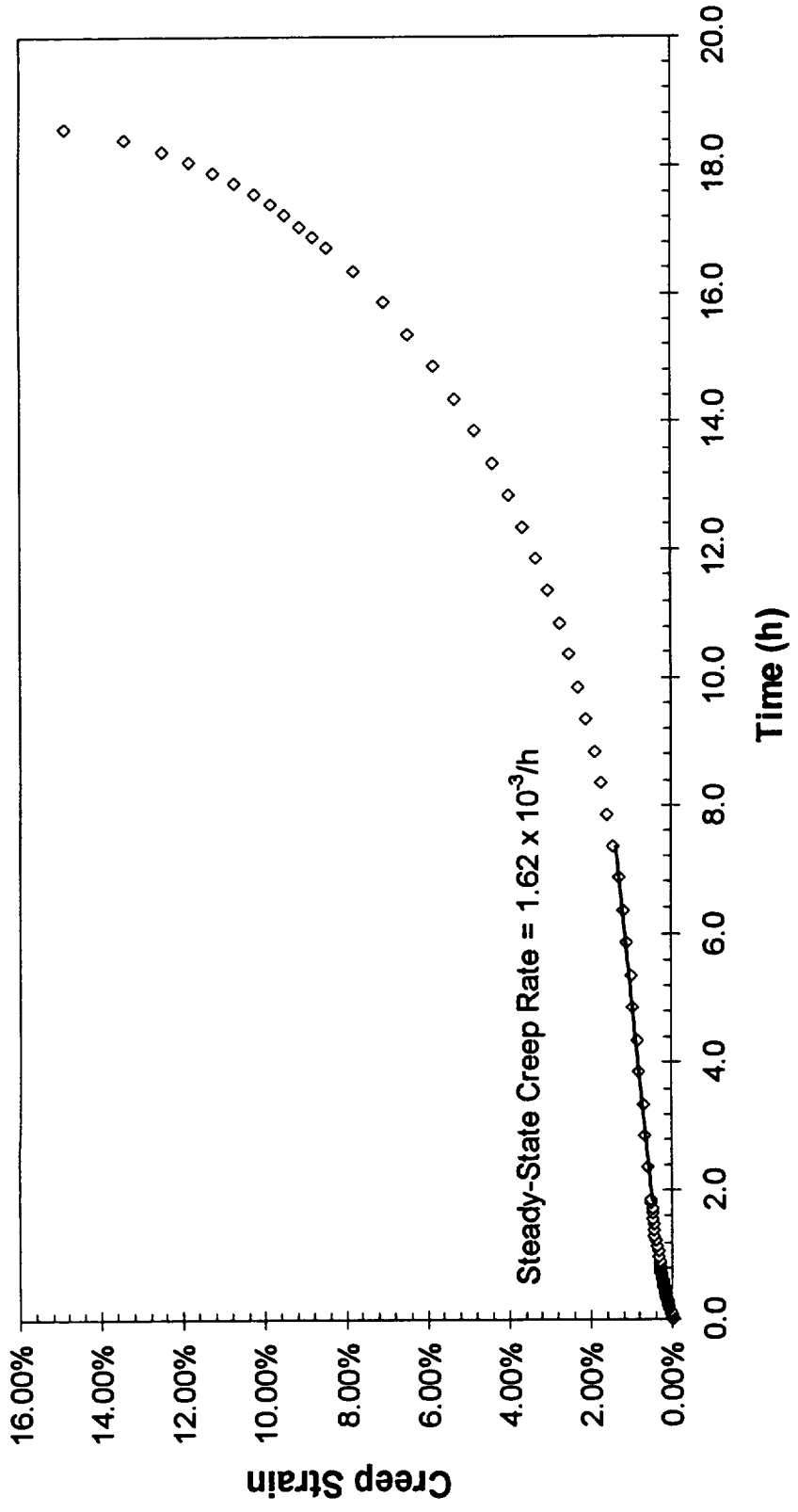


Figure C - 7 -
 Plate 6 Tested At 500°C/72.9 MPa

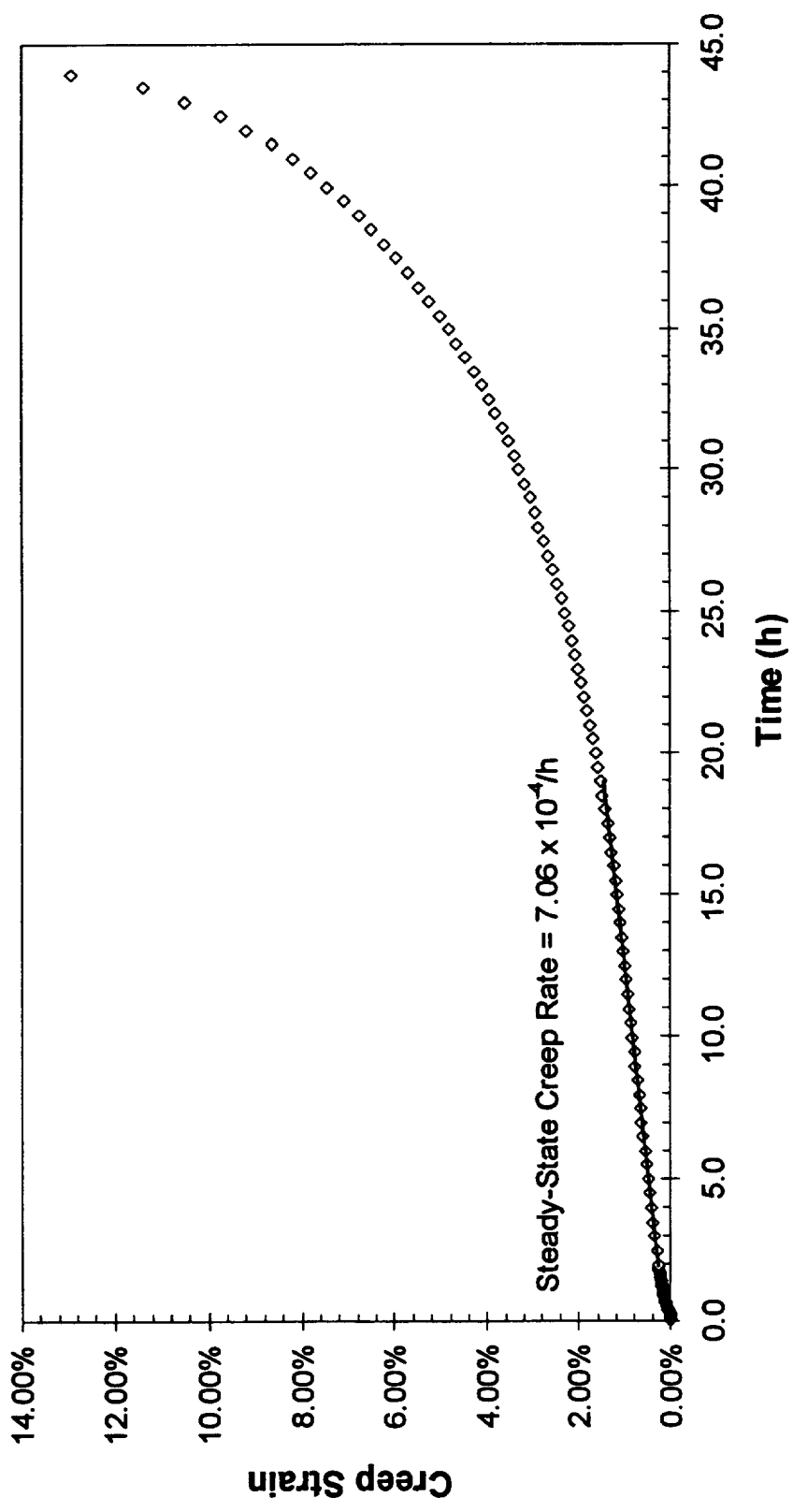


Figure C - 8 -
Plate 8 Tested At 500°C/72.9 MPa

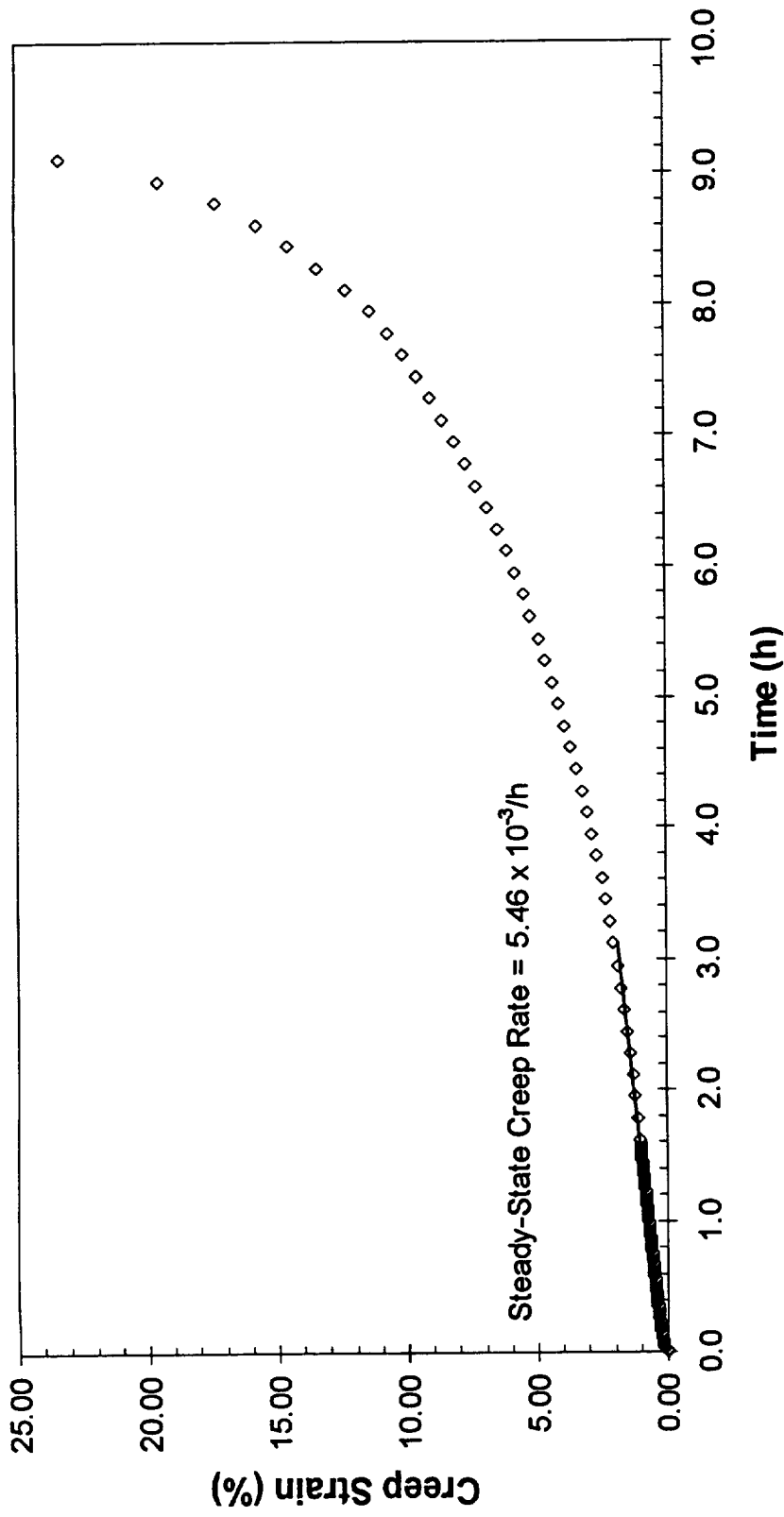


Figure C - 9 -
Plate 3 Tested At 500°C/84.0 MPa

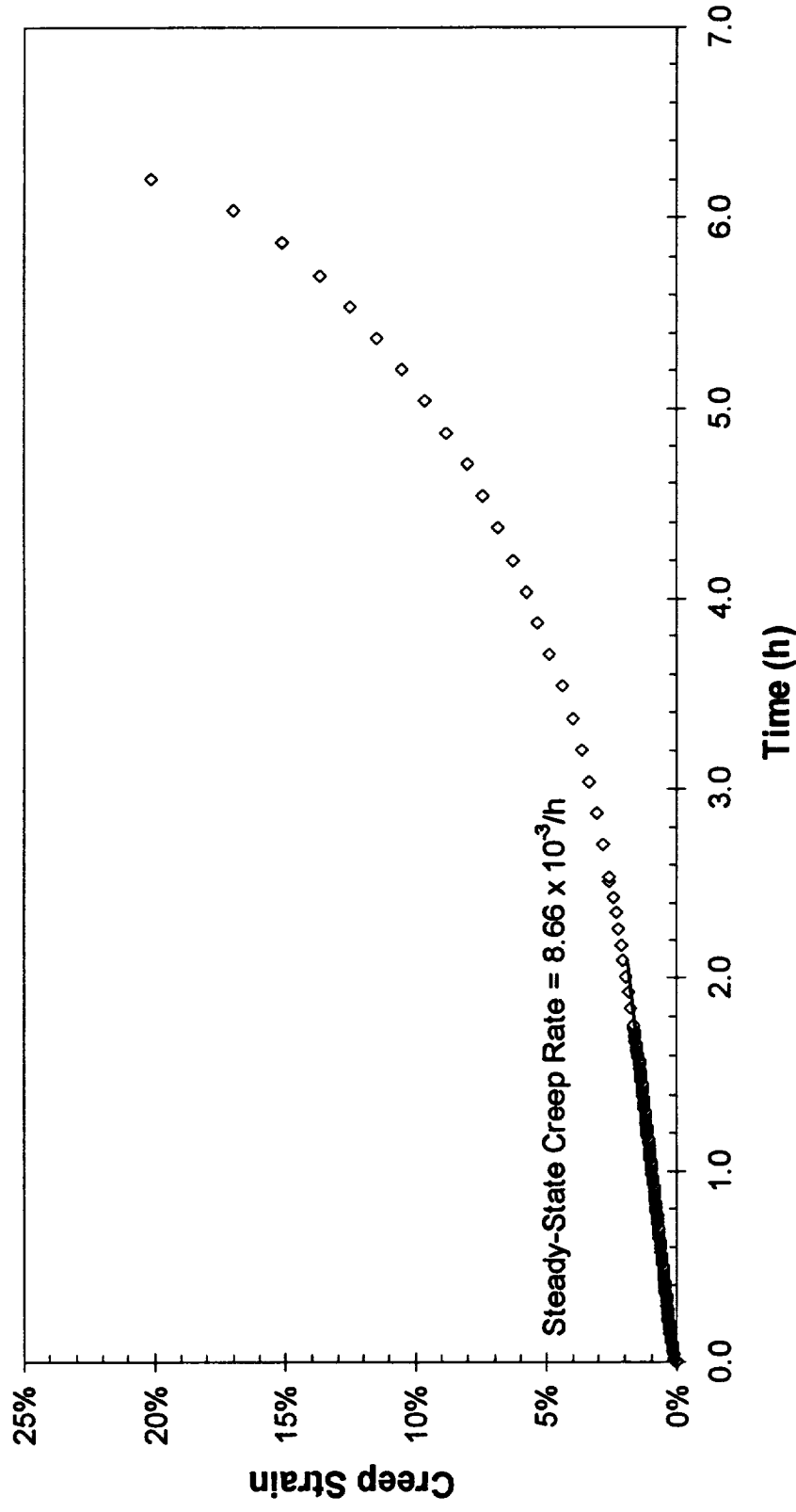


Figure C - 10 -
 Plate 5 Tested At 500°C/84.0 MPa

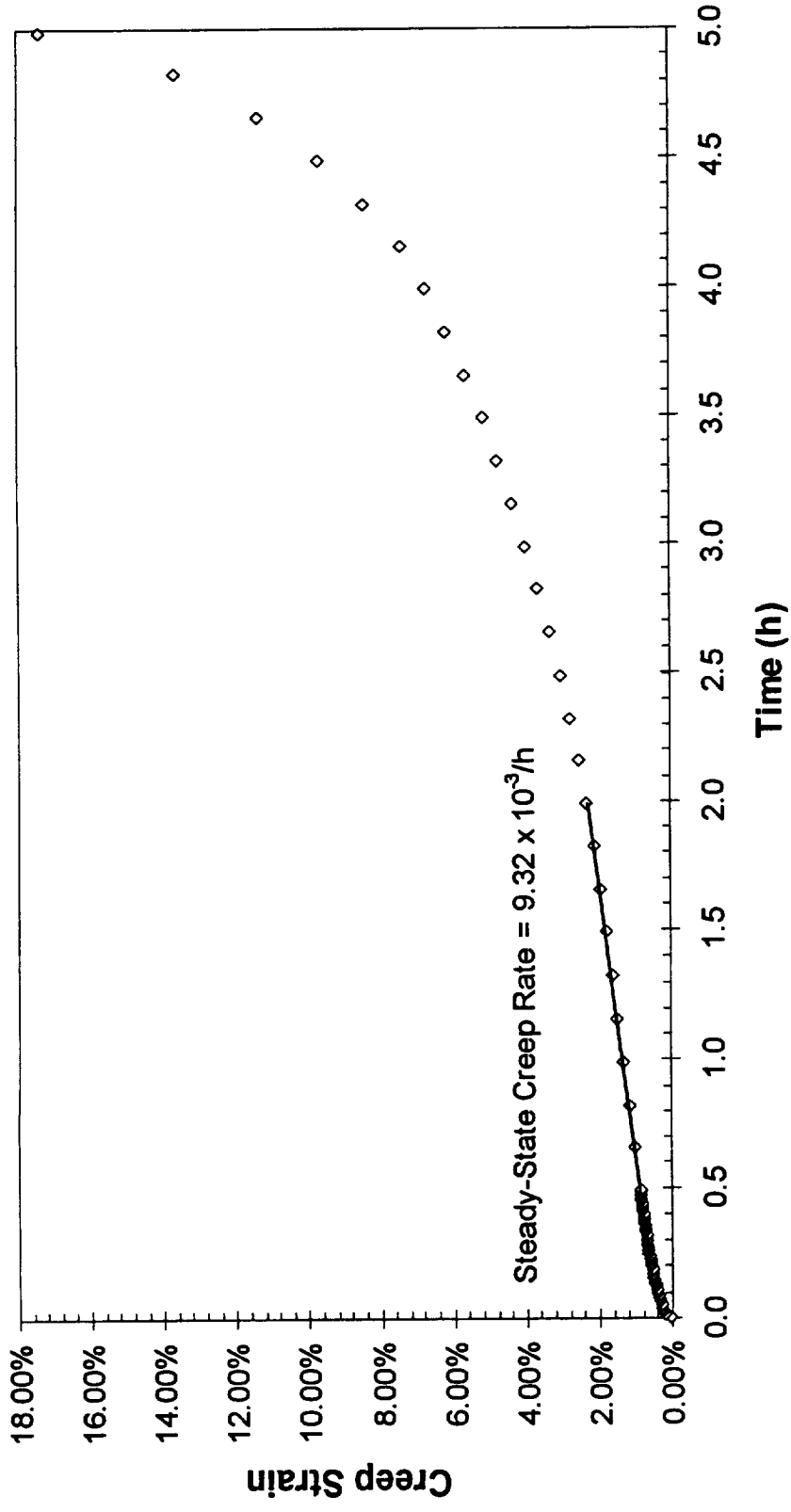


Figure C - 11 -
 Plate 6 Tested At 500°C/84.0 MPa

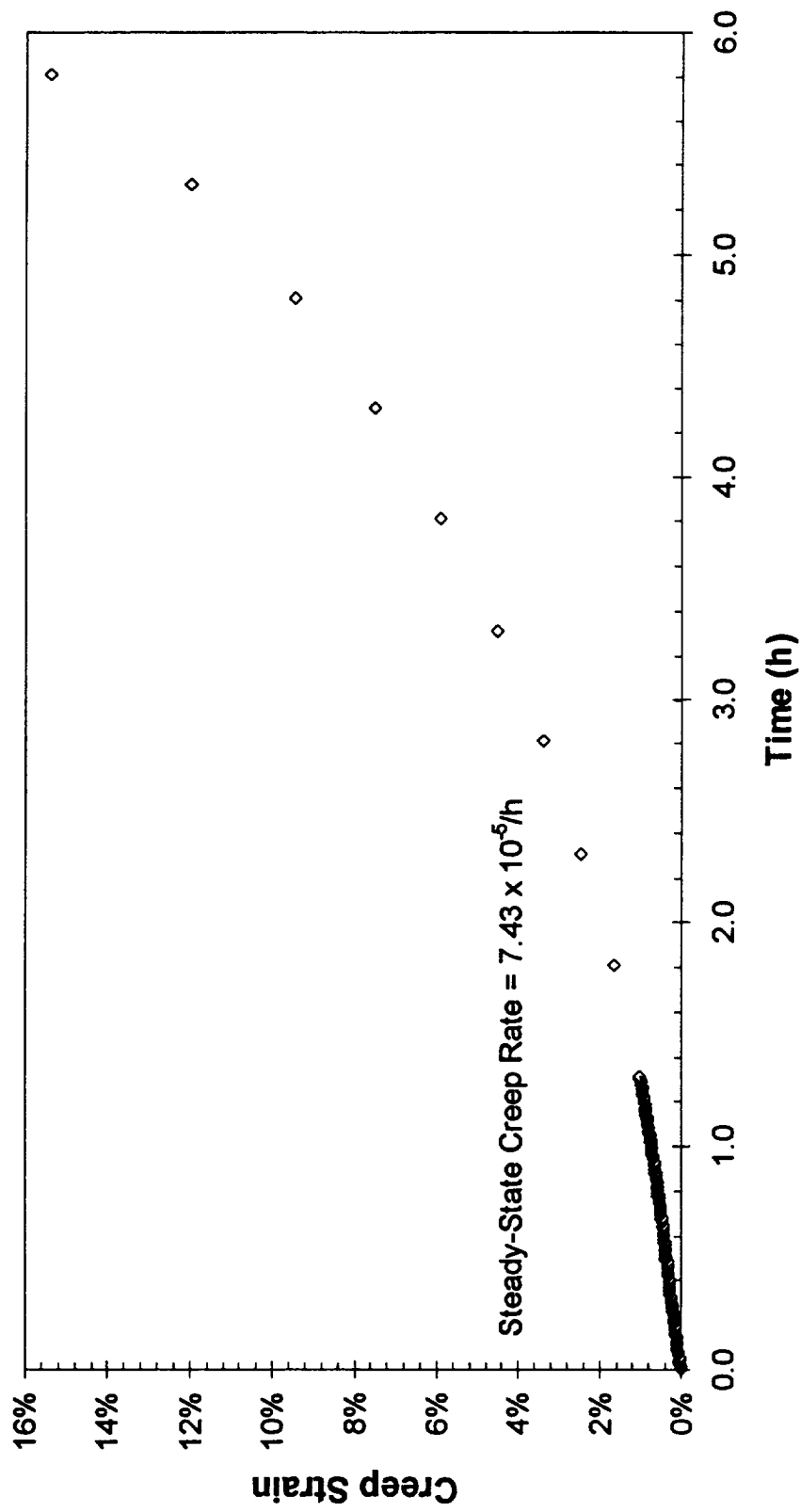


Figure C - 12 -
Plate 8 Tested At 500°C/84.0 MPa

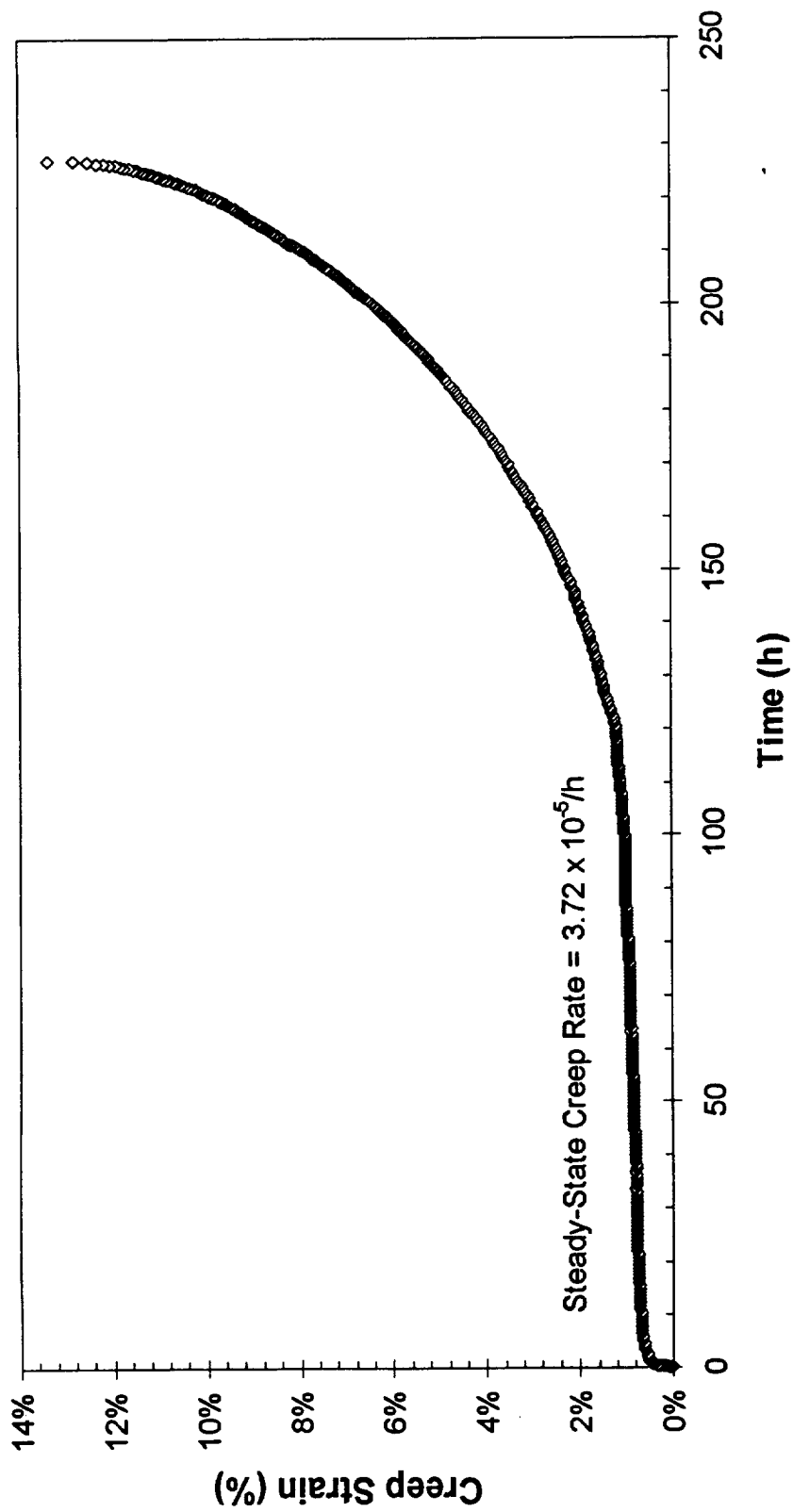


Figure C - 13 -
Plate 3 Tested At 650°C/17.9 MPa

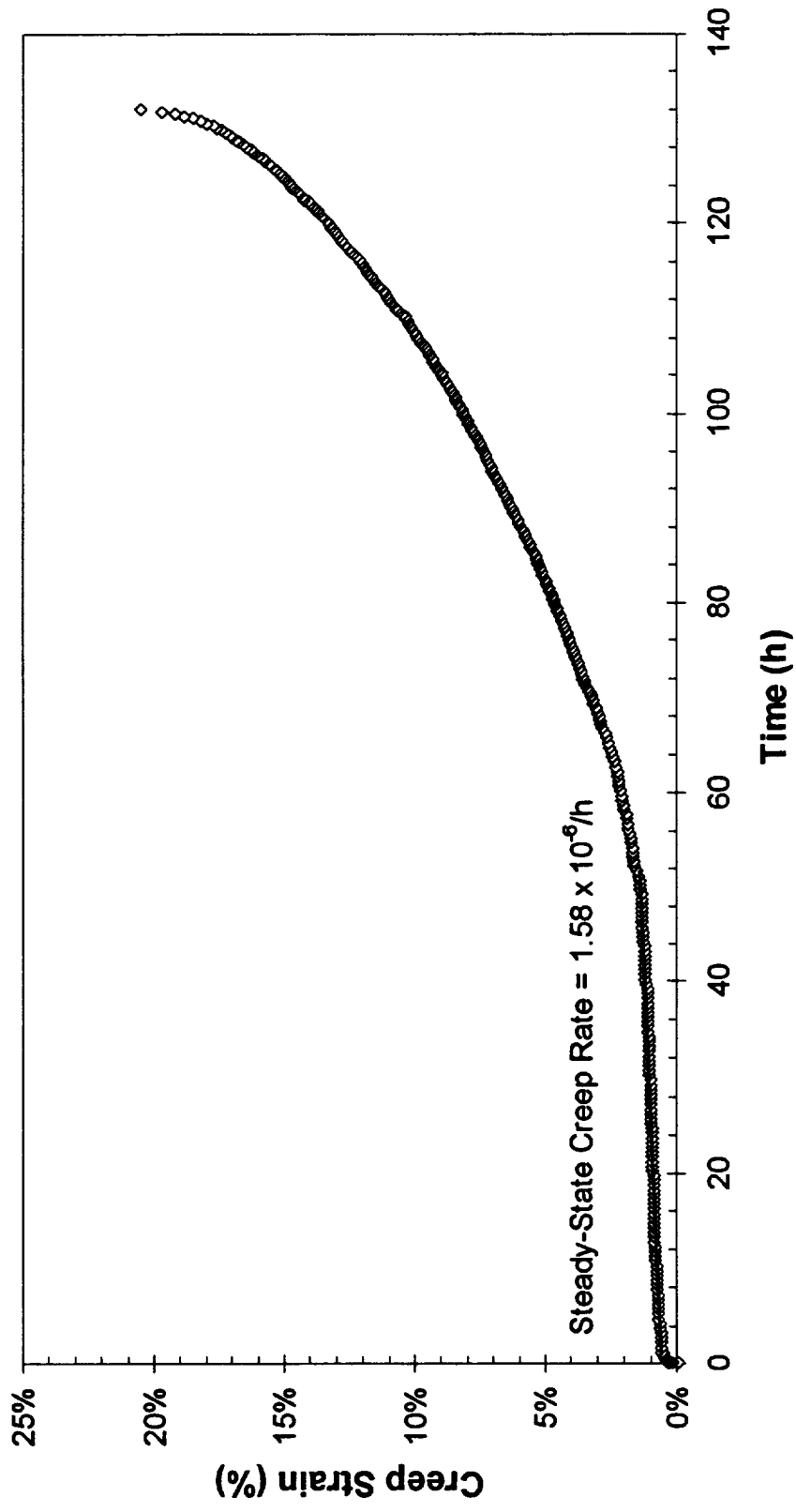


Figure C - 14 -
Plate 5 Tested At 650°C/17.7 MPa

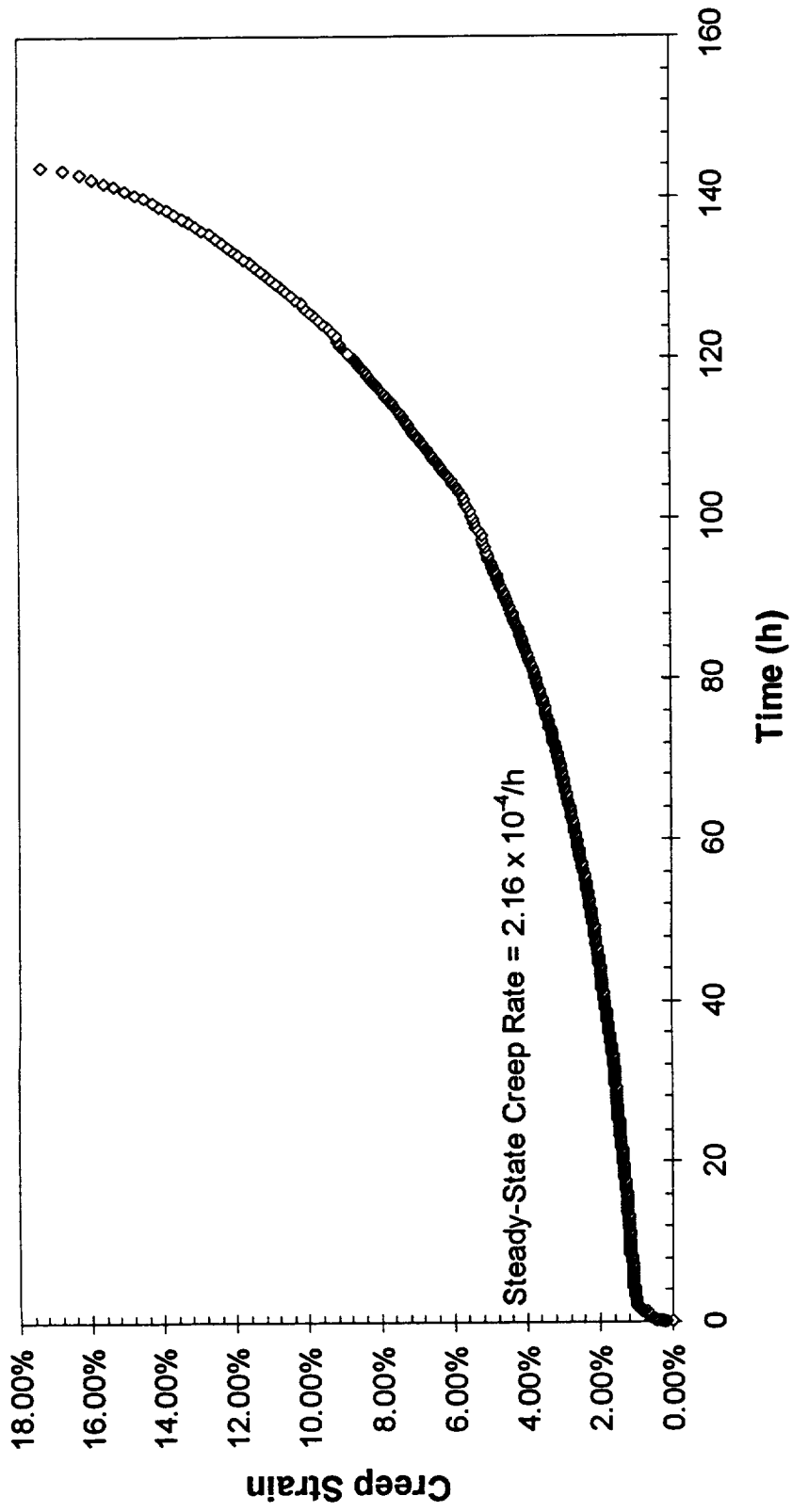


Figure C - 15 -
Plate 6 Tested At 650°C/17.8 MPa

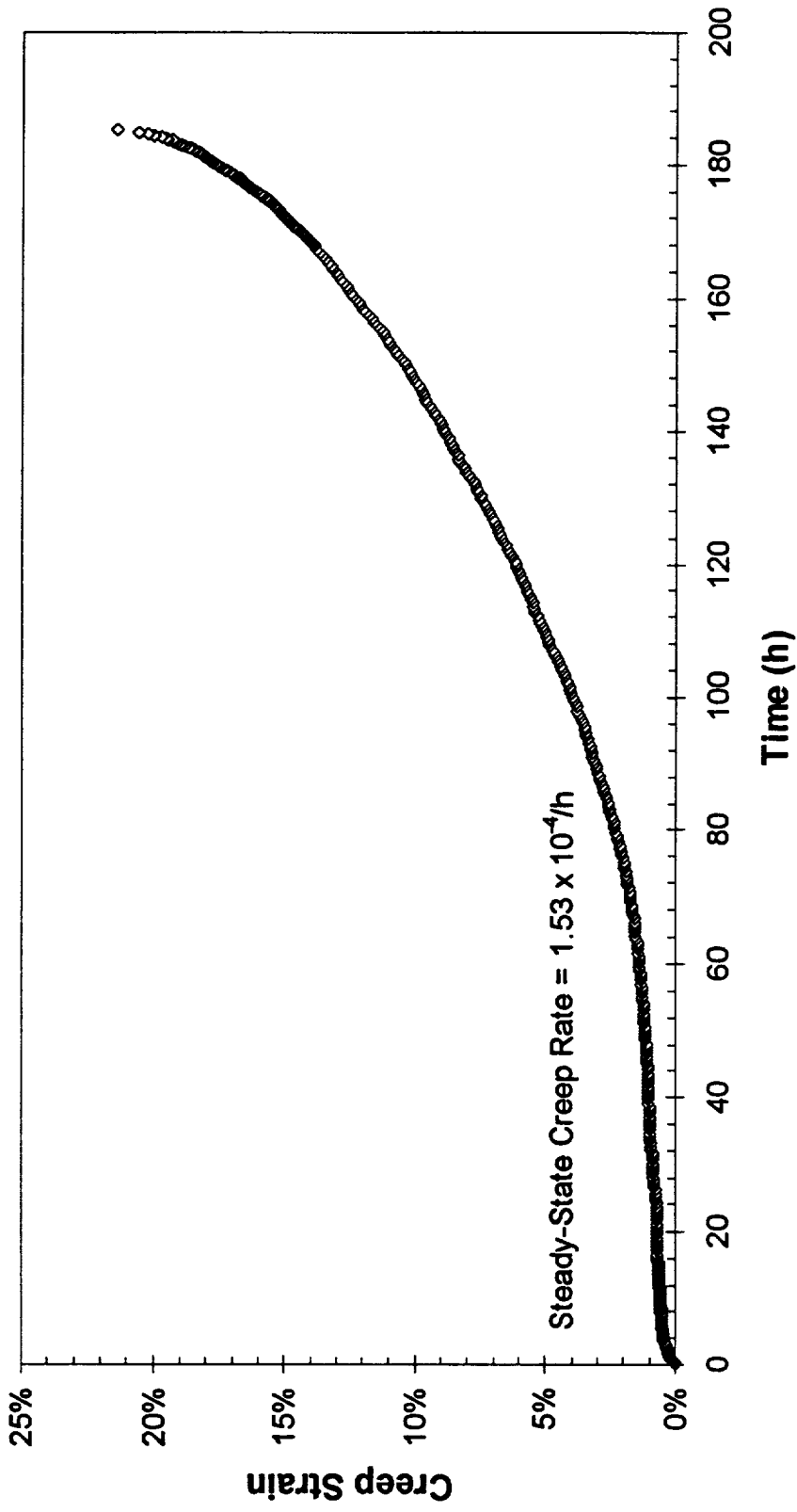


Figure C - 16 -
Plate 8 Tested At 650°C/17.8 MPa

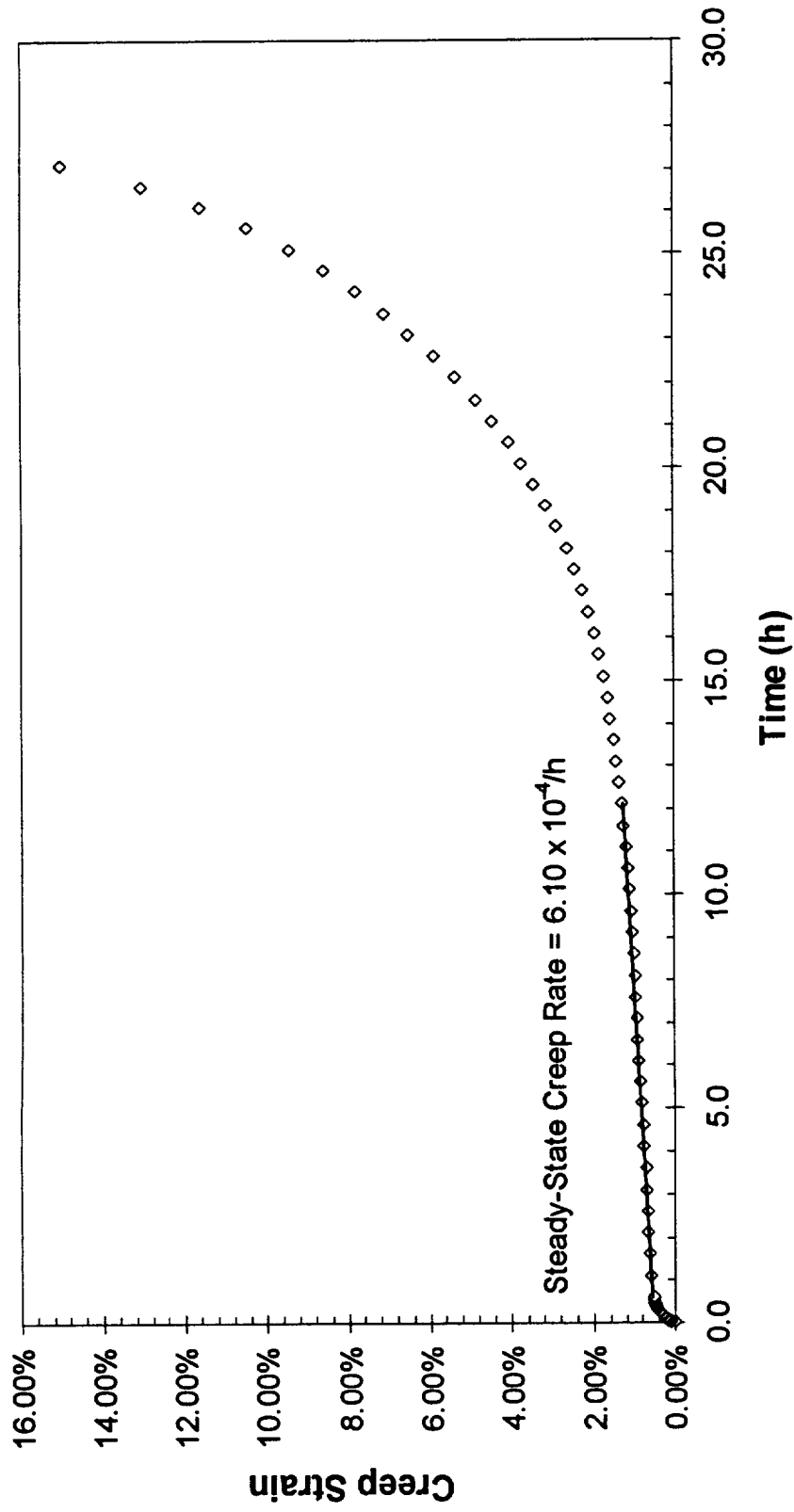


Figure C - 17 -
Plate 3 Tested At 650°C/27.6 MPa

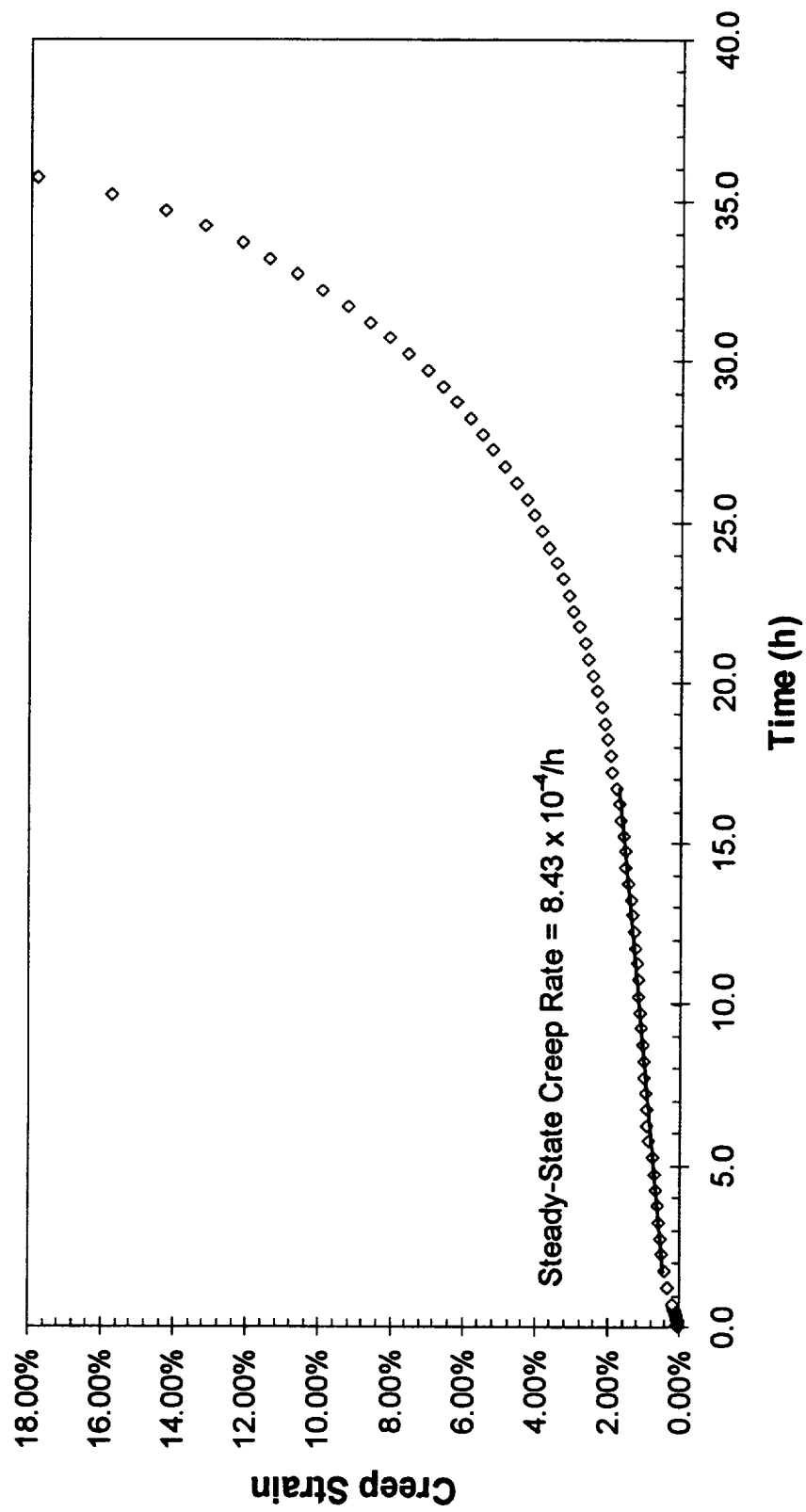


Figure C - 18 -
Plate 5 Tested At 650°C/27.6 MPa

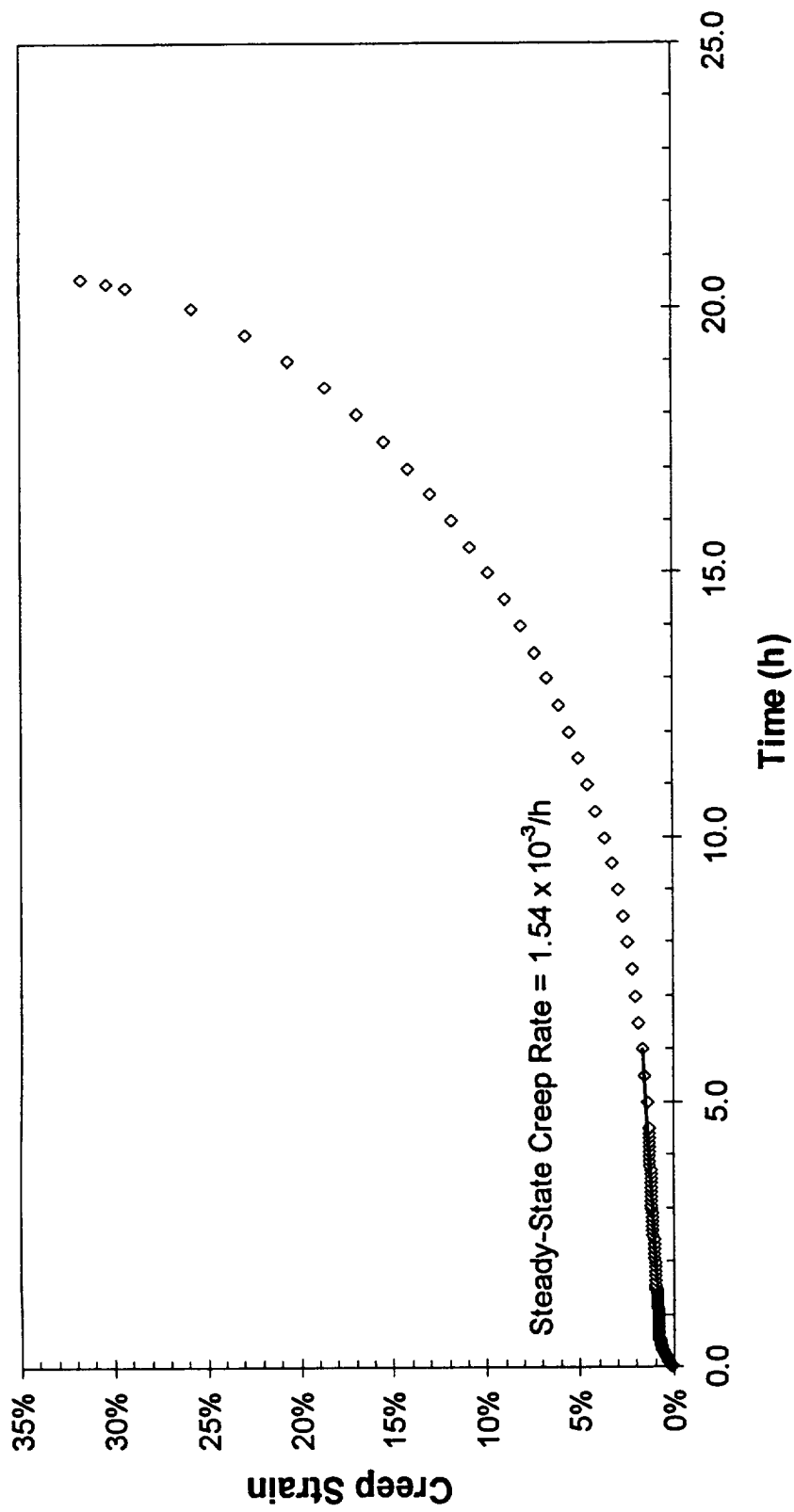


Figure C - 19 -
Plate 6 Tested At 650°C/27.6 MPa

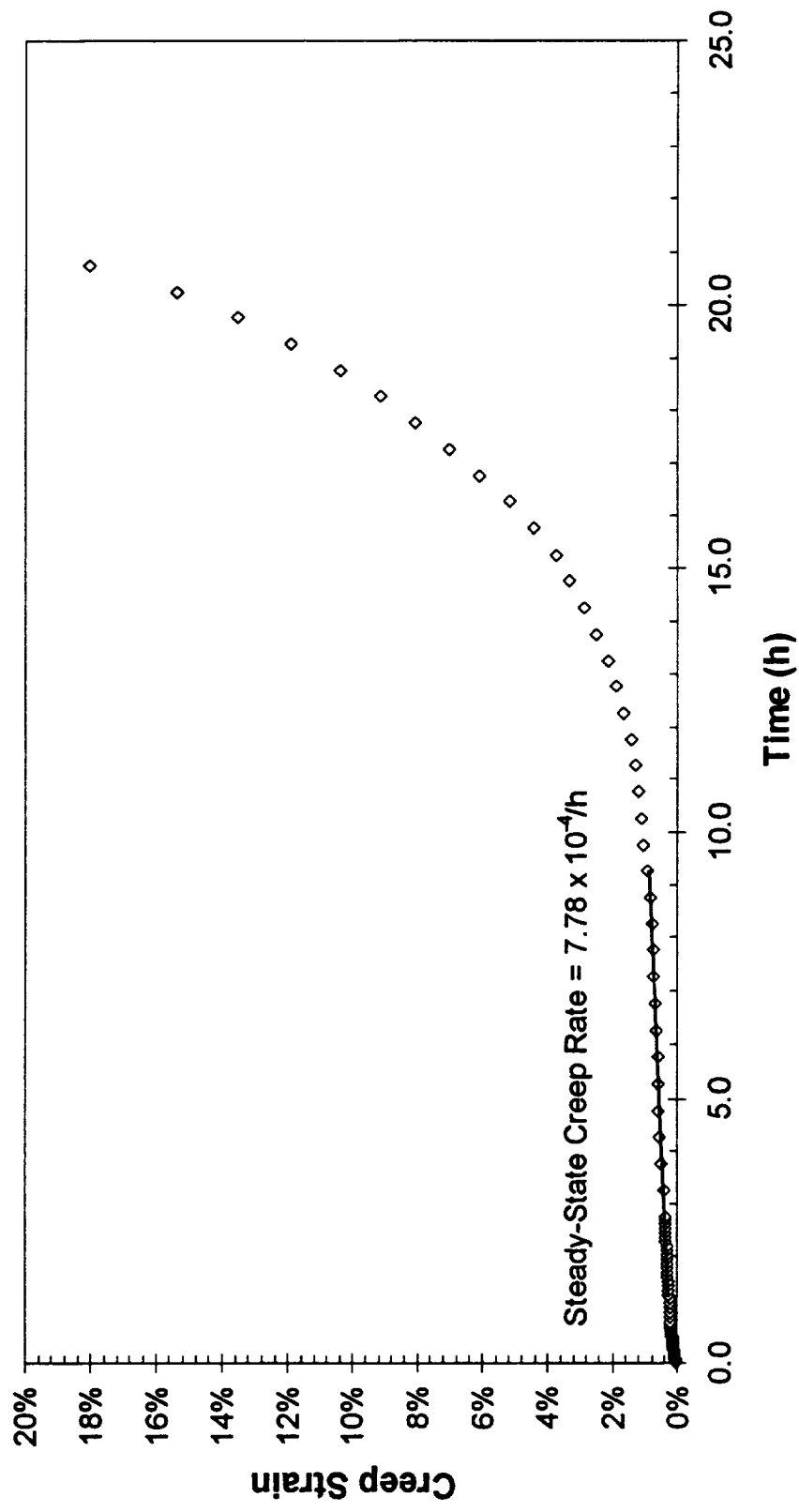


Figure C - 20 -
 Plate 8 Tested At 650°C/27.6 MPa

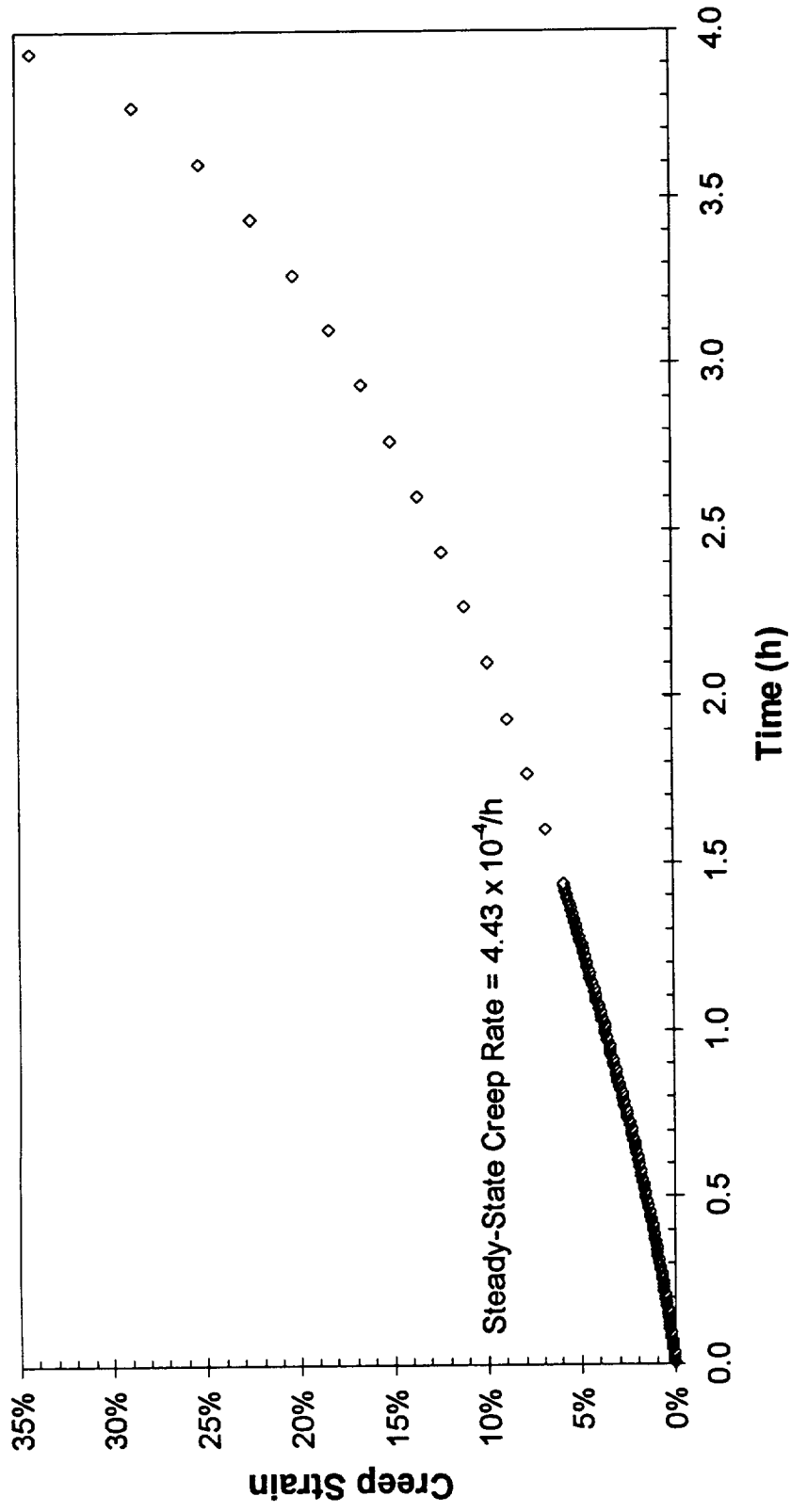


Figure C - 21 -
 Plate 3 Tested At 650°C/37.4 MPa

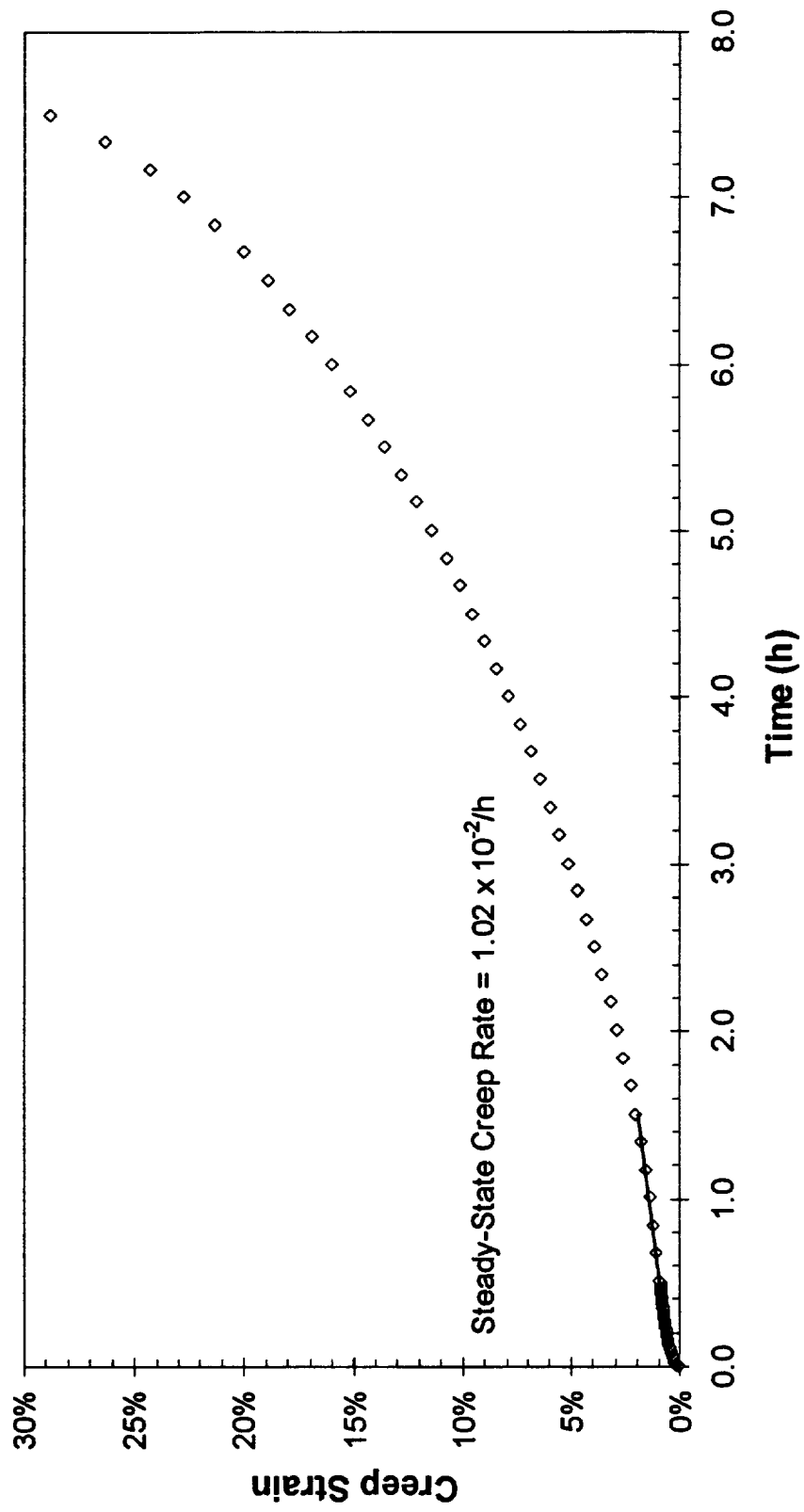


Figure C - 22 -
Plate 5 Tested At 650°C/37.4 MPa

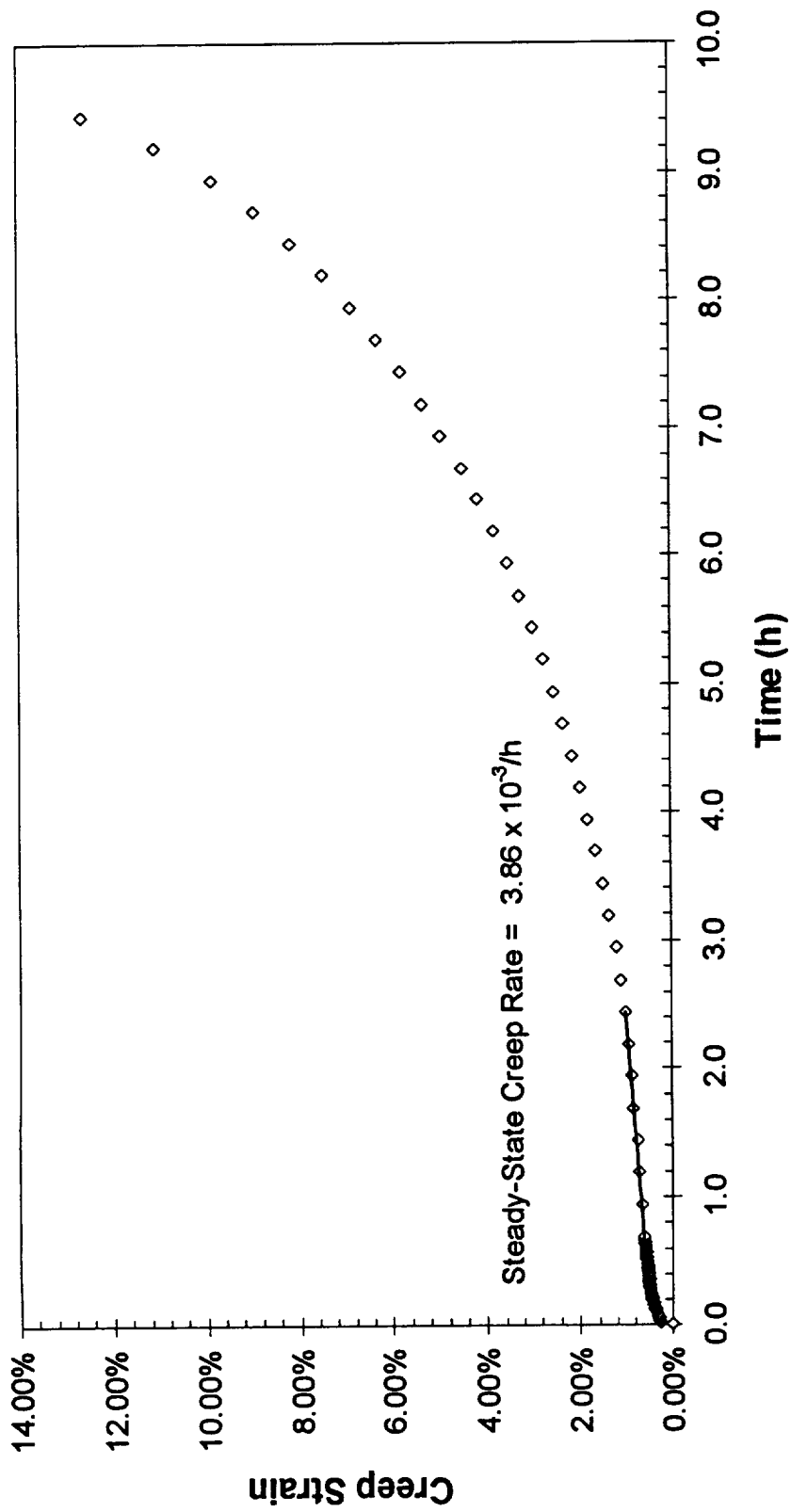


Figure C - 23 -
 Plate 6 Tested At 650°C/37.4 MPa

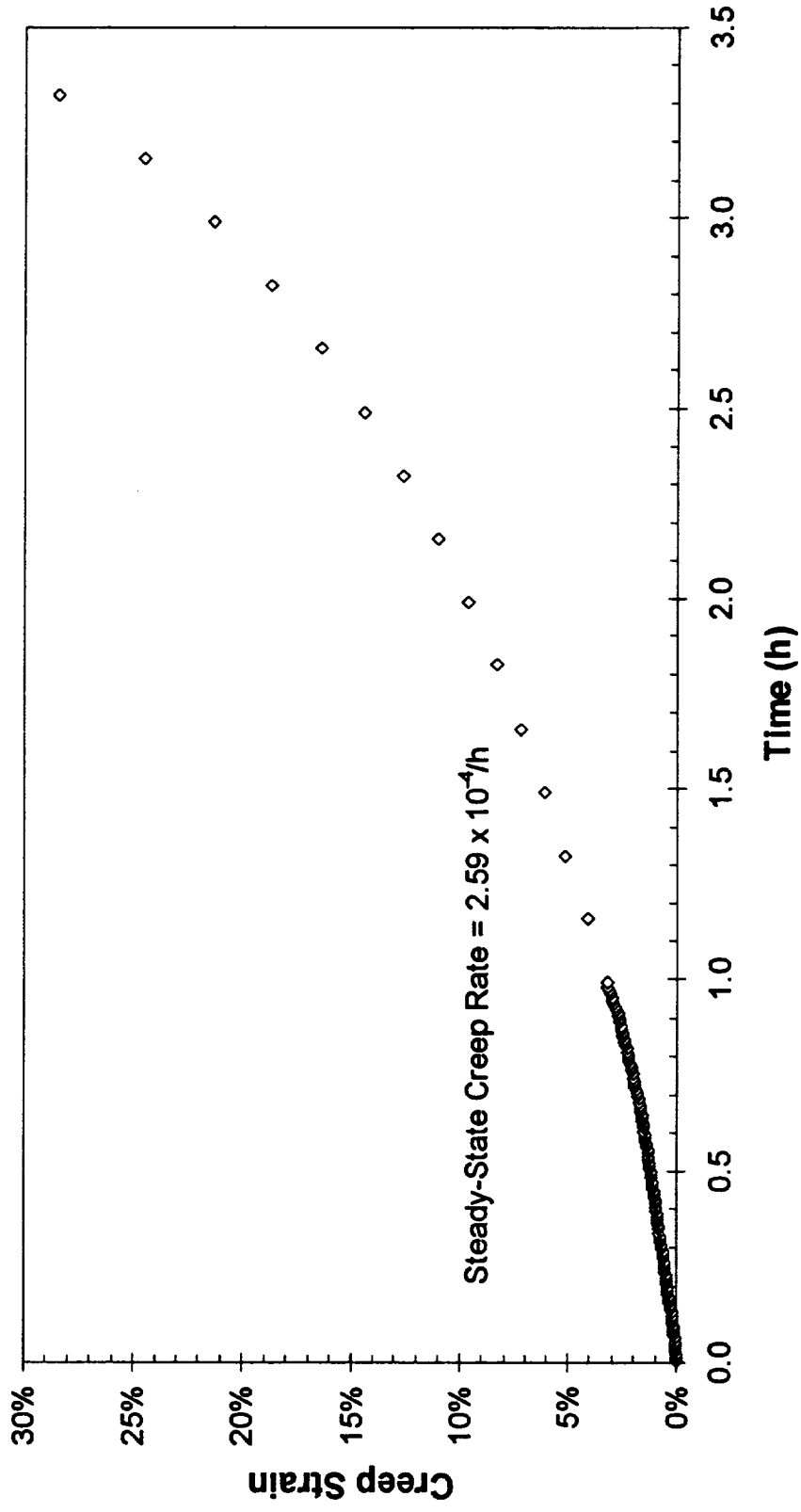


Figure C - 24 -
Plate 8 Tested At 650°C/37.4 MPa

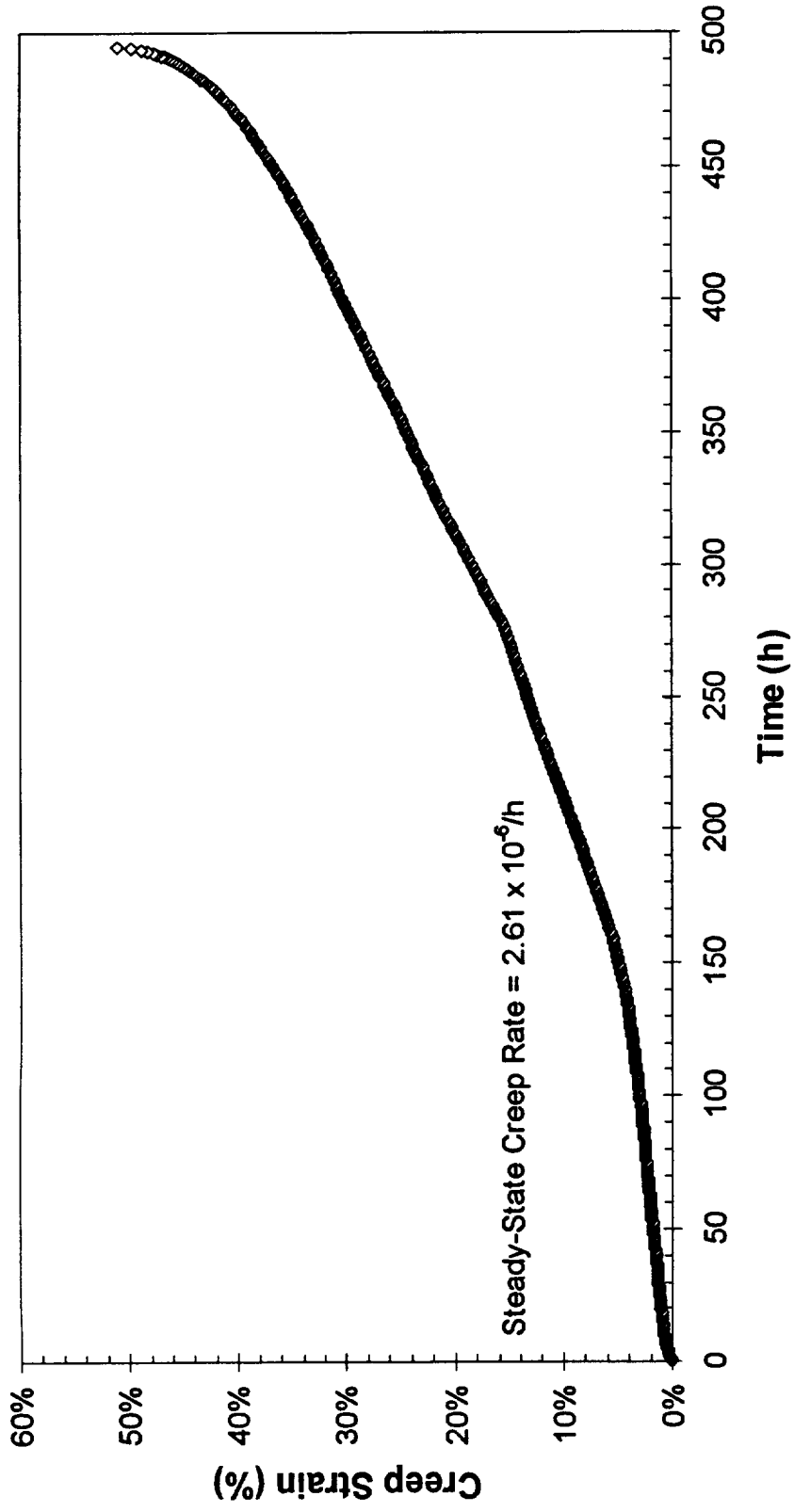


Figure C - 25 -
Plate 3 Tested At 800°C/6.2 MPa

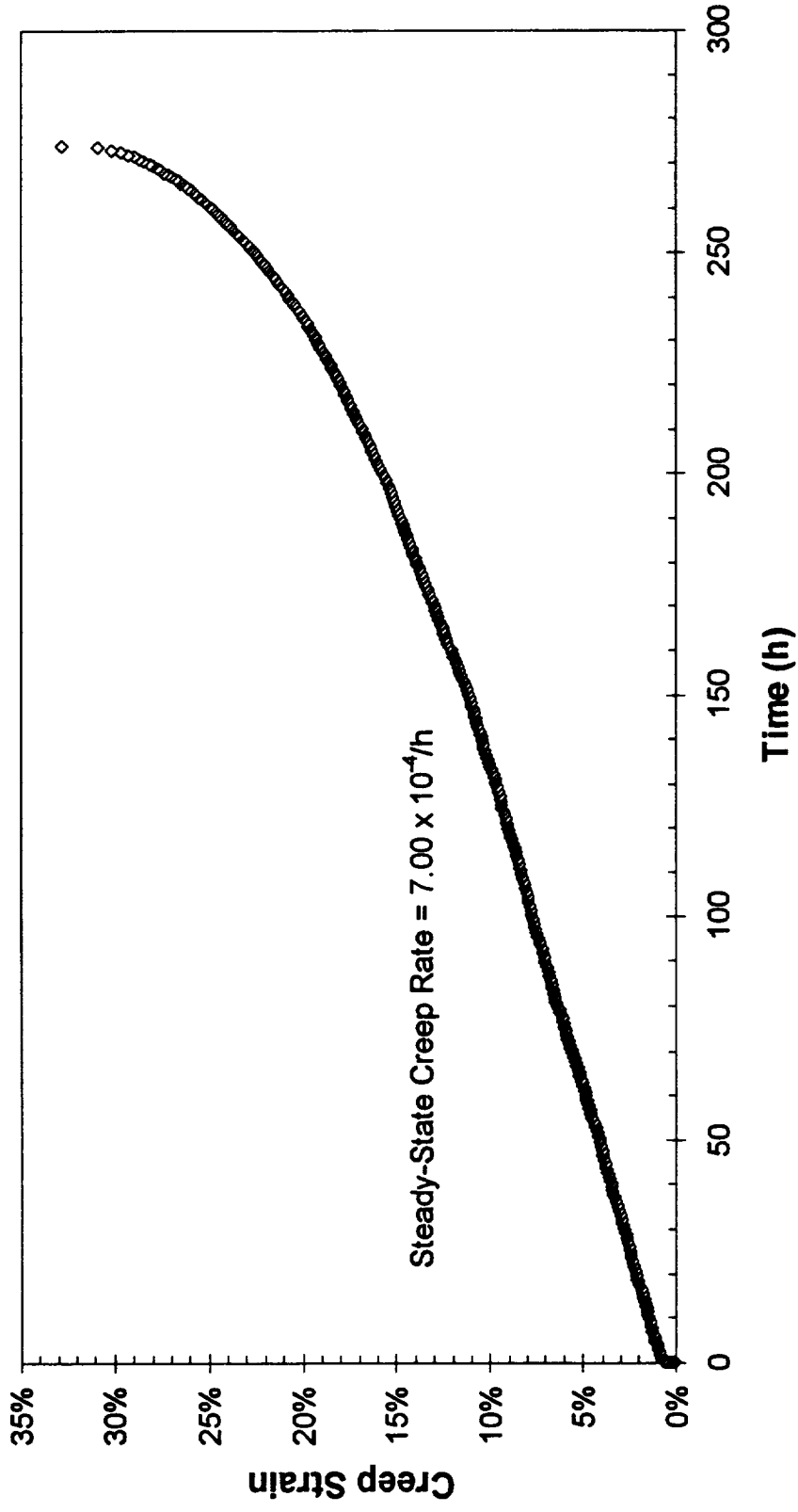


Figure C - 26 -
Plate 5 Tested At 800°C/6.2 MPa

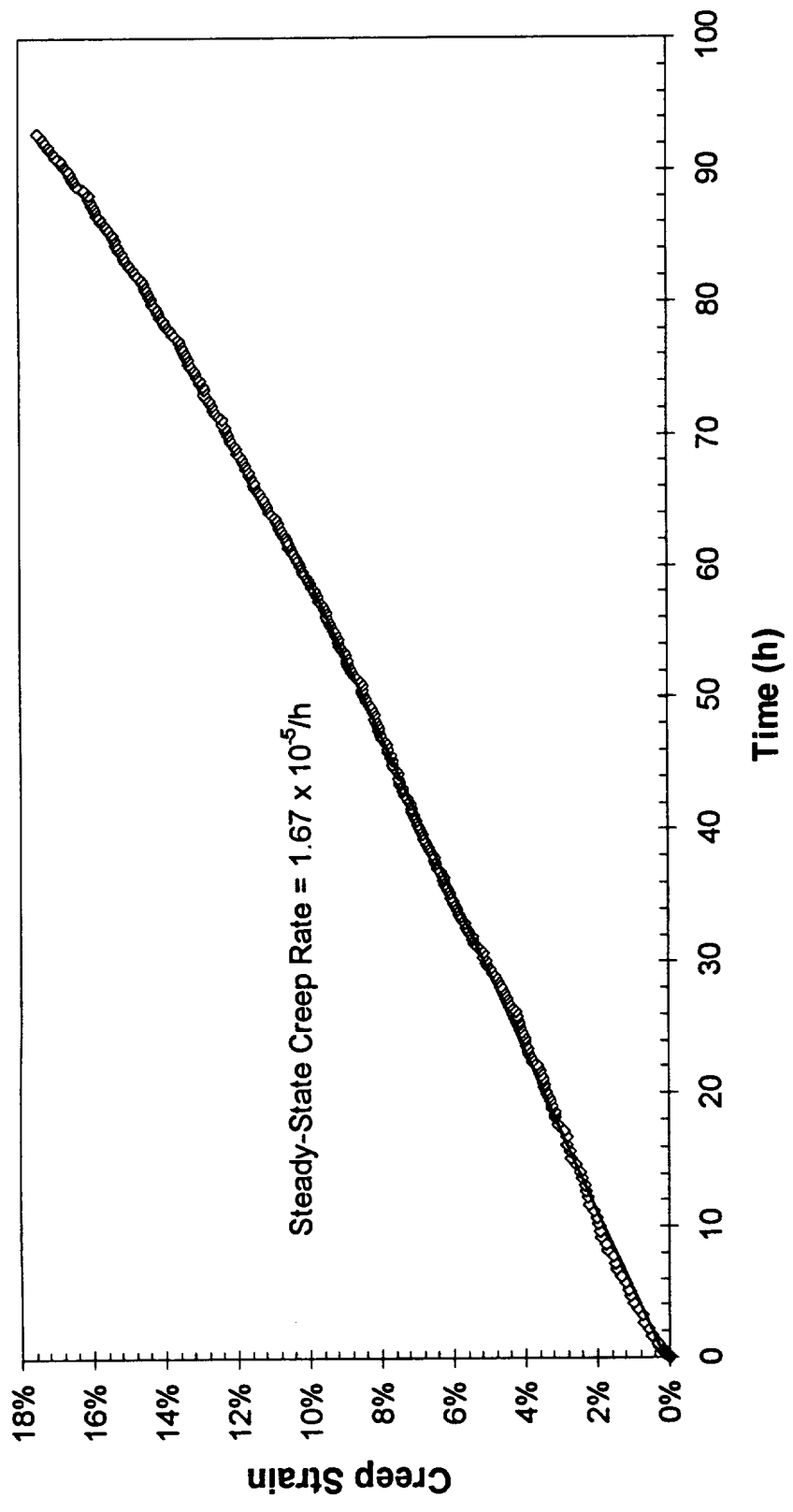


Figure C - 27 -
Plate 6 Tested At 800°C/6.2 MPa

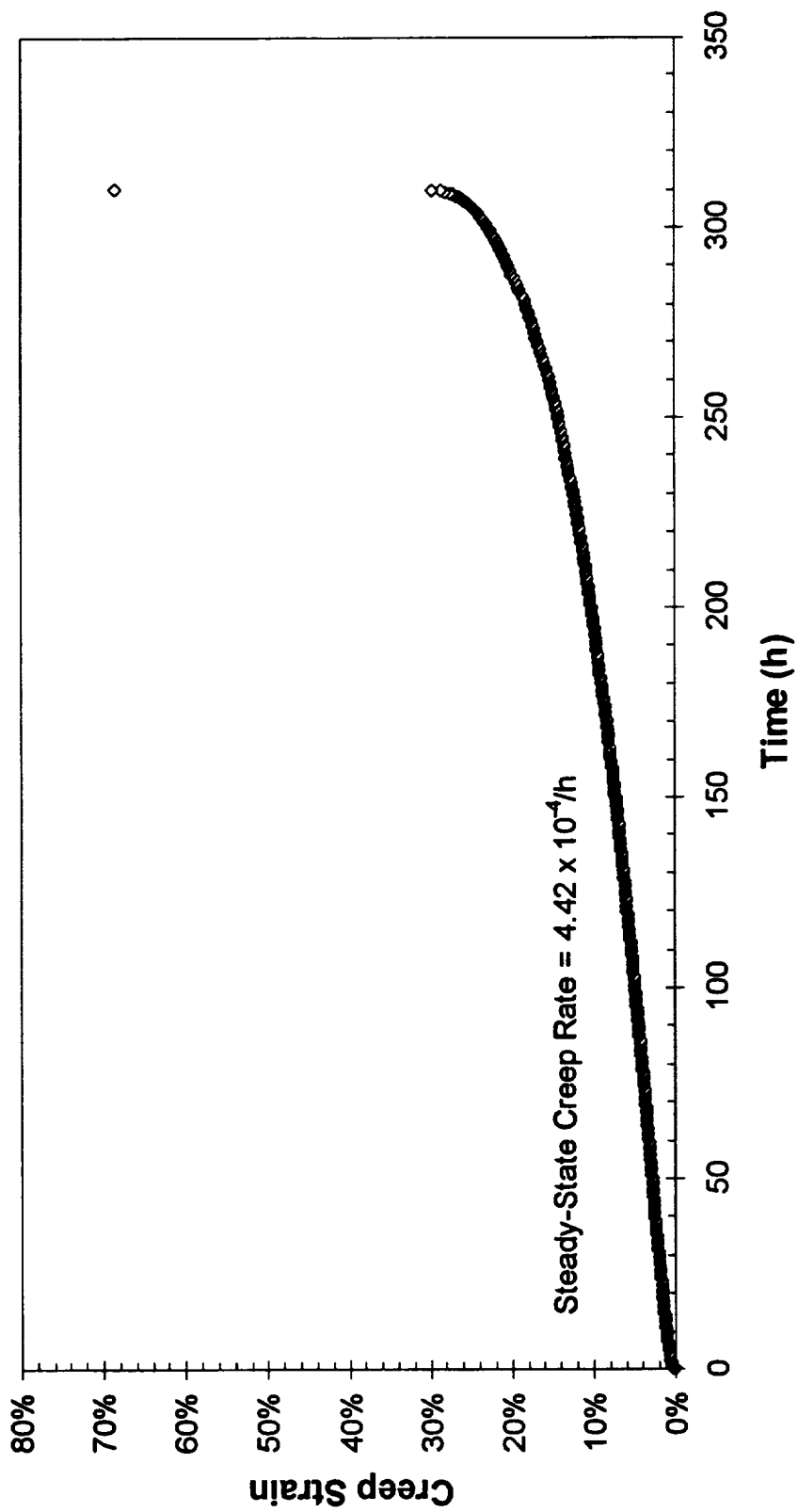


Figure C - 28 -
Plate 8 Tested At 800°C/6.2 MPa

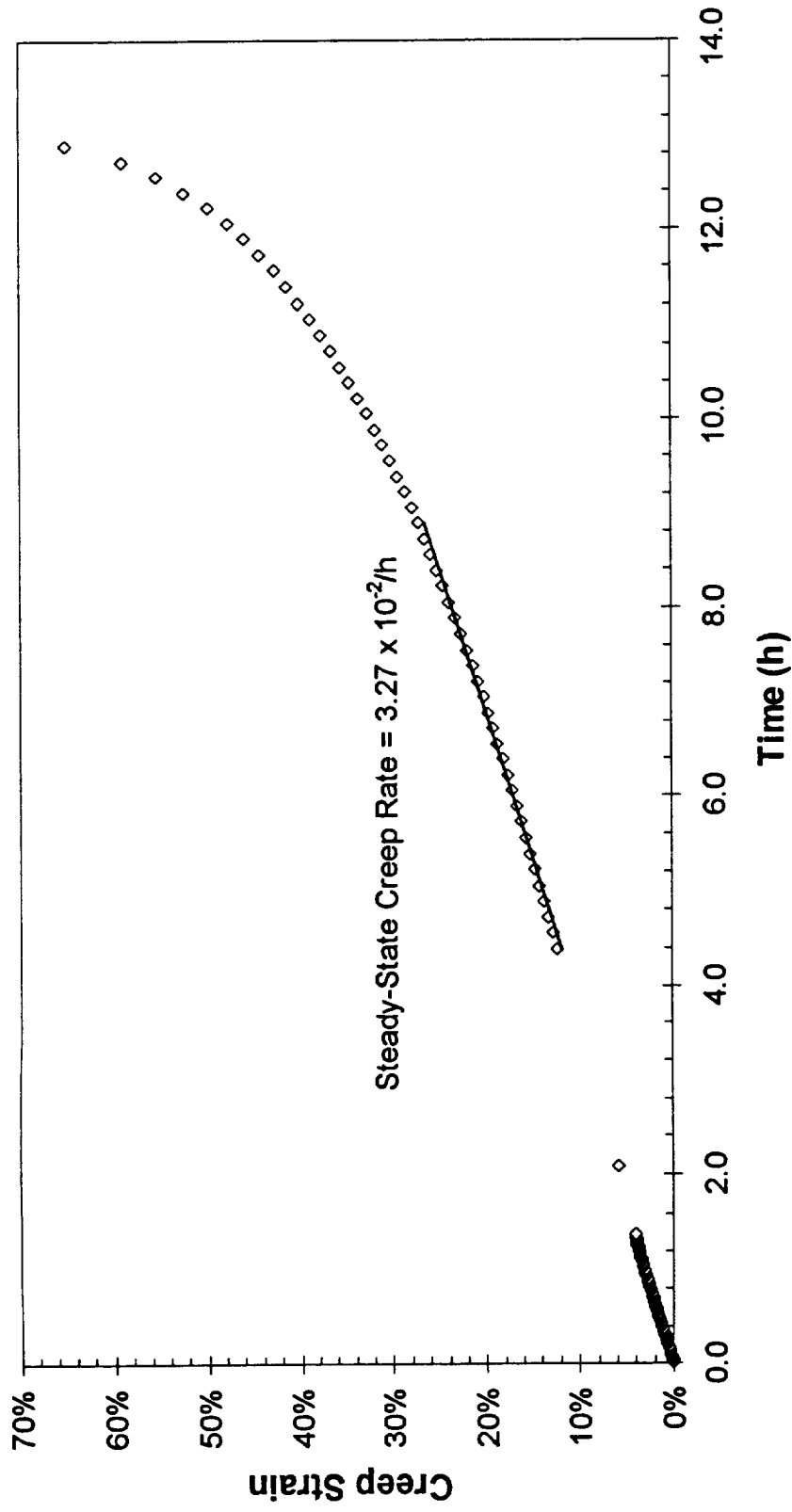


Figure C - 29 -
Plate 3 Tested At 800°C/10.4 MPa

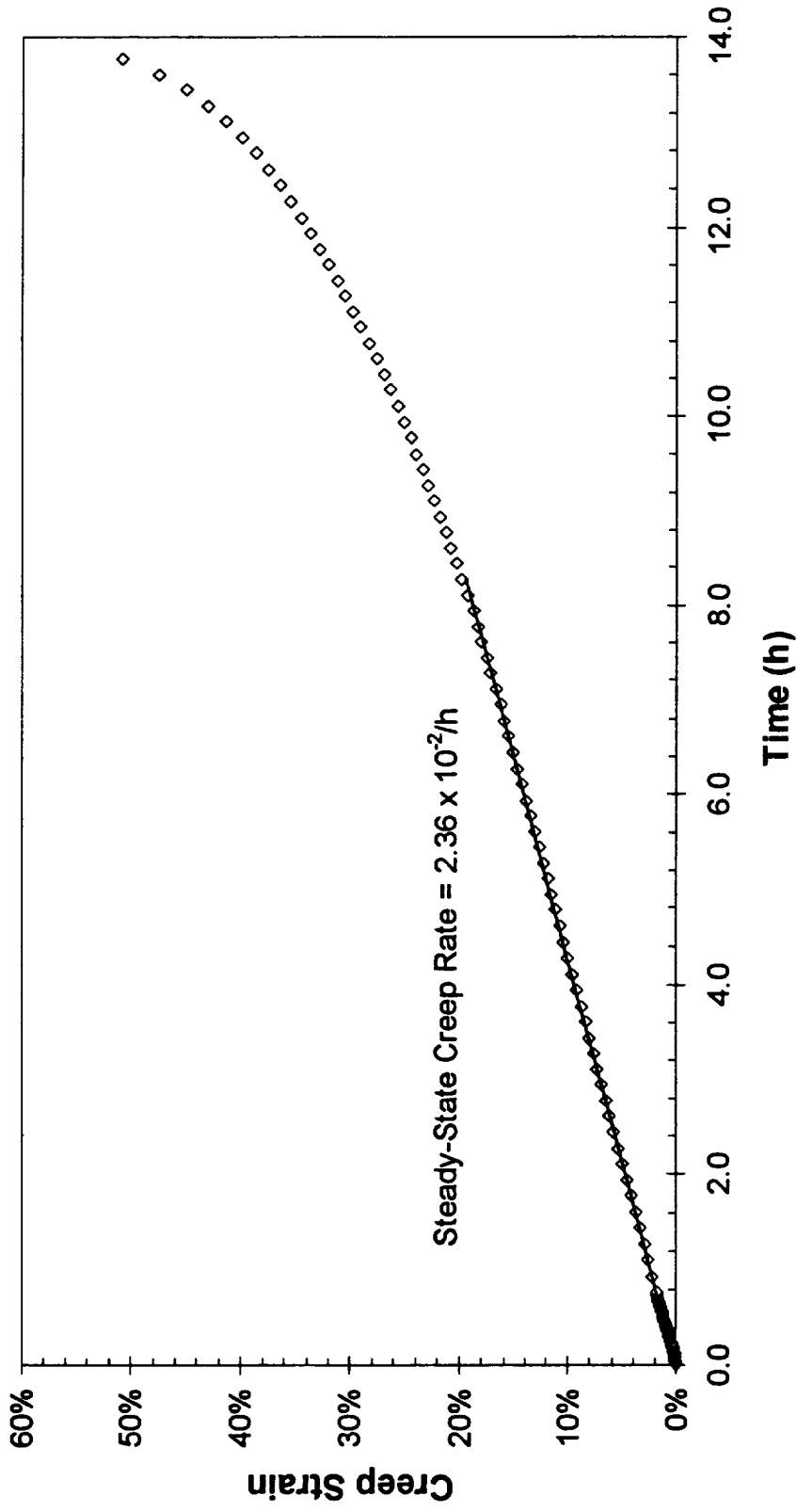


Figure C - 30 -
Plate 5 Tested At 800°C/10.4 MPa

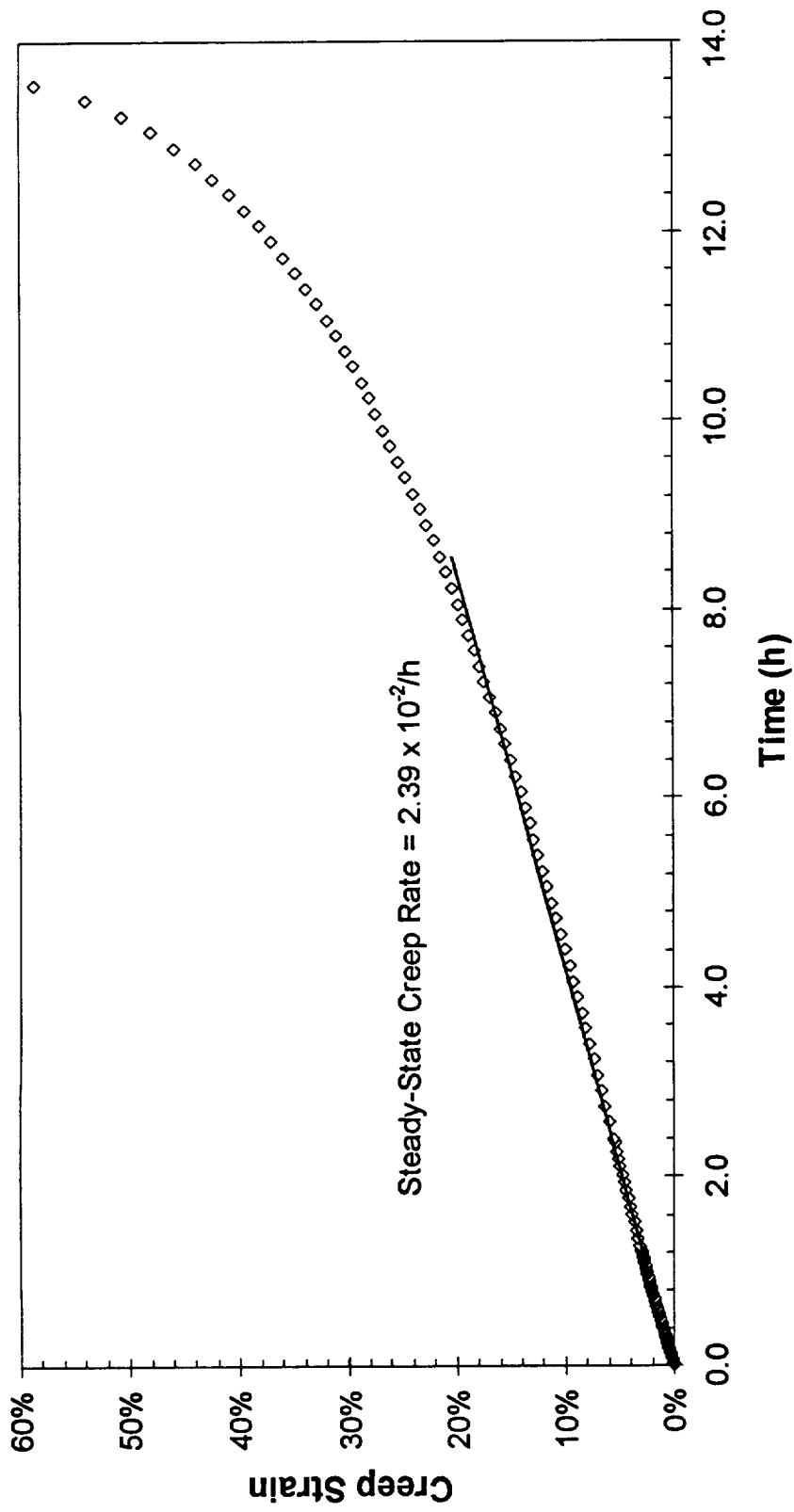


Figure C - 31 -
Plate 6 Tested At 800°C/10.4 MPa

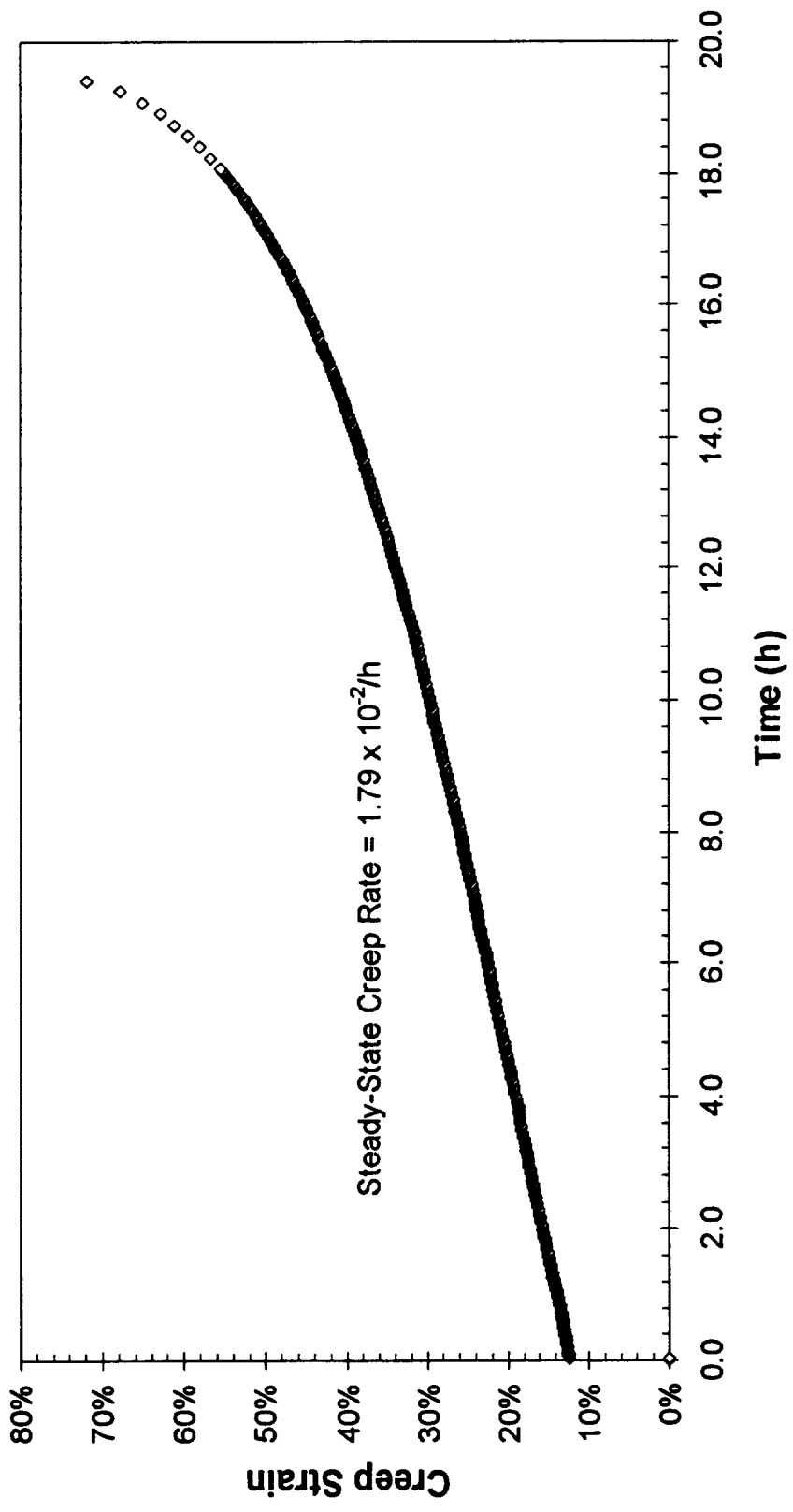


Figure C - 32 -
Plate 8 Tested At 800°C/10.4 MPa

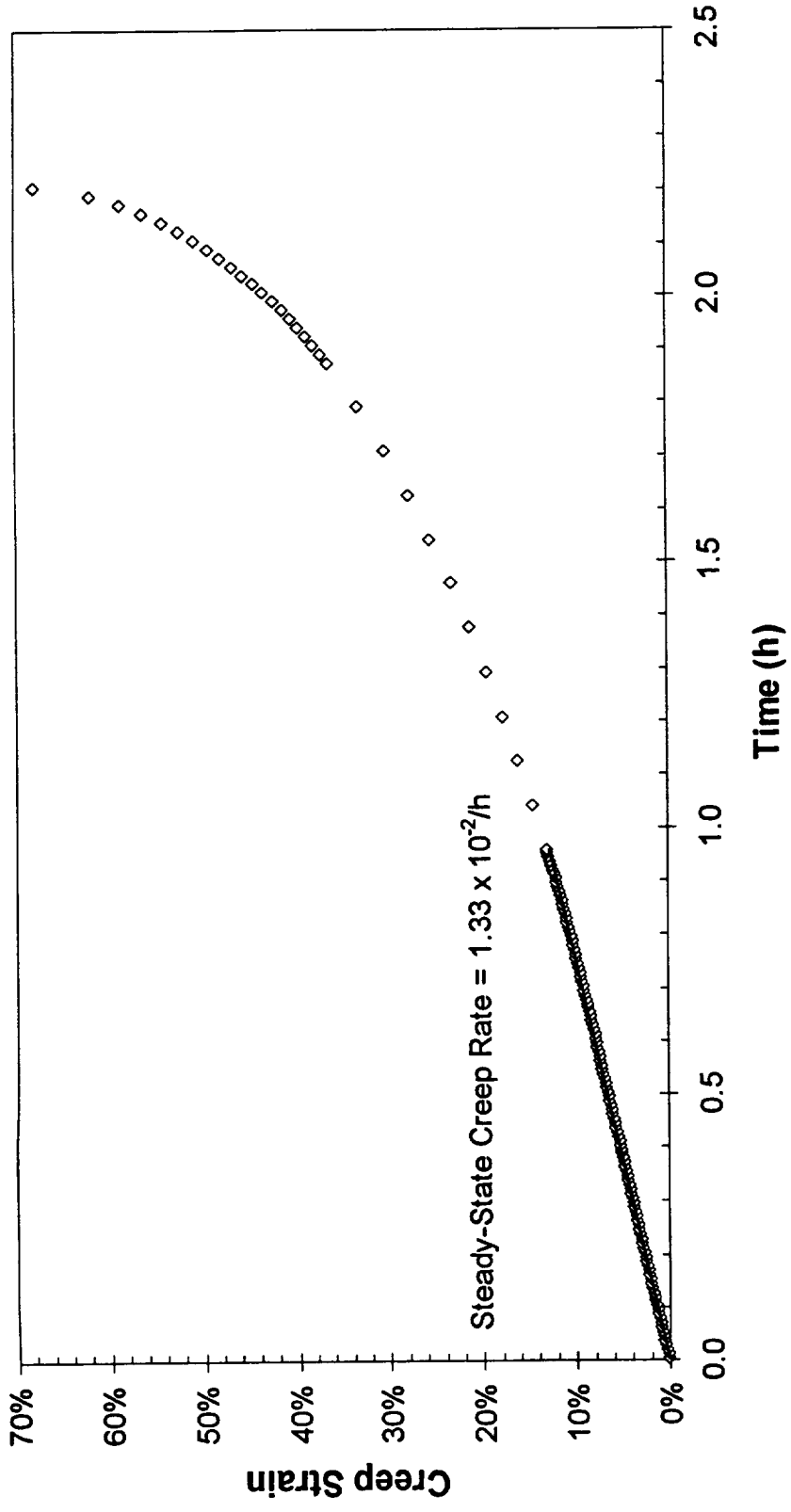


Figure C - 33 -
Plate 3 Tested At 800°C/14.6 MPa

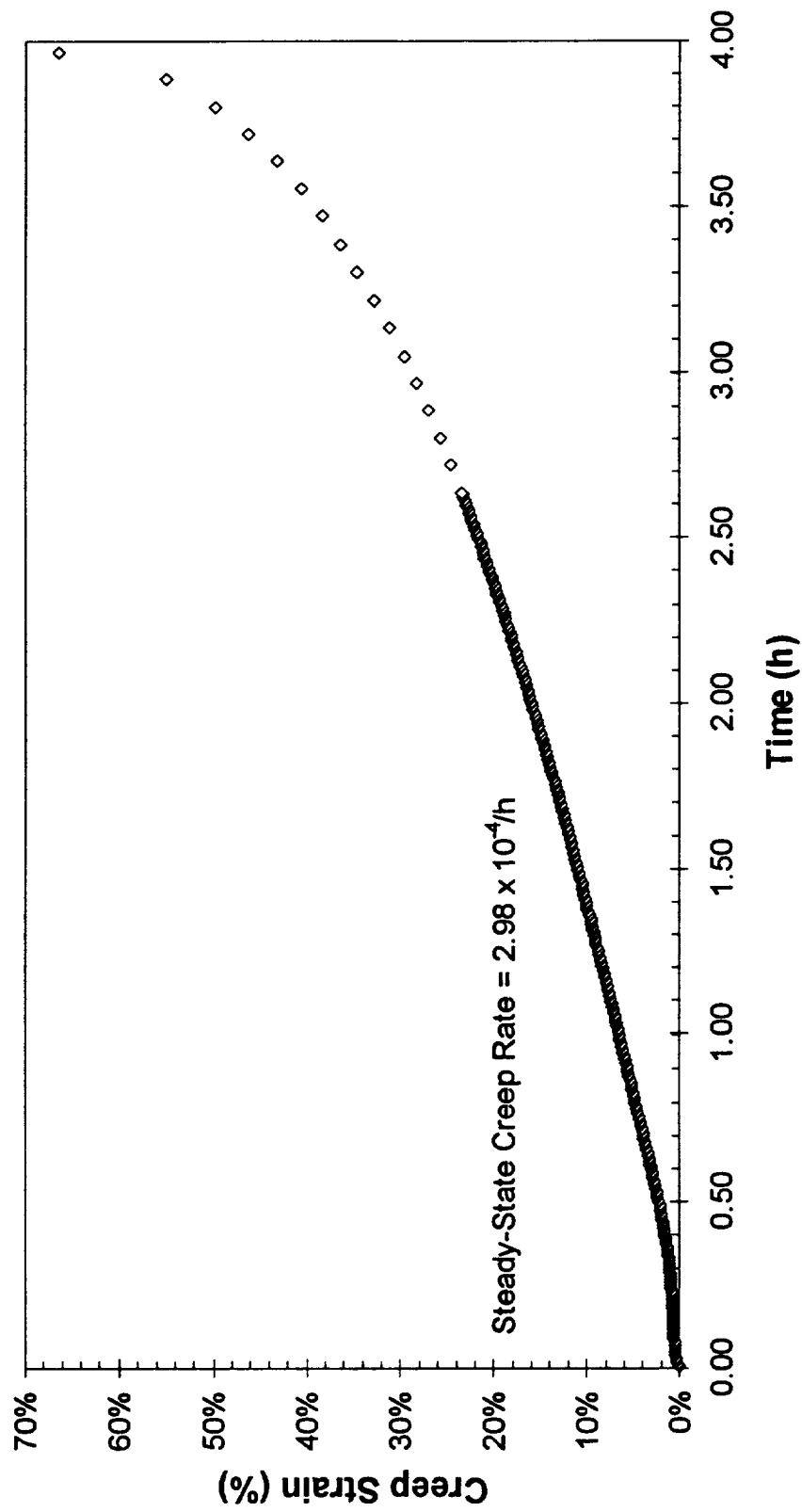


Figure C - 34 -
Plate 5 Tested At 800°C/14.6 MPa

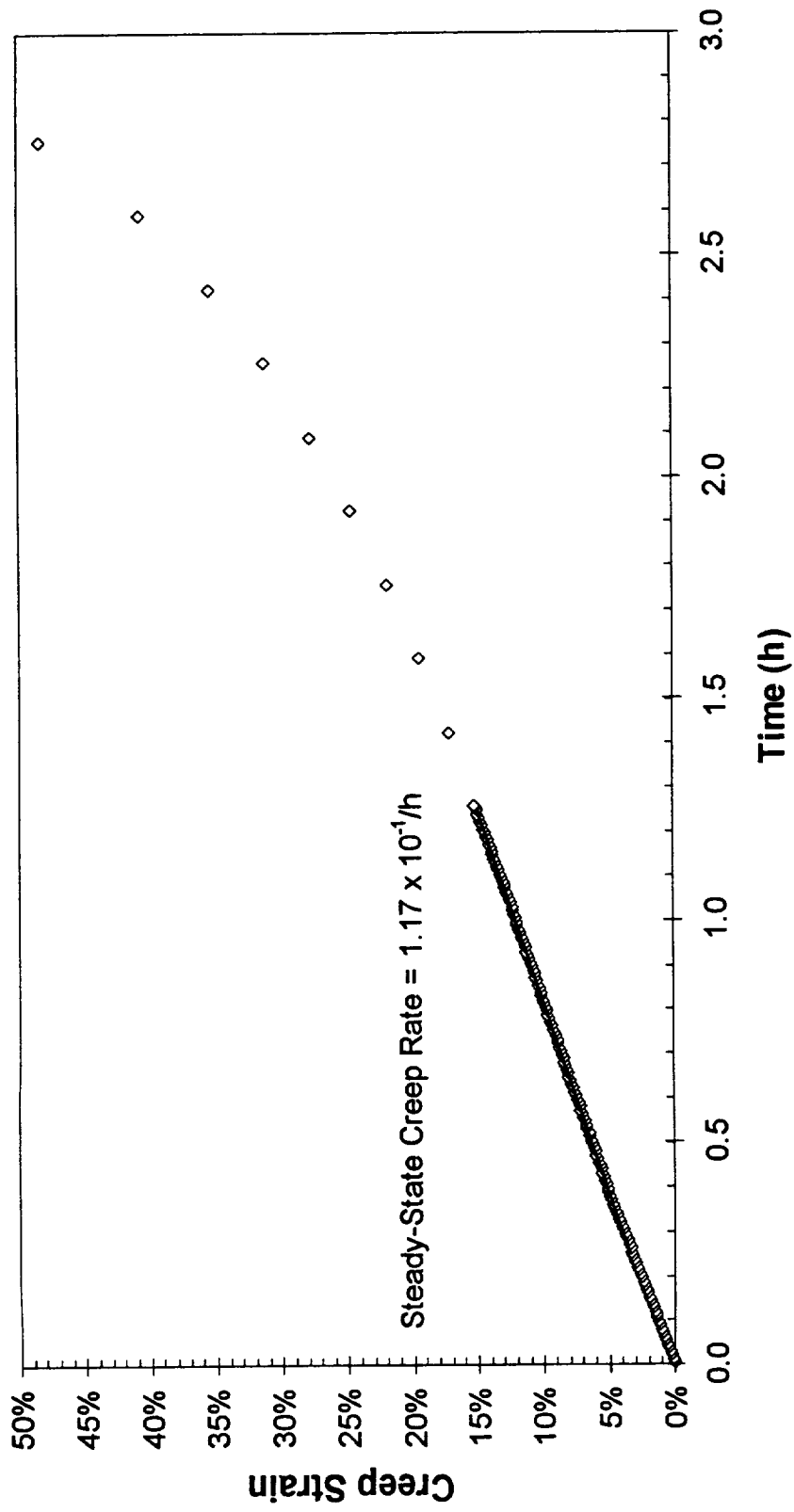


Figure C - 35 -
Plate 6 Tested At 800°C/14.6 MPa

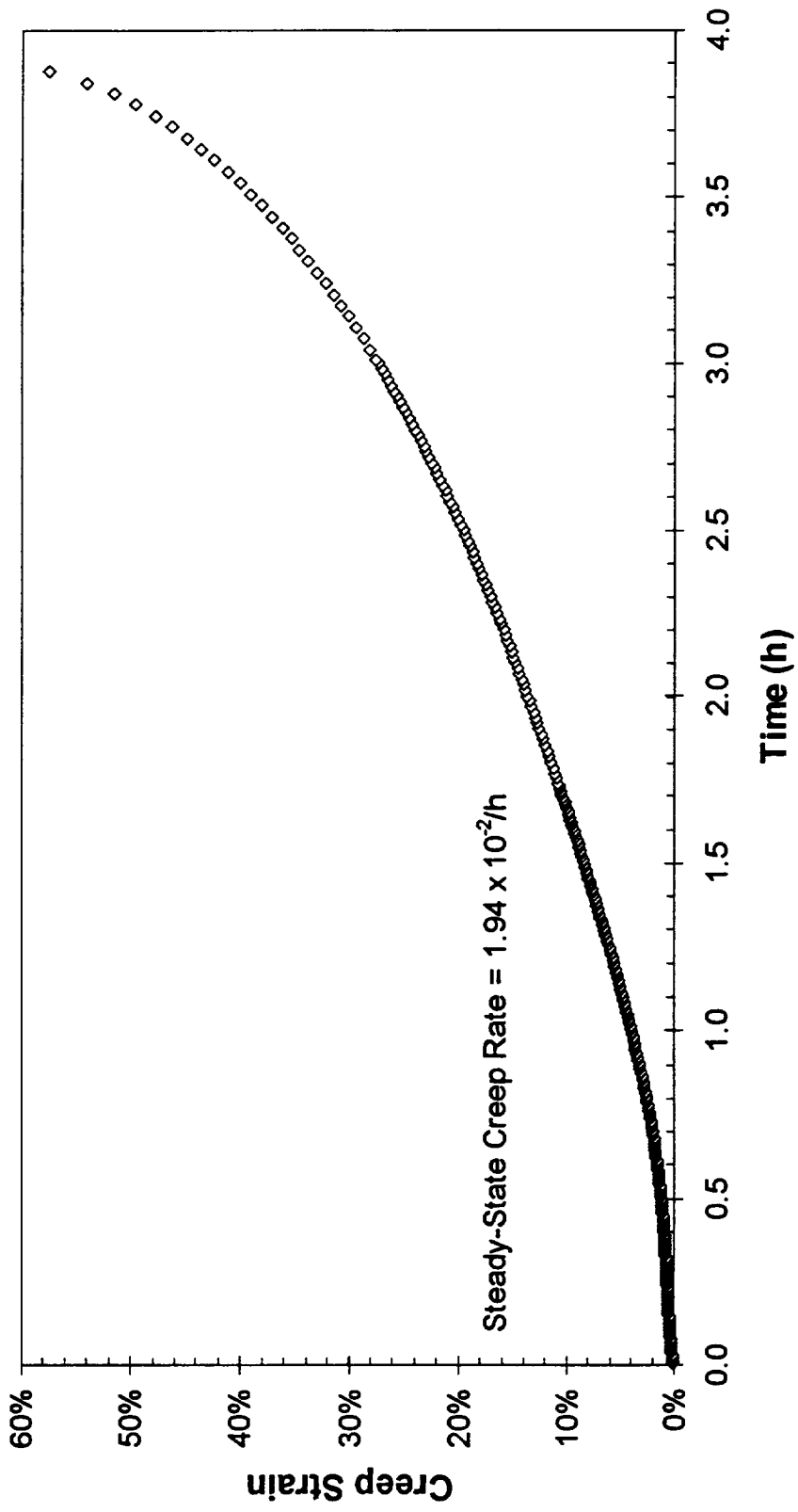


Figure C - 36 -
Plate 8 Tested At 800°C/14.6 MPa

Appendix D - Cu-8 Cr-4 Nb Low Cycle Fatigue Loops

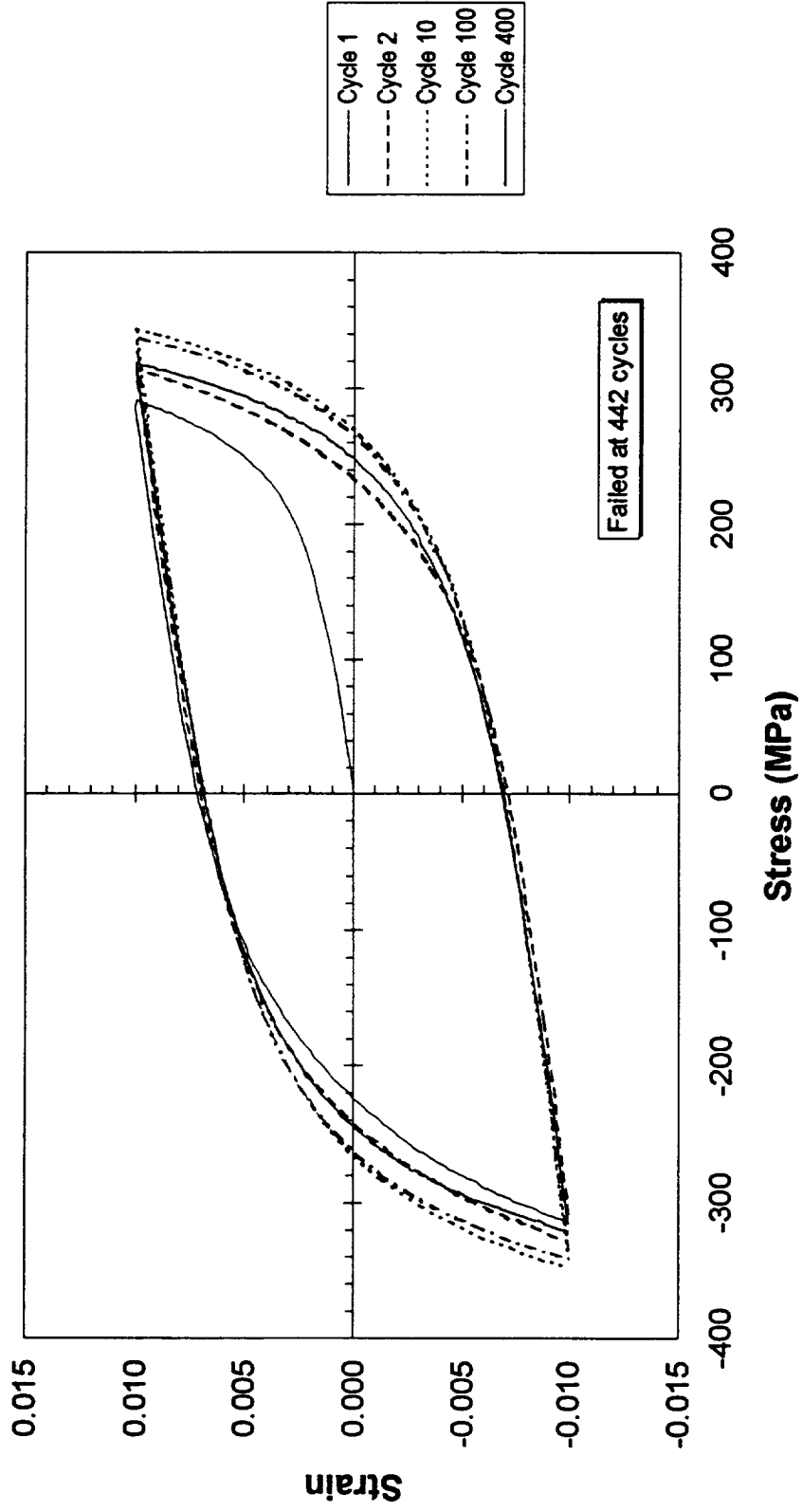


Figure D - 1 -
 Cu-8 Cr-4 Nb Sample 1-1 LCF Tested At Room Temperature / 2.0% Total Strain

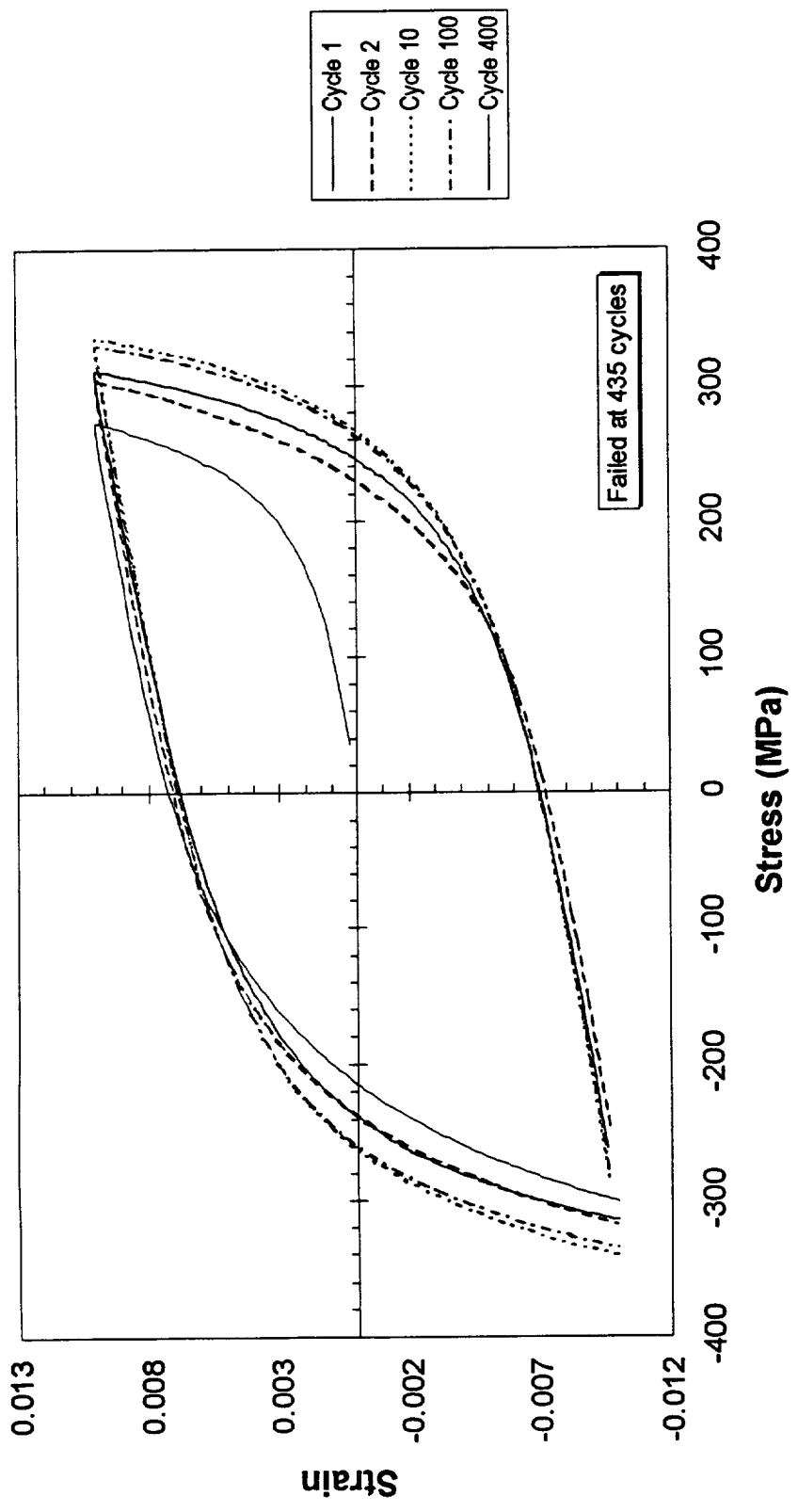


Figure D - 2 -
 Cu-8 Cr-4 Nb Sample 6-2 LCF Tested At Room Temperature / 2.0% Total Strain

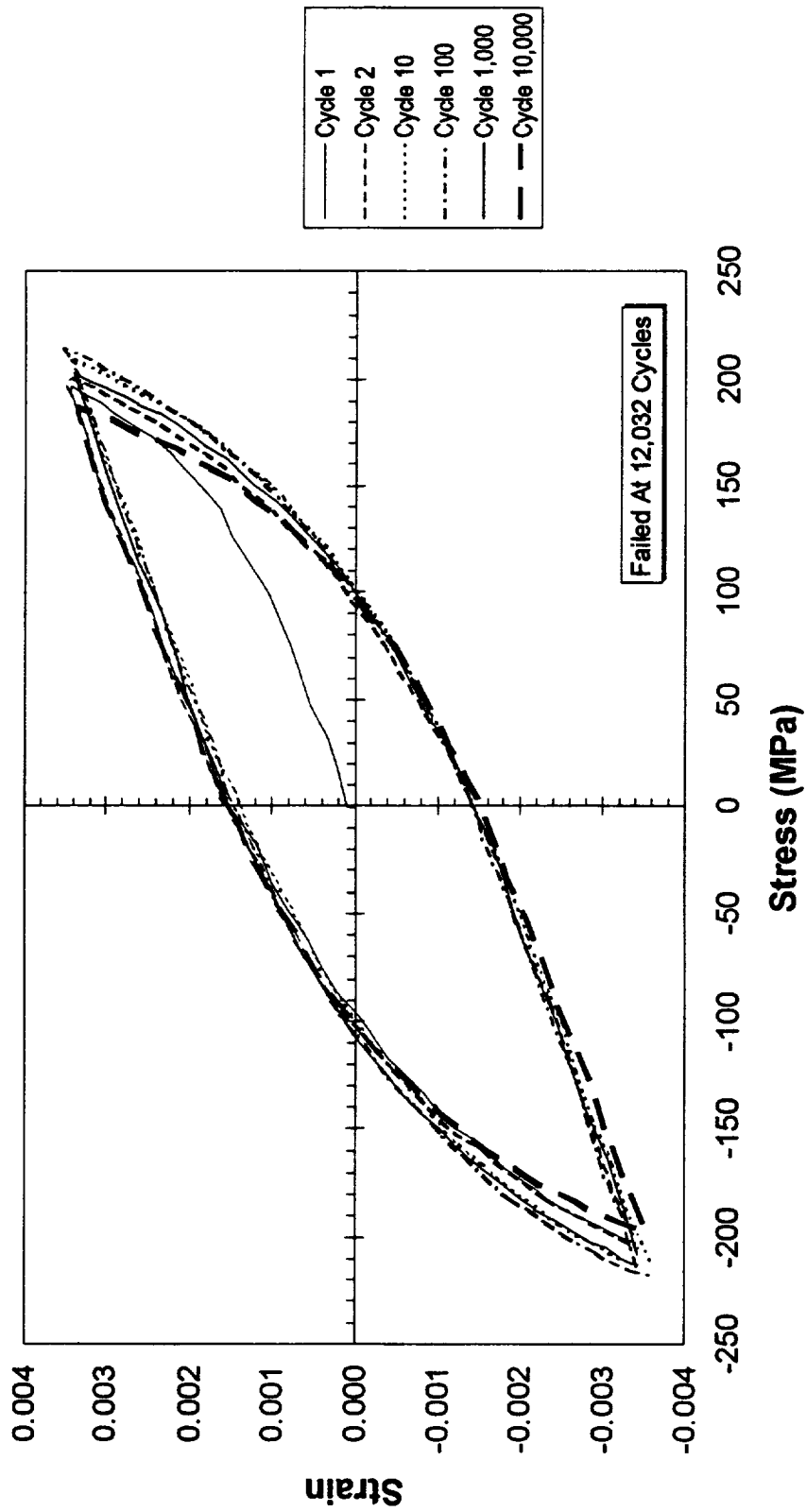


Figure D - 3 -
 Cu-8 Cr-4 Nb Sample 1-5 LCF Tested At 538°C (1000°F) / 0.7% Total Strain

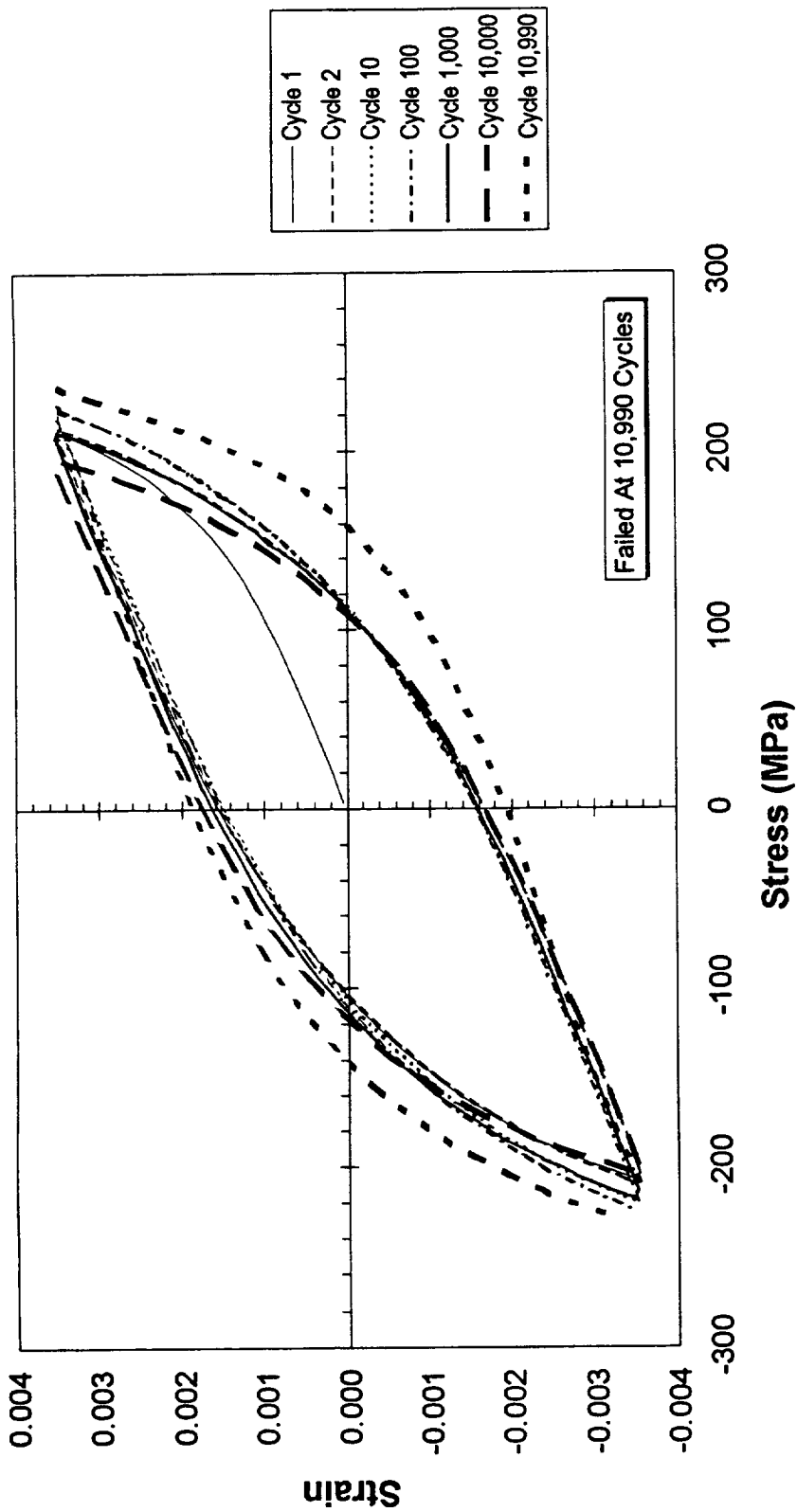


Figure D - 4 -
 Cu-8 Cr-4 Nb Sample 7-4 LCF Tested At 538°C (1000°F) / 0.7% Total Strain

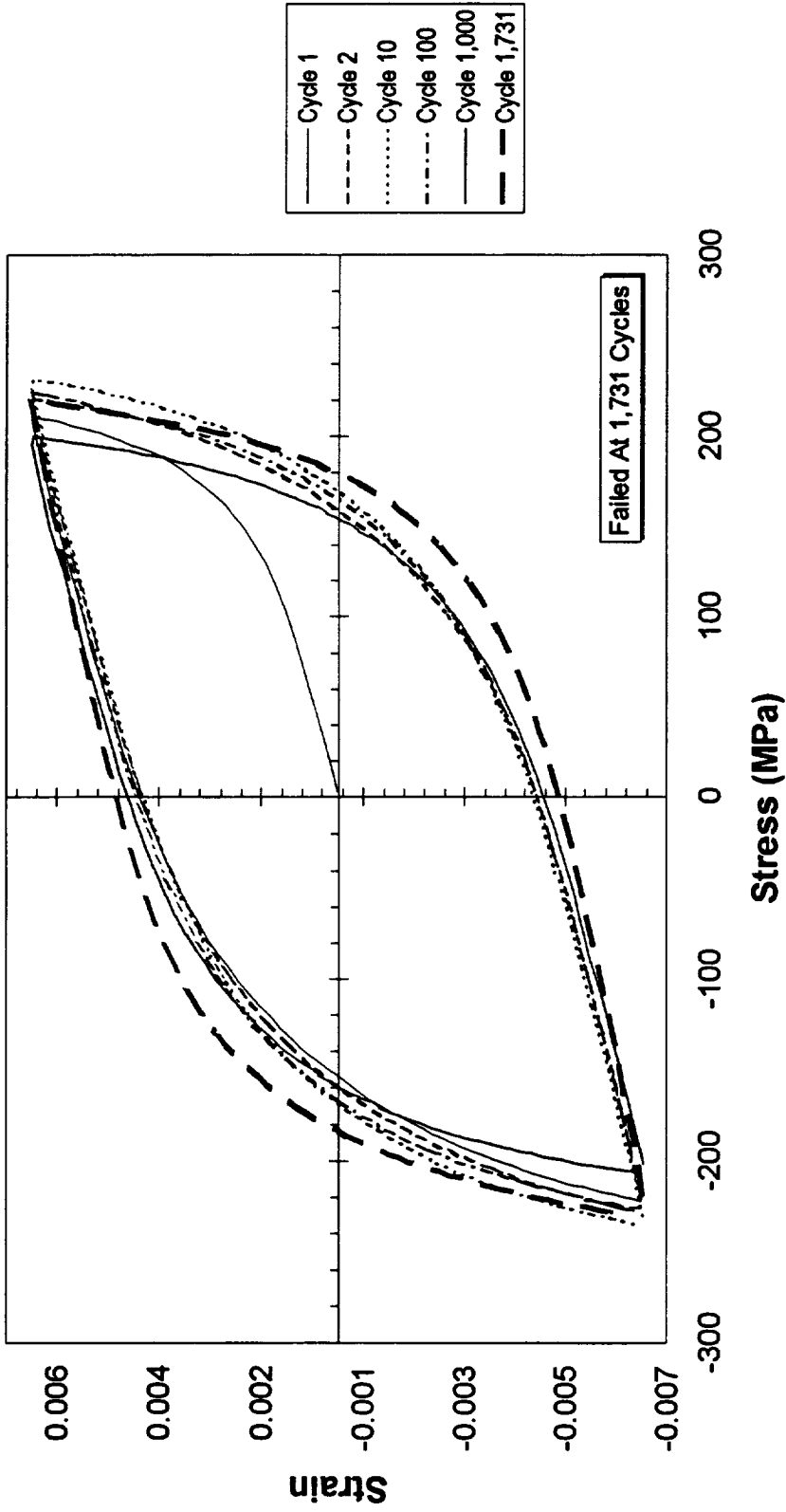


Figure D - 5 -
 Cu-8 Cr-4 Nb Sample 6-4 LCF Tested At 538°C (1000°F) / 1.2% Total Strain

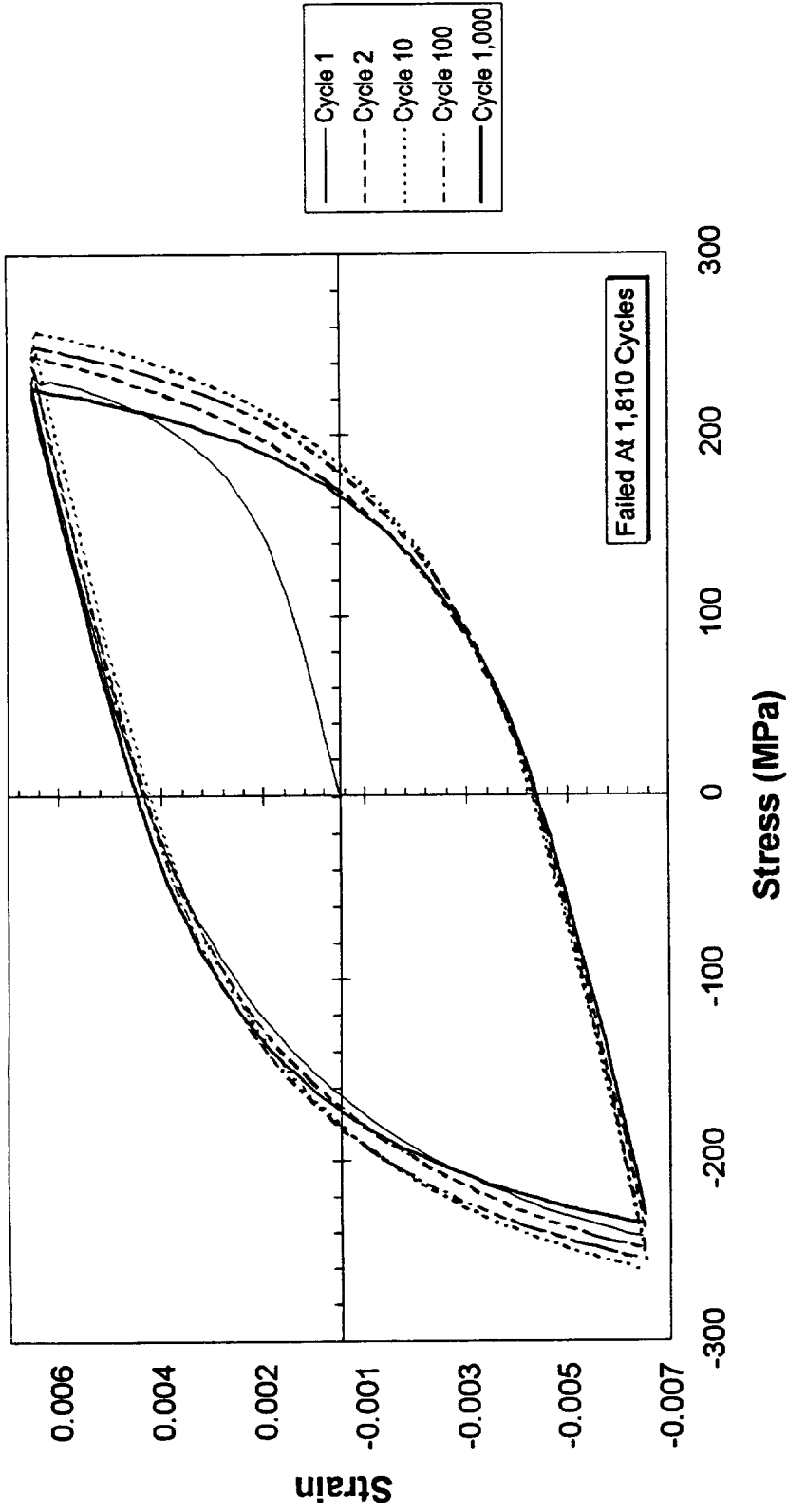


Figure D - 6 -
 Cu-8 Cr-4 Nb Sample 7-1 LCF Tested At 538°C (1000°F) / 1.2% Total Strain

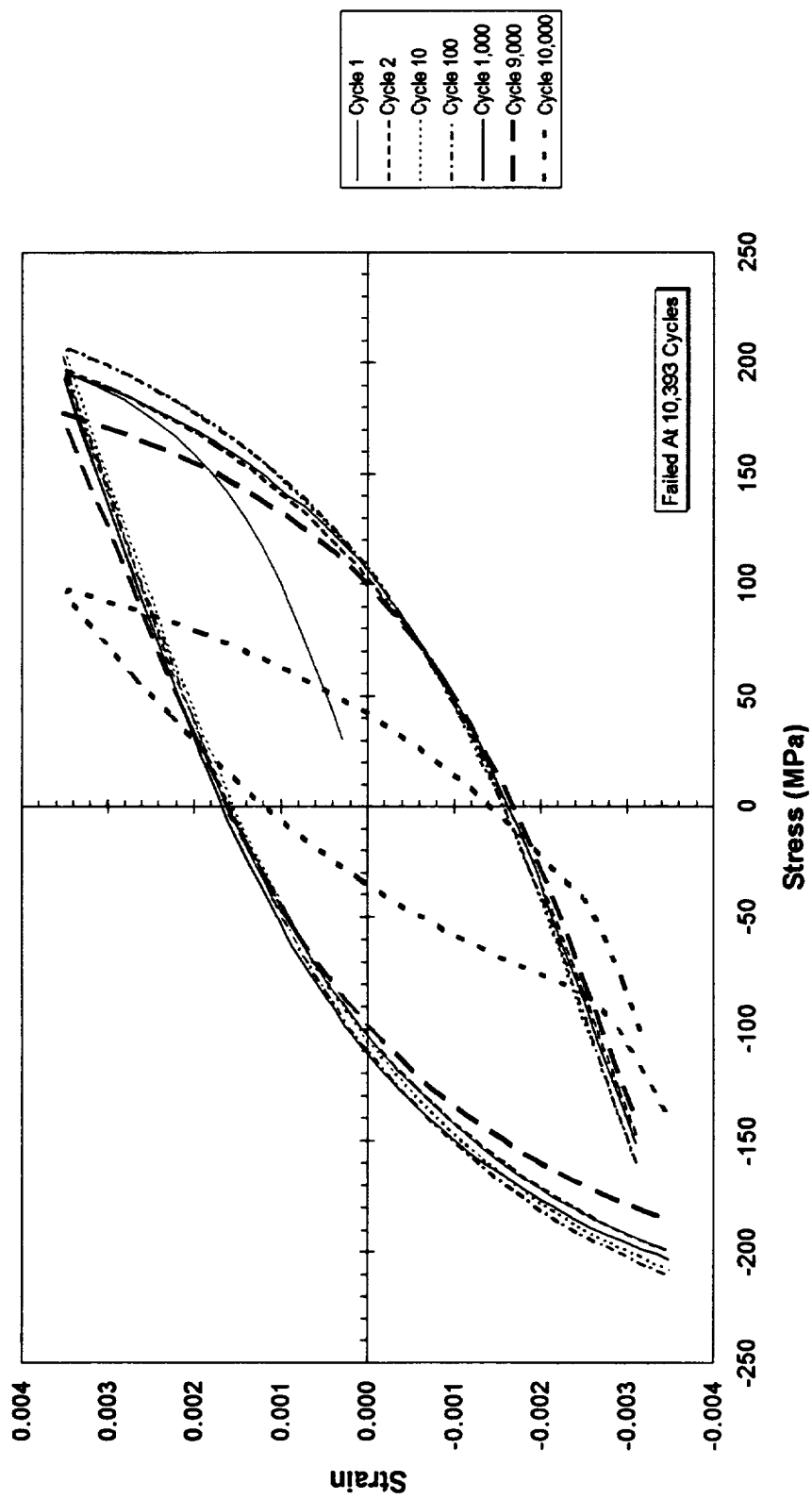


Figure D - 7 -
 Cu-8 Cr-4 Nb Sample 1-2 LCF Tested At 650°C (1200°F) / 0.7% Total Strain

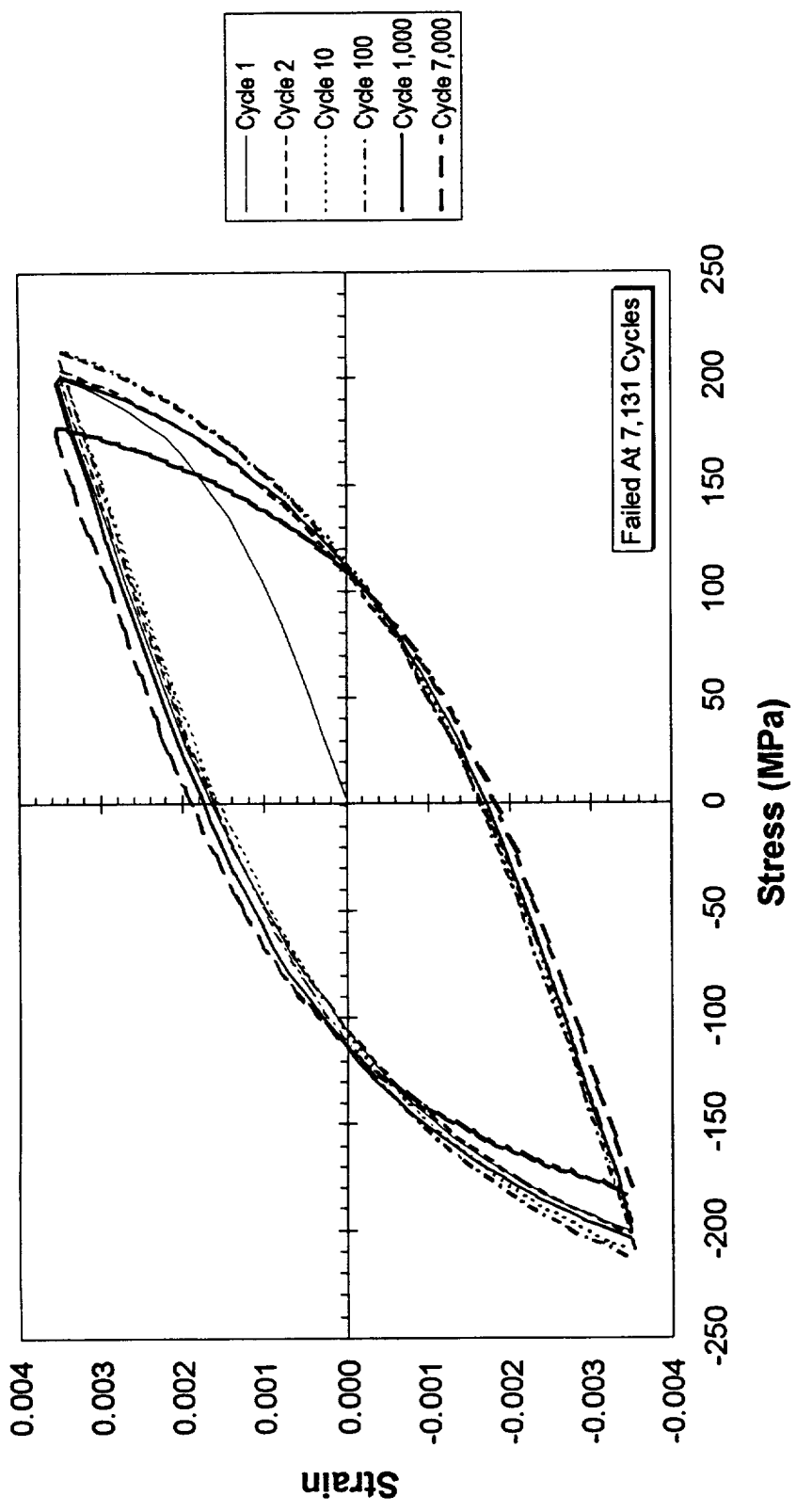


Figure D - 8 -
 Cu-8 Cr-4 Nb Sample 7-3 LCF Tested At 650°C (1200°F) / 0.7% Total Strain

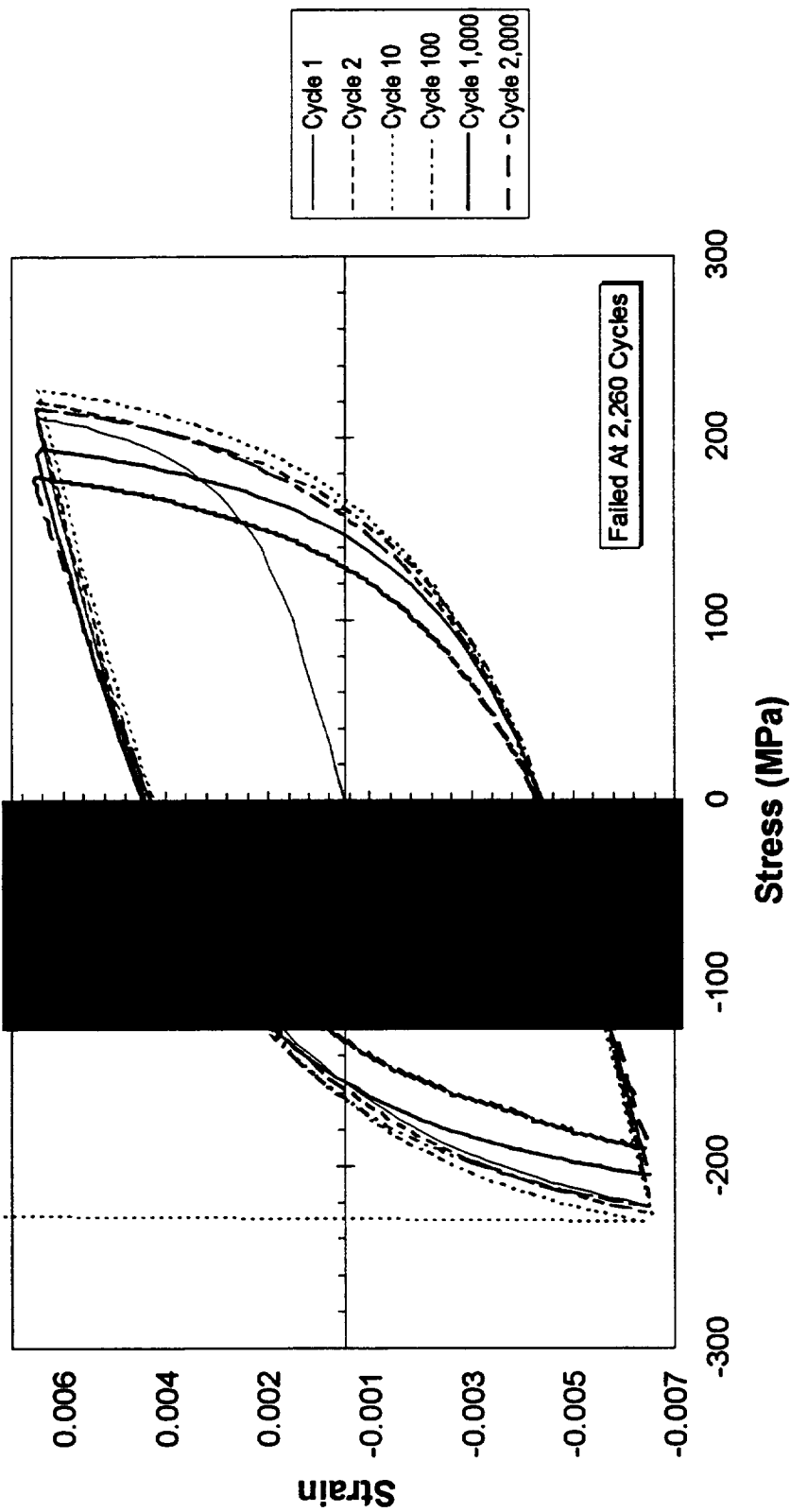


Figure D - 9 -
 Cu-8 Cr-4 Nb Sample 1-4 LCF Tested At 650°C (1200°F) / 1.2% Total Strain

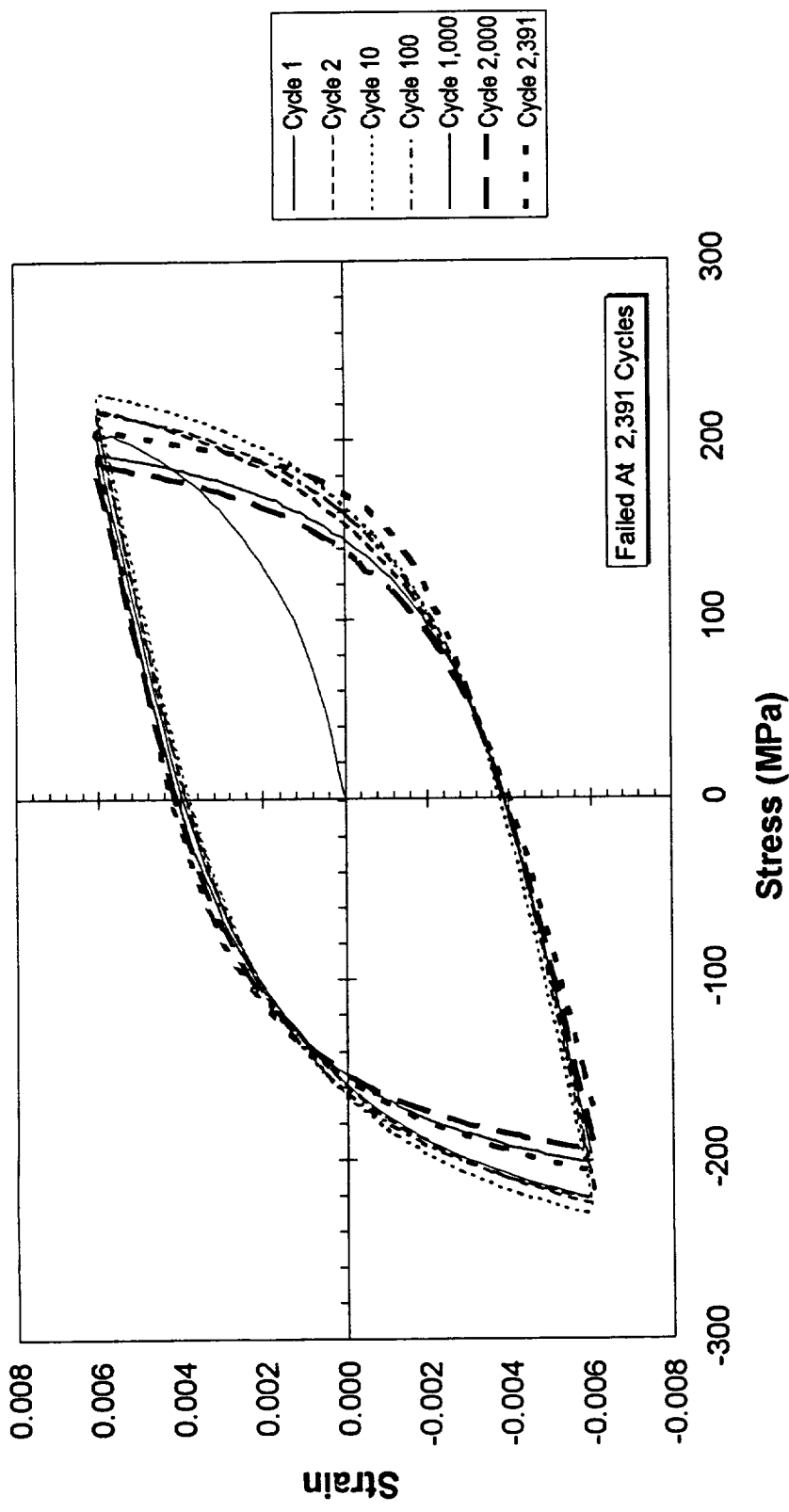


Figure D - 10 -
 Cu-8 Cr-4 Nb Sample 6-1 LCF Tested At 650°C (1200°F) / 1.2% Total Strain

REPORT DOCUMENTATION PAGE

Form Approved
OMB No. 0704-0188

Public reporting burden for this collection of information is estimated to average 1 hour per response, including the time for reviewing instructions, searching existing data sources, gathering and maintaining the data needed, and completing and reviewing the collection of information. Send comments regarding this burden estimate or any other aspect of this collection of information, including suggestions for reducing this burden, to Washington Headquarters Services, Directorate for Information Operations and Reports, 1215 Jefferson Davis Highway, Suite 1204, Arlington, VA 22202-4302, and to the Office of Management and Budget, Paperwork Reduction Project (0704-0188), Washington, DC 20503.

1. AGENCY USE ONLY (<i>Leave blank</i>)	2. REPORT DATE October 1996	3. REPORT TYPE AND DATES COVERED Final Contractor Report	
4. TITLE AND SUBTITLE Mechanical and Thermal Properties of Two Cu-Cr-Nb Alloys and NARloy-Z		5. FUNDING NUMBERS WU-505-63-52 NCC3-94	
6. AUTHOR(S) David L. Ellis and Gary M. Michal		8. PERFORMING ORGANIZATION REPORT NUMBER E-10428	
7. PERFORMING ORGANIZATION NAME(S) AND ADDRESS(ES) Case Western Reserve University 10900 Euclid Avenue Cleveland, Ohio 44106		10. SPONSORING/MONITORING AGENCY REPORT NUMBER NASA CR-198529	
9. SPONSORING/MONITORING AGENCY NAME(S) AND ADDRESS(ES) National Aeronautics and Space Administration Lewis Research Center Cleveland, Ohio 44135-3191		11. SUPPLEMENTARY NOTES Project Manager, Michael V. Nathal, Materials Division, organization code 5120, (216) 433-9516.	
12a. DISTRIBUTION/AVAILABILITY STATEMENT Unclassified - Unlimited Subject Category 26 This publication is available from the NASA Center for AeroSpace Information, (301) 621-0390.		12b. DISTRIBUTION CODE	
13. ABSTRACT (<i>Maximum 200 words</i>) A series of creep tests were conducted on Cu-8 Cr-4 Nb (Cu-8 at.% Cr-4 at.% Nb), Cu-4 Cr-2 Nb (Cu-4 at.% Cr-2 at.% Nb), and NARloy-Z (Cu-3 wt.% Ag-0.5 wt.% Zr) samples to determine their creep properties. In addition, a limited number of low cycle fatigue and thermal conductivity tests were conducted. The Cu-Cr-Nb alloys showed a clear advantage in creep life and sustainable load over the currently used NARloy-Z. Increases in life at a given stress were between 100% and 250% greater for the Cu-Cr-Nb alloys depending on the stress and temperature. For a given life, the Cu-Cr-Nb alloys could support a stress between 60% and 160% greater than NARloy-Z. Low cycle fatigue lives of the Cu-8 Cr-4 Nb alloy were equivalent to NARloy-Z at room temperature. At elevated temperatures (538 °C and 650 °C), the fatigue lives were 50% to 200% longer than NARloy-Z samples tested at 538 °C. The thermal conductivities of the Cu-Cr-Nb alloys remained high, but were lower than NARloy-Z and pure Cu. The Cu-Cr-Nb thermal conductivities were between 72% and 96% that of pure Cu with the Cu-4 Cr-2 Nb alloy having a significant advantage in thermal conductivity over Cu-8 Cr-4 Nb. In comparison, stainless steels with equivalent strengths would have thermal conductivities less than 25% the thermal conductivity of pure Cu. The combined results indicate that the Cu-Cr-Nb alloys offer an attractive alternative to current high temperature Cu-based alloys such as NARloy-Z.			
14. SUBJECT TERMS Cu-based alloys; Creep; Low cycle fatigue (LCF); Thermal conductivity			15. NUMBER OF PAGES 206
			16. PRICE CODE A10
17. SECURITY CLASSIFICATION OF REPORT Unclassified	18. SECURITY CLASSIFICATION OF THIS PAGE Unclassified	19. SECURITY CLASSIFICATION OF ABSTRACT Unclassified	20. LIMITATION OF ABSTRACT